DEVELOPMENT OF ULTRA-FINE SLAG BASED GEOPOLYMER MORTAR AND CONCRETE FOR REPAIRING AND STRENGTHENING OF REINFORCED CONCRETE BEAMS

A Thesis Submitted in
Partial Fulfillment of the Requirements
for the Degree of

DOCTOR OF PHILOSOPHY

By

Sulaem Musaddiq Laskar
Roll No.: 146104005

DEPARTMENT OF CIVIL ENGINEERING
INDIAN INSTITUTE OF TECHNOLOGY GUWAHATI
SEPTEMBER, 2018

Certificate

It is certified that the work contained in the thesis entitled **Development of Ultra-Fine Slag Based Geopolymer Mortar and Concrete for Repairing and Strengthening of Reinforced Concrete Beams** by **Sulaem Musaddiq Laskar** (Roll No.: 146104005), a student of the Department of Civil Engineering, Indian Institute of Technology Guwahati, submitted for the award of the degree of Doctor of Philosophy, has been carried out under my supervision and that this work has not been submitted elsewhere for a degree.

September, 2018

Prof. S. Talukdar
Department of Civil Engineering
Indian Institute of Technology Guwahati
Assam, India

Dedicated to my

mother, ***Mrs. Laila Begum Mazumder***

and

father, ***Prof. Zahir Uddin Ahmed Laskar***

Acknowledgement

At the onset, I would like to express my sincere gratitude to my supervisor, Prof. S. Talukdar for his constant guidance and valuable advices throughout my research work. His continuous encouragement, suggestions and effusive co-operation have been a great driving force for me while carrying out my work. I will remain grateful to him throughout my life for the knowledge he imparted from his vast experience in the field of research.

Besides my supervisor, I would like to thank the rest of my Doctoral Committee members: Prof. K. D. Singh, Dr. Karuna Kalita and Dr. A. Shelke for their encouragement and valuable suggestions.

I also thank Head of Civil Engineering Department for providing financial grant for purchasing materials for conducting laboratory experiments. I am also thankful to Counto Microfine Products Private Limited, India and Fosroc Chemicals India Private Limited, India for providing materials free of cost for the laboratory tests. I am also thankful to Prof. P.K. Khaund, JEC for his help and support during the period of thesis writing.

I am grateful to Central Library, IIT Guwahati for offering such a vast resource of research material and making it easily accessible.

I also acknowledge the good times shared with Dr. Palash Dey, Abu Saeed, Koushik, Baharul, Pranjal, Pallab, Lavish, Arnab, Nitu, Mitu and friends at IIT Guwahati. They have been a source of great help and co-operation at times of need. Last but not the least, I extend my gratefulness to my parents, Ms. Elina Amin Majumder, my sister and my brother-in-law for their support, encouragement, inspiration and all of their sacrifices during my research period.

September, 2018 Sulaem Musaddiq Laskar

Abstract

Geopolymer is an emerging material and has found profound research attention in construction industry as sustainable supplementary cementitious material. Geopolymer is prepared using industrial by-products such as flyash, ground granulated blast furnace slag, silica fume, etc. It is a chain of mineral molecules formed by the process of an exothermic reaction known as geopolymerisation. Geopolymerisation binds together the naturally occurring silica and alumina and/or silica and calcium oxide to form an amorphous material with high structural strength. The process is activated with the help of an alkali component, termed as alkali activator which is a compound from the element of first group in the periodic table. As geopolymer is prepared employing by-products of various industrial processes, its use in mortar and concrete can reduce carbon dioxide accumulation in the environment which is otherwise contributed during manufacture of Portland cement in cement factories. It is reported that manufacturing of Portland cement results in release of large amount of carbon dioxide which accounts to 7 % of the green-house gas emission annually. It is an established fact that, 1 ton of Portland cement preparation releases about 1 ton of carbon dioxide as waste.

Many studies have been performed to investigate the fresh and hardened state properties of flyash, ground granulated blast furnace slag, silica fume , metakaolin based geopolymer as binder in mortar and concrete including the durability studies. Geopolymer being able to offer early strength, needs further study for its application in repair and strengthening of reinforced concrete structures. However, application of geopolymer as a concrete repairing agent is relatively new and till date scanty number of literatures are only available.

The present research study deals with the development of ultra-fine ground granulated blast furnace slag based geopolymer mortar and concrete for using them as repairing and strengthening agent for concrete structures.

The geopolymer mortar was developed using ultra-fine ground granulated blast furnace slag where flyash and superplasticizers were added as admixtures. The alkali activator concentration and time of addition of superplasticizers were also varied to observe the effect. Total 32 numbers of geopolymer mortar mixes were prepared for conducting the laboratory

tests for evaluation of the fresh and hardened state properties. The microstructure of geopolymer matrix was studied with the help of field emission scanning electron microscope to interpret the change in the properties. The ultra-fine ground granulated blast furnace slag based geopolymer mortar showed excellent strength gain property when admixtures were added in lower quantity. At 1 day, ultra-fine ground granulated blast furnace slag based geopolymer mortar was found to develop about 60 % of the strength at 28 days. High amount of admixtures led to positive influence on the fresh state properties, but the strength at early and later age was reduced. Alkali activator concentration also significantly influenced the fresh and hardened state properties. It was found that there is an optimum alkali concentration which results in geopolymer with satisfactory setting time, workability and strength gain property. The results from the tests indicated positive sign of geopolymer mortar to be used for repairing concrete structures.

Having found the properties of geopolymer mortar developed in the present study, the research was then directed to develop ultra-fine ground granulated blast furnace slag based geopolymer concrete. Fresh and hardened state tests were conducted on total 21 numbers of ultra-fine ground granulated blast furnace slag based geopolymer concrete. Bond strength of geopolymer concrete with reinforcement bars and also with old concrete was also determined by conducting pull out and slant shear tests. Special arrangements in the specimen moulds were fabricated for developing the samples for conducting pull out and slant shear tests on geopolymer concrete. The bond study was performed to examine the effectiveness of geopolymer as repairing and strengthening material in damaged concrete structures. Ultra-fine ground granulated blast furnace slag based geopolymer concrete possess strong potential for using as jacketing agent as it can develop high early strength. Addition of admixtures such as flyash and superplasticizers showed positive effect in influencing the workability, however it led to decrease in the strength including the bond strength. The bond strength of geopolymer concrete improved on addition of the admixtures at lower quantity and at optimum alkali concentration.

In the final phase of the thesis, the ‘geopolymer’ developed was intended to be used in repairing and strengthening of reinforced concrete structures. The ultra-fine ground granulated blast furnace slag based geopolymer mortar was engaged for repairing 7 numbers of reinforced concrete beams which were damaged at 2 levels i.e. partially damaged and fully damaged level. Results from experimental investigation focus on the study of the behaviour of the repaired reinforced concrete beams under static flexural load monotonically applied using actuator. Due to the early strength gain property of geopolymer, the repaired beams

could attain appreciable load when subjected to static flexural load. The ductility of the geopolymer repaired beams also enhanced compared to the controlled beams. The partially damaged and repaired beams showed superior behaviour than the fully damaged and repaired beams. Remarkable strength gain upto 110 % was achieved by adopting the present technique of repairing.

For examining the potential of geopolymer in strengthening of damaged concrete structures, jacketing technique was adopted where 9 numbers of reinforced concrete beams were jacketed using ultra-fine ground granulated blast furnace slag based geopolymer concrete. The reinforced concrete beams were either fully damaged, partially damaged or undamaged. The jacketed beams were also subjected to static flexural load monotonically applied using actuator. Geopolymer concrete jacketed beams exhibited superior performance than Portland cement concrete jacketed beams as the load carrying capacity of geopolymer concrete jacketed beams enhanced by higher amounts than the increase in load capacity of Portland cement concrete jacketed beams. Higher increase in ductility was also observed in the geopolymer concrete jacketed beams. The results from tests on the jacketed beams damaged at various levels indicated that strengthening of the damaged structural members at early period with geopolymer concrete can effectively restore the structure to its functional use at the earliest possible time. The experimental study reveals that using geopolymer concrete jacket, the strength of damaged beam can be restored even exceeding the strength of original beam by approximately 3 times by providing thin layer of jacket. This is mainly attributed to the improved bond strength between old concrete and geopolymer concrete which could not be observed in the jacketing using Portland cement concrete.

Contents

List of Tables

List of Figures

Nomenclature

An overview of the most important symbols and abbreviations used in the present thesis:

Symbols

μ	Mean
ρ	Coefficient of variation
σ	Standard deviation
R^2	Coefficient of determination
A_{sc}	Area of compression steel
A_{st}	Area of tension steel
A_{sv}	Area of steel as shear reinforcement
b	Breadth of the beam specimen
BS_r	Bond strength with rebar
BS_c	Bond strength with old PCC substrate
C_{uc}	Resultant compressive force in concrete
C_{us}	Resultant compressive force in the compressive steel
D	Overall depth of the beam specimen
d	Effective depth
d_c	Effective cover
E_s	Modulus of elasticity of steel

ϵ_{s1}	Strain in compression steel
f_{ck}	Compressive strength of concrete
f_{ck}'	Target strength of concrete at 28 days
f_y	Yield stress of steel
f_y'	$f_y/0.87$
Fr	loads carried by the specimen at failure in pull-out
Fc	loads carried by the specimen at failure in slant shear tests
L	Span of the beam speciemen
M_u	Moment carrying capacity of beam speciemen
p_t	Percentage of tensile reinforcement
S_v	Spacing of the stirrups
T_u	Resultant tensile force in tension steel
W_u	Ultimate load carrying capacity of beam speciemen
V_u	Shear force
V_c	Shear resistance of concrete
V_{us}	Shear resistance of steel
x	Neutral axis depth
τ_c	Shear strength of concrete

Abbreviations

a/b	Alkali activator solution/total binding agent ratio
ACV	Aggregate crushing value
ASTM	American Society for Testing and Materials
BFRP	Basalt fiber-reinforced polymer

BFS	Blast furnace slag
CASH	Calcium-alumino-silicate-hydrate
CFW	Carbon fibre waste
CFRP	Carbon fibre reinforced polymer
CSF	Condensed silica fume
CSH	Calcium silicate hydrate
CTM	Compressive strength testing machine
DR	Ductility ratio
FA	Flyash
FESEM	Field emission scanning electron microscope
FI	Flow index
GBP	Ground basaltic pumic
GGBS	Ground granulated blast furnace slag
GGBOS	Ground granulated basic oxygen furnace slag
GGFAC	Granulated blast furnace slag flyash concrete
GPC	Geopolymer concrete
GPM	Geopolymer mortar
GPP	Geopolymer paste
GUSMRC	Green-USM-reinforced concrete
H/C	Heat-cool
HFAC	High volume FA high strength concrete
ITZ	Interfacial transition zone
LS	Lignosulfonate
LVDT	Linear variable differential transformer
MK	Metakaolin

OPC	Ordinary Portland cement
PC	Portland cement
PCC	Portland cement concrete
PCM	Portland cement mortar
PCP	Portland cement paste
PE	Polycarboxylate ether
PMM	Polymer modified mortar
PVC	Poly vinyl chloride
RC	Reinforced concrete
RH	Relative humidity
RHA	Rice husk ash
RM	Repair materials
SEM	Scanning electron microscope
SER	Strength enhancement ratio
SF	Silica fume
SN	Sulphonated naphthalene
SP	Superplasticizer
UFA	Ultrafine flyash
UFS	Ultrafine slag
UGGBS	Ultra-fine ground granulated blast furnace slag
UTM	Universal testing machine
w/c	Water/cement
w/s	Water/solid
XRF	X-ray fluorescence

Chapter 1

Introduction

1.1 Overview

Numerous technologies including high-tech machinery, selection of materials, test equipment, and other sciences have assisted in the advancement of Civil Engineering in the modern world, However, the most prominent contributor to be considered in this field are the "newer materials". The majority of Civil Engineering structures are massive and require utilization of concrete, brick and stone masonry. Due to constraints in space and time; and exposure conditions, at the present age there is a large demand of high strength and durable materials. Research in the development of high strength and durable materials is in full swing in various parts of the world. Most of the outcomes of the research in construction materials are already delivered to the society, however, cost effectiveness and sustainability of the materials are of most concern that requires further attention.

Portland cement (PC) based concrete is one of the most widely used building materials in construction industry today. Portland cement concrete (PCC) is the second most consumed material by the human society, with nearly one ton of the material used annually by each person on the planet [1]. Some of the reasons of popularity of PCC are simplicity in its preparation,

availability and low cost of its ingredients; and satisfactory strength and durability performance when prepared as per the standard guidelines.

With the changing economic condition and rapid urbanization of large number of countries of the world, consumption of cement for construction of infrastructures has risen. The demand of cement has enhanced with time. About 1 m^3 of concrete per year per person is required to meet the infrastructure development demand in the world. The demand of cement in construction industry in India has taken pace since the beginning of twentieth century. India ranks second in the world in producing cement. The cement production in India from 2012 to 2017 was on average of about 275 million metric tons [2]. Due to improvement in infrastructure, investment cycle and overall economy, cement consumption in India has increased from 166 million metric tons in the year 2011 to 270 million metric tons in 2017. The demand for cement is likely to grow by nearly 4.5 % during the year 2019 [3]. Fig. 1.1 and 1.2 present the scenario of production of cement in selected countries from 2012 to 2017 and cement consumption in India from 2012 to 2017 respectively [4, 5]. In the succeeding years, it is expected that demand of concrete and hence cement will increase as a result of improvement of human life. Global cement production is expected to increase from 3.27 billion metric tons in 2010 to 4.83 billion metric tons in 2030 [6].

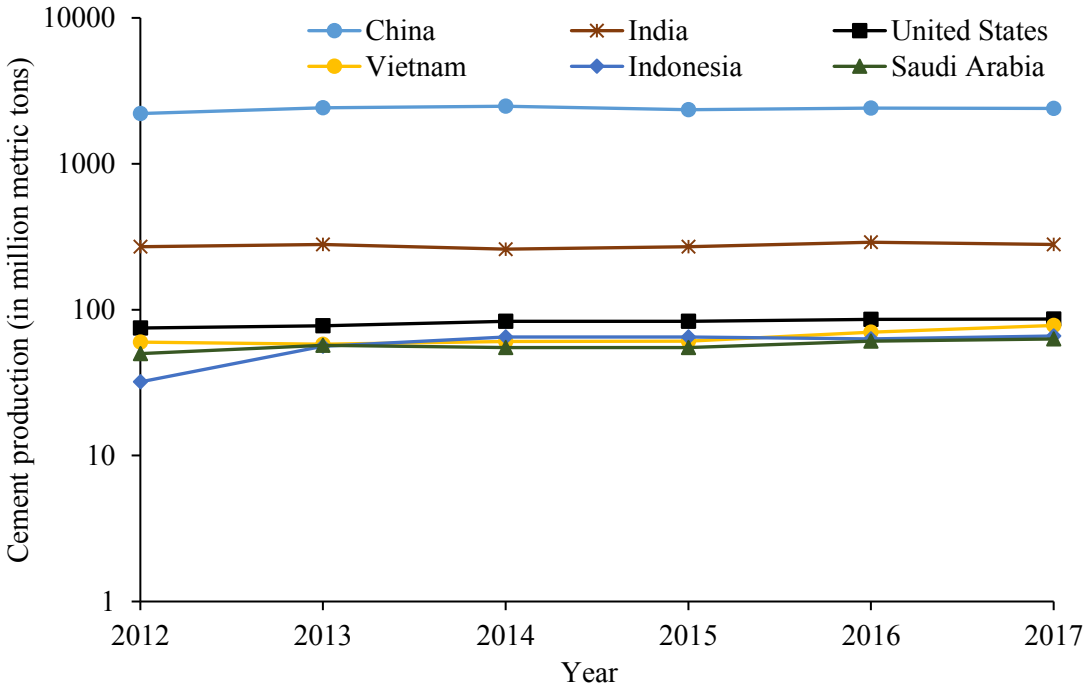

Figure 1.1: Cement production in selected countries from 2012 to 2017 (*Statista, the statistics portal, www.statista.com* [4]).

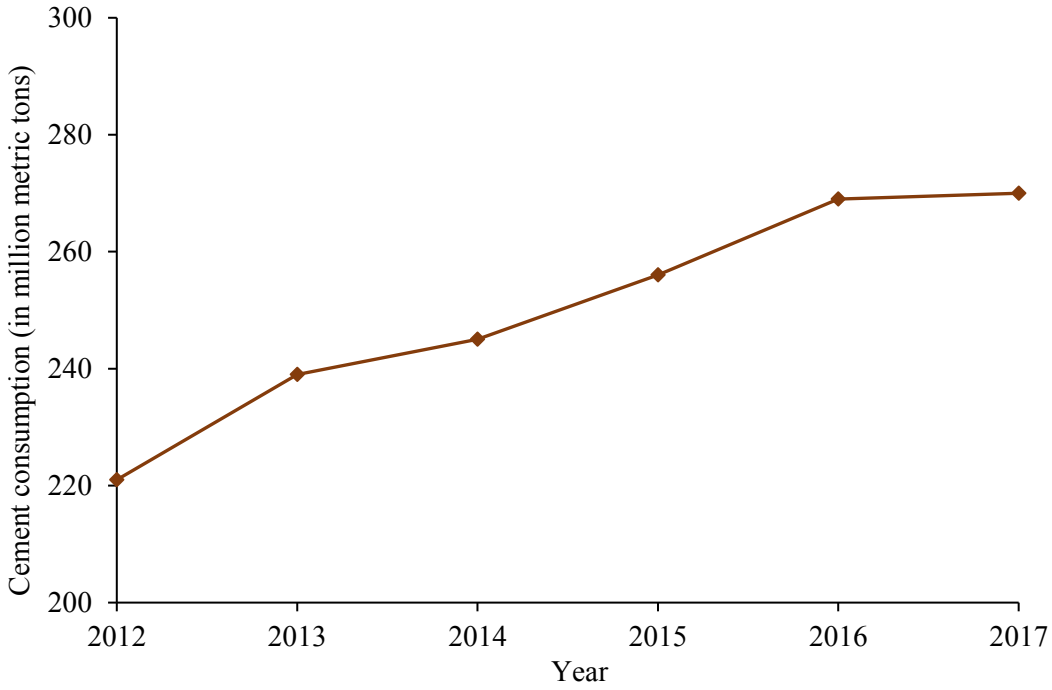

Figure 1.2: Cement consumption in India, 2012-17
(*Statista, the statistics portal, www.statista.com* [5]).

Portland cement production necessarily involves breakdown of calcium carbonate ($CaCO_3$) into calcium oxide (CaO) and carbon dioxide (CO_2). The process of manufacturing of PC not only involves considerable amount of energy but also produces substantial amount of CO_2 followed by other greenhouse gases [7]. Around 13,500 tons of CO_2 is released into the Earth's atmosphere every year due to manufacturing of PC. This accounts to 7 % of the green-house gas emission annually [8]. It is worthy to note that manufacture of 1 ton of PC releases about 1 ton of CO_2 as waste, which is a serious threat to the environment.

In recent years, awareness on the quantity and diversity of hazardous solid waste generation and its impact on human health and natural environment has enhanced. The concern about the consequences of waste generation and disposal has led to investigation associated with various utilization methods. Safe and effective disposal of effluent, sludge and by-products from industrial processes is one of the greatest problems faced by industries. Most of the wastes are disposed in landfills at suitable sites. However, landfilling is not a desirable solution to waste disposal because it is not only costly, but also increases load of toxic metals in the landfill that potentially increases the threat to ground water contamination. Furthermore, increasing economic factors has also dictated the industry to look forward for recycling and reuse of waste materials as a better alternate to landfilling and discarding. Thus, in order to

keep pace with the rapid industrialization necessity has been felt towards development of materials and processes causing minimum pollution in the environment. The use of waste materials or by-products as an alternate to existing construction materials that cause environmental hazard can fulfill the objective of development of waste utilization technique.

The restriction imposed by the ecological constraints and environmental regulations, followed by the demand for sustainable technology in construction industry has compelled the researchers to look for use of alternative cementitious materials using industrial by-products such as fly ash (FA), ground granulated blast furnace slag (GGBS), silica fume (SF), rice husk ash (RHA), etc. in concrete. These materials can be used either as partial or full replacement of PC in mortar and concrete. When PC cement is partially replaced by such by-products, the concrete is known blended cement concrete. On the other hand, the concrete in which PC is fully replaced by the by-products possessing pozzolanic property is known as geopolymer concrete and the corresponding mortar is geopolymer mortar. Some researchers also use the term alkali activated concrete to indicate geopolymer concrete.

As geopolymer is prepared using by-product materials, its use in concrete can reduce the CO_2 accumulation in the environment which is otherwise contributed during the manufacturing of PC used in PCC. Moreover, the utilization of these by-products greatly cater the need of recycle and reuse of waste materials avoiding the trouble of their disposal in the form of landfills which leads to soil toxication and ground water contamination. Hence, the use of these by-products in concrete preparation eradicates the problem of disposal and eventually minimize the environmental impact caused by the industrial processes.

1.2 Geopolymer

Geopolymer is a chain of mineral molecules formed by the process of an exothermic reaction known as geopolymerisation. Geopolymer was first patented by J. Davidovits, a French scientist in 1982 [9]. He brought to light the fact that geopolymer has been existing since 5000 years back. The Pyramids in Egypt and the Great Wall in China were constructed using geopolymer technology [10].

Geopolymerisation process binds together the naturally occurring silica (SiO_2) and alumina (Al_2O_3) which are dissolvable in alkaline solution to form an amorphous material with high structural strength. The process is activated with the help of an alkali component, which is a compound from the element of first group in the periodic table. Under the alkaline

conditions, when reactive aluminosilicates are rapidly dissolved and free $[SiO_4]^-$ and $[AlO_4]^-$ tetrahedral units are released in solution, polymerization occurs. The tetrahedral units are alternately linked to each other by sharing oxygen atoms, forming the polymeric Si-O-Al-O bonds, Eq. (1). However, in case of GGBS based geopolymer, the end product is a linear chain of calcium-silicate hydrate (C-S-H) and calcium-alumino-silicate-hydrate (C-A-S-H).

$$(Si_2O_5.Al_2O_2)_n + H_2O + OH^- \longrightarrow (\text{-Si-O-Al-O-})_n + 4H_2O$$

Geopolymer consists of silicon (Si) and aluminum (Al) tetrahedrally interlinked alternately by sharing all the oxygen (O) atoms, Fig. 1.3. It is constituted of repeated units of sialate monomer (–Si–O–Al–O–). Geopolymer is characterized by amorphous to semi-crystalline three dimensional alumino-silicate structures. These three dimensional structures are of poly-sialate type (Si–O–Al–O–), poly-sialate-siloxo type (Si–O–Al–O–Si–O–) and poly-sialate-disiloxo) type (Si–O–Al–O–Si–O–Si–O) [11]. The empirical formula for these mineral polymers is given by:

$$M_n[\text{-}(Si\text{-}O_2)_z\text{-}Al\text{-}O]_n \cdot wH_2O$$

where M is the alkaline element, *z* is 1, 2 or 3 for poly(sialate), poly(sialate-siloxo) and poly(sialate-disiloxo) respectively and *n* is the degree of polymerization. Hardening and strength gain in geopolymers occur due to the formation of these polymeric Si-O-Al-O bonds. A conceptual model of geopolymerization is provided in Fig. 1.4 which consists of varios steps such as dissolution; speciation equilibrium; gelation; reorganization; and polymerization and hardening [12].

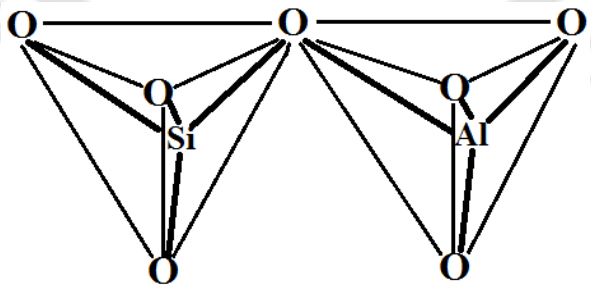

Figure 1.3: Molecular structure of geopolymer.

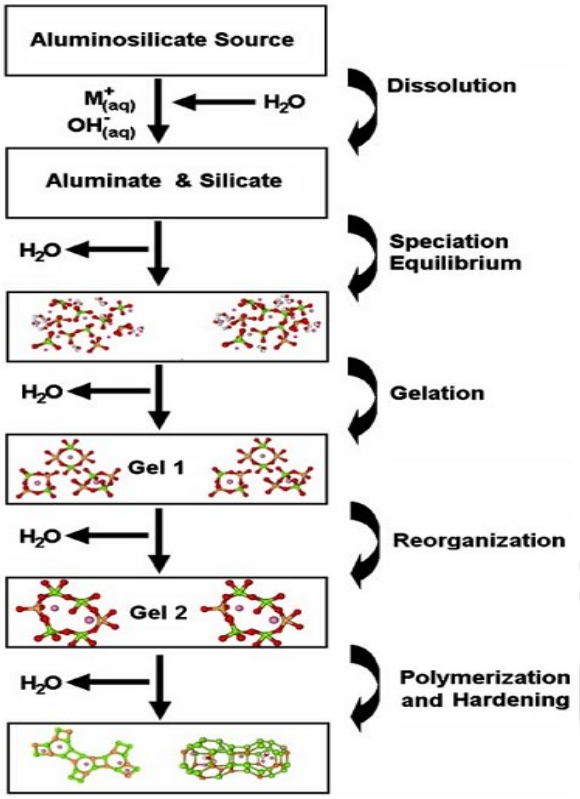

Figure 1.4: Flow diagram of geopolymerisation process (*Duxson et al.* [12]).

Geopolymer mortar (GPM) and concrete (GPC) differ significantly from PC based mortar and concrete, as it uses totally different reaction pathway in order to attain structural integrity. PCC depends on the presence of C-S-H for matrix formation and strength whereas GPC utilizes raw materials with low calcium and high SiO_2 and Al_2O_3 content such as FA, metakaolin (MK), etc or low Al_2O_3 and high SiO_2 and calcium oxide (CaO) content such as GGBS. When these are activated with alkali compounds in solution form such as sodium hydroxide (NaOH), sodium silicate (Na_2SiO_3), potassium silicate (K_2SiO_3) and potassium hydroxide (KOH) form the alumino-silicate compound. Some secondary products are also formed in geopolymerisation process which also contribute to strength gain and durability. In many cases, the secondary products improve the properties of GPM and GPC in fresh and hardened state apart from improving its durability. Geopolymer as binder shows good bonding properties, better abrasion and impact resistance and is less susceptible to chemical attack.

Geopolymer is prepared by by-product materials, its use in concrete can reduce CO_2 accumulation in the environment which is otherwise contributed during manufacture of PC used in PCC. Moreover, the utilization of these by-products greatly cater the need of recycle and reuse of waste materials avoiding the trouble of their disposal in landfills at suitable sites

which leads to soil toxication and ground water contamination. Hence, the use of these by-products in concrete preparation eradicates the problem of disposal and eventually minimize the environmental impact caused by the industrial processes.

1.3 Sources of Geopolymer

Geopolymer can be prepared using industrial by-products. Apart from that, it can also be prepared using metakaolin and volcanic ash. The process of preparation is similar in all the cases though the source material may be different. The physical and chemical properties of the source materials vary and hence the end products of the geopolymerisation process involved also vary. Following are few materials used for preparation of geopolymer mortar and concrete:-

i. Blast furnace slag
ii. Flyash
iii. Silica fume
iv. Rice husk ash
v. Metakaolin

1.3.1 Blast furnace slag

Blast Furnace Slag (BFS) is a by-product obtained in iron and steel producing industries. In the process of production of iron and steel, the iron-ore, coke and a flux (either limestone or dolomite) are melted together in a blast furnace. On completion of the metallurgical smelting process, the lime in the flux chemically combines with the aluminates and silicates of the iron-ore and coke ash to form a non-metallic product, termed as blast furnace slag. It is a nonmetallic co-product produced in this process. The molten slag comprises about 20 % by mass of iron production. Silicates, aluminosilicates and calcium-alumina-silicates are the primary constituents of BFS. Fig. 1.5 presents a schematic view of which shows the production of iron and BFS.

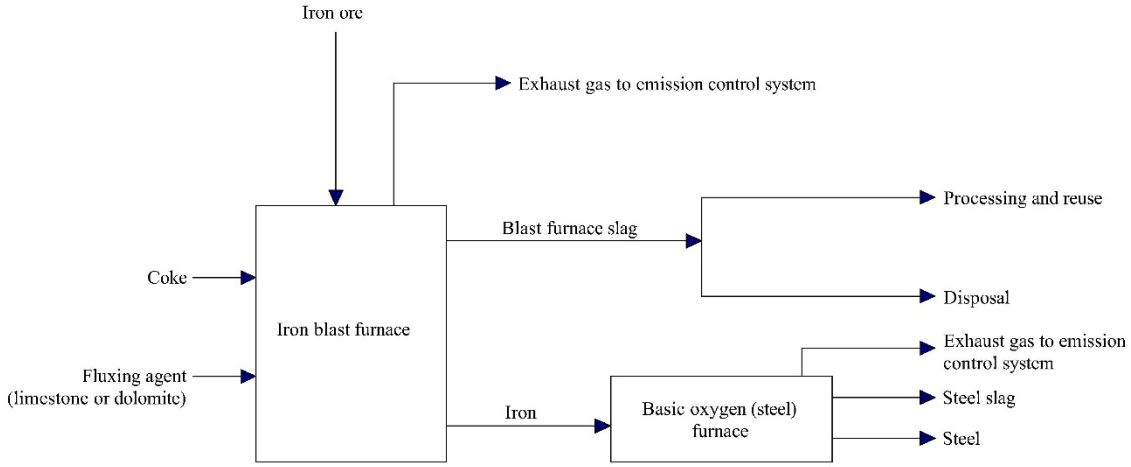

Figure 1.5: A schematic view of production of iron and BFS.

The chemical composition of BFS varies depending upon the composition of the raw materials involved in the process of production of iron. The main components of blast furnace slag are CaO (30 – 50 %), SiO_2 (28 – 38 %), Al_2O_3 (8 – 24 %), and MgO (1 – 18 %). Increasing the CaO content of the slag results in raised slag basicity and an increase in its compressive strength.

During the production process, the slag floats on top of the iron in the blast furnace and is drawn out for separation. Slow cooling of the molten slag results in an unreactive crystalline material consisting of an assemblage of Ca-Al-Mg silicates. However, when the molten slag is rapidly cooled or quenched below 800 °C, crystallization of merwinite and melilite is prevented. Thus, a good slag reactivity is obtained. The cooling and granulation/fragmentation process is carried out by subjecting the slag to jet streams of water or air under pressure.

The process of cooling and hardening of BFS from its molten state is carried out in several ways to form several types of BFS. The various type of BFS are:-

i. Ground granulated blast furnace slag (GGBS): When the molten slag is cooled and solidified to a glassy state by rapid water quenching. In this process, crystallization does not occur and sand size fragments are formed. These are known as GGBS. The physical structure and gradation of GGBS depend on the chemical composition of the slag, its temperature at the time of water quenching and the method of production. When crushed or milled to very fine cement-sized particles, GGBS show cementitious properties.

ii. Air-cooled blast furnace slag: This type of BFS is formed when the liquid slag is poured into beds and slowly cooled under ambient conditions. A crystalline structure is formed in this process and a hard lump slag is produced, which is subsequently crushed and screened.

iii. Expanded or foamed blast furnace slag: The cellular nature of the slag can be increased by accelerated cooling and solidifying molten slag by adding controlled quantities of water, air or steam. The resultant slag is a lightweight expanded or foamed product. This type of blast furnace slag is known as expanded or foamed blast furnace slag. It is differs from air-cooled blast furnace slag by its relatively high porosity and low bulk density.

iv. Pelletized blast furnace slag: This type of slag is produced when molten slag is cooled and solidified with water and air quenched in a spinning drum. Slag pellets are formed in this process instead of solid slag mass. The pellets can be made more crystalline by controlling the process of its formation. The crystalline pellets can be used as aggregate. On the other hand, more vitrified (glassy) pellets can also be formed which results in slag with cementitious nature. More rapid quenching results in greater vitrification and less crystallization.

The production of iron ore was at 192.08 million tons in the year 2016-17. India is currently the 3rd largest producer of pig iron in the world. The production of pig iron was 9.39 million tons in the year 2016-17. Typically, for ore feed containing 60 to 65 % iron, BFS production ranges from about 300 to 540 kg per ton of pig iron produced [13].

1.3.2 Flyash

The residue that results from the combustion of pulverized coal and is transported from the combustion chamber by exhaust gases and collected by electrostatic precipitators known as flyash (FA). FA consists of particles which are generally spherical, typically ranging in size between 10 and 100 micron. These spherical shape contributes towards improving the fluidity and reducing the viscosity within the mix consisting of flyash and concrete preparing materials. Fineness is one of the important property and contributes to the pozzolanic reactivity of FA.

FA is produced in the coal fired electric and steam generating plants. Usually, coal is pulverized and blown with air into the boiler's combustion chamber where it is ignited immediately. This generates heat and produces a molten mineral residue. Boiler tubes extract

heat from the boiler and cool the flue gas. This causes the molten mineral residue to harden and form ash. Coarse ash particles fall to the bottom of the combustion chamber. They are referred to as bottom ash. The lighter fine ash particles remain suspended in the flue gas. These are termed as FA. It is removed by particulate emission control devices, such as electrostatic precipitators or filter fabric baghouses before the flue gas exhausts.

FA primarily consists of silicon dioxide (SiO_2), aluminium oxide (Al_2O_3) and calcium oxide (CaO). Very tiny amount of magnesium, potassium, sodium, titanium, and sulfur also remain in it. FA is classified as either Class C or Class F based on its chemical composition [14].

Class C FA is produced from younger lignite or sub-bituminous coals. Class C FA has the capacity of hardening and gaining strength when mixed with water. It consist primarily of calcium alumino-sulfate, quartz, tricalcium aluminate and calcium oxide (CaO). Due to presence of more than 20 % CaO, it is also known as high calcium FA. On the other hand, bituminous and anthracite coals are the sources of Class F FA. The primary constituent of Class F FA are alumino-silicate glass, quartz, mullite and magnetite. It consists of less than 10 % CaO and hence it is also known as low calcium FA. When it combines with a chemical activator such as alkali compound, it exhibits binding capacity.

In India, coal production was 662.79 million ton in 2016-17. This production amount was 3.69 % higher compared to that of the previous year. Around 82 % of coal produced was used in the Power Sector. In the year 2015, India ranked 3rd in the world in coal production [13].

1.3.3 Silica fume

Silica fume (SF) is obtained as byproduct from the process of production of silicon metal or ferrosilicon alloys. It is produced in the carbo-thermic reduction of high-purity quartz with carbonaceous materials like coal, coke, wood-chips, in electric arc furnaces. It is amorphous in nature. The silica fume is formed as an ultrafine powder consisting of spherical particles of size of less than 1 μm in diameter with an average particle size of about 0.15 μm diameter. It is also termed as micro silica. Due to the fine particles, large surface area and high SiO_2 content, silica fume possess high pozzolanic characteristics.

1.3.4 Rice husk ash

Rice husk is an agricultural waste generated in the countries which produce rice. It is a hard protective covering of rice grains. About 22 % of the weight of paddy is received as husk. The husk is used as fuel for combustion in many industries, especially in rice mills. Combustion of the husk, produces rice husk ash (RHA). It consists of 85 - 90 % amorphous silica. The particles of RHA are usually finer than Portland cement particles when the rice husk is burnt completely. Since, it is a potential source of amorphous reactive silica, it is used for preparation of geopolymer by allowing it to react with alkali compounds. In India, around 20 million tons of rice husk ash is produced per year [15].

1.3.5 Metakaolin

Metakaolin (MK) is obtained by heating china clay (mineral kaolin) to a temperature between 600 and 800 ºC. It is rather an industry manufactured product than a byproduct from industrial processes. Formation of metakaolin from kaolin is an endothermic process which involves large amount of energy to remove the chemically bonded hydroxyl ions in kaolin. Due to the pozzolanic nature of metakaolin, it is also used to prepare geopolymer.

1.4 Defects in Reinforced Concrete Structural Members

Concrete cracks due to its ageing, corrosion of steel, overloading, earthquake and other environmental effects, accidental impacts on the structures, etc. and leads to damage of reinforced concrete (RC) structures. Cracks that are related to plastic concrete are plastic shrinkage cracking and settlement cracking while cracks in hardened concrete are occur basically due to drying shrinkage, thermal stresses, chemical reaction, weathering, corrosion of reinforcement, poor construction practices, construction overloads and errors in design and detailing. The cracks that are induced in concrete provide pathway for intrusion of moisture and harmful ions in it leading to further enlargement of the cracks that ultimately causes weakness and lack of durability of the structural members. Added to this, presence of cracks in the structural members also affects the overall appearance of the structure. Due to the application of repeated loads, a crack may propagate until it reaches a point where fracture occurs and failure results. The presence of a crack causes the strength of the structure to reduce a lower amount than the original strength it is designed for. The micro-cracks present in the concrete propagate due to the monotonic or cyclic loading. This leads to failure in the concrete

either by crushing, splitting or bending.

Repair of deteriorated concrete structural members is essential to assure their safety and serviceability. By virtue of repairing, the structural members can also be utilize satisfactorily for their intended service life. Repairing of concrete structural members is important because structural degradations and durability of reinforced concrete structures are accelerated by cracks formation. Repairing improves the function and performance of a structure, restores or increases its strength and stiffness, improves the appearance of the damaged concrete surface, provides water tightness, prevents ingress of moisture, oxygen, chloride, carbon dioxide etc. to the reinforcing steel and improves its durability. Effective repairing of cracks depends on knowing the causes and selecting the appropriate repairing procedures.

Repairing is also followed by retrofitting of a damaged structural member. Retrofitting is defined as the process of enhancement of load carrying capacity of a structural member. The structural member on being retrofitted may be able to carry load which is multiple times higher the its original load carrying capacity. Some of the situations in which retrofitting is adopted include upgradation of the capacity of structure to resist the underestimated loads and design flaws, to eliminate premature failure due to inadequate detailing, seismic retrofit to satisfy the standard/codal requirement, restoration of the load carrying capacity of corrosion affected or cracked structures, etc.

Among all the crack repairing techniques, the epoxy injection method is conventionally utilized because of its stable structural performance. The epoxy adhesives represent a wide range of chemical polymers with diverse chemical, mechanical and thermal properties. Some of the favourable characteristics of epoxy, which make them desirable for use with concrete are excellent adhesion and bond to surfaces of nearly all construction materials, the system of a resin and hardener constitutes a thermosetting plastic, which when mixed together changes from liquid to a solid state and cannot melt back thereafter. Thus, the use of epoxy increases tensile and compressive strengths across a crack, if further cracking is not anticipated. However, epoxy is very costly, its application requires skilled labour and also, the use of epoxy alone may not be sufficient sometimes to restore the damage in a structure and require other repair methods in addition such as additional reinforcement or using post-tensioning.

1.5 Historical Background

1.5.1 Geopolymer and geopolymeric systems

Long since, a number of studies were performed on the strength, durability and flow properties of geopolymer mortar and concrete to find the feasibility of its practical application.

Davidovits [16] in one of his study reports on geopolymer described the synthesis and hardening mechanism of geopolymers. Terminologies attributed to geopolymer have been presented in this report. Here, geopolymers are defined as amorphous to semi crystalline three dimensional silico-aluminate-structures. Application of geopolymer in different industries were brought forward highlighting the potential of use of geopolymer as binder in concrete. Compressive strength test results of concretes prepared from blended geopolymer Portland cements and blended geopolymers confirmed that such type of concrete can attain satisfactory strength and also have the capacity of retaining strengths when exposed to high temperature of the order of 600 - 1100 $^{\circ}$C.

1.5.1.1 Fresh and hardened state properties of geopolymer

Works to find the effect of use of various additives in modifying the properties of ground granulated blast furnace slag (GGBS) based geopolymer mortar (GPM) were undertaken by Douglas and Brandstetr [17]. Additives such as Portland cement (PC), silica fume (SF), flyash (FA), calcium hydroxide ($Ca(OH)_2$), lignosulfonate (LS), sodium sulphate (Na_2SO_4) and sulfonated naphthalene-based superplasticizer (SN) were added in various proportions in GPM. GPM was prepared using GGBS from three different sources and activated with sodium silicate (Na_2SiO_3) of two varied silicate modulus. Mortar samples were prepared in accordance with procedure mentioned in ASTM C 109 [18] and moist cured until the age of testing. It was observed that addition of SF and $Ca(OH)_2$ results in mortar samples with higher 7 and 28 days compressive strength compared to the controlled ones prepared with PC. GGBS from all the three sources outperformed PC in developing 28 days strength. However, rate of strength gain was comparatively slow, implying that mortars from such material will always show satisfactory performance in terms of strength at later ages. Use of small amount of PC (2 – 5 %) increased the rate of strength gain. Na_2SO_4 addition further enhanced the rate of strength gain of GPM. Na_2SO_4 added GPM samples attained strength higher than controlled samples even at 1 day. No significant change in GPM property was observed due to addition of FA. On the

other hand, use of lignosulphonate for improving GPM consistency was not beneficial. Instead it decreased 1 day strength and increased 7 and 28 days strength. Workability of GPM could be improved only by adding SN but at the cost of its compressive strength compared to controlled samples.

Douglas et al. [19] preformed laboratory experiments to arrive at conclusions related to workability and strength characteristics of GGBS based GPC. Five GPC mixes were prepared by varying water-to-binder (w/b) ratios and silicate modulus of Na_2SiO_3 which is used as activator. From the results it was concluded that GGBS can be used to prepare concrete with satisfactory workability and strength. Significant strength gain occurred at 7 days compared to 14, 28 and 91 days for all the five concrete mixes. Lime slurry and air entrainer which were added in an attempt to act as retarder and to improve workability respectively, performed satisfactorily.

To understand the effect of ultrafine materials such as ultrafine FA (UFA), ultrafine slag (UFS) and condensed SF (CSF) on GGBS based GPC laboratory investigation was performed by Collins and Sanjayan [20]. Concrete specimens were prepared by 10 % replacement of slag binder by UFA, UFS and CSF and tested for workability and strength. Results were compared with GGBS based GPC without any ultrafine material and PCC of similar mix proportions. Slump retention was observed for each concrete specimen by performing slump test at the time of mixing and at 30, 60, 90 and 120 minutes after mixing. GGBS based GPC exhibited better workability and suffered lesser slump loss then PCC. CSF and UFS addition reduced workability of GGBS based GPC. However, in terms of slump loss, UFS based GPC specimens showed minimal slump loss over period of 120 minutes. UFA based GPC showed best workability among all. From the strength test results it was found that GPC with and without the ultrafine additives outperformed PCC. CSF addition in GPC though reduced workability, it increased the strength and attained highest strength among all.

Alonso and Palomo [21] studied the effect of metakaolin (MK)/calcium hydroxide ($Ca(OH)_2$) ratio, alkaline solution concentration and reaction temperature on reaction of metakaolin based geopolymer in strong alkaline medium and presence of $Ca(OH)_2$. $Ca(OH)_2$ is added to increase the calcium oxide (CaO) percentage in the geopolymer mix. $Ca(OH)_2$ was added to metakaolin in 30 and 50 % of total mix content. Each mix was activated with NaOH solutions of 10, 12, 15 and 18 M concentrations. Activation process was carried out at 35, 45 and 65 $^{\circ}$C. Results indicated involvement of three step reaction in the geopolymerisation

process viz: dissolution, induction period and massive precipitation for the formation of final product. It was also suggested that alkaline solution concentration higher than 10 M delays formation of alkaline polymer and temperature increase accelerates the alkaline activation process and hence increases strength gain. This fact is indicated in the Fig. 1.6. Mechanical strength of geopolymer with higher metakaolin proportion was found to be higher. This indicated that due to higher amount of available reactants, there was an increase of reaction intensity and hence larger amount of end products were available at the end of the geopolymerisation process.

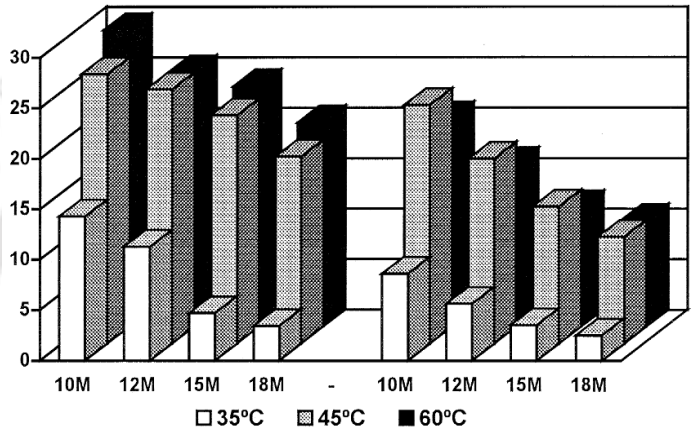

Figure 1.6: Flexural strength of specimens cured during 24 hours (*Alonso and Palomo* [21]).

Investigation on waterglass (Na_2SiO_3) based alkali activated slag mortars was performed by Brough and Atkinson [22] for determination of strength, hydration and the microstructure. An attempt was also made to develop suitable retarder and workable concretes. The mortars exhibited early strength development and attained high strength in the order of 80 MPa (cured at room temperature, 20 ºC). The slag specimens were found to be glassy with insignificant amount of crystalline hydration products. Setting time varied widely between different mixes. Three heat evolution peaks were presumed from the Calorimetry test, namely, wetting of slag, gelation of Na_2SiO_3 and bulk reaction of slag. At 5 ºC hydration process was very slow while that at 40 ºC was faster resulting in accelerated strength development. Steam cured samples at 80 ºC showed even better strength development. When potassium hydroxide (KOH) was used as activator, the mortar samples exhibited better 1 day strength compared to Na_2SiO_3 activated mortars. However, at later ages, the strength gain rate reduced and hence lower strengths were exhibited by KOH activated mortars, Fig. 1.7. Microstructural analysis of the slag systems were also carried out. The systems were subjected to SEM, EDX, XRD for

obtaining definite conclusions. The slag systems showed no crystalline products.

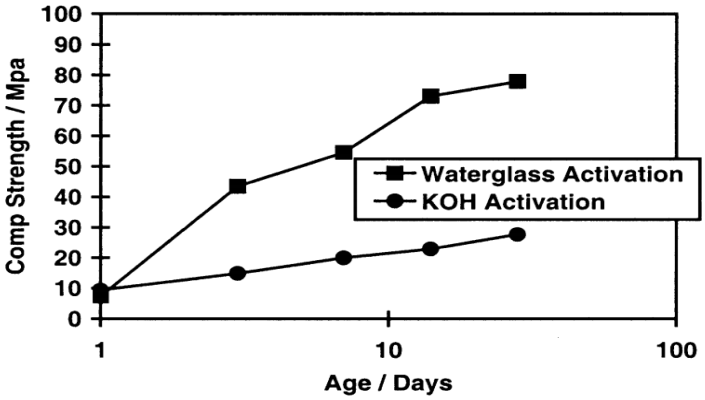

Figure 1.7: Strength development in mortars with Na_2SiO_3 and KOH (*Brough and Atkinson* [22]).

Hardjito et al. [23] prepared FA based geopolymer concrete (GPC) activated using Na_2SiO_3 and NaOH . Fresh and hardened state tests were conducted on the GPC such as workability and compressive strength test at 1, 7 and 28 days strengths. The results revealed that higher activator concentration led to higher strength. The increase in curing time put positive impact on the strength enhancement (Fig. 1.33). Minute amount of drying shrinkage and creep was observed in the GPC.

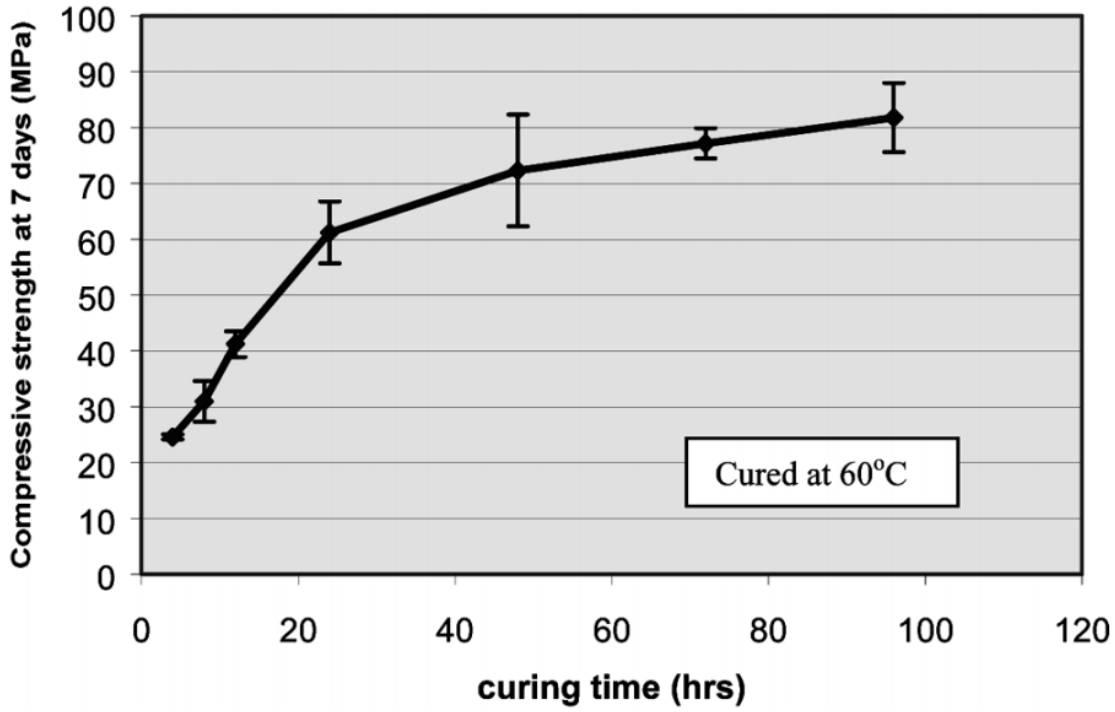

Figure 1.8: Influence of curing temperature on compressive strength of GPC (*Hardjito et al.* [23]).

Rangan and Hardjito [24] from their extensive research on FA based GPC concluded concentration of NaOH as alkali activator in GPC play significant role in strength attainment. As the concentration of NaOH increased in the GPC, the strength enhanced. The increase in extra water in the fresh GPC monotonously increased the workability. However, the compressive strength decreased due to increase in H_2O-to-Na_2O molar ratio. The density of GPC and OPC were found to be similar.

Oner et al. [25] from his work on strength development of blast furnace slag cement suggested that fineness of individual component of blended cement is an important parameter that affects strength attainment. Increase in fineness of slag increased the strength gain, however caused normal consistency and setting time reduction. It was suggested that grinding of slag components to higher degree results in higher strength. The cost effectiveness of such grinding protocol was not taken into account and suggested for further investigation taking this in consideration.

At higher levels of GGBS in PC based mortar, early age strength development is dependent on temperature as found by Barnett et al. [26]. Strength gain in PC-GGBS mortar was investigated by performing laboratory experiments on mortars prepared with varying content of GGBS in the binder (0, 20, 35, 50 and 70 %), water/binder (w/b) ratio and curing temperature (20, 30, 40 and 50 ºC). Results ascertained that higher temperature leads to high early strength regardless of GGBS content and w/b ratio. However, the improvement in early strength is more significant at higher levels of GGBS.

Atis and Bilim [27] investigated the influence of curing conditions for different relative humidity (RH), 65 % and 100 % on the compressive strength of GGBS and PCC concrete. Both the concrete types were prepared varying the binder content and w/b ratio. Concrete samples were dry and wet cured maintaining temperature of 22 ± 2 ºC and tested at 28 day and 3 months for compressive strength. When the results were compared, it was observed that the reduction in the strength of dry cured specimens due to addition of GGBS is more pronounced than that of wet cured ones. It was also concluded that an optimum w/b ratio exists for which the influence of curing conditions becomes minimum for a concrete.

Chindraprasirt et al. [28] investigated the effect of SiO_2 and Al_2O_3 content on setting, phase development and strength of high calcium based geopolymer systems. SiO_2 and Al_2O_3 contents were varied to attain SiO_2/Al_2O_3 ratio in the range 2.57 to 4.79. Rapid setting property of high calcium based geopolymer systems as mentioned in the report is primarily attributed to

calcium silicate hydrate (CSH) and calcium alumina silicate hydrate (CASH) formation. It was observed that SiO_2/Al_2O_3 ratios in the range of 3.20 to 3.70 produced geopolymer systems with high strengths and delayed setting times, Fig. 1.8. Moreover, at this SiO_2/Al_2O_3 ratio, strength was found to be higher than that with other SiO_2/Al_2O_3 ratios. Increase in SiO_2/Al_2O_3 ratio decreased both rate of strength development and compressive strength.

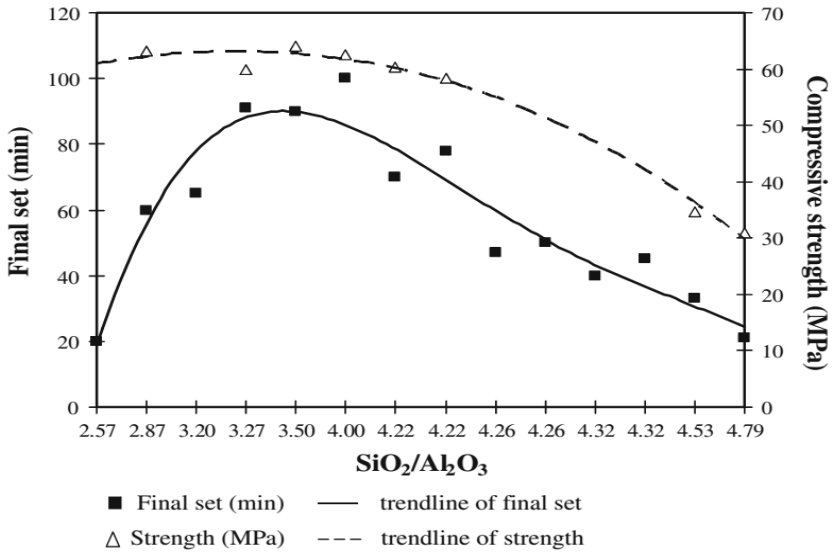

Figure 1.9: Final setting times and compressive strength with respect to SiO_2/Al_2O_3 ratio (Chindraprasirt et al. [28]).

Laboratory experimental works on strength development of alkali activated slag mortars using alkali hydroxide (KOH or NaOH) and Na_2SiO_3, undertaken by Altan and Erdogan [29] brought to light some facts regarding the curing conditions. Slag mortar samples prepared as per European Standards were cured at both room temperature and elevated temperature of 60, 80 and 95 ºC maintaining both dry and humid curing conditions. Results from the compressive strength tests indicated that samples cured at 80 ºC attained higher strength than other samples. Ambient temperature cured samples were also able to attain similar strength as that of 80 ºC temperature cured samples but at later ages (beyond 60 days), Fig. 1.9 (a) and (b). Humid curing was found to be beneficial in the strength gain process compared to dry curing condition. KOH with Na_2SiO_3 activated samples exhibited higher strength than NaOH with Na_2SiO_3 activated samples at early ages. But later, the strength gain decreased in KOH with Na_2SiO_3 activated samples as result of which 28 days strength was found to be less than NaOH with Na_2SiO_3 activated samples. Effect of NaOH concentration variation was also observed in the samples. Increase in NaOH concentration increased the strength at all ages

regardless of curing temperature.

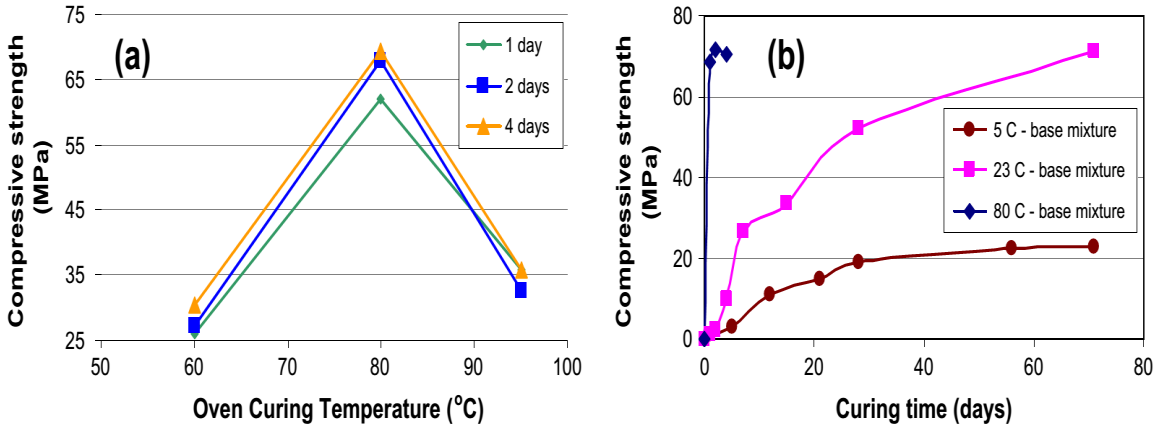

Figure 1.10: Effect of: (a) three different elevated curing temperatures on compressive strength and (b) curing temperature on compressive strength (*Altan and Erdogan,* [29]).

Alkali activated mortars with high aggregate/binder (a/b) ratios of 10:1 and 8:1 were prepared using blast furnace slag by Burciaga-Diaz et al. [30] to investigate the effect of Na_2O content and temperature on strength development. Alkali activator of varying percentage of Na_2O relative to the mass of slag (2.5, 3.5, 4.5 and 6.5 %) was used. These mortars having low water/binder ratio and cured at 20 and 60 °C were used for preparing brick samples and tested under compressive load. It was observed that, 8:1 a/b ratio produce mortar with higher strength when cured at 60 °C and consist of 3.5 % Na_2O. Similar strength was also achieved by mortar at 20 °C having 6.5 % Na_2O.

Tsai et al. [31] attempted to prepare a new type of blended cementitious material using GGBS and ground granulated basic oxygen furnace slag (GGBOS). The strength results of mortar samples of GGBS and GGBOS were compared with that of OPC mortar. GGBOS was mixed in 9 different proportions i.e. 10 - 90 % of cementitious material content (GGBS and GGBOS). Numerous tests were performed on these mixes so as to ascertain the compressive strength, time of setting, durability, etc., of the mortar samples. However, the compressive strength test was performed only on three mixes containing 30, 40 and 50 % GGBOS. Decision for compressive strength test on these mixes was taken on the grounds of chemical and physical requirement of lime in the blended mix. Samples with GGBS more than 70 % take prolonged setting time. 40 % and 50 % GGBOS containing samples could only meet the setting time requirements. This indicated that higher dosage of GGBS delays setting time, while higher

usage of GGBOS decreases setting time. Rate of strength gain in all the GGBS and GGBOS mortar samples was observed to be low. At 28 days, the samples could attain compressive strength as low as 50 % of that of OPC mortar samples. This trend was rather changed at later ages in 40 % GGBOS contained mortar samples. The samples could attain 90 % of the strength of OPC samples. From the Fig. 1.10, it can be seen that significant strength development occurred past 28 days.

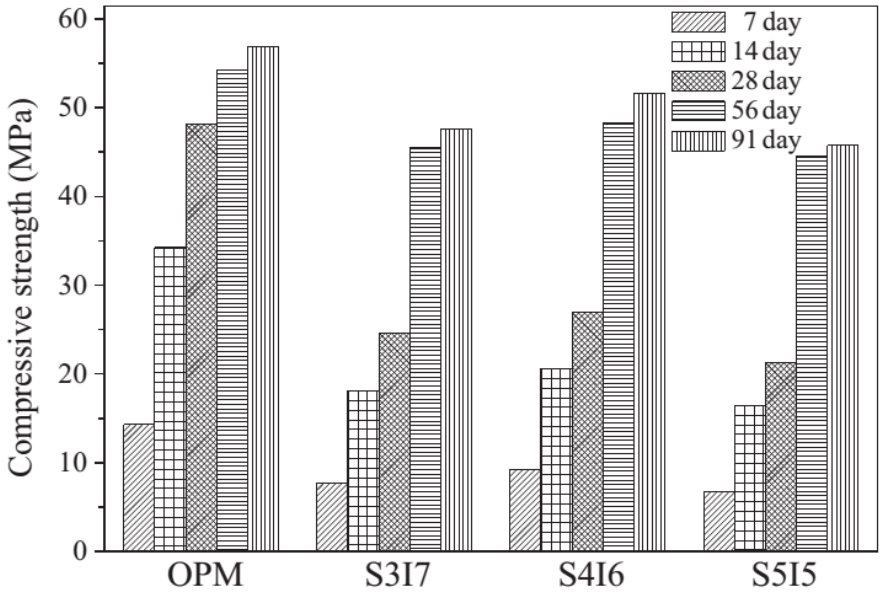

Figure 1.11: Compressive strength GGBS and GGBOS blended cements mortar (*Tsai et al.* [31]).

Atis et al. [32] reported maximum compressive and flexure strength of 120 and 15 MPa respectively for FA based GPM. Experimental investigation on GPM was carried out to find the influence of heat curing temperature, duration and alkali concentration on the strength characteristics. NaOH was used as alkali activator where Na concentration was varied to get desired alkali concentration. Curing temperature was varied from 45 to 115 $^{\circ}$C with 10 $^{\circ}$C increment and curing duration of 24, 48 and 72 hours were selected. It was observed that GPM cured at 45 $^{\circ}$C couldnot attain any strength even after 72 hours of curing for all alkali concentration. Highest strengths as mentioned were obtained using 14% Na concentration cured at 115 $^{\circ}$C for 24 hour. For low alkali concentration samples, increase in curing temperature increases the strength but upto a certain temperature point, beyond which, temperature increase decreases the strength. This is common phenomenon observed for all curing duration. It was also observed that two beneficial curing combination existed viz: low temperature curing for longer duration and high temperature curing for shorter duration.

Kartik et al. [33] also conducted physico-chemical test on FA-BFS based geopolymer consisting of bio-additives. FA and BFS were added in the amount of 60 and 40 %. Terminalia chebula and natural sugars were the bio-additives. The test results hold that due to addition of bio-additive in the geopolymer, stable geopolymer matrix forms as a result of intense structural reorganization. the geopolymer gel structures grow more stronger due to the bio-additive addition. the micro-structure as observed in the SEM were found to be compact and dense. Unreacted/partially reacted FA and BFS particles were observed in the FA-BFS based geopolymer without bio-additives. On contrary, less unreacted FA and BFS particles were observed in the microstructure of FA-BFS based geopolymer with bio-additives. The strength results indicated that the presence of sucrose in the bio-additives added geopolymer contributed towards attainment of higher strength.

Patel and Shah [34] added rice husk ash (RHA) to self-compacting geopolymer concrete prepared using BFS as primary binder. RHA was added as replacement in various percentages such as 5, 15 and 25 % by weight of the primary binder. The addition of RHA resulted in loss of workability due to the presence of micro pores in the RHA and its multilayered surface with irregular shape. Moreover, RHA is finer than BFS and hence led to absorption of the liquid component in the fresh geopolymer concrete. On contrary, improvement in strength was observed due to RHA addition of low amount (5 %). Higher amount of RHA in geopolymer concrete increased the amount if SiO_2 in the mix and thus contributed towards delay in the reaction of Si and Al ions. This in turn, produced weak geopolymer matrix and thus the concrete exhibited lower strength due to RHA addition of amount higher than 5 %.

Parveen et al. [35] prepared FA based geopolymer concrete consisting of high fineness slag of 10 % by weight. Laboratory tests were conducted on the geopolymer concrete in both fresh and hardened state. Slag addition in the geopolymer concrete improved its strength attainment capacity even when cured at ambient temperature. The high fineness slag caused hydration in the geopolymer concrete along with the polymerisation process. This resulted in compacted geopolymer structure and dense geopolymer matrix. This also reduced the water absorption of the geopolymer concrete.

Askarian et al. [36] developed FA-slag based geopolymer concrete consisting of various amount of ordinary PC (OPC). The geopolymer concrete was activated using solid potassium carbonate. The addition of OPC in the mix reduced the workability and setting time of

geopolymer concrete due to rapid reaction of OPC with alkali activator. On contrary, the compressive strength was found to enhance due to addition of OPC in the geopolymer concrete. Due to rapid reaction of OPC with alkali activator, the early ager strength of OPC P added geopolymer concrete was found to be significantly higher that the geopolymer concrete without OPC. The microstructure study revealed that OPC facilitated better reaction product formation in the geopolymer matrix. Thus, the geopolymer matrix developed was more compact and less porous compared to the geopolymer matrix without OPC.

1.5.1.2 Durability of geopolymer

Influence of combination of FA and on the properties of granulated blast furnace slag flyash concrete (GGFAC) and high volume FA high strength concrete (HFAC) was studied by Li and Zhao [37]. GGFAC was prepared by partial replacement of cement in PCC with 25% FA and 15% GGBS while HFAC with 40% of FA. Assessments of the concrete mixes were based on short and long-term performance of concrete and included compressive strength and resistance to sulphate (H_2SO_4) attack observation. The results showed that the GGFAC have higher early strength compared to HFAC, similar strength development as of PCC. GGFAC also showed better resistance to H_2SO_4 attack as the strength degradation rate of GGFAC was lowest among all.

Binci et al. [38] from his works on slag and basaltic pumic blended cement and PC came up with the fact that ground basaltic pumic (GBP) and clinker have lower grindibilty than GGBS. GGBS has higher pozzolanic activity as a pozzolanic material than GBP. Strength test as performed on mortar samples cured at 20 ± 3 ºC and 70 ± 5 % RH; and tested at 3, 7, 28, 90 and 180 days indicated that finer ground blended cements contributed to similar strength as that by PC. Though at early ages, the strength gain were lower for ground blended cements but later the rate of strength gain increased. Resistance to sulphate attack was found to be higher in finer ground blended cement mortar samples which is attributed to the presence of decreased amount of $Ca(OH)_2$ in the matrix.

Teng et al. [39] investigated the effects of ultra fine ground granulated blast furnace slag (UGGBS) as mineral admixture on fresh and hardened properties of PCC including durability. UGGBS was added in amount of 30 % of total cementitious material. Two different grades of concrete were studied with varying amount of water/cementitious material (w/c) ratio. It is found that, the addition of UGGBS improved the workability and consistency of

fresh concrete and also increased compressive and flexural strength compared to control PCC samples, Fig. 1.11. The effectiveness in enhancing the properties of PCC was more pronounced when w/c ratio was lower. UGGBS had increased surface area which increased the apparent rate of hydration and pozzolanic reactions. Moreover, due to better filling effect and reduction in pore connectivity, chloride penetration into the concrete was reduced in the test for chloride resistivity. Therefore, for all the mentioned reasons, concrete with UGGBS showed higher early strength, lower permeability and improved durability.

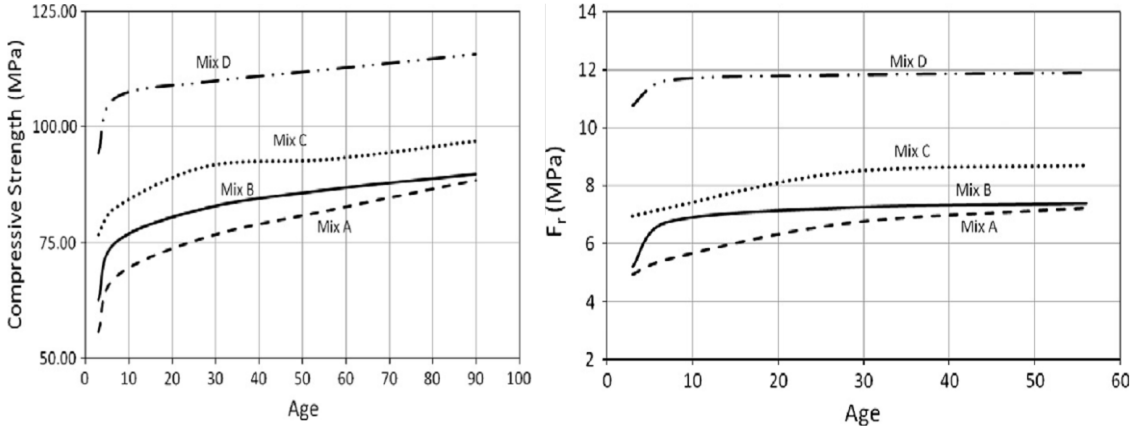

Figure 1.12: Compressive and flexural strength development (*Teng et al.* [39]).

Salas et al. [40] conducted the life cycle assessment geopolymer concrete. The researchers identified the significant raw materials and processes that contribute to its environmental performance. The researchers pointed out that the production of sodium hydroxide is the most relevant process in all life cycle impact categories. It was concluded that the global warming potential for geopolymer concrete is 64% lower than Portland cement concrete.

FA based rubberized geopolymer concrete was developed using the waste rubber tire fibres by Luhar et al. [41]. Test were conducted to investigate the thermal resistance of the concrete after subjection to temperatures of 200, 400, 600 and 800 ºC for 2 hours. The rubberized geopolymer concrete was developed with the aim of providing a solution to the disposal problem of both waste rubber and FA. The rubber tire fibres were added as partial replacement of natural fine aggregate. It was observed that the loss in mass and strength in the rubberized geopolymer concrete was not significantly higher than that of geopolymer concrete without rubber fibres. The authors ascertained that the minute difference in the result was due to the early decomposition of rubber fibres at elevated temperatures. Therefore, voids in the

concrete matrix formed and reduced its compactness.

1.5.1.3 Bond strength of geopolymer

Khan et al. [42] presented before the world facts relating to adhesion strength, setting time, microstructure and thermal stability of FA based geopolymer coating materials from some laboratory experiments performed on the same. Tests were performed on samples prepared by varying Na/Al and water/solids (w/s)ratio to observe the effect on the mentioned properties. It is worthy to mention that geopolymer systems were activated using only NaOH solutions. This was done with the aim of making the systems economical. The adhesion strength test revealed that 3 days of curing at 60 °C was adequate for developing the strength. Samples cured beyond 3 days till 7, 28 and 180 days showed negligible variation in the adhesion strength. Fig. 1.12 shows that maximum adhesion strength of 3.8 MPa could be attained at Na/Al ratio of 1 and w/s ratio 0.33, however this strength was attained after 3 days of curing. Water content also played important role in adhesion strength as it was observed that increase in water content decreased the bonding between geopolymer and substrate considerably. The total setting times for all the geopolymer systems were within 4 hours and those systems with high and low setting times showed weaker adhesion compared to the others. On exposing to high temperature of 800 °C, the geopolymer systems exhibited only 12 % of mass loss due to dehydration and dehydroxylation. The alkali concentration did not show any effect on the thermal stability of geopolymer systems.

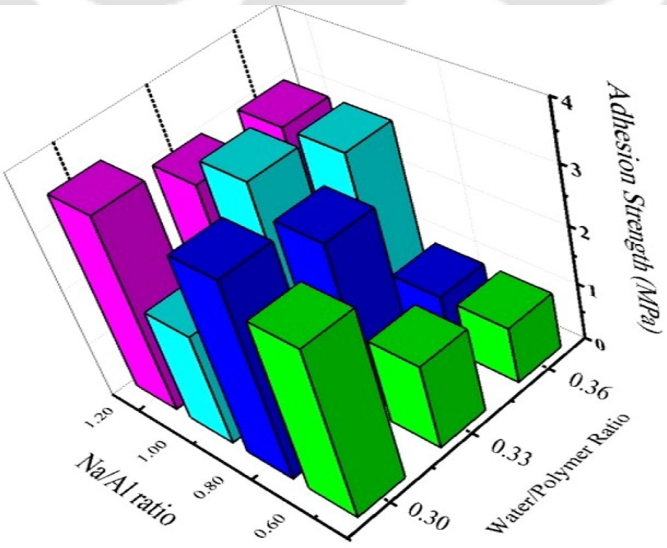

Figure 1.13: Correlation of Na/Al and w/s ratios with adhesion strength of geopolymers (*Khan et al.* [42]).

Sarker [43] evaluated the bond strength of FA based GPC with reinforcing steel. Pull-out test in accordance with American Society for Testing and Materials (ASTM) standard was carried out on 24 GPC and 24 PCC beam samples with varying concrete strength, bar diameter and concrete cover. The results were compared for conclusions. Crack patterns in GPC were similar to that of PCC under the pull out load. Both GPC and PCC samples failed in brittle manner by splitting of concrete along the bonded length of the pull out bar. The bond strength increased with the increase of concrete cover and compressive strength. Increase in concrete cover to bar diameter ratio also increased the bond strength. In all, GPC possessed higher bond strength than PCC which is attributed to the fact that GPC have higher splitting tensile strength.

Useng et al. [44] performed series of laboratory experiments to investigate the adhesion property at the interface of cement mortar and geopolymer. A simple mechanical model using the factors affecting various components at interface was developed to ascertain the strength properties, failure modes and deformational moduli. Fig. 1.13 shows the typical prism sample used for the interface adhesion study. The geopolymer interlayer was applied with various dip angles (β) in the prisms and subjected to uniaxial and triaxial compressive loads. The stress-strain curve under uniaxial loading exhibited brittleness and tensile splitting at failure. Whereas, increase in ductility was observed as the confining pressure was increased under triaxial loading. The failure was observed to be due to shearing. At the geopolymer interlayer, basically two modes of failure were noticeable. First involved major fractured plane passing through the interlayer (I) and second involved shear sliding along the interface between cement mortar and geopolymer (II). Prism samples with β between 0 to 45° and 90° suffered type I failure mode while type II is shown by prism samples with β between 50° to 60°. From the analysis of the results using the mechanical model, it was found that interface adhesion between cement mortar and geopolymer was 34 - 43% as strong as the cohesions of the two components. Load causing failure mode I in the prism was found to be higher than that causing failure mode II.

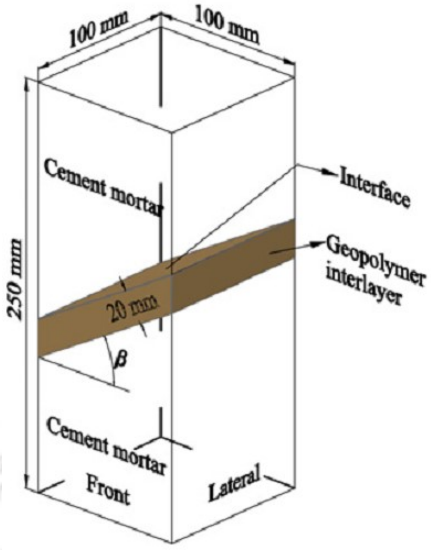

Figure 1.14: Dimensions of prism cement mortar specimen containing a geopolymer interlayer (*Ueng et al.* [44]).

Experimental study on bond performance of GGBS based geopolymer paste on exposure to 20 - 500 °C was undertaken by Zheng and Zhu [45]. The aim was to develop GGBS based geopolymer paste as construction adhesive. Geopolymer prism samples were prepared and subjected to high temperature exposure to study its microstructure and thermostability. PCC prism samples were also prepared and cured at ambient temperature to observe the bond performance of geopolymer pastes. Geopolymer paste was applied to the hardened concrete surface of each prism sample, CFRP sheet was placed over it, pressed gently to remove entrapped air and the whole system was covered with a film to prevent moisture loss. The prism samples were subjected to temperature of 20, 100, 200, 300, 400 and 500 °C for 2 hours. Later, double shear test was performed on these samples. On studying the test results, it was found that thermostability and mechanical properties of GGBS based geopolymer paste deteriorate after exposure to 800 °C and above. Ultimate load in the double shear test decreased with the increase in temperature. Enhanced rate of load capacity reduction was observed beyond 300 °C. Modes of failure as observed were concrete failure and CFRP rupture. The absence CFRP-adhesive interface failure and adhesive failure confirmed that GGBS based geopolymer paste possessed strong adhesive bond and hence can be used efficiently as construction adhesive.

Phoo-ngernkham et al. [46] attempted to develop a type of repair material using high calcium FA based GPM containing some amount PC. PC was added in 5, 10 and 15% by weight of the cementitious material. Performance of the GPM was evaluated by performing tests for

slant shear and bending stress on the specimens shown in Fig. 1.14 and compared with results from similar tests on similar specimens prepared with five types of commercially available repair materials (RM). NaOH and Na_2SiO_3 were used as activators. Three NaOH concentrations 6, 10, 14 M were used to study the influence of alkali concentration on the mentioned strength parameters. Results provided positive indications for use of GPM as repair material in place of commercially available repair material. GPM prepared with higher alkali concentration (14 M) and 10 % PC was found to exhibit highest strength in both the tests as indicated in the Fig. 1.15 and 1.16. The failure of samples in slant shear test for GPM with this alkali concentration and PC content was in the monolithic mode where cracks were formed in both sections of GPM and PCC substrate indicating the relatively high bonding between the two surfaces.

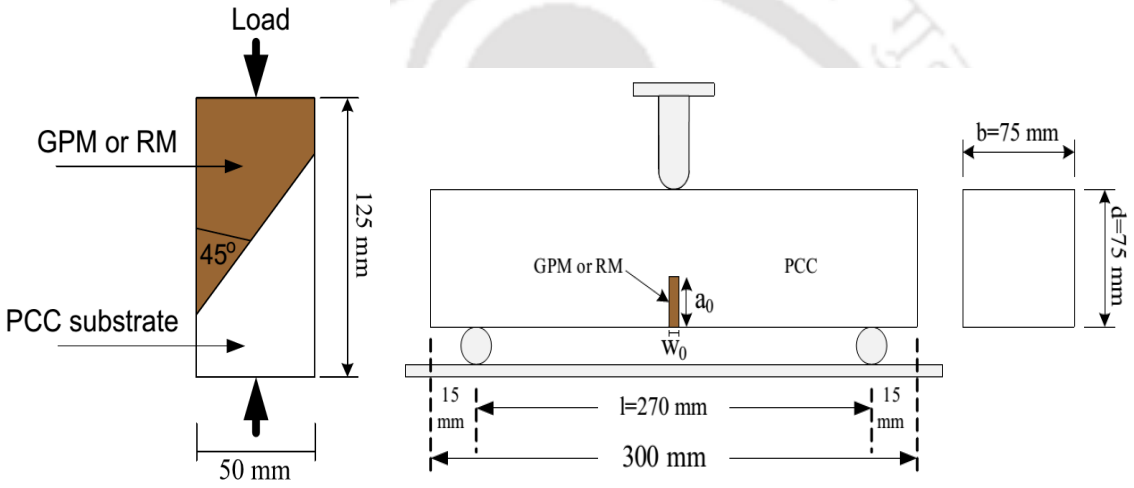

Figure 1.15: Test set up of slant shear specimens and bending stress of PCC notched beam with filled GPM or RM specimens (*Phoo-ngernkham et al.* [46]).

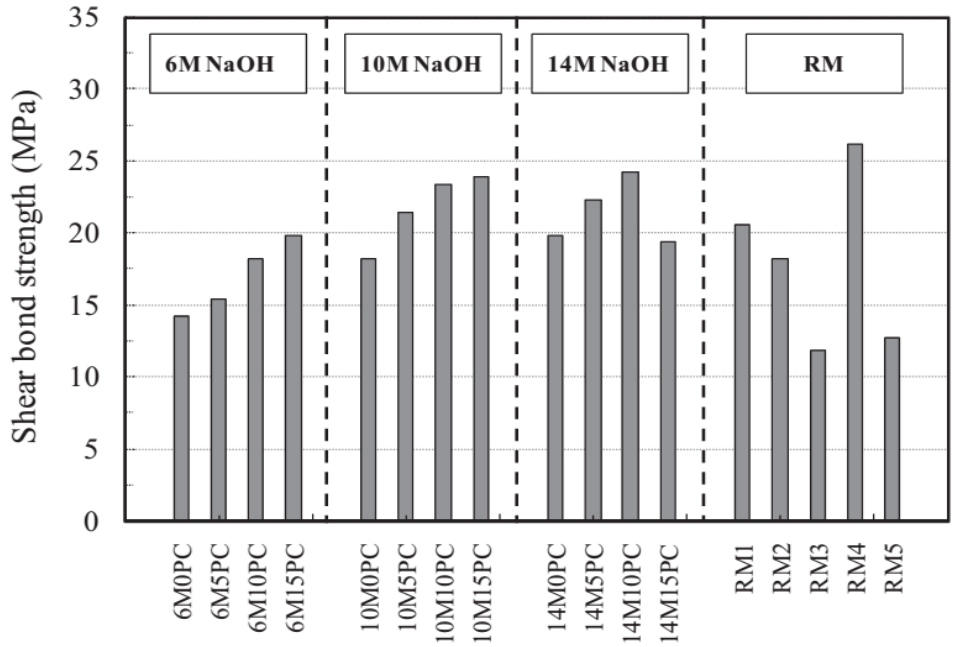

Figure 1.16: Shear bond strength of GPM and RM (*Phoongernkham et al.* [46]).

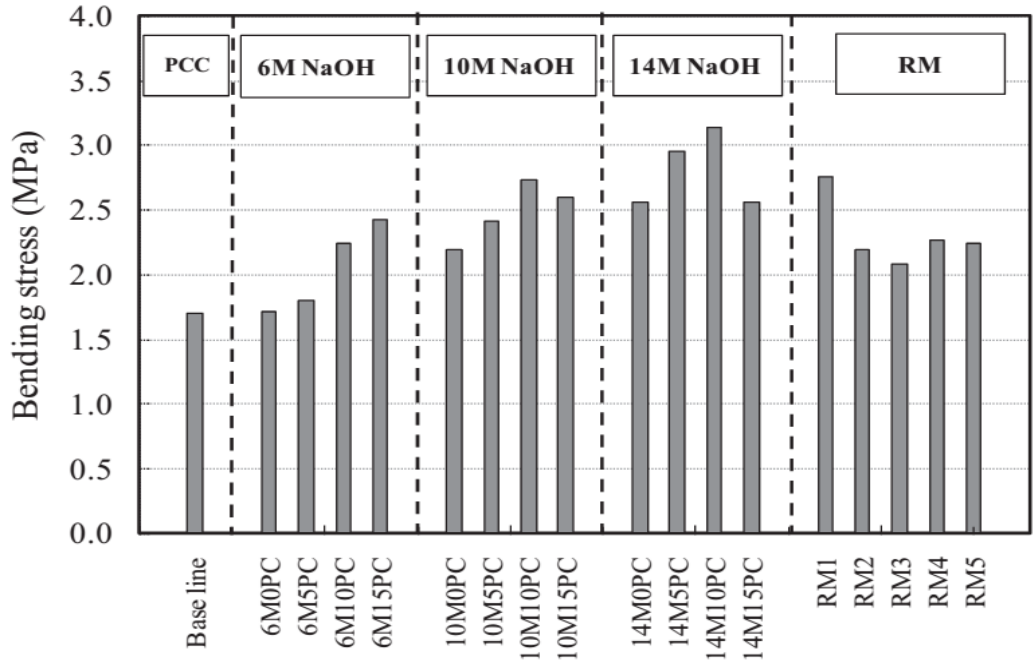

Figure 1.17: Bending stress of PCC notched beam with filled GPM or RM as repair materials (*Phoongernkham et al.* [46]).

Al-Azzawi et al. [47] investigated on the bond strength of FA based geopolymer concrete with steel reinforcement. The bond strength showed increasing trend due to increment of FA content in the concrete. The characteristic of FA, its particle size and chemical

composition significantly affected the bond strength.

1.5.1.4 Geopolymer as repairing agent

Perna and Hanzlicek [48] investigated the possibility of altering the setting time of clay/slag geopolymer matrix by modifying clay/slag ratio and by using different methods of mixing clay and slag with the aim of developing it as repairing agent. The geopolymer system was activated using potassium silicate (K_2SiO_3) as it was found to produce such systems of high compressive strength. Three variation of slag content were considered (50, 60 and 70 % of total clay content) for mix proportioning of the geopolymer systems. Components mixing included two methods, first involved mixing of clay material with alkaline activator for 10 minutes, then addition of slag and further mixing 10 minutes. Second method involved mixing clay material and slag in dry state till homogenized dry mix was obtained. Later, alkali activator was added and mixing of components were carried out for 20 minutes. The results indicated that increase in slag content reduce setting time regardless of mixing methods. Collective mixing reduced the setting times by more 5 and 10 minutes for 60 and 70 % slag containing systems respectively as compared to separate mixing, Fig. 1.17 and 1.18. The authors recommended that such accelerated setting type geopolymer systems can be used as repair material.

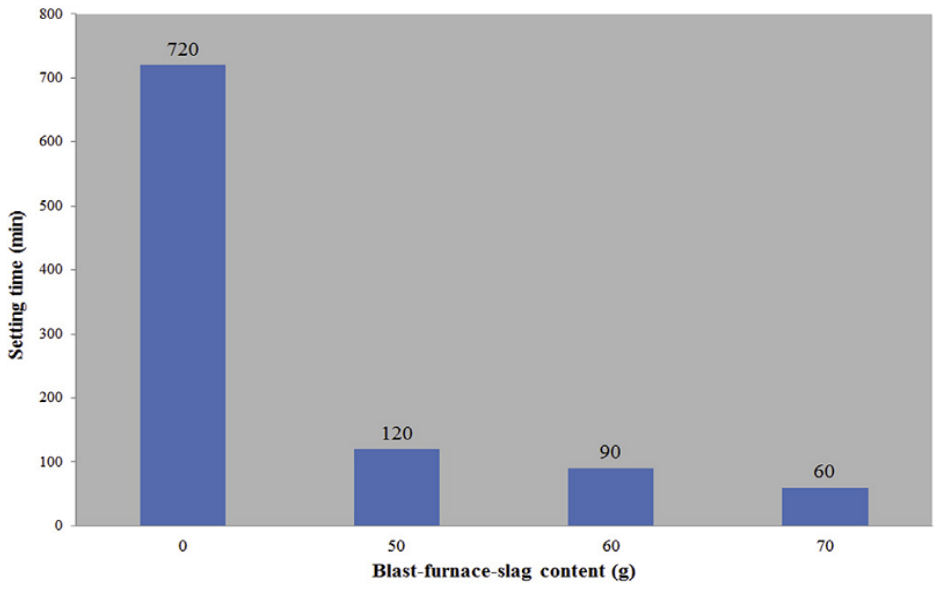

Figure 1.18: Setting time of separate mixing with different additions of slag (*Perna and Hanzlicek* [48]).

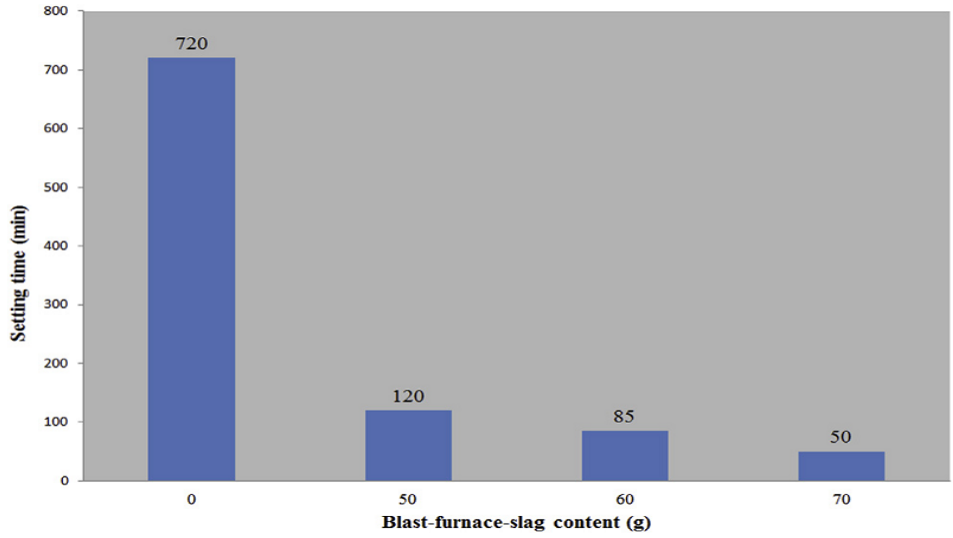

Figure 1.19: Setting time of collective mixing with different additions of slag (*Perna and Hanzlicek* [48]).

Xiong et al. [49] proposed to modify the repair interfacial transition zone by introducing fly ash into a primer between concrete substrate and repair materials. A comparison test was carried out for five different bond interfaces coated with five kinds of primers, namely neat cement paste, expansive paste, cement mortar, water-dispersible epoxy resin and fly ash-modified mortar. The test results showed that the fly ash-modified primer made the microstructure of the repaired interface zone more dense and uniform. As a result, the splitting bond strength of the interface coated with the fly ash-modified primer was significantly higher than those coated with the other kinds of primers and results from intermolecular force, mechanical interlocking and chemical reaction.

Hu et al. [50] attempted to develop efficient repair material by investigating the mechanical properties of three types of binders. The binders were cement based binders, metakaolin based geopolymeric binders and geopolymeric binders containing steel slag. Compressive strength, bond strength and abrasion resistance were examined by performing laboratory tests. Compressive strength tests were performed on 40 × 40 × 40 mm cubes at curing ages of 8 hour, 1, 3, 7 and 28 days. Bond strength test was performed on a specially prepared specimen as shown in Fig. 1.19. Abrasion resistance test were performed in accordance to Chinese code. It was observed that geopolymeric repair materials possess better repair characteristics than cement based materials. Irrespective of curing ages, geopolymeric repair materials exhibited higher strength compared to cement based materials. Geopolymeric

repair materials even possessed better transition zone bonding than cement based materials. The modes of failure for the three repair materials in the bond test is given in Fig. 1.20. Mode A was basically exhibited by cement based repair material while Modes B and C were exhibited by geopolymeric repair materials for different curing ages. The abrasion resistance of geopolymeric repair materials was also found to be better than cement based materials at all curing ages. Addition of steel slag enhanced the mechanical properties of geopolymeric repair materials.

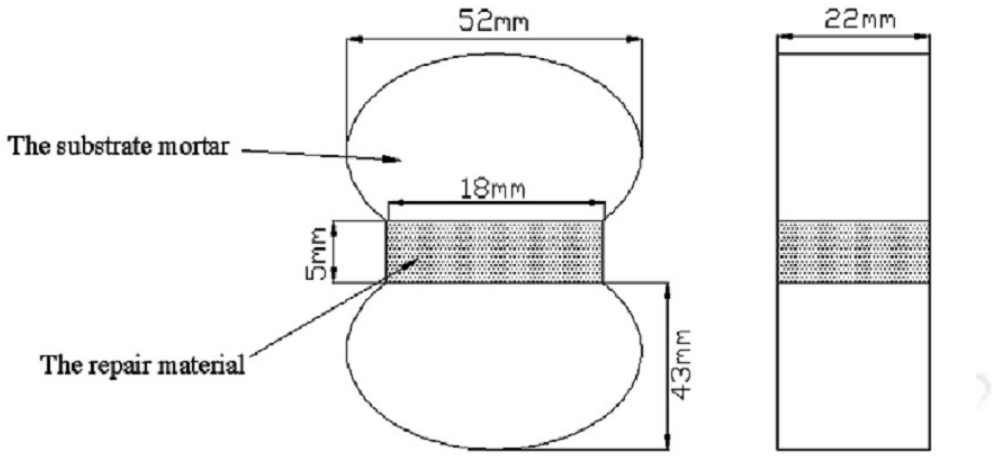

Figure 1.20: Test set-up of for bond strength between substrate and mortar repair materials (*Hu et al.* [50]).

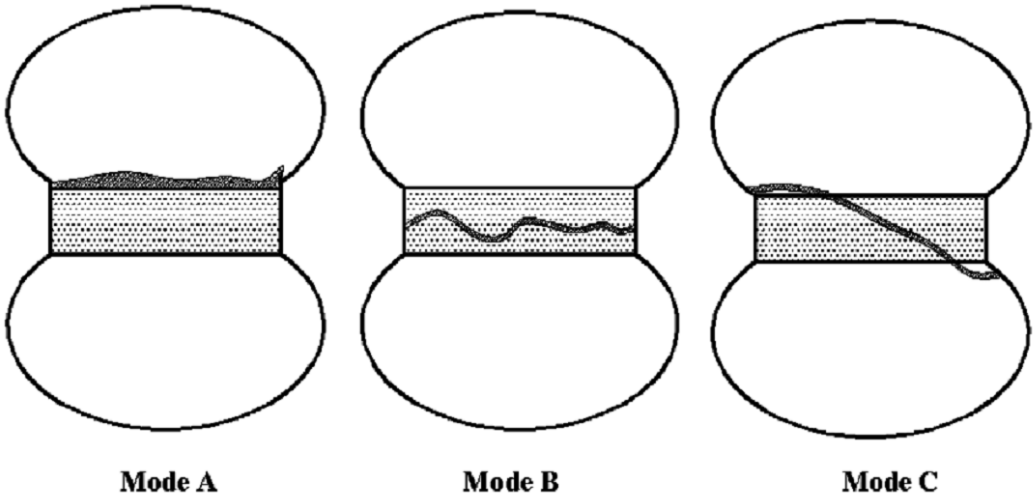

Figure 1.21: Failure modes of specimens in bond strength test (*Hu et al.* [50]).

Geopolymer can also be used as retrofitting agent. The effectiveness of geopolymer mortars for retrofitting of structures was investigated by Vasconcelos et al. [51]. Metakaolin

(MK) geopolymer mortar was used as both repairing layer and binding agent for adhesion of carbon fibre reinforced polymer (CFRP) sheets with concrete, Fig. 1.21. It was concluded that the geopolymer mortars are cost effective repairing agents, which show satisfactory result. But as binding agent, its performance was found not to be appropriate considering the fact that the CFRP used was not prone to this kind of application.

Figure 1.22: Placing CFRP sheet and geopolymeric on the concrete surface (*Vasconcelos et al.* [51]).

1.5.2 Repairing and strengthening of reinforced concrete members

Popov and Bertero [52] evaluated the performance of epoxy resin and PCC repaired reinforced concrete (RC) members under cyclic loading. The RC members were severely cracked by applying monotonic load in two opposite directions to form large closed hysteretic cycle. The members were then repair using either epoxy resin or PCC and subjected to both monotonic and cyclic load of gradually increasing magnitude. Results of RC members at both original uncracked stage and post repair stage were compared to conclude about the repairing methods' efficiency. Epoxy repairing proved to be very efficient in crack repairing as the repaired RC members could sustain several load cycles. However, due to insufficient repairing of finer cracks and inability of restoring bond fully, the repaired RC members were less stiff than the original ones. It was advised that PCC repairing should be practiced when original RC members are severely damaged leading to local disintegration of concrete materials. It was also concluded from the test results that, repaired RC members become 2 to 2.5 times more flexible compared to the original members.

Research outcome of torsion failed RC beams repaired using adhesive bonded steel

plates were presented by Holman and Cook [53]. Three sets of RC beams were prepared, (A) control beams i.e., RC beams without plates, (B) externally reinforced RC beams with epoxy bonded plates and (C) 'A' type torsion failed RC beams repaired with epoxy bonded plates. All the three sets of RC beams were subjected to identical loading. From the experimental data, it was found that externally reinforced RC beams possessed 43 % higher strength than the controlled beams. The failure mode was observed to be in flexure, rather than in torsion. The repaired beams also showed higher load capacity of 33 % and failed in flexure. In all the cases, the experimental strength values were greater than the calculated values, Table 1.1.

Table 1.1: Failure loads of the beam specimens (*Holman and Cook* [53]).

Beam	Load (kN)	Average load (kN)	Calculated load (kN)
A1	31.2		
A2	31.2	31.2	26.7
A3	31.2		
B1	42.3		
B2	44.5	44.5	36.8
B3	46.7		
C1	35.6		
C2	49.0	41.3	36.8
C3	39.2		

Al-Mandil et al. [54] prepared concrete beams with simulated cracks and injected three types of commercially available epoxy compounds. The repaired beams were then exposed to a heat-cool (H/C) cyclic system. The beams were tested in flexure, where the epoxy concrete interface was subjected to tensile stresses. Concrete cylinders with embedded inclined cracks were repaired by the same epoxy compounds, exposed to similar H/C cyclic system and tested in compression, where the epoxy concrete interface was subjected to combined compressive and shear stresses. The results indicated considerable reduction in the bonding strength of epoxies in the repaired beams due to H/C cycling. An average reduction of 80% in the epoxy bonding capacity was obtained after beams were subjected to 150 H/C cycles and tested in flexure. The adverse effect of H/C cycles on the bond strength was more noticeable when the epoxy concrete interface was subjected to tensile stresses in compared to the case where the interface is subjected to combined compression and shear.

Chajes et al. [55] presented some of the results from their research project on flexural

strengthening of RC beams using externally bonded composite fabrics. The fabrics were of three types, amramid, E-glass and graphite fibres which were bonded using epoxy resin. The results dealt with the durability of the same when subjected to varying number of wet/dry and freeze/thaw cycles in calcium chloride solution. Evaluation of durability property was done by performing four point flexural test on the aggressive environment exposed and controlled beams and hence comparing the results. Results given in Table 1.2, 1.3 and 1.4 show increase in load carrying capacity of the beams due to externally bonded composite fabrics compared to the controlled beams. However, exposure to aggressive environment caused reduction in the ultimate strength of externally bonded composite fabrics beams compared to those at controlled condition. The degradation of strength due to varying exposure duration to aggressive environments varied for all the three types of externally bonded composite fabrics beams. It was found that wet/dry cycles caused higher strength degradation than freeze/thaw cycles. Of the three types, graphite strengthened beams were most durable, losing less than 15% of their increased strength in the strengthened beams under controlled condition.

Table 1.2: Average beam strength (Chajes et al. [55]).

Environmental condition	Unwrapped (N)	Aramid (N)	E-glass (N)	Graphite (N)
Control	1203	3504	2267	2873
50 cycle freeze/thaw	1033	2295	1932	2358
100 cycle freeze/thaw	1000	3183	1665	2267
50 cycle wet/dry	1045	2803	1455	2591
100 cycle wet/dry	1058	2237	1447	2332

Table 1.3: Variation in beam strength due to environmental conditions (*Chajes et al.* [55]).

Environmental condition	Unwrapped (%)	Aramid (%)	E-glass (%)	Graphite (%)
Control	-	-	-	-
50 cycle freeze/thaw	14	17	15	18
100 cycle freeze/thaw	17	9	27	21
50 cycle wet/dry	13	20	36	10
100 cycle wet/dry	12	36	36	19

Table 1.4: Variation in beam strength due to external fabric (*Chajes et al.* [55]).

Environmental condition	Unwrapped (%)	Aramid (%)	E-glass (%)	Graphite (%)
Control	-	191	88	139
50 cycle freeze/thaw	-	183	87	128
100 cycle freeze/thaw	-	218	67	127
50 cycle wet/dry	-	168	39	148
100 cycle wet/dry	-	11	37	120

Efficiency of external unbonded reinforcement for strengthening flexure deficient RC beams was experimentally investigated by Cairns and Rafeeqi [56]. The research was concerned with the flexural behaviour and performance of RC beams with variation in loading arrangement (shear span), effective depth of external reinforcement and quantity of internal reinforcement. A new method for determining the ultimate load capacity of beams with external reinforcement was proposed and the results were compared with the experimentally obtained ultimate load capacity. The results indicated considerable improvement in ultimate flexural strength in RC beams with unbonded external reinforcement. Ductility was reduced in such beams due to external reinforcement compared to the beams with internal reinforcement only. However, the reduction in ductility was not considered to be a problem as the warning of failure of beams were given by development of large number of structural cracks. At constant loading, reduction in shear span and increase in effective depth of the external unbonded reinforcement lead to higher stresses in them, Fig. 1.22. In case of beams which were lightly reinforced with internal bars, the improvement in ultimate flexural strength due to unbonded external reinforcement was more pronounced. Calculated results tallied with the measured results and also revealed that the strength obtained by unbonded external reinforcement were lower than that would have been with fully bonded additional reinforcement.

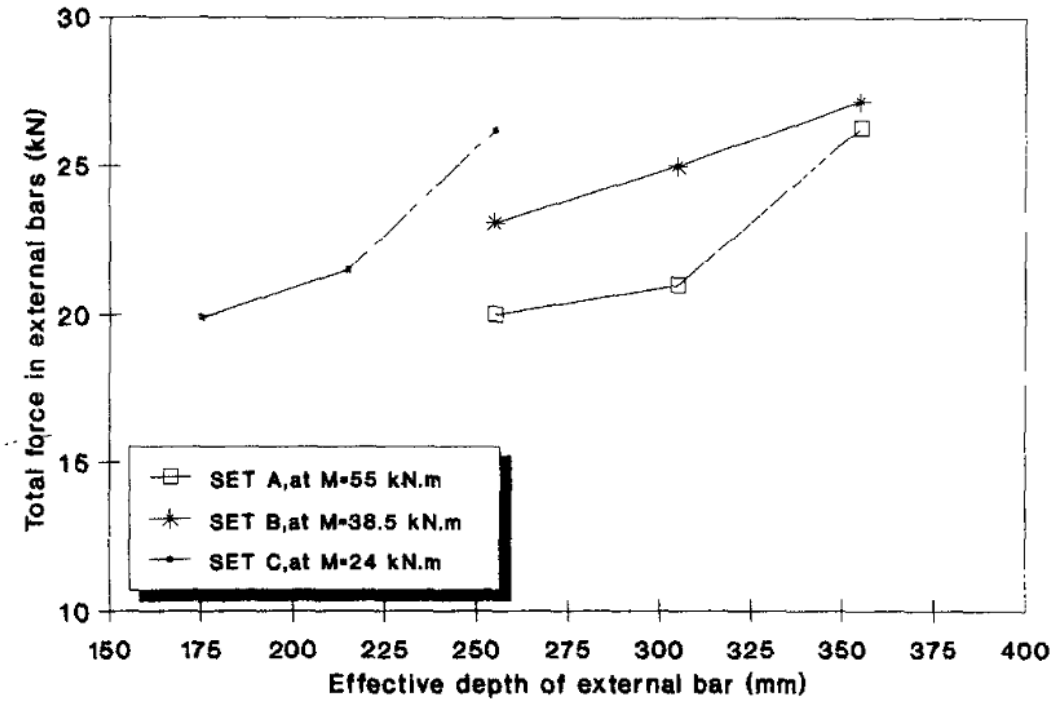

Figure 1.23: Variation in force in external unbonded bars with effective depth (*Cairns and Rafeeqi* [56]).

Nounu and Chaudhary [57] assessed the corrosion resistance of OPC mortar and free flowing micro-concrete repaired RC beams when exposed to chloride environment. RC beams were tested for load capacity at different stages starting right from casting-curing stage to the end of weathering stage. RC beams that were repaired were subjected to preliminary corrosion at predetermined section. Later, these were exposed to chloride environment at varying temperature conditions in a weathering chamber. Comparing the test results performed after short time duration curing, it was found that OPC mortar and free flowing micro-concrete had similar load capacity restoring property for the repaired beams. However, at long term duration, free flowing micro concrete showed better performance in terms of weathering restriction and strength gain. In terms of serviceability, the repaired beams couldnot match up the performance of the original controlled beams tested after casting and curing. This was attributed to the fact that the repair process couldnot develop full bond between the overlapped bars. The cracks developed in the repaired beams indicated that bonding capacity of free flowing micro concrete was found to be better than OPC mortar.

Li et al. [58] investigated the different strength schemes of RC beams shear strengthened with carbon-fiber–reinforced plastic (CFRP) sheets. The investigation primarily

dealt with the stress distribution, appearance of first crack, crack propagation and ultimate strength of the strengthened beams. The five strengthening schemes included beams strengthened in flexure and shear-flexure, Fig. 1.23. The modes of failure involved flexure failure, shear failure and hybrid shear/flexure failure. Initial stiffnesses within service load range, stiffnesses beyond service load range and ultimate load were found to be higher in beams strengthened in both shear and flexure compared to that in beams strengthened in flexure only. Appearance of first crack was delayed in the beams strengthened in both shear and flexure, Fig. 1.24. Increase in CFRP sheet area improved the stiffnesses of beams at higher loads due to better restraining effect on crack development. The bond between concrete and CFRP sheets remained intact till the end of load application, proving the fact that epoxy adhesive used for bond CFRP sheets with RC beams performed with high levels of satisfaction.

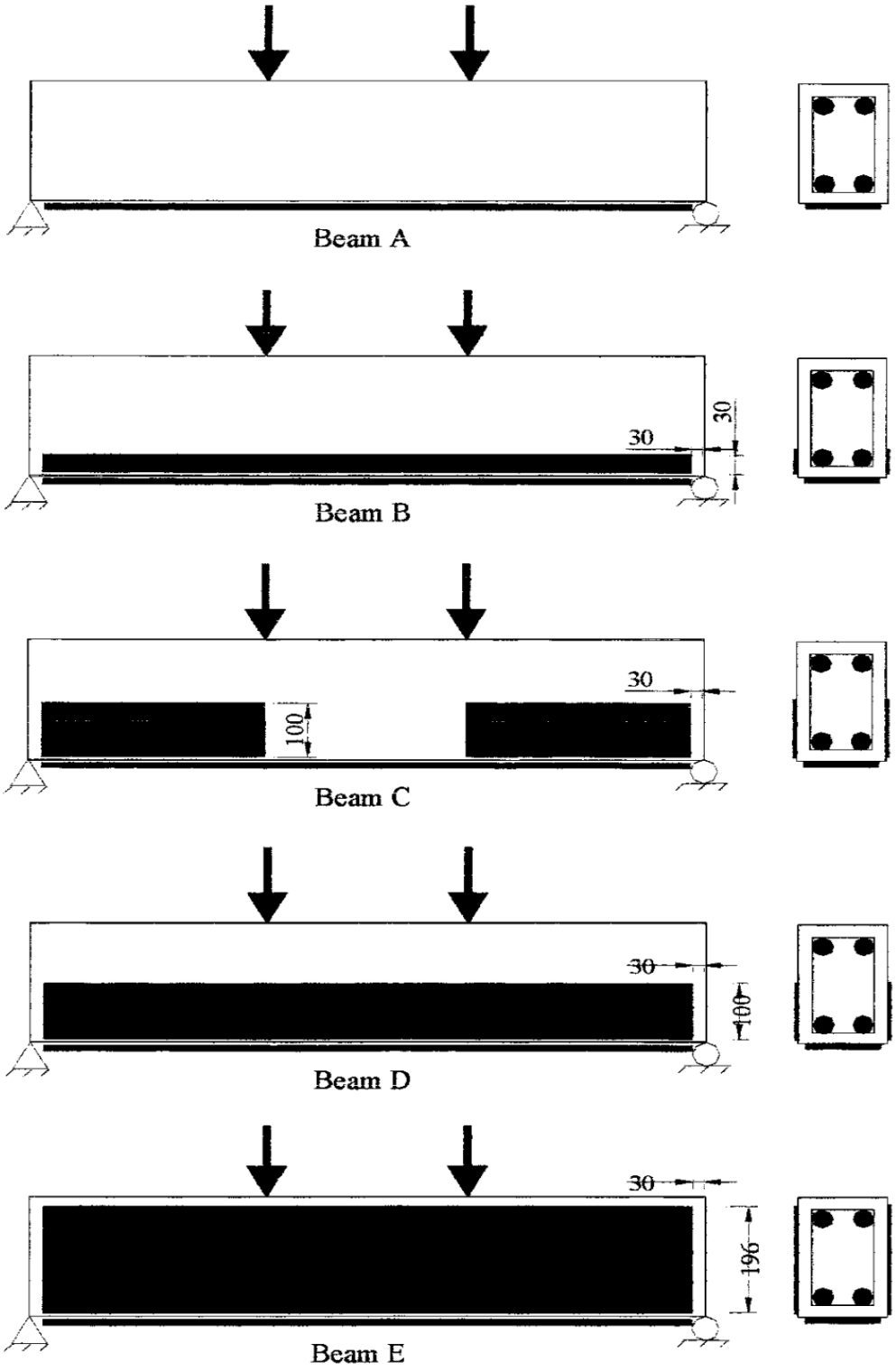

Figure 1.24: Different shear strengthening beams (*Li et al.* [58]).

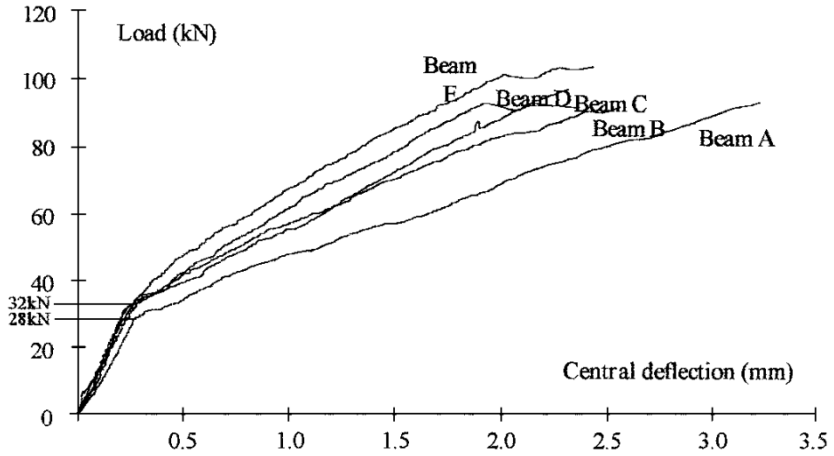

Figure 1.25: Load versus central deflection (*Li et al.* [58]).

Effectiveness of concrete jacketing of damaged RC beams was studied by Altun [59]. Under reinforced RC beams which were fully plastic yielded by applying flexural loading were repaired by concrete jacketing and tested for bending stiffness, ultimate load capacity and ductility under static loading, Fig. 1.25 and 1.26. Parameter variations included jacket thickness, aspect ratio of cross-section and amount of reinforcement. Theoretically calculated values were compared with the experimentally obtained ones for validation of results. Load deflection results revealed that jacketed RC beams behaved similar to original RC beams. Ductility of the RC beams varied with variation in aspect ratio of cross-section and amount of reinforcement. Experimentally obtained values were found to be higher than the calculated ones. The reasons for this was cited as assumption of certain parameters while calculating the ultimate load values theoretically neglecting the actual phenomenon.

Figure 1.26: Jacketing reinforcement around the damaged initial RC beams (*Altun,* [59]).

Figure 1.27: Concrete of the jacketed RC beams (*Altun* [59]).

Issa and Deb [60] studied the effectiveness of application of gravity filled epoxy in concrete. Concrete cubes with artificially induced crack, with gravity filled epoxy in the artificially induced crack and with no cracks were crushed and their compressive strengths were obtained. The test results indicated that the cracks caused a reduction in compressive strength up to 40.93 % whereas the epoxy system, when properly applied, restored the compressive strength by decreasing the reduction down to 8.23 %.

Ahmad et al. [61] used polymer modified mortar (PMM) for controlling cracks in RC beams. In the study, locally available PMM was used in filling the cracks of damaged beams which were loaded initially till development of cracks with maximum width of 1 mm. These crack damaged RC beams were later tested till failure again after 3 days of moist curing. The PMM repaired beams attained 36 % higher load capacity compared to the controlled ones i.e. RC beams with no cracks. PMM could effectively repair the flexural cracks, as all the repaired beams failed in shear. However, stiffness improvement was not achieved due to the application of PMM at initial loading stages.

Pattnaik and Rangaraju [62] suggested that due consideration should be given to the strength compatibility of the repair material and the substrate to be provided with the repair material. The negligence to which may lead to failure of the repaired concrete members in incompatible modes such as bond failure, failure due to accumulation of excessive stresses at the interfaces, etc. In the study performed by the researchers, prism specimens made out of concrete were provided with different commercially available repair materials with various strength. When subjected to four point flexural loading, some specimens failed by crack development at centre, indicating the compatible type of failure. On the other hand, as

presented in Table 1.5, when the strength of the repair material was higher than the strength of substrate material, cracks developed at the edge of the repair material filled notched section which indicated incompatible type of failure, Fig. 1.27.

Table 1.5: Strength of composite beams (*Pattnaik and Rangaraju* [62]).

Repair Material (RM)	Compressive strength (MPa)		Flexural strength (MPa)	Compressive strength ratio	Failure pattern
	RM	Substrate			
A	65.0	56.0	6.4	1.2	Compatible
B	63.2	50.1	6.5	1.3	Incompatible
C	66.6	50.3	5.5	1.3	Incompatible
D	80.9	56.0	6.1	1.4	Incompatible
E	30.6	50.1	7.0	0.6	Compatible
F	55.2	50.1	5.2	1.1	Incompatible
G	43.6	56.3	6.0	0.8	Compatible
H	45.6	50.3	5.5	0.9	Compatible

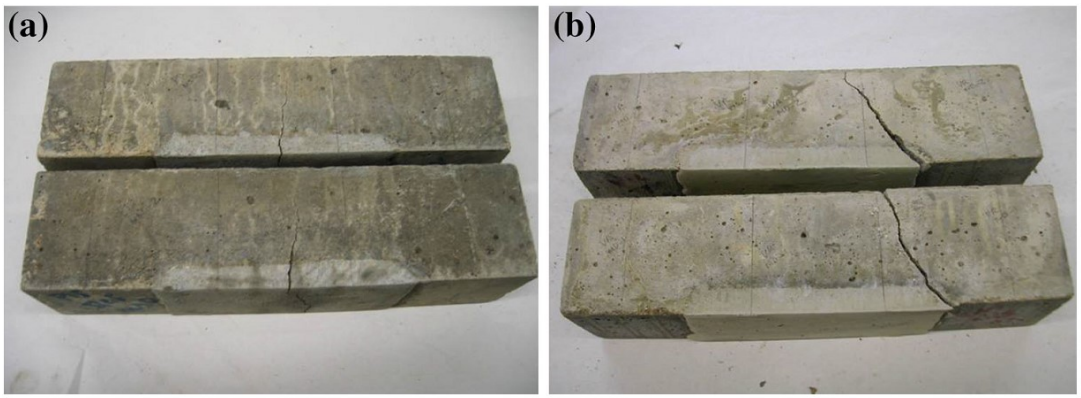

Figure 1.28: Failure patterns of composite beam (a) Failure at centre (b) Failure at the edge of repair (*Pattnaik and Rangaraju,* [62]).

Tomlinson and Fam [63] studied the behaviour of concrete beams reinforced with basalt fiber-reinforced polymer (BFRP) rebar and strips when subjected to four point loading. Beams with various BFRP flexural reinforcement ratios, various shear reinforcement conditions and no shear reinforcement conditions were tested. From the test observations, it was found that all the beams behaved in similar manner till the appearance of first crack. At service loads,

cracking was observed to be in flexure for all the beams. Reinforcement ratios had no effect on the cracking loads and precracked stiffnesses, as they were found to be same in all the beams. However, ultimate load capacities of the beams were influenced with the reinforcement ratio irrespective of failure mode. Increase in BFRP flexural reinforcement increased the load for shear cracking in beams without shear reinforcement. Ultimate shear capacities also increased with increase in the flexural reinforcement ratios. In all, BFRP successfully enhanced the load capacities of the beams.

Luna-Galiano et al. [64] developed composites from carbon fibre waste (CFW) and blast furnace slag based geopolymer. the carbon fibre waste was obtained from aircraft industry. Due to the addition of CFW in the geopolymer, the porosity of the system enhanced. The authors suggested that the porosity enhancement was either due to the increase in water content in the geopolymer-CFW composite to keep it workable or due to the voids developed in the geopolymeric gel and the CFW particles interface. The compressive strength reduced due to CFW addition. The reason was attribute to the development of higher amount of pores due to CFW content enhancement. The composite was acid resistant as the pore provided space for accommodation of products formed due to the acid attack. Thermal resistivity was also high due to the presence of pores.

Raval and Dave [65] studied the performance to micro-concrete jacketed reinforced concrete beams due static loading. Various bonding methods were applied in combined and solo form during the jacketing process which involved dowel connectors, bonding agent and surface roughening. The results were compared with controlled beams which were not jacketed. It was observed that surface chipping of the beams contributed towards better performance of the various bonding methods in jacketed beams on contrary to the performance of smooth beam surface jacketing. Combined action of dowel connectors and bonding agent led to highest load carrying capacity of the beams.

Belal et al. [66] employed various techniques of steel jacketing for strengthening of RC columns. Variations included shape of the strengthening systems, sizes and number of batten plates used for connection. Total five numbers of RC columns were strengthened and then subjected to uniaxial loading. Two numbers of beams were also tested without jacketing and were considered as controlled specimens. Test results revealed that the steel jacketing technique is an effective method of strengthening of RC columns. The minimum strength enhancement in RC columns in the investigation was 20 %. Moreover, the steel jacketing provided ductility

to the RC columns. The increase of contact area between concrete and steel jacket increased the effect of confinement.

Jamil et al. [67] accomplished numerical analysis of RC beams using finite element software ANSYS to evaluate the behavior of cracked and un-cracked beam under different loading conditions. The analysis was also done for the RC beams re-strengthened by concrete jacketing. From the analysis it was suggested that the damage level plays significant role on the stresses condition at crack tip of the cracked beam. Jacketing is very effective in reducing the stress at crack tip. Application of jacketing also increases the stiffness and load carrying capacity of beam because of larger cross section of the jacketed member. Perfect bonding between old and new concrete and addition of extra longitudinal reinforcement is very necessary for the jacketing to be effective.

Julio et al. [68] studied the influence of the interface treatment on the structural behavior of seven full-scale columns models strengthened by RC jacketing after their surface was prepared considering various techniques. The column models were tested under monotonic loading. Several parameters such as cracking pattern, yielding load, maximum load, stiffness, etc. were taken into consideration. The jacketing of the columns led to higher load carrying capacity. All the column models behaved monolithically independent of the adopted interface preparation method. However, the column model in which a non-adherent jacket was provided showed varying behaviour due to prominence of non-adherence. The jacketing of the columns also led to increase in the stiffness of the column.

Flyash (FA) was utilized as a basic ingredient of a new geopolymeric material in a study carried out by Swanepoel and Strydom [69]. FA was obtained from a large coal based fuel producing plant. The authors described the proposed mechanisms of formation of reaction products in a flyash based geopolymer as dissolution, transportation or orientation, as well as a reprecipitation (polycondensation) step. Geopolymer was prepared by mixing FA, kaolinite, sodium silicate solution, sodium hydroxide and water. The samples were cured at different temperatures for different time span. The geopolymer cured at 60 ºC for 48 hours provided optimal result by attaining maximum strength of almost 8 MPa after 28 days as seen from Fig. 1.28.

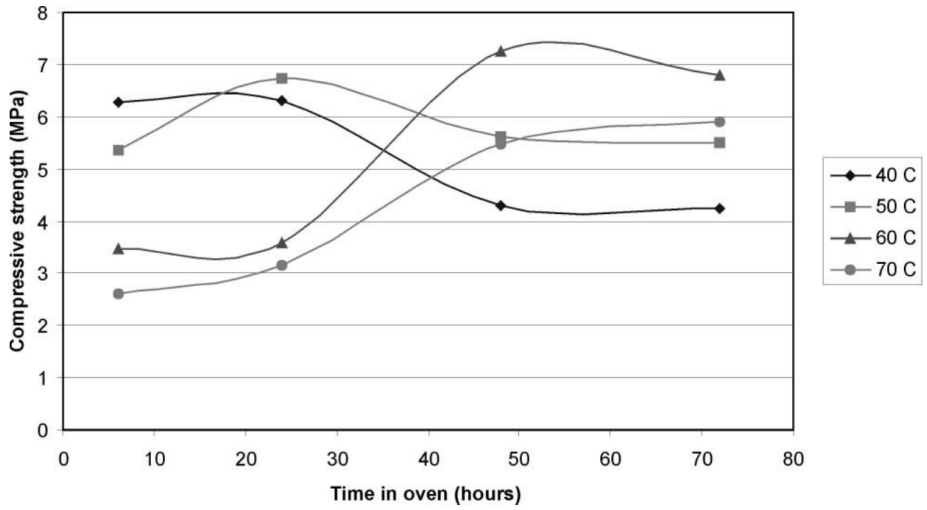

Figure 1.29: Compressive strength development after 28 days at different temperatures (*Swanepoel and Strydom* [69]).

Fernandez-Jimenez et al. [70] carried out microscopic study FA based geopolymer paste. The FA was activated using sodium hydroxide solution and oven-cured at 85 ºC for 5 h, 24 h and 60 days. Results showed from the study showed continuous increase in the degree of reaction with time (Fig. 1.29). It was concluded that the activation reaction rate and chemical composition of the production of geopolymerisation depend on particle size distribution and the mineral composition of fly ash, type and concentration of activator, etc.

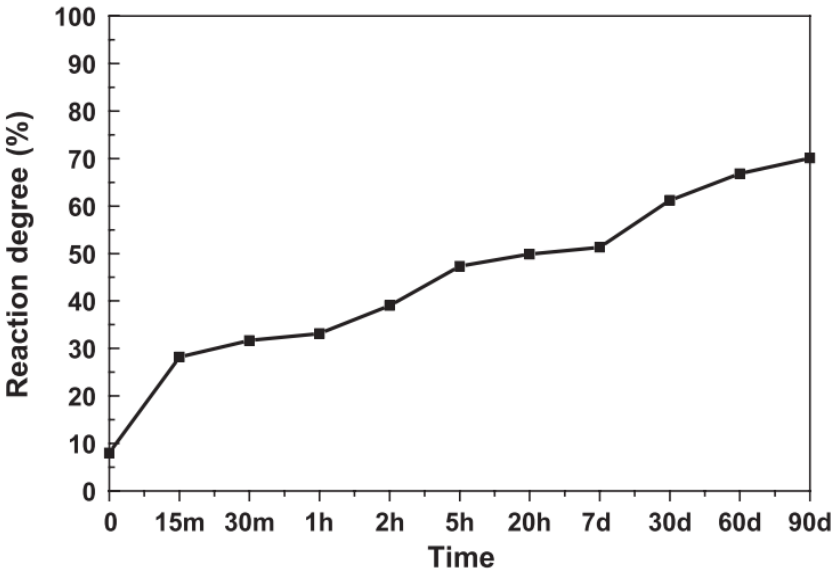

Figure 1.30: Evolution of the reaction degree of FA activated with 8 molar NaOH solution (*Fernandez-Jimenez et al.* [70]).

Duan et al. [71] prepared a novel concrete repairing agent using metakaolin (MK) based geopolymer activated using combination of sodium silicate and sodium hydroxide. A coating hydrophobic modification agent was applied over the surface of the samples to act as waterproof layer. The modification agent was in liquid state and consisted of water, aluminum tri-chloride (as a catalyst) and fatty acid. From the Fig. 1.30 it can be observed that the contact angle on the surface of geopolymer after modification significantly increased compared to that of before modification. Thus, the surface treatment achieved successful hydrophobic modification of geopolymer. The MK based geopolymer also possessed properties such as high workability (high flow diameter of 212 mm), fast setting (24 minutes), high compressive and bond strength.

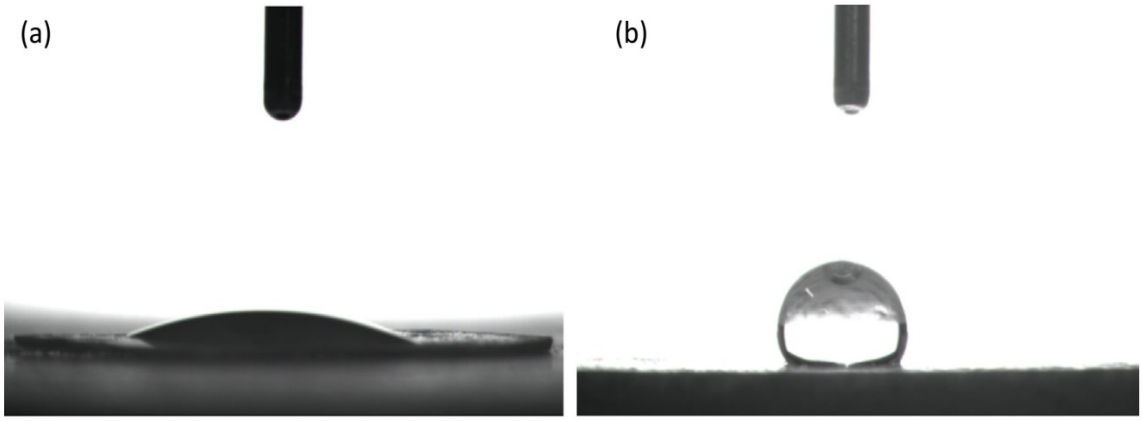

Figure 1.31: Contact angle of geopolymer before (a) and after (b) modification (*Duan et al.* [71]).

MK based geopolymer mortar (GPM) was also employed for preparing PCC pavement repair agent by Alanazi [72]. Both sodium silicate and sodium hydroxide solution were used as alkali activator. The 3 days compressive strength of GPM was found to be as high as 80% of its 28 days strength. It also outperformed the other commercial materials available for concrete repairing. The duration of curing affected the strength results as 24 hour cured specimens showed very low strength (Fig. 1.31). The bond strength decreased as the Portland cement mortar (PCM) deteriorated due to soaking in hydrochloric acid. As the substrate was soaked in hydrochloric acid, calcium chloride ($CaCl_2$) was formed due to reaction between hydrochloric acid and calcium hydroxide ($Ca(OH)_2$) of hydrated cement paste. Due to the formation of $CaCl_2$ the substrate became more porous and hence added to bond strength deterioration. Fig. 1.32 shows that increase in submersion time led to decrease in bond strength.

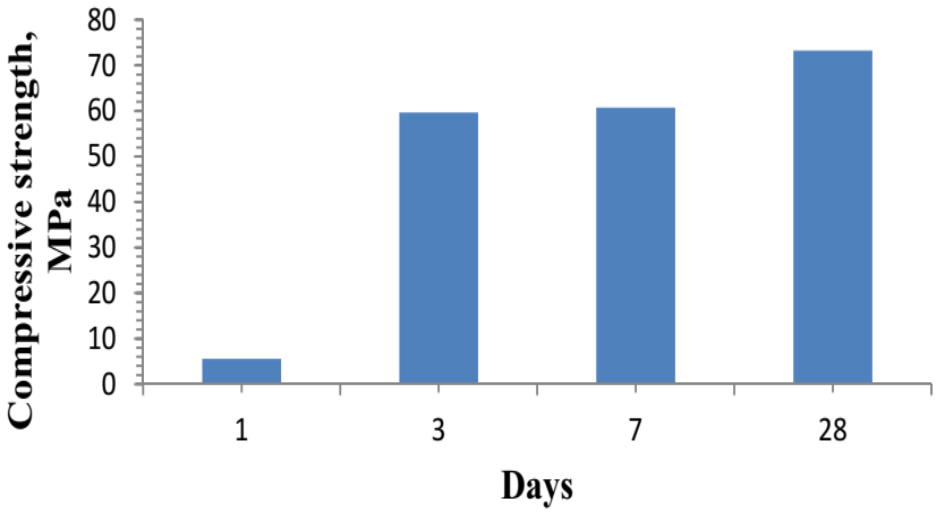

Figure 1.32: Compressive strength of MK based GPM (*Alanazi et al.* [72]).

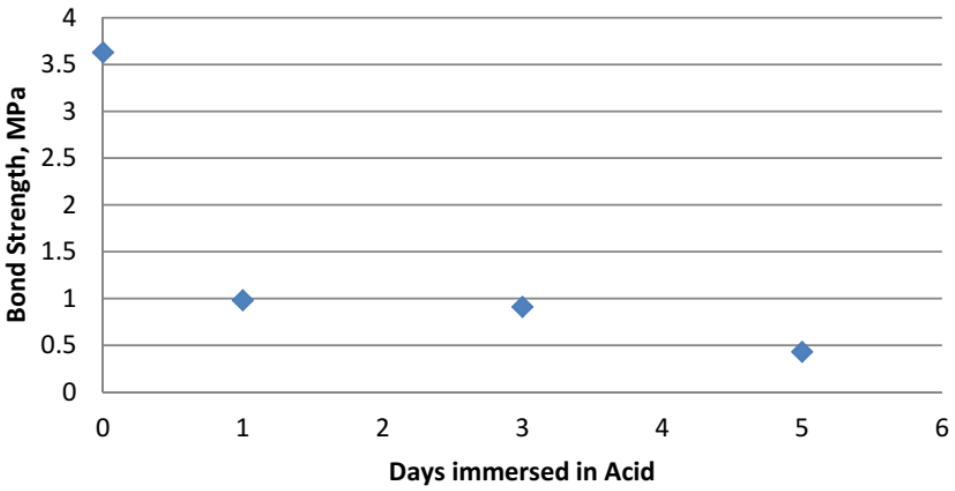

Figure 1.33: Bond strength between GPM and PCM with different deterioration time (*Alanazi et al.* [72]).

Zanotti et al. [73] prepared and tested MK based GPM for using as concrete repair agent. Bond strength was accessed by conducting slant shear tests on PCC substrate. Significant early-age cracking was observed in the repair mortar and along the substrate-GPM interface due to ambient curing of the specimens. Mild heat curing of the specimens prevented the early-age cracking and thus enhanced the bond strength. Addition of polyvinyl alcohol fibers to the GPM improved its cohesion with the substrate.

A new green retrofitting material, Green-USM-Reinforced Concrete (GUSMRC), developed and employed by Aldahdooh et al. [74] retrofitting damaged concrete beams and

flexural behavior was observed. GUSMRC was prepared using ordinary Portland cement (OPC), ultrafine flyash (FA), densified silica fume (SF), mining sand, short brass-coated micro-steel fiber and polycarboxylic ether-based superplasticizer. GUSMRC strips were provided as shown in Fig. 1.34. GUSMRC improved the flexural, shear behavior and serviceability of damaged concrete beams. The crack development and crack modes in the retrofitted beams were independent of thickness of the GUSMRC strips. Thicker strip led to higher failure load .

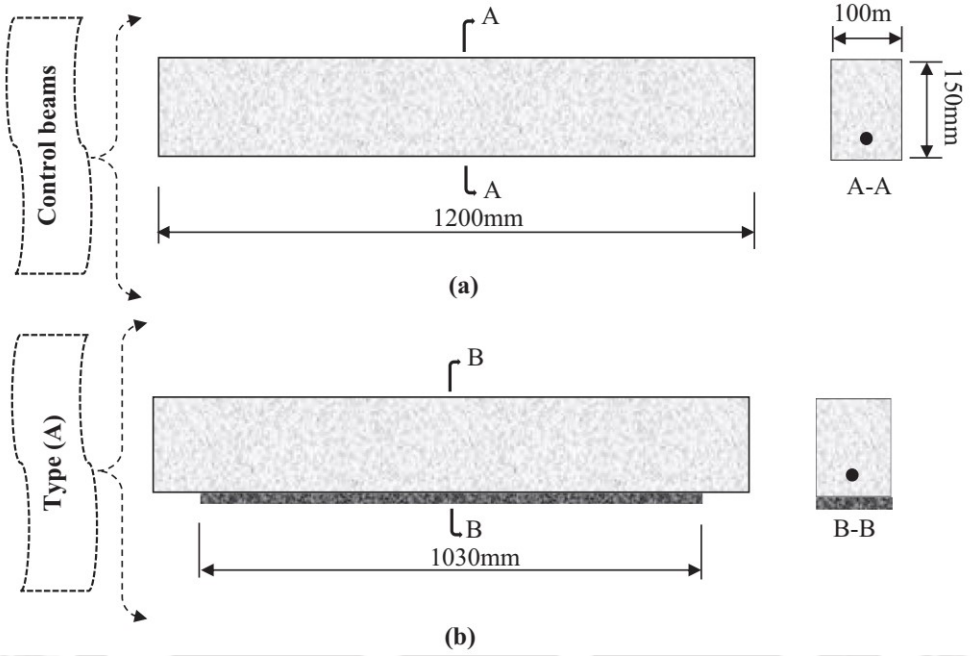

Figure 1.34: Retrofitting configuration: (a) control beams and (b) retrofitted beams (*Aldahdooh et al.* [74]).

1.6 Scope of the Present Study

Geopolymer has sturdy potential to replace the present binding materials in mortar and concrete and can bring a revolution in the construction industry. Review of literature on geopolymer reveals that investigation of geopolymer as concrete binder has been carried out in abundance. Many studies have been performed to investigate the fresh and hardened state properties of flyash, ground granulated blast furnace slag, metakaolin based geopolymer as binder in mortar and concrete including the durability studies. Geopolymer being able to offer early strength, needs further study for its application in repair and strengthening of reinforced concrete structures. Early strength development is a positive sign for early removal of form work so that damaged structures can be put to re-use earlier. However, application of geopolymer as a concrete repairing agent is relatively new and till date scanty number of literatures are only

available. There are numerous materials and technology which are readily available for application for concrete repairing and strengthening. Some of the repairing and strengthening materials are: epoxy resin, fibre reinforced polymer, steel plates, etc. However, these repairing and strengthening materials are expensive materials and the techniques involved in repairing and strengthening using these materials are sophisticated and hence, require skilled labourer for the engagement. Although several researchers have prepared geopolymer using various industrial by-product, very limited study is available on ultra-fine ground granulated blast furnace slag based geopolymer. Geopolymer, being a by-product and having potential to be used as repairing and strengthening material can be used as replacement of these expensive materials and sophisticated technologies. Geopolymer mortar and concrete preparation being similar to that of Portland cement mortar and concrete can be prepared easily. Since geopolymer preparation involves low cost, it can greatly influence the economy of developing nations, especially India.

1.7 Objectives of the Thesis

The objectives of the present thesis are listed below :

1. To prepare ultra-fine ground granulated blast furnace slag (UGGBS) based geopolymer mortar (GPM) containing varying amounts of flyash (FA) and superplasticizer (SP) and evaluate the fresh and hardened state properties by means of laboratory tests.
2. To prepare UGGBS based geopolymer concrete (GPC) containing varying amounts of FA and SP and evaluate the fresh and hardened state properties including bond strength by means of laboratory tests.
3. To repair damaged reinforced concrete (RC) beams by identifying and filling of induced cracks using UGGBS based GPM and Portland cement mortar (PCM); and study the behaviour under monotonic static load.
4. To strengthen damaged and undamaged RC beams by jacketing using UGGBS based GPC and Portland cement concrete (PCC); and study the behaviour under monotonic static load.

1.8. Organization of the Thesis

The content of the thesis is organized in seven major chapters in addition to abstract and

references. **Chapter 1** covers the introduction, literature review, research scope and objectives of the work. **Chapter 2** describes the various engineering properties of the materials and methods of laboratory testing involved in the work. **Chapter 3** presents the development of GPM and the laboratory tests for evaluation of the fresh and hardened state properties. **Chapter 4** presents the development of GPC and laboratory tests for evaluation of fresh and hardened state properties of GPC including bond strength. **Chapter 5** illustrates the method of repairing damaged RC beams using GPM and PCM; and presents the results from experimental investigation on the behaviour under monotonic static load. **Chapter 6** demonstrates the method of strengthening damaged and undamaged RC beams by jacketing using GPC and PCC; and presents the results from experimental investigation on the behaviour under monotonic static load. **Chapter 7** presents the summary and the major conclusions from this study, followed by some suggestions for future work. **Appendix** is added to provide detailed calculation of mix design and prediction of load carrying capacity of the test beams.

1.9 Closure

This chapter includes the introduction of geopolymer technology and the techniques used in repairing and strengthening of damaged and undamaged concrete. An extensive literature review is presented in this chapter related to the subject matter. The literatures are presented in groups which are mainly divided into: (i) geopolymer as binder, (ii) geopolymer as repairing and strengthening agent and (iii) concrete repairing and strengthening techniques. Finally on observing the various inadequacies in the earlier studies on geopolymer, the scope and objectives of the present study have been listed in this chapter. The organisation of the thesis is also outlined in the present chapter.

Chapter 2

Material Characterization

2.1 Overview

This chapter describes the properties of the materials involved in the preparation geopolymer mortar (GPM) and geopolymer concrete (GPC) along with Portland cement mortar (PCM) and Portland cement concrete (PCC). The desired mix proportions of the concrete for preparing the specimens that were tested in the laboratory were composed by carrying out proper mix design. The details of the mix design are stated in this chapter. The properties of materials of concrete required for the mix design were evaluated by conducting laboratory tests as per the relevant Indian Standards Codes of Practice.

In the present study, reinforced concrete (RC) beams were also developed to facilitate the investigation on repairing and strengthening capacity of geopolymeric systems. The RC beams were cast to size as per the design performed to decide the size of the beams, reinforcement required, etc. based on the load carrying capacity of the beams. This chapter also describes the method of designing the RC beams.

2.2 Materials

2.2.1 Portland cement

The Portland cement mortar (PCM) and concrete (PCC) specimens were cast using ordinary Portland cement (OPC) 43 grade cement. The cement was tested in the laboratory for evaluation of physical properties such as fineness, standard consistency, setting time and specific gravity. The tests were conducted as per the provisions mentioned in relevant Indian Standard Codes of Practice.

Additionally, compressive strength of the cement was also evaluated as per provisions of IS 4031 (Part 6) 1988 [75]. Table 2.1 presents the results of the tests performed on the Portland cement (PC). The values of various properties of the PC were found to be within the range mention in the relevant Indian Standard Codes of Practice.

Table 2.1: Results from tests on Portland cement.

Name of the test	Relevant Indian Standard Codes of Practice	Test Result
Fineness	IS 4031 (Part 1) 1996 [76]	280 m^2/kg
Standard Consistency	IS 4031 (Part 4) 1988 [77]	29 %
Initial Setting Time	IS 4031 (Part 5) 1988 [78]	95 mins
Final Setting Time	IS 4031 (Part 5) 1988 [78]	310 mins
Specific Gravity	IS 4031 (Part 11) 1988 [79]	3.08
Compressive strength (at 3 days)		24.34 N/mm^2
Compressive strength (at 7 days)	IS 8112 2013 [80]	33.86 N/mm^2
Compressive strength (at 28 days)		44.78 N/mm^2

2.2.2 Ultra-fine ground granulated blast furnace slag

Ultra-fine ground granulated blast furnace slag (UGGBS) available indigenously was used as primary binding agent in the geopolymer mixes. The chemical property i.e. oxide composition of the UGGBS as determined by X-Ray Fluorescence (XRF) Spectrometer (Make - PANalytical, Nottingham, U.K.) is given in Table 2.2. The XRF analysis was carried out by the Quality Control Department of the manufacturer.

The colour of the UGGBS was whitish grey, Fig. 2.1. The specific gravity was determined as per the provisions mentioned in IS 1727 1967 [81]. The fineness was evaluated based on median particle size and specific surface area. Laser particle size analyzer (Make - Malvern Instruments Ltd, UK; Model - Hydro 2000MU) was employed for the determination of median particle size and specific surface area. Table 2.3 presents the physical properties of UGGBS. Field emission scanning electron microscopic (FESEM) image of UGGBS is presented in Fig. 2.2. The FESEM image was captured using Field Emission Scanning Electron Microscope (Make - Zeiss, Oberkochen, Germany; Model - Sigma) at 7500x magnification.

Table 2.2: Chemical composition of UGGBS.

Oxides	Amount (%)
Silicon dioxide (SiO_2)	33.60
Aluminium oxide (Al_2O_3)	22.50
Ferric oxide (Fe_2O_3)	1.30
Calcium oxide (CaO)	34.00
Magnesium oxide (MgO)	6.80
Sulphur oxide (SO_3)	0.15

Figure 2.1: Physical appearance of UGGBS.

Table 2.3: Physical properties of UGGBS.

Physical properties	Value
Specific gravity	2.84
Median particle sized d50	3.58 µm
Specific surface area	3010 m^2/kg

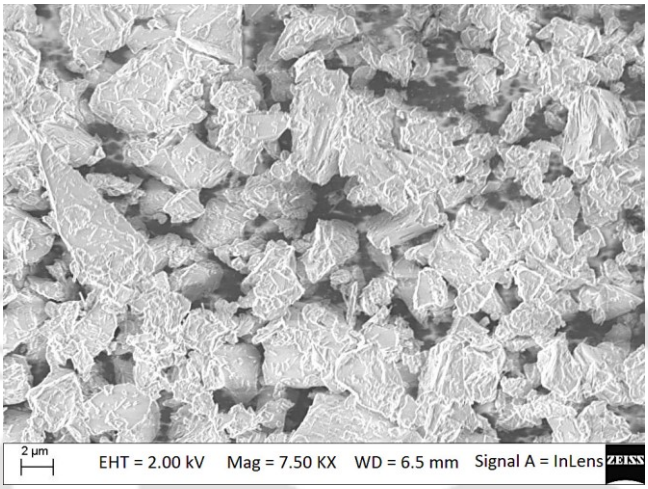

Figure 2.2: FESEM image of UGGBS.

2.2.3 Flyash

Class F flyash (FA) obtained from thermal power plant at Farakka, India was used for preparation of geopolymer mixes along with UGGBS. Class F FA is produced on burning older anthracite and bituminous coal. This fly ash exhibits pozzolanic characterstics, and contains less than 7 % lime (CaO). Table 2.4 presents the chemical property i.e. oxide composition of the FA.

Table 2.4: Chemical composition of FA.

Oxides	Amount (%)
Silicon dioxide (SiO_2)	55.47
Aluminium oxide (Al_2O_3)	25.37
Ferric oxide (Fe_2O_3)	6.20
Calcium oxide (CaO)	6.24
Magnesium oxide (MgO)	1.55
Sulphur oxide (SO_3)	0.90

The FA was of dark grey colour in appearance (Fig. 2.3). Alike UGGBS, the specific gravity was determined as per the provisions mentioned in IS 1727 1967 [80]. The fineness

was evaluated with the help of laser particle size analyzer. The physical properties of FA is presented in Table 2.5. Field emission scanning electron microscopic (FESEM) image of FA captured at 7500x magnification is presented in Fig. 2.4.

Figure 2.3: Physical appearance of FA.

Table 2.5: Physical properties of FA.

Physical properties	Value
Specific gravity	2.42
Median particle sized d50	26.33 µm
Specific surface area	894 m^2/kg

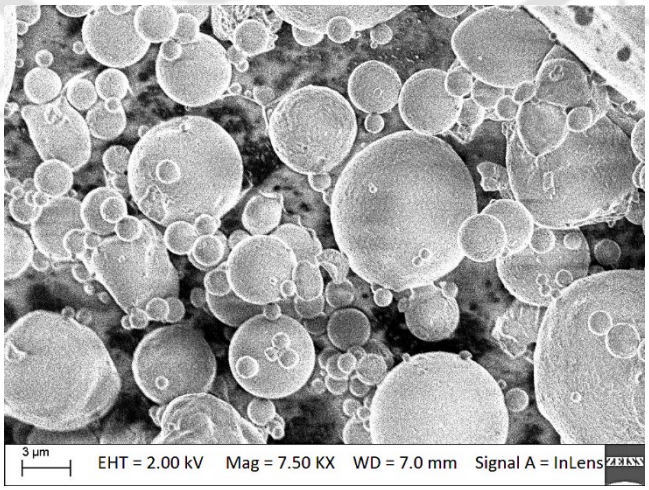

Figure 2.4: FESEM image of FA.

2.2.4 Alkali activators

In the present study, for activation of geopolymerisation process in the UGGBS mixes, sodium silicate (Na_2SiO_3) and sodium hydroxide (NaOH) were used as the alkali activator. Numerous types of alkali activators were used in geopolymer mixes by researchers for starting of the geopolymerisation process. The alkali activators were used in both isolated and combined form [22, 42, 82 - 86]. In this study, sodium based activators were preferred as alkali activator since they are cheaper than potassium based ones.

Alkali metal silicates and/or hydroxides are found to be the most suitable for using as alkali activator. Sakulich et al. [87] found an average strength of 64±3 MPa at 28 days in Na_2SiO_3 and NaOH activated geopolymer whereas, sodium carbonate (Na_2CO_3) activated ones could attain only 36±2 MPa. Altan and Erdogan [29] reported that Na_2SiO_3 and NaOH activated geopolymer showed approximately 22 % higher strength than geopolymer activated with Na_2SiO_3 and potassium hydroxide (KOH). Due to issues related to short and long term strength development and cost effectiveness, Na_2SiO_3 and NaOH are considered as suitable alkali activators for geopolymerisation process [23, 88 - 89]. However, alkali silicates are expensive. Moreover, they cause shortening of setting time and reduce workability [42]. Hence, to get rid of such disadvantages, alkali metal hydroxides can be better option. NaOH activated geopolymer can attain higher strength of around 400 % compared to Na_2SiO_3 activated geopolymer when cured at ambient temperature [29]. Carbon footprint of alkali metal hydroxide based geopolymer is lower than alkali metal silicate based ones [89]. It is observed that high amount of calcium hydroxide ($Ca(OH)_2$) in geopolymer results in unstable strength over period of time since strength at later ages are found to be much lower than the early ages strength. NaOH exhibits increase in strength over period of time [83]. Solubility of Al^{3+} and Si^{4+} ions is higher in NaOH solution than other alkali metal hydroxides [90] and usually, higher strength is attained after geopolymerisation due to higher dissolution [91]. NaOH is found to be the most suitable as activator in alkali metal silicate free geopolymers. Hence, in this study Na_2SiO_3 and NaOH; and only NaOH solution were used as alkali activators.

Commercially available Na_2SiO_3 solution and NaOH pellets were used to prepare the alkali activator. Fig. 2.5 shows the NaOH pellets. The Na_2SiO_3 solution consisted of 26.5 % SiO_2, 8 % Na_2O and 65.5 % H_2O. Physical properties of sodium silicate are furnished in Table 2.6. The NaOH solution of required concentration was prepared by mixing NaOH pellets

having 97-98 % purity with distilled water. The quantity of NaOH pellets (solids) in a solution varied depending on the concentration of the solution. The concentration of the NaOH solution is expressed in terms of molar (M).

For example, NaOH solution possessing a concentration of 10 M consisted 10 × 40 = 400 grams of NaOH solids (in pellet form) in 1000 grams of distilled water. Here, 40 is the molecular weight of NaOH.

Figure 2.5: Sodium hydroxide pellets.

Table 2.6: Physical properties of sodium silicate.

Property	Specification
Colour	colourless
Specific gravity	1.6 g/cm^3
Total solids content, by mass %	49

2.2.5 Aggregates

Alluvial sand was used as fine aggregate. The fine aggregate was acquired from a locally available source. The specific gravity of the sand was found to be 2.69 and water absorption to be 1.7 % when tested as per the provisions mentioned in IS 2386 (Part 3) 1963 [92]. On conducting the sieve analysis as per IS 2386 (Part 1) 1963 [93], the fine aggregate was found to be conforming to zone III of IS 383 1970 [94]. Table 2.7 presents the test result from sieve analysis of fine aggregate.

Table 2.7: Result from sieve analysis on fine aggregate.

Sieve sizes	Weight retained (g)	Percentage weight retained (%)	Cumulative percentage weight retained (%)	Percentage finer (%)	Remarks
4.75 mm	8	0.8	0.8	99.2	Zone III and fineness modulus: 3.33
2.36 mm	13	1.3	2.1	97.9	
1.18 mm	86	8.6	10.7	89.3	
600 μ	290	29	39.7	60.3	
300 μ	436	43.6	83.3	16.7	
150 μ	142	14.2	97.5	2.5	
75 μ	19	1.9	99.4	0.6	
Pan	6	0.6	100	0	

Well-graded crushed coarse aggregate of maximum 20 mm size was used for the concrete preparation. On testing for specific gravity of coarse aggregate as per the provisions of IS 2386 (Part 3) 1963 [92], it was found to be 2.61. The water absorption of coarse aggregate was 0.7 %.

To access the strength of coarse aggregate, aggregate crushing value (ACV) test was performed. ACV provides a relative measure of the resistance of an aggregate to crushing under a gradually applied compressive load. Higher the value of ACV of coarse aggregate, lower is the resistance against crushing under gradually applied load. The ACV of the coarse aggregate in this study was found to be 17.63. Sieve analysis of coarse aggregates was carried out as per IS 2386 (Part 1) 1963 [93]. The result of the sieve analysis is presented in Table 2.8. The fineness modulus of coarse aggregate was found to be 2.97.

2.2.6 Admixture

To modify the workability and setting time of the mortar and concrete mixes, superplasticizer (SP) was used. The SP was supplied by Fosroc Chemicals (India) Pvt. Ltd. Both sulfonated naphthalene based SP namely Conplast SP430SRV having specific gravity of 1.260 and polycarboxylate ether based SP namely Structuro 201 having specific gravity of 1.090 were used.

Table 2.8: Result from sieve analysis on coarse aggregate.

Sieve sizes	Weight retained (g)	Percentage weight retained (%)	Cumulative percentage weight retained (%)	Percentage finer (%)
20 mm	0	0	0	100
16 mm	349	6.98	6.98	93.02
12.5 mm	1107	22.14	29.12	70.88
10 mm	2182	43.64	72.76	27.24
6.3 mm	780	15.6	88.36	11.64
4.75 mm	574	11.48	99.84	0.16
Pan	8	0.16	100	0

2.2.7 Steel reinforcement bars

Reinforcement bars of grade Fe 550 SD conforming to IS 432 (Part 1) 1982 [95] were used in the study for preparation of concrete specimens and reinforced concrete beams. The reinforcement bars were tested in the universal testing machine (UTM) as per provisions of IS 1608 2005 [96] to determine the yield and ultimate strength. The average length of test specimen was 370 mm. The material properties of reinforcement bars of various sizes as obtained from the tests are presented in Table 2.9. The stress strain curve of a 12 mm bar is presented in Fig. 2.6.

Table 2.9: Properties of rebar.

Diameter of rebar (mm)	Yield stress (N/mm^2)	Ultimate stress (N/mm^2)	Young's modulus (N/mm^2)	Elongation (%)
16	547.4	675.62		17.25
12	550.87	681.94	200000	16.62
8	542.74	648.31		16.78

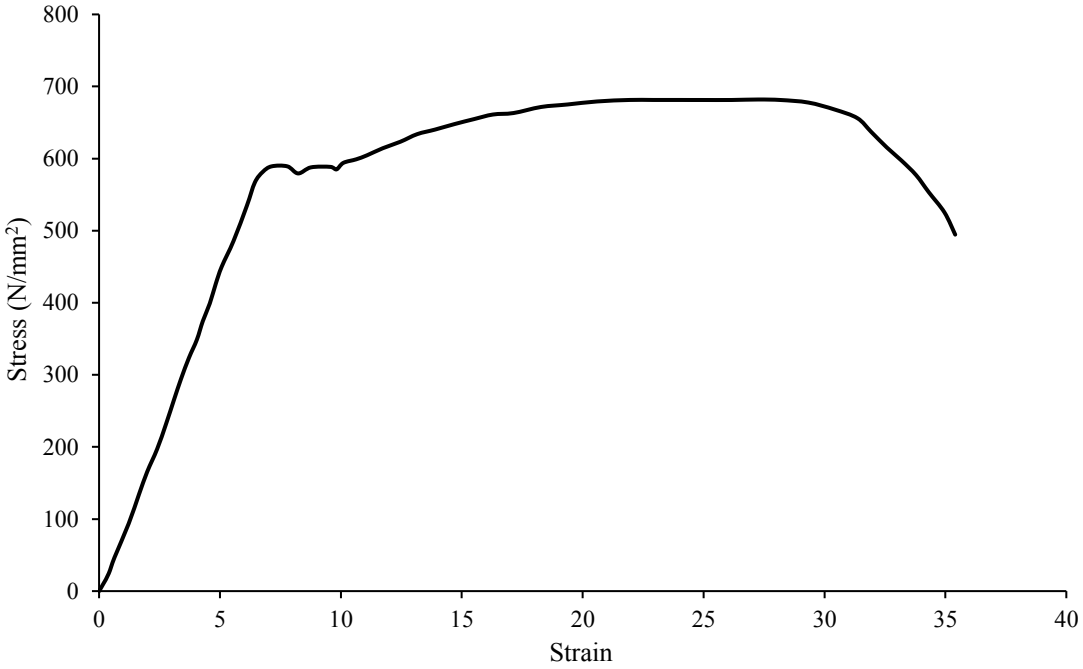

Figure 2.6: Stress-strain curve of grade Fe 550 SD 12 mm diameter rebar.

2.3 Mix Design

For better precision of the experimental work involving concrete, mix design was conducted to arrive at mix proportions of the concrete with desired strength. Appendix A describes the mix design conducted. The mix design was prepared following the provisions mentioned in IS 10262 2009 [97]. The properties of materials of concrete required for the mix design were evaluated by conducting laboratory tests as per the relevant Indian Standards codes. The mix design was done only for Portland cement concrete (PCC). In case of GPC, the mix proportion of PCC was modified maintaining constant quantity of fine aggregate and coarse aggregate and constant value of water to solids (w/s) ratio. In case of PCC, two concrete mix proportions were prepared with target strength 20 N/mm^2 and 35 N/mm^2. The former was used for preparation of PCC for casting of reinforced concrete beams, while the later was used for preparing the PCC for strengthening of the beams. Table 2.10 shows the result of the mix design for concrete.

Table 2.10: Mix proportion for PCC (kg/m^3).

Mix	Cement	Fine Aggregate	Coarse aggregate	Water/cement (w/c)
CC1	360	680	1128	0.55
CC2	425	611	1208	0.40

2.4 Design of Reinforced Concrete Beam

The reinforced concrete (RC) beams were designed as per IS 456 2000 [98]. The beams were designed as doubly reinforced beam possessing flexural load carrying capacity of 53.78 kN. The cross-sectional area was 150 mm × 200 mm and length was 2000 mm. The span of the beams while testing was 1800 mm. Appendix B presents the procedure of the design of the RC beam. The typical load carrying capacities of the beam evaluated by theoretical and experimental methods are presented in Table 2.11.

Table 2.11: Load carrying capacity of RC beam.

Theoretical load carrying capacity	Experimental load carrying capacity
53.78 kN	62.84 kN

2.5 Closure

A detailed description about the properties of all materials essential for casting, repairing and strengthening of reinforced concrete (RC) beams is presented in this chapter. Mix designs were carried out for deciding the mix proportion of concrete for casting of the RC beams. The various methods for testing of the materials are mentioned in this chapter. Design of RC beams were carried out for deciding the beam size and is reported in this chapter.

Chapter 3

Development and Testing of Geopolymer Mortar

3.1 Introduction

Geopolymer has strong potential to replace the conventional Portland cement (PC) in the construction industry. It can be used as sustainable supplementary cementitious material for the preparation of mortar and concrete. Geopolymer can be prepared by using silica, alumina and calcium oxide rich materials such as slag, flyash (FA), rice husk ash, etc. However, to attain strength, some of the geopolymeric systems have to be cured at elevated temperature [99]. Among the popular types of geopolymer, slag based geopolymer can gain strength even when cured at ambient temperature [88]. Numerous research works were carried out to study the behaviour of both slag and FA based geopolymeric systems in terms of workability, strength, durability, etc. [22, 83, 84, 90, 100 - 103].

Due to better strength and bonding capacity, geopolymer is used as repairing material by few researchers. Special attention to bonding capacity of geopolymer was provided in many investigations. Sarker [43], Wenzhong and Jing [45], Hu et al. [50] and Phoo-ngernkham et al. [89] worked on bond strength of geopolymeric systems. Results indicated that the geopolymer can be used effectively as concrete repairing agent as it possesses

appreciable bond strength.

Early strength development was observed in geopolymer mortar by various researchers such as Brough and Atkinson [22], Oner et al. [25] and Binici et al. [38]. Pozzolanic activity increases due to increase in fineness of binder which contribute to early formation of reaction products and thus leads to early strength [104]. However, such mortar or concrete exhibit lower setting time and workability compared to the mortar or concrete prepared with same binder of lower fineness [20]. Higher available particle surface area of binder facilitates increased pozzolanic activity for formation of reaction products instantaneously. Again, high particle surface area requires higher amount of alkali solution for reaction process, therefore decreasing the available amount of solution for providing mobility to particles within the mix [104, 105]. These reasons are to be attributed for the lower setting time and loss of workability in mortar and concrete mixes. In case of slag based geopolymer, the angular shape of slag particles obstruct their mobility and thus cause poor workability of mixes.

This chapter reports the works performed in the thesis to develop ultra-fine ground granulated blast furnace slag (UGGBS) based geopolymer mortar (GPM) for using as concrete repairing agent. The materials used, methodology for the mortar development and results of the laboratory investigations performed for this purpose are reported in this chapter. Such mortar have the potential to repair damaged RC members to withstand the loads for which it is designed. Flyash (FA) and superplasticizer (SP) were added to the GPM to alter the properties and to arrive at satisfactory setting time and workability while retaining the early strength gain property. Effect of variation of alkali activator concentration and time of addition of SP in GPM was also noted and compared with that of Portland cement mortar (PCM). In this study, laboratory experiments were conducted on total 33 numbers of mortar mixes including a controlled mix prepared using Portland cement.

3.2 Experimental Investigation

Geopolymer mortar (GPM) specimens were cast using ultra-fine ground granulated blast furnace slag (UGGBS) to conduct laboratory experiments for evaluating the fresh and hardened state properties. The tests included setting time test of the mixes, workability test and compressive strength test. Each mortar mix was tested at 1, 3, 7, 28, 56, and 91 days to access the strength gain behaviour at both early and later ages.

3.2.1 Materials

3.2.1.1 Geopolymer mortar

Ultra-fine ground granulated blast furnace slag (UGGBS) available indigenously was used as primary binding agent in the geopolymer mortar (GPM). Various amounts of Class F flyash (FA) and superplasticizer (SP) were used as additive in the GPM. Details of the properties of UGGBS, FA and SP are furnished in sub-section *2.2.2 Ultra-fine ground granulated blast furnace slag, 2.2.3 Flyash* and *2.2.6 Admixture* of Chapter 2. SP that was used was of sulfonated naphthalene (SN) and polycarboxylate ether (PE) type. Commercially available sodium silicate (Na_2SiO_3) solution and sodium hydroxide (NaOH) pellets were used to prepare the alkali activator for activation of the geopolymerisation process in GPM. Sub-section, *2.2.4 Alkali activators* of Chapter 2 presents the details of the Na_2SiO_3 and NaOH. NaOH solution of required concentration was prepared by mixing the NaOH pellets having with distilled water 24 hours before the casting of specimens. Alluvial sand that was locally available and conforming to zone III [94] was used as fine aggregate. The properties of fine aggregate is discussed in sub-section, *2.2.5 Aggregates* of Chapter 2.

3.2.1.2 Portland cement mortar

Ordinary Portland cement (OPC) 43 grade was utilized for preparing the Portland cement mortar (PCM). The details of the properties of OPC are presented in sub-section *2.2.1 Portland cement* of Chapter 2. The fine aggregates used in the preparation of PCM was same as used in preparation of GPM. Portable water available in the laboratory was mixed with dry Portland cement-fine aggregate mix for preparation of PCM.

3.2.2 Mix proportions

Mix proportion of the UGGBS based GPM was prepared based on provisions mentioned in IS 1727 1967 [81] and is presented in Table 3.1. The total binding agent mentioned here is defined as the total amount of UGGBS and FA in the mix. Na_2SiO_3 and/or NaOH solution was used as the alkali activator.

Table 3.1: Mix proportion for GPM (kg).

Mix	UGGBS	FA	a/b	Na_2SiO_3	NaOH (Molarity)	SP dosage (%)	SP Type	SP addition type
GM1	100	-	0.50	25	25 (10 M)	-	-	-
GM2	100	-	0.50	-	50 (10 M)	-	-	-
GM3	100	-	0.55	27.5	27.5 (10 M)	-	-	-
GM4	100	-	0.55	-	55 (10 M)	-	-	-
GM5	100	-	0.60	30	30 (10 M)	-	-	-
GM6	100	-	0.60	-	60 (10 M)	-	-	-
GM7	100	-	0.65	32.5	32.5 (10M)	-	-	-
GM8	100	-	0.65	-	65 (10 M)	-	-	-
GM9	80	20	0.60	-	60 (10 M)	-	-	-
GM10	70	30		-	60 (10 M)	-	-	-
GM11	60	40		-	60 (10 M)	-	-	-
GM12	50	50		-	60 (10 M)	-	-	-
GM13	80	20	0.65	-	65 (10 M)	-	-	-
GM14	70	30		-	65 (10 M)	-	-	-
GM15	60	40		-	65 (10 M)	-	-	-
GM16	50	50		-	65 (10 M)	-	-	-
GM17	70	30	0.60	-	60 (10 M)	0.5	SN	Type I
GM18	70	30		-	60 (10 M)	0.5	PE	Type I
GM19	70	30		-	60 (10 M)	1.5	SN	Type I
GM20	7 0	30		-	60 (10 M)	1.5	PE	Type I
GM21	70	30		-	60 (10 M)	3.0	SN	Type I
GM22	70	30		-	60 (10 M)	3.0	PE	Type I
GM23	70	30	0.60	-	60 (8 M)	1.5	SN	Type I
GM24	70	30		-	60 (8 M)	1.5	PE	Type I
GM25	70	30		-	60 (12 M)	1.5	SN	Type I
GM26	70	30		-	60 (12 M)	1.5	PE	Type I
GM27	70	30		-	60 (14M)	1.5	SN	Type I
GM28	70	30		-	60 (14 M)	1.5	PE	Type I
GM29	70	30	0.60	-	60 (10 M)	1.5	PE	Type II
GM30	70	30		-	60 (10 M)	1.5	SN	Type II
GM31	70	30		-	60 (10 M)	1.5	PE	Type III
GM32	70	30		-	60 (10 M)	1.5	SN	Type III

Note: *Total binder: fine aggregate = 1:3, a/b = alkali/total binder.*

The mortar mixes presented in Table 3.1 were prepared and tested to study the effect of following on setting time, workability and strength gain of GPM :-

i. Use of Na_2SiO_3 and NaOH; and only NaOH as alkali activator.
ii. Variation in the amount of alkali activator in the mortar.
iii. Addition of FA of varying amounts of 20, 30, 40 and 50 % by weight of total binding agent in the mortar.
iv. Addition of SP of varying amounts of 0.5, 1.5 and 3 % by weight of total binding agent in the mortar.
v. Variations of NaOH concentrations of 8, 10, 12 and 14 molar (M) in the mortar.
vi. Variation in the time of addition of SP.

Total 32 numbers of GPM mixes were prepared for conducting the laboratory tests. Mixes GM1 to GM8 consisted of only UGGBS and no FA and were prepared using varying amount of alkali activator. The mixes either consisted of both Na_2SiO_3 and NaOH or only NaOH as alkali activator. Mixes GM9 to GM12 and GM13 to GM16 having alkali/total binder (a/b) ratio of 0.6 and 0.65 respectively consisted FA of varying amounts along with UGGBS and were activated by NaOH only. Mixes GM17 to GM22 were modifications of GM10 where, two different types of SP of varying amounts were added. In mixes GM23 to GM28, consisting of UGGBS, FA and SP, the concentration of alkali activator (NaOH) was varied. GM29 and GM30; and GM31 and GM32 were similar to GM19 and GM20 respectively having difference in method of SP addition only.

The ratio of total binding agent to fine aggregate was 1:3 [81] . The ratio of Na_2SiO_3 to NaOH solution was kept constant at 1 when both Na_2SiO_3 and NaOH were used as alkali activator. Na_2SiO_3 and/or NaOH were used as alkali activator based on the works and recommendations of the researchers dedicated in the field of geopolymeric systems. The a/b ratios were selected within the range of 0.50 - 0.65 because a/b ratio less than 0.50 causes the mix to be quite dry which leads to trouble of handling (workability). Upper limit was set as 0.65 so as to avoid the occurrence of bleeding and segregation in the mixes. Maximum content of FA was kept at 50 % since studies showed that amount higher than this causes significant reduction of early and later compressive strength of geopolymer cured at ambient temperature [106 - 109]. Moreover, addition of FA of amount lower than 20 % cannot produce significant change in the properties of UGGBS based geopolymer. Lower limit of SP content was selected 0.5 % because amount lower than that have minimal effect in altering the properties of fresh geopolymer mortar and concrete, especially in case of PE based SP [110]. Meanwhile,

upper limit was set as 3 % to observe the effect of high dosage of SP on geopolymeric systems.

SP of both SN and PE types were added to the GPM in either of the following three types:-

i. Type I: SP added after the addition of NaOH solution to the mix.
ii. Type II: SP was mixed with NaOH solution and then added to the mix.
iii. Type III: SP added before the addition of NaOH solution to the mix.

The difference in all the three types depends upon the time of SP addition. In Type I, the SP was added to the wet mix which consisted of UGGBS, FA, fine aggregates and NaOH solution. After the addition of SP to the wet mix, it was blended thoroughly so that the SP got homogenously distributed. In Type II, SP was added to the NaOH solution and stirred properly. Later, the SP contained NaOH solution was added to the dry mix. In Type III, SP was added to the dry mix prior to the addition of NaOH solution. On addition of the SP, it was thoroughly mixed for homogenous distribution. NaOH solution was added to the mix at the end of this step of SP addition.

Table 3.2 presents the mix proportion of PCM. The mix proportion was prepared as per the recommendations in IS 1727 1967 [81] for testing of cementitious mortar. Controlled mix, CM1 was prepared using PCM. The water/cement (w/c) ratio of PCM was equal to the water/solid (w/s) ratios of the GPM mixes, excluding some mixes. Water/solid (w/s) ratios of GPM is the ratio between water and total solids in the GPM mix excluding fine aggregates.

Table 3.2: Mix proportion for PCM (kg).

Mix	Cement	Fine Aggregate	Water/cement (w/c)
CM1	100	300	0.40

3.2.3 Specimen preparation and curing

Prior to casting of geopolymer mortar specimens, alkali activator was prepared. NaOH solution was prepared by mixing NaOH pellets with distilled water as per desired molarity 24 hours before the casting of specimens and then allowed to cool. Fig. 3.1 shows preparation of NaOH solution. When Na_2SiO_3 and NaOH were used together as alkali activator, they were mixed with each other one hour prior to mixing with other mortar components.

Figure 3.1: Sodium hydroxide solution.

Following are the steps that were involved while preparing UGGBS based GPM specimens:-

i. Dry mix was composed manually by thoroughly mixing UGGBS, FA and fine aggregates for 2 minutes, Fig. 3.2.

ii. To this dry mix, alkali activator solution was added and the mixing processes was further continued for 3 minutes.

iii. SP was added to the mix by either of Type I, Type II or Type III method.

iv. On being ready, the fresh GPM was placed into the cube moulds for compressive strength test. Workability test was conducted using the GPM in fresh state. Fig. 3.3 shows GPM in fresh state. The colour of the fresh GPM was noted to be dark brownish grey colour.

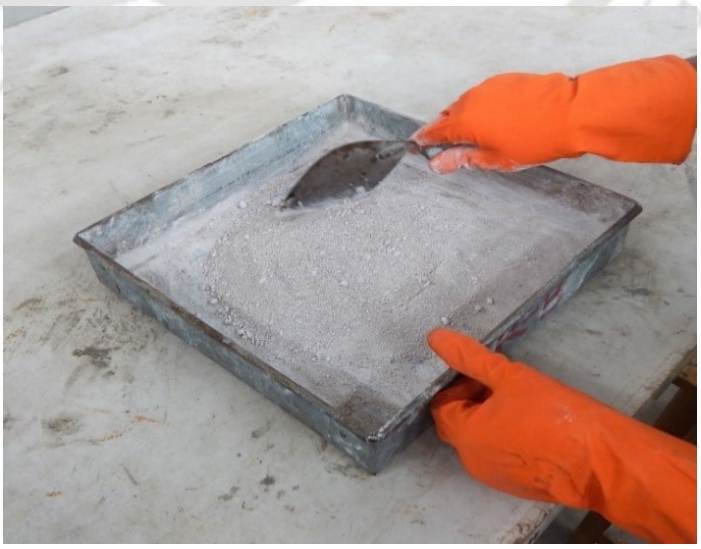

Figure 3.2: Dry mix consisting of UGGBS, FA and fine aggregate.

Figure 3.3: Geopolymer mortar in fresh state.

Geopolymer paste (GPP) and Portland cement paste (PCP) in fresh state were used for carrying out the setting time test. For GPP and PCP preparation, similar procedure and mix proportions were maintained as that of corresponding GPM and PCM excluding fine aggregate addition.

Cube specimens of size 50 mm were used to conduct the compressive strength test of mortar. Fresh mortar mixes were placed into cubes in two layers, each layer being tamped 25 times by tamping rod. Fig. 3.4 shows the GPM inside the cube mould. Later, these were placed under ambient temperature of 20 ± 2 ºC. After 24 hours of casting, the cubes were demolded (Fig. 3.5) and completely submerged inside water tank maintaining temperature of 20 ± 2 ºC and stored till the arrival of test day, Fig. 3.6.

Figure 3.4: Geopolymer mortar inside the cube mould.

Figure 3.5: Geopolymer mortar cubes ready for curing after 24 hours from casting time.

Figure 3.6: Geopolymer mortar cubes submerged inside water tank for curing.

3.2.4 Experiments

The provisions mentioned in IS 1727 1967 [81] were adopted for performing setting time tests of geopolymer pastes using Vicat apparatus, workability test and compressive strength tests of GPM and PCM. Fig. 3.7 presents setting time test on GPP. For assessing workability property of fresh mortars, flow table test was conducted immediately after mixing the mortar ingredients. A flow table is shown in Fig. 3.8. Fig. 3.9 (a) and (b) present flow table test on GPM. The results are specified in terms of flow index as given below:-

$$FI = \frac{FD - ID}{ID} \times 100 \quad (1)$$

Here, FI is the flow index in percent. FD is the average final base diameter of mortar mass measured on four diameters after jolting as per the codal provisions, ID is the original base diameter, which is 100 mm. Compressive strength tests were conducted at 1, 3, 7, 28, 56 and 91 days to assess the strength gain property of the mortars. Fig. 3.10 shows the crushing of cube in the compressive testing machine.

Figure 3.7: Vicat apparatus used for setting time test.

Figure 3.8: Flow table.

Figure 3.9 (a): Flow table test (Before the jolting of the flow table).

Figure 3.9 (b): Flow table test (After the jolting of the flow table).

Figure 3.10: Geopolymer mortar cube crushed in the compressive testing machine.

Field emission scanning electron microscopic (FESEM) images of UGGBS, FA, combination of 80 % UGGBS and 20 % FA; and 50 % UGGBS and 50 % FA were obtained and given in Fig. 3.11 (a) - (d) respectively. FESEM images of microstructure of mortar mixes at different ages were also captured and presented in the sub-section, *3.3.5 Microstructure study.*

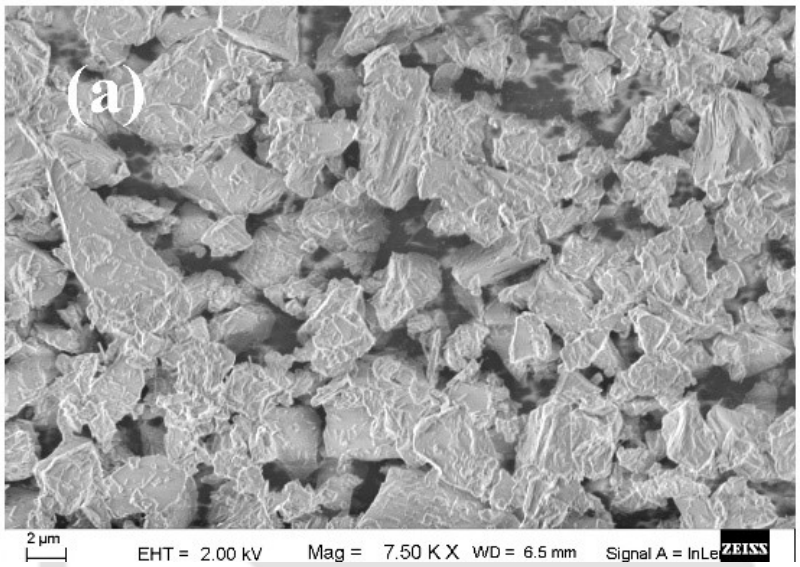

Figure 3.11 (a): FESEM image of UGGBS.

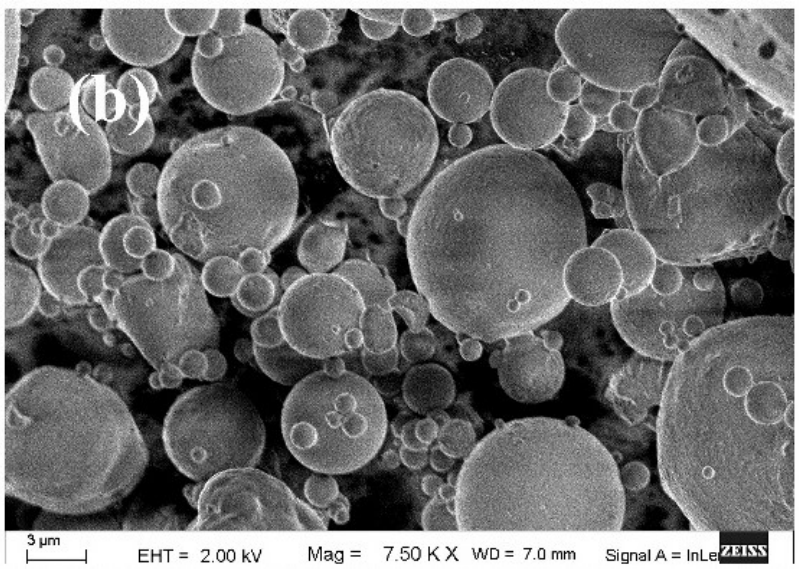

Figure 3.11 (b): FESEM image of Flyash.

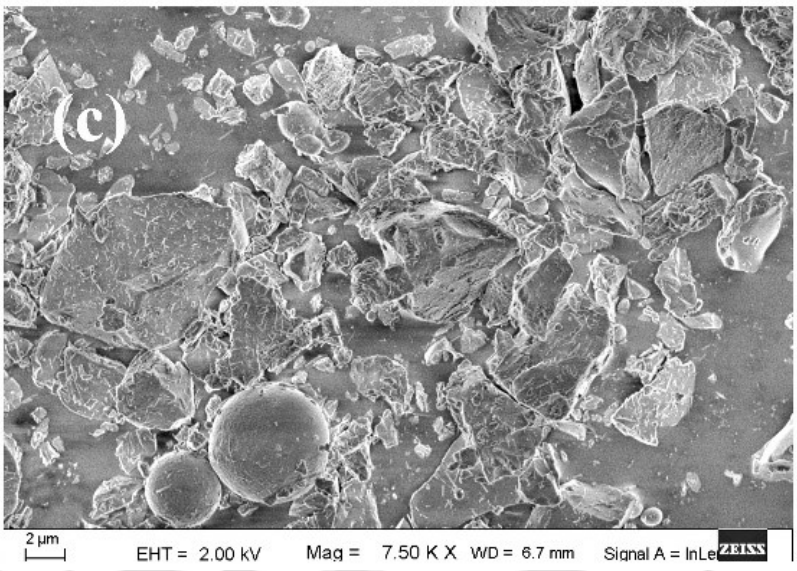

Figure 3.11 (c): FESEM image of mix of 80 % UGGBS and 20 % Flyash.

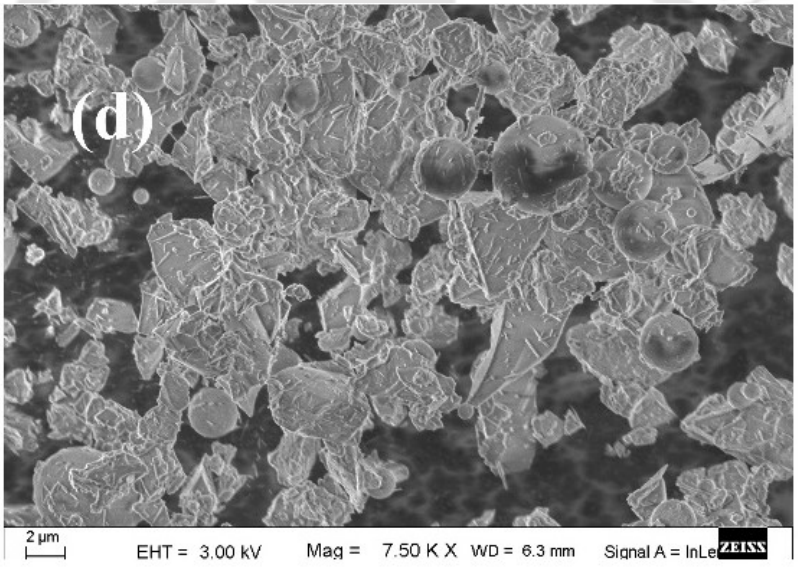

Figure 3.11 (d): FESEM image of mix of 50 % UGGBS and 50 % Flyash.

Statistical analysis was carried out from the data obtained from compressive strength to obtain mean (μ), standard deviation (σ) and coefficient of variation (ρ). The μ, σ and ρ of compressive strength test results at 3 and 28 days only are presented. The quality control in test procedures, precision and repeatability of the test method are indicated by σ and ρ.

3.3 Experimental Observations

3.3.1. Setting time

Fig 3.12, presents the setting times of the geopolymer mixes consisting of variation in the amount and type of alkali activator. Mix with a/b ratio 0.55 and consisting both Na_2SiO_3 and NaOH possessed workability issue due to its dryness. Hence, the setting time test gave erroneous results and therefore the setting time is presented here as zero. Mixes with NaOH as the alkali activator exhibited similar setting times for a/b in the range of 0.55 to 0.65. The mix with Na_2SiO_3 and NaOH as alkali activator with a/b ratio of 0.55, showed uneven distribution of the alkali activator due to poor workability (results are provided in the sub-section, *3.3.2. Workability*). Hence, the geopolymerisation process could not take place throughout the wet mix evenly and thus caused a lag in the setting. It was observed that setting times of mixes containing only NaOH as alkali activator were slightly more than the mixes containing Na_2SiO_3 and NaOH in combination as alkali activator. The reason for such behaviour has been explained by Karakoc et al. [111] and Chang [112] in their works on slag based geopolymeric systems. Mixes without Na_2SiO_3 are less viscous, allowing better mobility for the particles and thus require more time for setting.

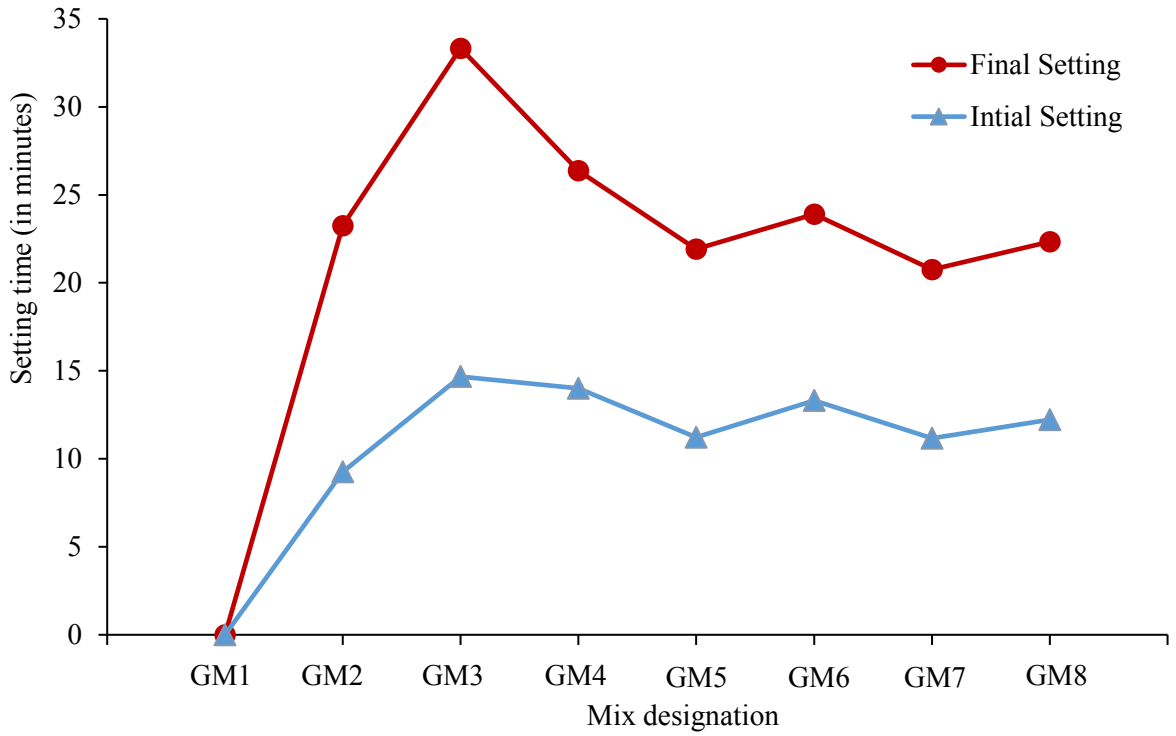

Figure 3.12: Effect of variation in the amount and type of alkali activator on setting times of GPM.

The effect of the addition of FA to the mixes containing only NaOH as alkali activator can be observed from Fig 3.13 and 3.14. Similar trends in the results were observed in mixes with a/b ratios 0.60 and 0.65. The addition of FA retarded the setting time of the mixes. Gradual increase in setting time occurred with the increase in FA content for both a/b ratios. This phenomenon is attributed to the fact that unlike UGGBS, FA cannot form geopolymerisation products instantly at early stages when subjected to curing at ambient temperature [106 – 107], thereby delaying the setting of the mixes. Moreover, since FA particles are spherical shaped as seen in Fig. 3.11. Hence, its addition allowed better mobility of particles in the mixes which eventually contributed to delay of setting time. However, the increase was more pronounced in mixes with FA content of 30 % and above, compared to those with FA content of 20 %.

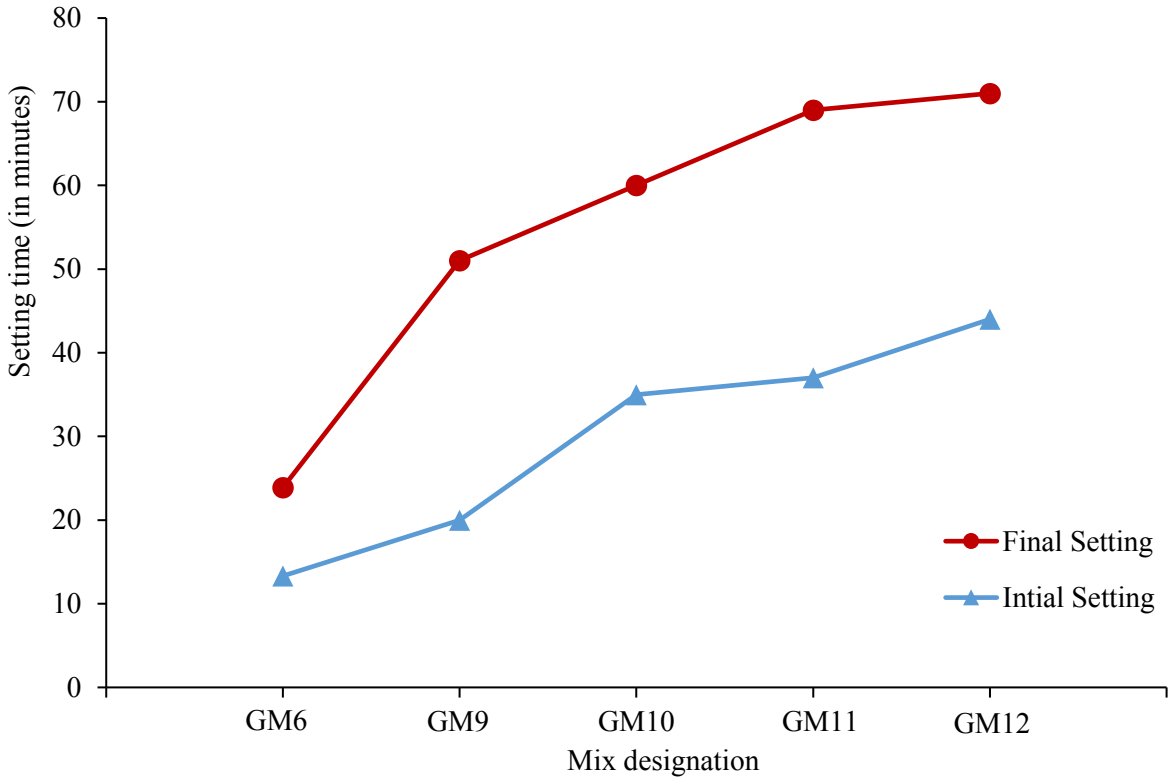

Figure 3.13: Effect of FA content on setting times of GPM for a/b of 0.6.

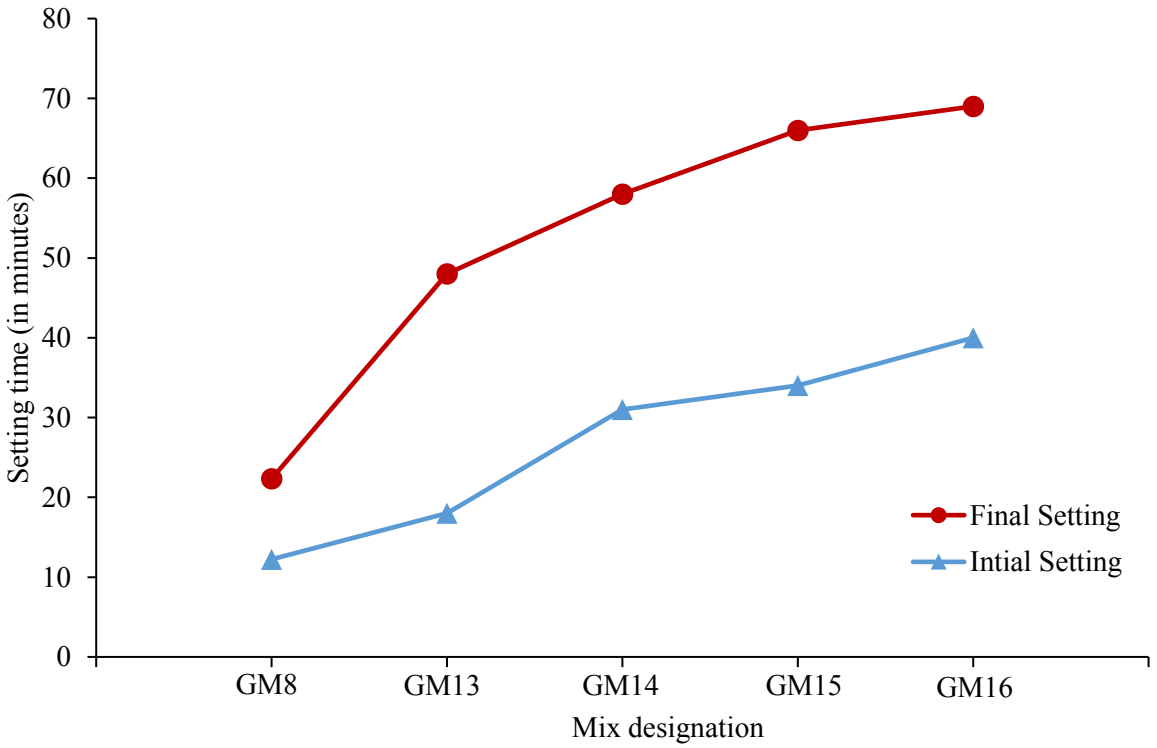

Figure 3.14: Effect of FA content on setting times of GPM for a/b of 0.65.

Addition of SP (both SN and PE based) to the mixes at constant FA content contributed to the retardation of early setting by preventing the geopolymerisation products from formation of bonds at early period, Fig. 3.15. The reason for this is similar to that of addition of FA in the mixes which provide better mobility to particles by producing less viscous mixes and thus retarding the setting times. In fact, the accelerating capacity of SP which is otherwise shown in decreasing the setting times of PC based systems is not shown in these geopolymeric mixes. Till 1.5 % SP dosage, the retarding effect was better exhibited by PE based SP compared to the SN based ones. In contrast to this, at SP dosage of 3 % high retarding effect was observed due to SN based SP in the mixes. It is presumed that addition of 3 % SN based SP caused new chemical reaction with NaOH, rendering it ineffective in carrying out the geopolymerisation process for instant formation of geopolymeric products. However, no such definite chemical reaction have been identified so far. But the sudden change of appearance of the dark greyish mortar to light brownish colour (see Fig. 3.16) and exhibition of segregation of particles give an impression of possible chemical reaction within the mix at SP content of 3 %. At lower dosage, however no such colour change could be observed. The phenomenon may indicate absence of chemical reaction at lower dosage. Laskar and Bhattacharjee [110] while carrying out study on geopolymer concrete reported that with

increased dosage of SP, segregation occurs forming a dense lower phase and a creamy upper phase within the mix. Criado et al. [113] observed similar changes due to addition of SP in the geopolymeric mixes.

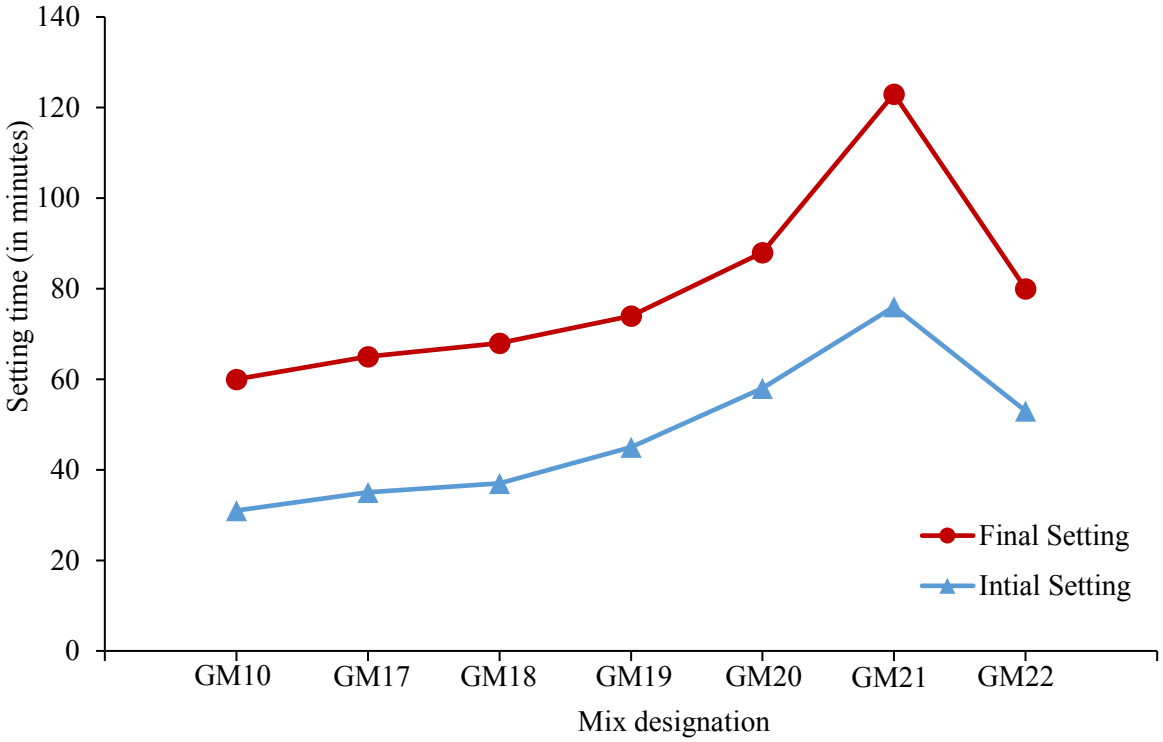

Figure 3.15: Effect of SP content and type on setting times of GPM.

Figure 3.16 (a): Appearance of fresh geopolymer mortar, GM 17 which consisted of 0.5 % SN based SP.

Figure 3.16 (b): Appearance of fresh geopolymer mortar, GM 19 which consisted of 1.5 % SN based SP.

Figure 3.16 (c): Appearance of fresh geopolymer mortar, GM 21 which consisted of 3.0 % SN based SP.

Figure 3.16 (d): Appearance of fresh geopolymer mortar, GM 22 which consisted of 3.0 % PE based SP.

Fig. 3.17 indicates that the change in alkali concentration changed the effect of SP on the setting behaviour of mixes. Increase in alkali concentration at constant FA content of 30 % and SP ratio of 1.5 % (both SN and PE based) decreased the setting time indicating the fact that increase in alkali concentration increased the rate of formation of bonds between the geopolymerisation products in the mixes. The trend that is observed by other researchers in geopolymeric systems without SP [108, 111], is also followed by these mixes containing SP. Drop in setting times for mixes with 10 M alkali activator was very less compared to that for mixes with 12 M and 14 M alkali activator when mixes with 8 M alkali activator were considered as reference. This was exhibited by mixes with both SN and PE based SP.

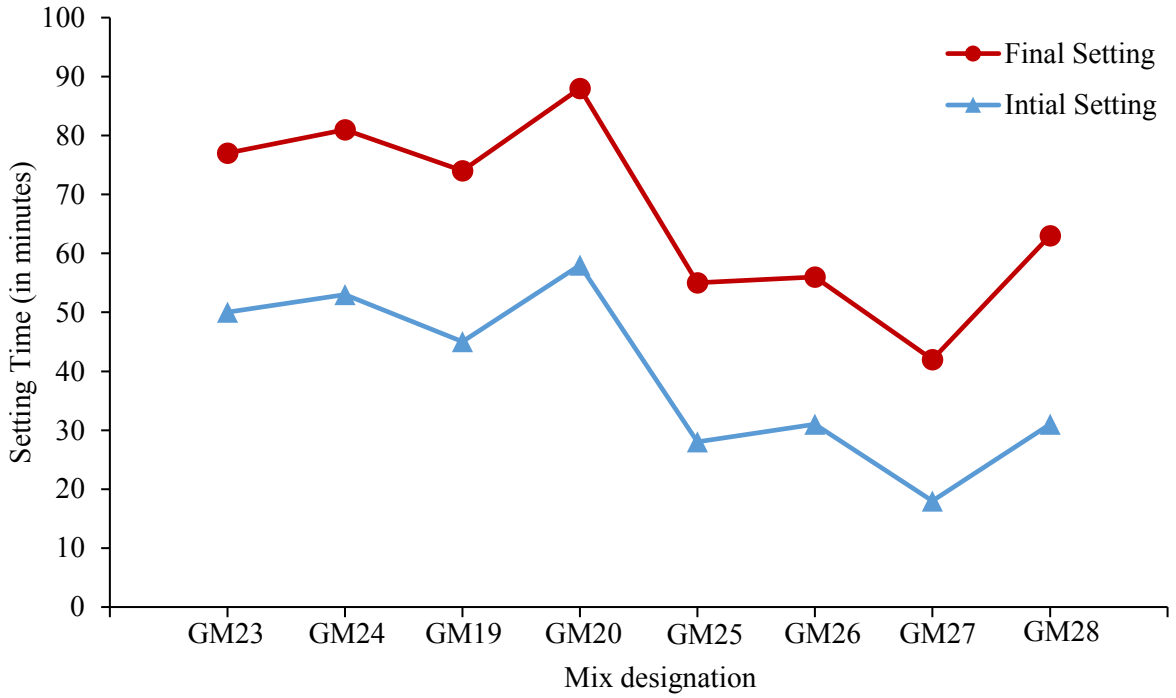

Figure 3.17: Effect of alkali activator concentration on setting times of GPM.

The time of SP addition also influenced the setting time of the mixes, Fig. 3.18. Setting retardation was highest in case of Type I SP addition. However, the difference in the setting times from the mixes with other mixing types is nominal. In all, PE based SP with Type I addition outperformed others in creating retarding effect in the mixes.

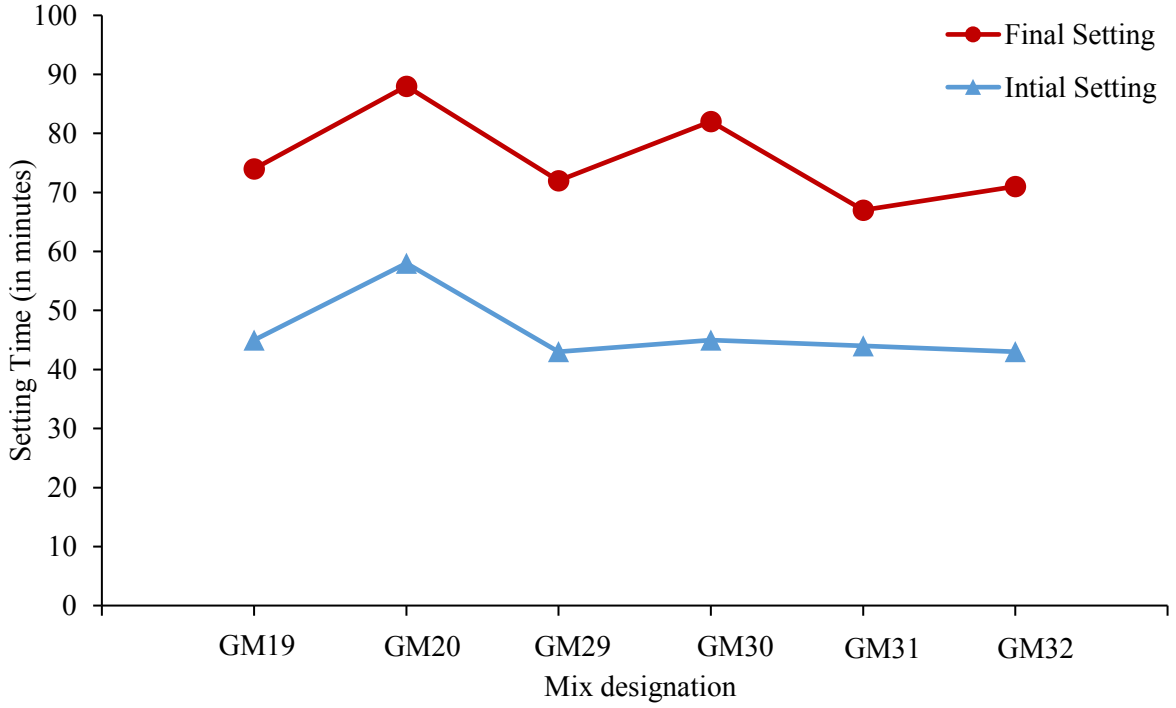

Figure 3.18: Effect of SP addition type on setting times of GPM.

The setting time of GPM was found to be much lower than that of PCM. Initial setting time of PCM mix, CM1 was 95 minutes and final setting time was 265 minutes. In some of the GPM mixes, the initial setting time was found to be lesser than that recommended in the IS 8112 2013 [114]. However, addition of admixture and alteration of alkali activator concentration led to enhanced initial setting time. The final setting time was significantly less than the maximum values in all the mixes which makes GPM a strong contender for recognizing it as a concrete repairing agent.

3.3.2 Workability

Workability was evaluated in terms of FI. It measures the ability of the mortar to flow due to specific numbers of jolts subjected when placed over the flow table. It is evident from results presented in Fig. 3.19 that workability of GPM mixes is influenced by the alkali activator type. FI of mixes containing both Na_2SiO_3 and NaOH as alkali activator were lower compared to the FI of mixes containing only NaOH as alkali activator. NaOH being less viscous than Na_2SiO_3 provided better facility for the movement of mix particles. Hence, mixes with NaOH as alkali activator exhibited better workability than the mixes with Na_2SiO_3 in combination as alkali activator. The increment in the a/b ratio monotonously enhanced the FI of the mixes.

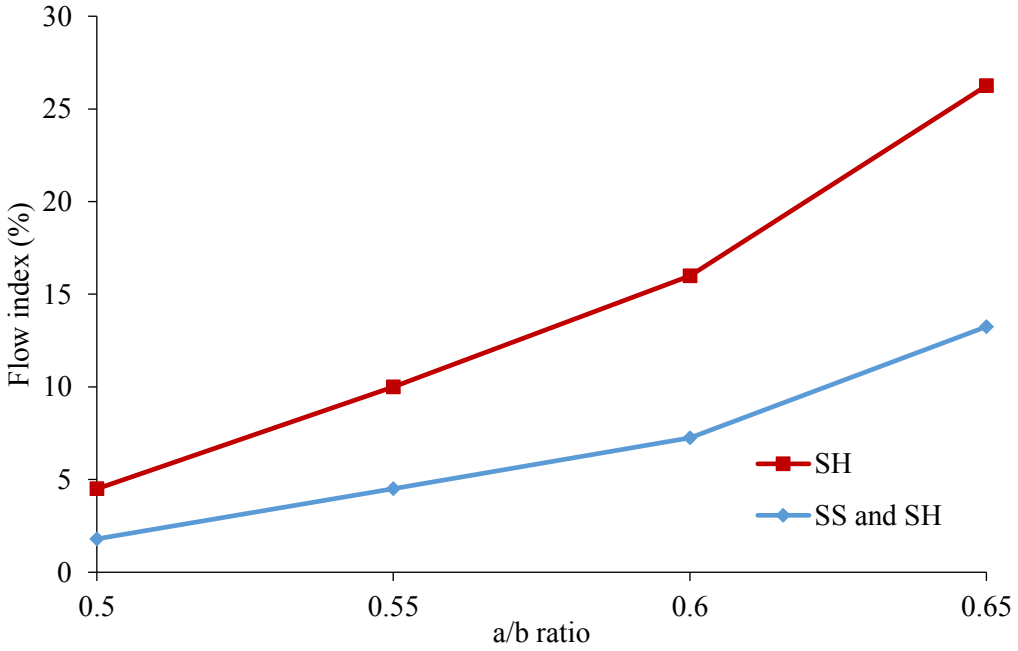

Figure 3.19: Effect of variation in the amount and type of alkali activator on workability of GPM.

Fig. 3.20 shows that by increasing the content of FA in the mixes, higher workability

can be attained. The steep rise of FI curve beyond 20 % FA content point indicated that increase in FI with increasing FA content was more for mixes with FA content higher than 20 %. This trend was exhibited by mixes with both a/b ratios. Increase in addition of FA increases the availability of smooth and spherical particles in the mixes which contribute to better sliding among the particles and reduction of friction which is otherwise caused due to presence of angular UGGBS particles. FESEM images in Fig. 3.11 show the particle shape and distribution in mixes. As FA content in the mixes increases, reduction of total friction among the particles occurs leading to better workability.

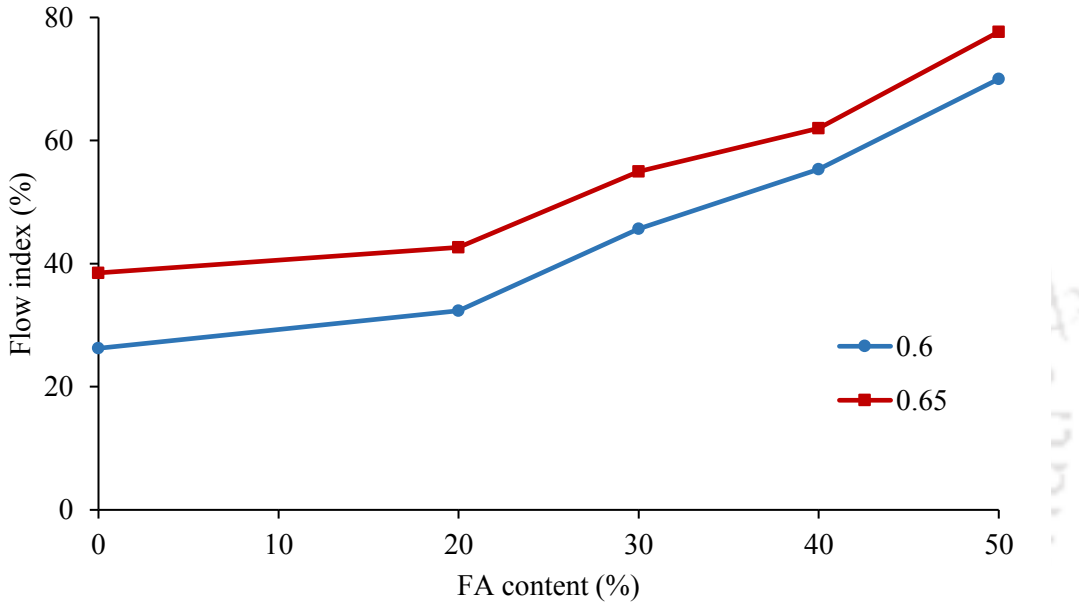

Figure 3.20: Effect of FA content on workability of GPM mixes for a/b of 0.6 and 0.65

Addition of SP (both SN and PE based) contributed towards increasing workability of the mixes with constant FA content of 30 % (see Fig. 3.21). Both the types of SP helped in releasing the liquid component in the mixes trapped in flocs by dispersing the solid particles. It is worth mentioning that the trend of increase in workability with the addition of higher dosage of SP changed for dosage between 1.5 to 3 %. At 0.5 % and 1.5 % SP dosage, mixes with PE based SP showed improved workability, on the other hand mixes with SN based ones showed higher FI at SP dosage of 3%. Such behaviour of mixes with SN and PE based SP have also been observed by Laskar and Bhattacharjee [110] in their work on FA based geopolymeric mixes consisting of SP. At SP dosage of 3 %, solid particles in the mixes got highly dispersed causing separation of semiliquid phase from the solid phase. Such segregation phenomenon was more prominent in mix with SN based SP. It is presumed that

this phenomenon has also caused the high retarding effect in the mix due to 3% SN based SP as seen from results in Fig. 3.15. Thus, it can be said that at very high SP dosage, SN based SP disperses the solid particles in mixes more than PE based SP but this also result in segregation.

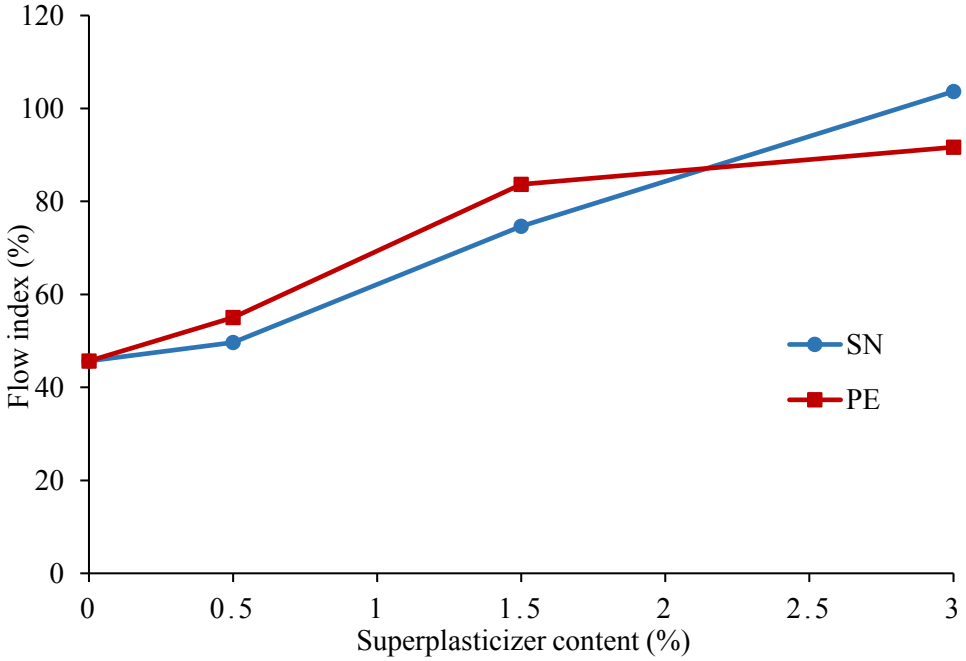

Figure 3.21: Effect of SP type and content on workability of GPM mixes.

The effect of change in alkali concentration on workability of mixes with constant FA content of 30 % and SP (both SN and PE based) dosage of 1.5 % is shown in Fig. 3.22. Increase in alkali concentration reduced the workability of the mixes. By increasing the alkali concentration, total solids in the solution was increased which resulted in more viscous alkali activator and caused obstruction to mobility of particles in the mixes. This resulted in decrease in workability. Such happening was also observed by Palacios and Puertas [115] while working with different types of SP in slag based geopolymeric mixes. The reduction in workability was higher for mixes with PE based SP. Addition of PE based SP to the mix with alkali concentration of 14 M caused formation of a very thick and viscous liquid phase in the mix which was not observed in other mixes. Therefore, it can be said that higher alkali concentration caused modification of chemical structure of PE based SP rendering it ineffective in improving the workability of the mixes. A steep fall of FI has been observed due to increase in alkalinity beyond 10 M for mix with PE based SP. But, for mixes with SN based SP, the fall was gradual and less steep than that of PE based SP ones. Henceforth, it is

understood that PE based SP can be used at alkali concentration upto 10 M without much loss of workability. As elaborated by Laskar and Bhattacharjee [110], this behaviour of geopolymeric systems donot lineup with that of PC based systems when alkali concentration is high. The mechanism related to this behaviour is not known so far.

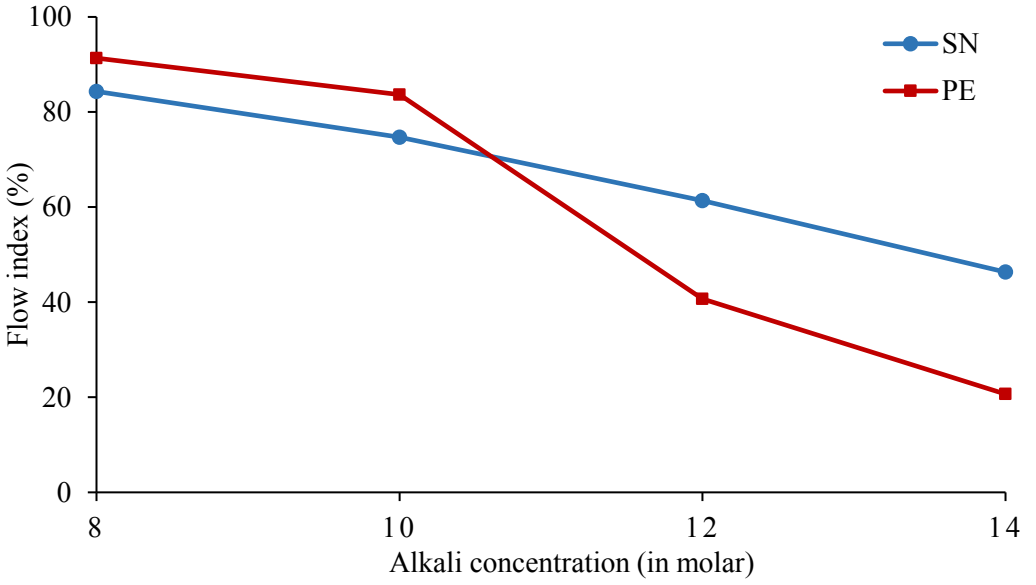

Figure 3.22: Effect of alkali concentration on workability of GPM mixes.

The mixes with Type I SP addition proved to be the most workable among the other types of SP addition. Flow indices of GPM mixes GM19, GM20, GM29, GM30, GM31 and GM32 are given in Table 3.3. When PE based SP was directly added to NaOH solution, appearance of the solution changed from transparent to whitish colour indicating some chemical change in the solution. Type I and III SP addition showed similar trend of workability affect. Mixes with SN based SP exhibited lower FI compared to PE based SP ones unless it is added to the mix by addition in the alkali activator directly.

Table 3.3. Effect of SP addition type on workability.

Mix	SP addition type	Flow index
GM19	Type I	74.67
GM20		83.67
GM29	Type II	62.33
GM30		50.67
GM31	Type III	45.67
GM32		64.33

3.3.3 Compressive strength

Influence of alkali activator type on the strength gain of mixes can be clearly seen in Fig. 3.23. Use of NaOH as alkali activator in the mixes contributed to better strength development compared to mixes with Na_2SiO_3 and NaOH together as alkali activator. This was observed for mixes with all the a/b ratios. NaOH being less viscous than Na_2SiO_3 and NaOH in combination, allows better mobility to particles in the mixes as seen from workability results. Due to this, particles got evenly distributed within the matrix and void spaces got reduced, leading to the development of homogenous geopolymeric product and early strength of the mixes. However, for mixes with Na_2SiO_3 and NaOH together as alkali activator, fast setting happened [42, 111, 112] and particles' mobility was restricted due to higher viscosity which caused uneven distribution of the geopolymeric products and hence, lower strength gain. The results are in conformity with the works of Lee and Lee [108] on FA/slag based concrete using Na_2SiO_3 and NaOH as alkali activator. Fig. 3.24 shows the crushed cubes post compressive strength test. The mix in which both Na_2SiO_3 and NaOH are used alkali activator showed low strength at early and later ages. The signs of incomplete geopolymerisation in the mortar were noted from the Fig. 3.24 (a) - (d) where the matrix of mixes (GM5 and GM7) with Na_2SiO_3 and NaOH showed light green colour appearance at 3 days. At 28 days, the matrix colour remained light green and unevenly spread throughout indicating incomplete geopolymerisation process in the mixes. On contrary, the matrix of mixes (GM6 and GM8) with NaOH as the only alkali activator showed dark green colour appearance even at 3 days {Fig 3.24 (e) and (f)}. Such mixes produced high early strength and hence the appearance of dark green colour of matrix indicated that most of the geopolymerisation products were formed at 3 days in the mixes. Similar appearance of matrix was observed at 28 days also {Fig 3.24 (g) and (h)}. In the mixes, GM6 and GM8 geopolymerisation process occurred evenly throughout the mix due to better workability.

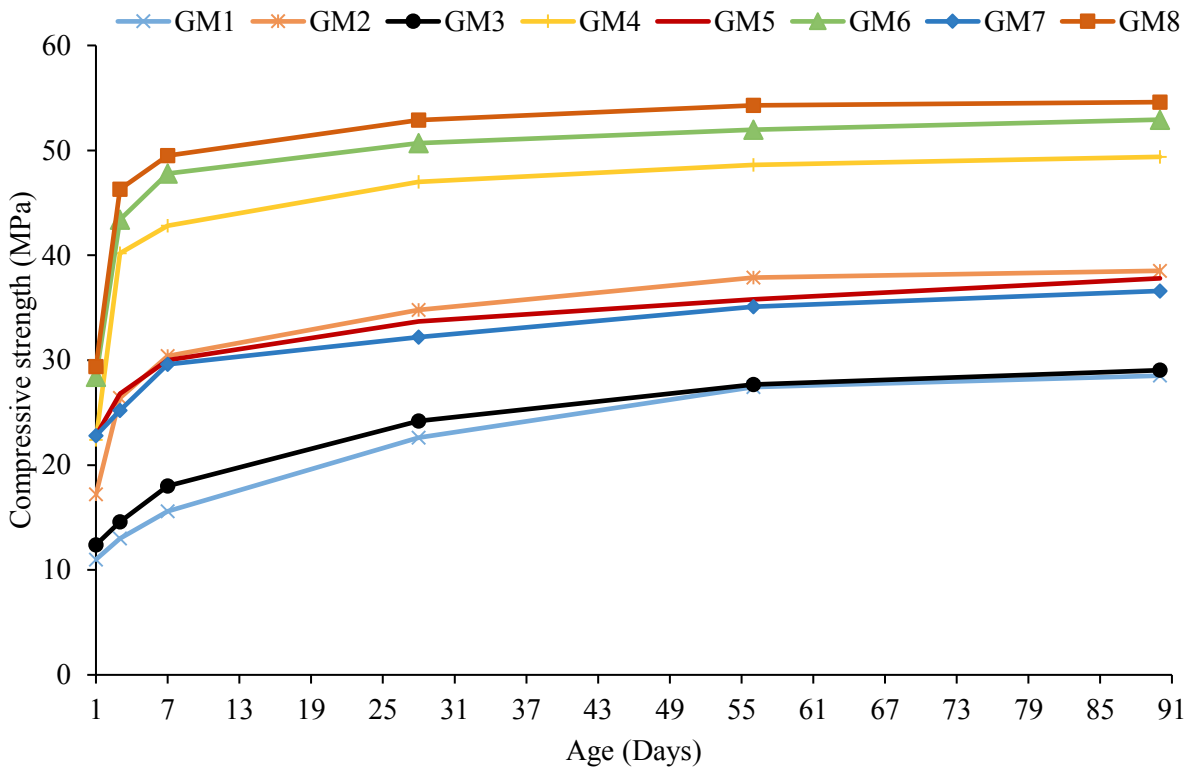

Figure 3.23: Effect of variation in amount and type of alkali activator on compressive strength of GPM.

Figure 3.24 (a): Crushed mortar cube at 3 days (GM5).

Figure 3.24 (b): Crushed mortar cube at 3 days (GM7).

Figure 3.24 (c): Crushed mortar cube at 28 days (GM5).

Figure 3.24 (d): Crushed mortar cube at 28 days (GM7).

Figure 3.24 (e): Crushed mortar cube at 3 days (GM6).

Figure 3.24 (f): Crushed mortar cube at 3 days (GM8).

Figure 3.24 (g): Crushed mortar cube at 28 days (GM6).

Figure 3.24 (h): Crushed mortar cube at 28 days (GM8).

Fig 3.25 and 3.26 show the effect of FA content on strength gain capacity of the mixes. Though addition of FA in the mixes retarded setting time and improved workability as seen in Fig. 3.12 and Fig. 3.19 respectively. However, it reduced the early strength gain property of mixes. This was common for mixes with both a/b ratios (0.6 and 0.65). The reduction in the early strength gain was more significant in mixes with FA content 40 and 50 %. Strengths of these mixes at later ages i.e. 28 days and beyond were notably higher than those at early ages indicating the contribution of FA in long term strength under curing at ambient temperature. However, such contribution could not help the mixes with FA content 40 and 50 % to attain strengths similar to that of the other mixes.

The main product in UGGBS based geopolymer is calcium silicate hydrate (C-S-H) when activated with alkaline solution [116]. The formation of C-S-H takes place even at ambient temperature. FA on the other hand is rich in SiO_2 and Al_2O_3. In alkaline medium, polymerisation occurs to transform aluminosilicates minerals to three dimensional polymeric chains [12]. However, FA can contribute to the strength development in geopolymer at early days only if cured at elevated temperature [106 , 109]. In this study, geopolymer mortars were cured at ambient temperature. Thus, contribution of FA in the strength development is insignificant at early ages.

In the mixes, angular UGGBS particles contributed to early strength gain by enhanced rate of geopolymerisation due to availability of higher particle surface areas. But, the angular shape and higher particle surface area reduced workability and accelerated setting of the mixes rendering it unsuitable for use as building material. On the other hand, though the

smooth and spherical FA particles led to lower rate of geopolymerisation, but they balanced the workability loss and retarded the setting because of the facts mentioned in the sub-section, *3.3.1 Setting time*. This was the reason behind exhibition of slow strength gain, higher workability and retarded setting time of the mixes with 40 % and 50 % FA content. The crushed cubes prepared by mixes GM11 and GM12 consisting of 40 % and 50 % of FA respectively are shown in Fig. 3.27. The matrix of the mixes were of unevenly distributed light green colour at 3 days similar to that of GM5 and GM7. However, at 28 days the matrix colour turn in slight dark green indicating that high amount of FA caused slow rate of strength development.

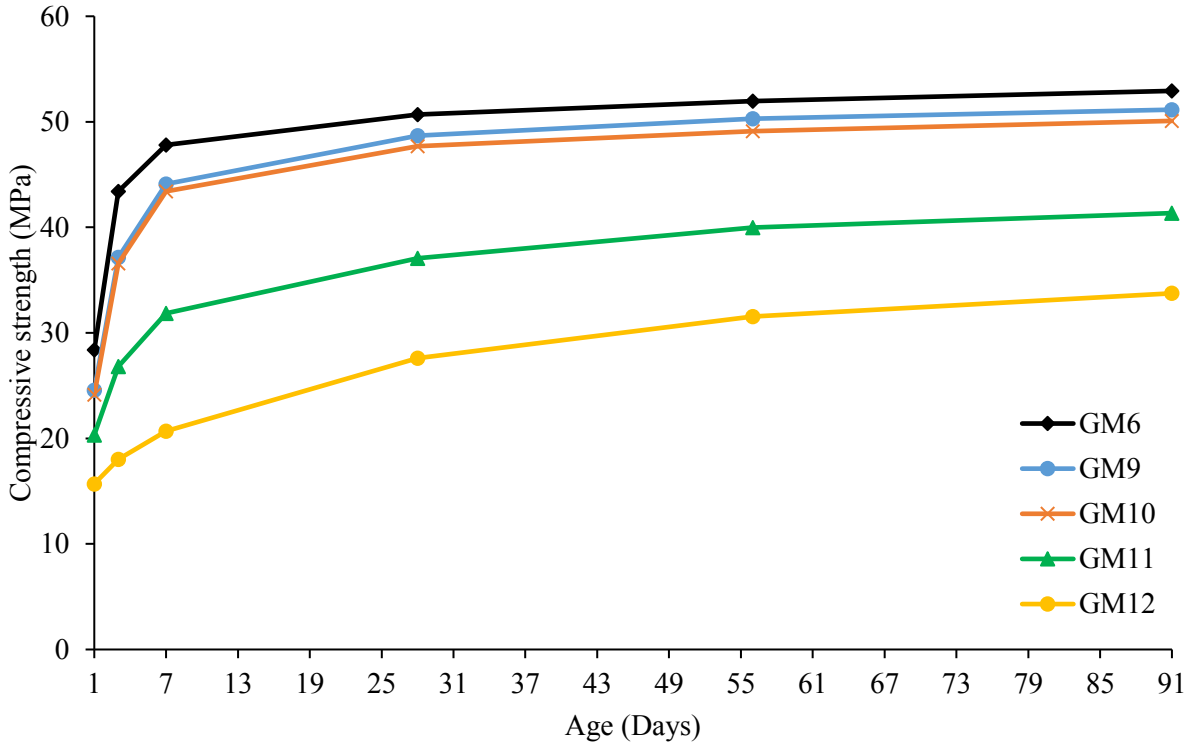

Figure 3.25: Effect of FA content on compressive strength of GPM mixes for a/b of 0.6.

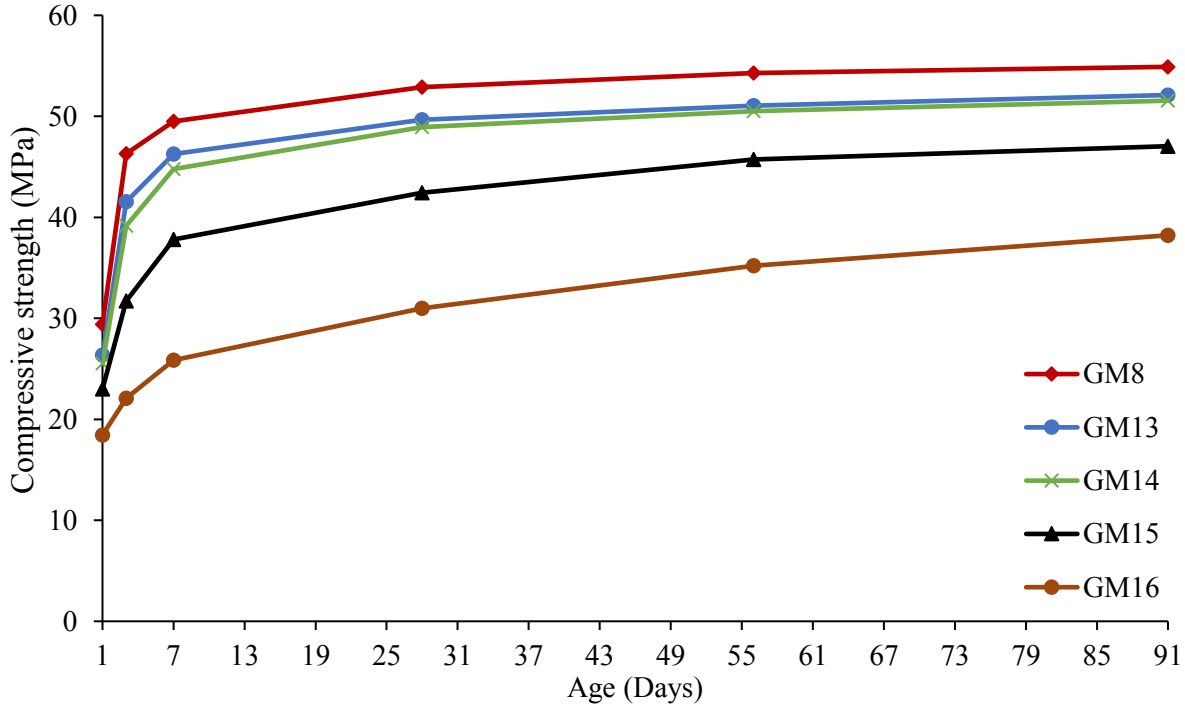

Figure 3.26: Effect of FA content on compressive strength of mixes with a/b of 0.65.

Figure 3.27 (a): Crushed mortar cube at 3 days (GM11).

Figure 3.27 (b): Crushed mortar cube at 3 days (GM12).

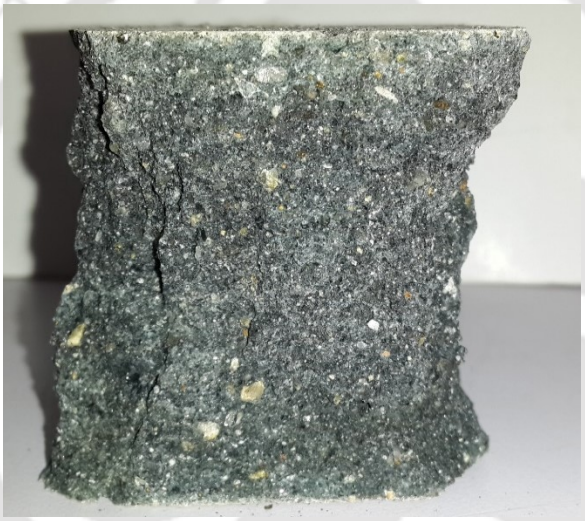

Figure 3.27 (c): Crushed mortar cube at 28 days (GM11).

Figure 3.27 (d): Crushed mortar cube at 28 days (GM12).

The amount of SP and its type significantly affected the strength gain process of the mixes. Huge variation in strength gain at various days was observed in mixes with both SN and PE based SP (see Fig. 3.28). Mixes with PE based SP attained higher strength at all days than SN based ones for all dosages. Among the two types of SP, the rate of strength development was higher in mixes with PE based SP. Compared to 28 days strength, about 80 and 90 % strength was attained at 3 and 7 days respectively by the mixes with PE based SP. In contrast, mixes with SN based SP could attain 70 and 80 % of the 28 days strength at 3 and 7 days respectively. Mixes with 0.5 % content of both types of SP exhibited highest strength at each selected day. For each type of SP, dosage higher than this amount lead to lower strength. Though in mixes with 1.5 % SP (SN and PE based) dosage, the strength drop compared to mixes with 0.5 % SP dosage was lower but pronounced strength drop was observed for mixes with 3 % SP (SN and PE based) dosage. This is an indication of possible occurrence of chemical reaction within the mix at SP content beyond 1.5 % which creates hindrance to the geopolymerisation process rendering the mix to gain strength slowly and also attain lower strength compared to that at lower dosage. Similar strength reduction with increase of SP content was observed by Douglas and Brandstetr [17].

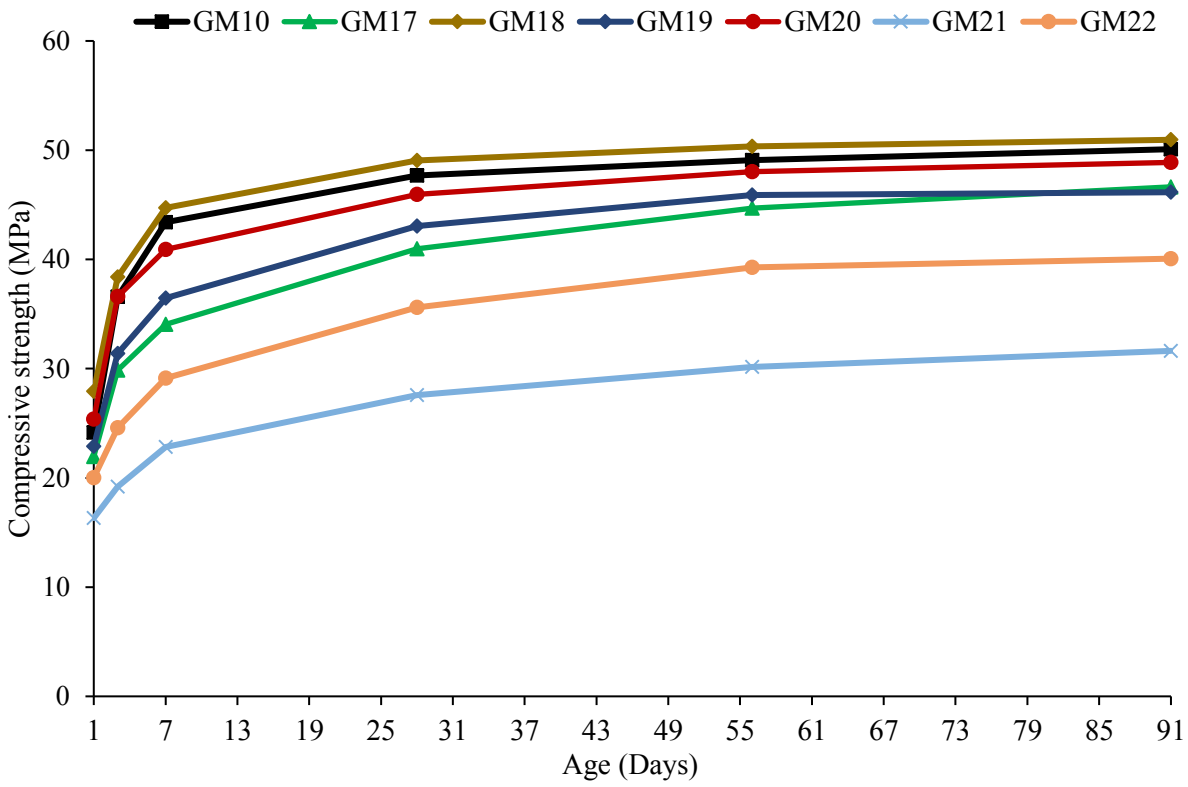

Figure 3.28: Effect of SP type and content on strength gain of GPM mixes.

Fig. 3.29 shows the effect of alkali concentration on strength gain rate of mixes containing 30 % FA and both SN and PE based SP of 1.5 % dosage. It was noted that at 8 M and 14 M alkali concentration, rate of strength gain was slow for mixes with both types of SP. Maximum rate of strength gain was observed in mixes with alkali concentration of 10 M. Several other researchers have observed similar behaviour which is in line with the exhibition of low rate of strength gain and attainment of low ultimate strength in mixes with 8 M concentration [21, 117]. But, the contradiction arises in case of mixes with 12 M and 14 M alkali concentration. Other researchers observed that with increase in alkali activator concentration, rate of strength gain and attainment of ultimate strength increases [29 , 42], but in case of present work, higher concentration of alkali beyond 10 M in the mixes with SP content causes negative effect on the strength gain rate. At concentration 14 M, the rate of strength gain dropped drastically. PE based SP performed better than SN based ones for all the mixes. Thus, it is understood that performance of SN based SP in strength gain process in the mixes is more affected by the alkali concentration, especially when the alkali concentration is high.

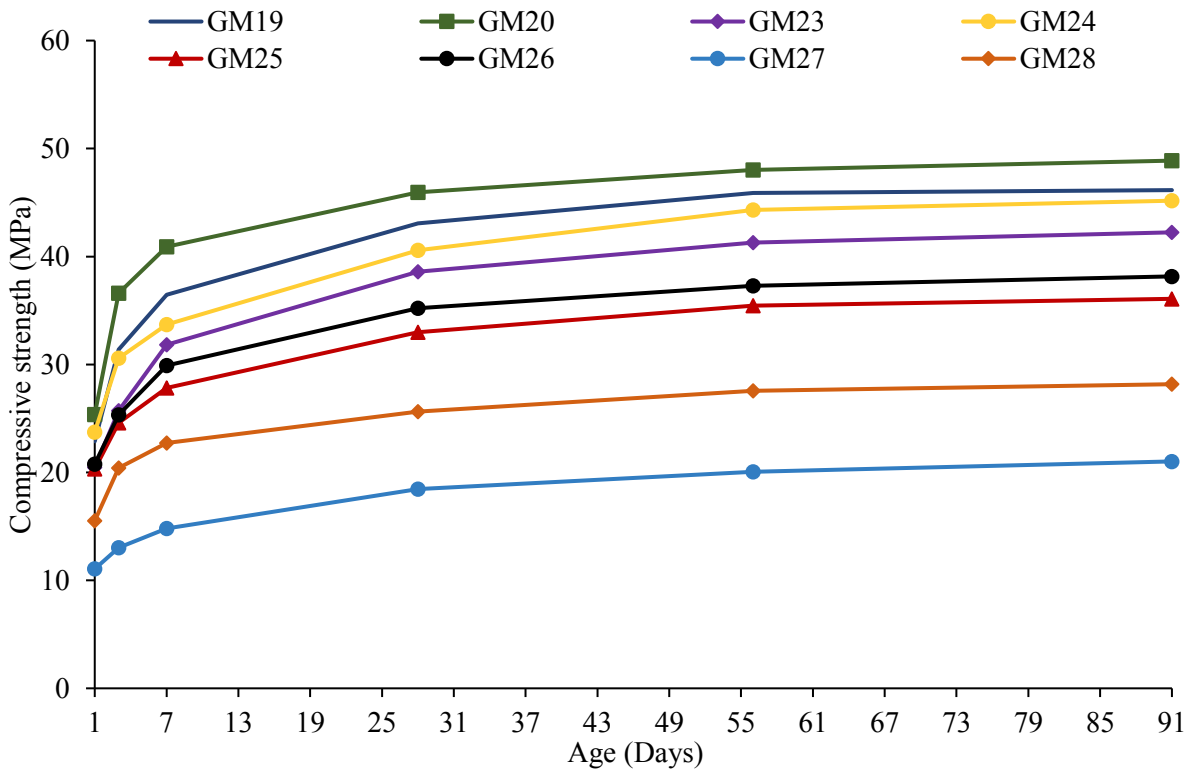

Figure 3.29: Effect of alkali concentration on compressive strength gain of GPM mixes.

Results in Fig. 3.30 show that Type I SP addition contributed to better strength gain than Type II and III. Mixes prepared with Type I SP addition could attain significantly higher

strength at ages 3 days and beyond than those with Type II and III SP addition. Though at early ages, the strength attained by mixes for all types of SP addition was apparently same, however mixes with Type I PE based SP addition attained highest strength at all ages. Type II SP addition proved to be the most ineffective.

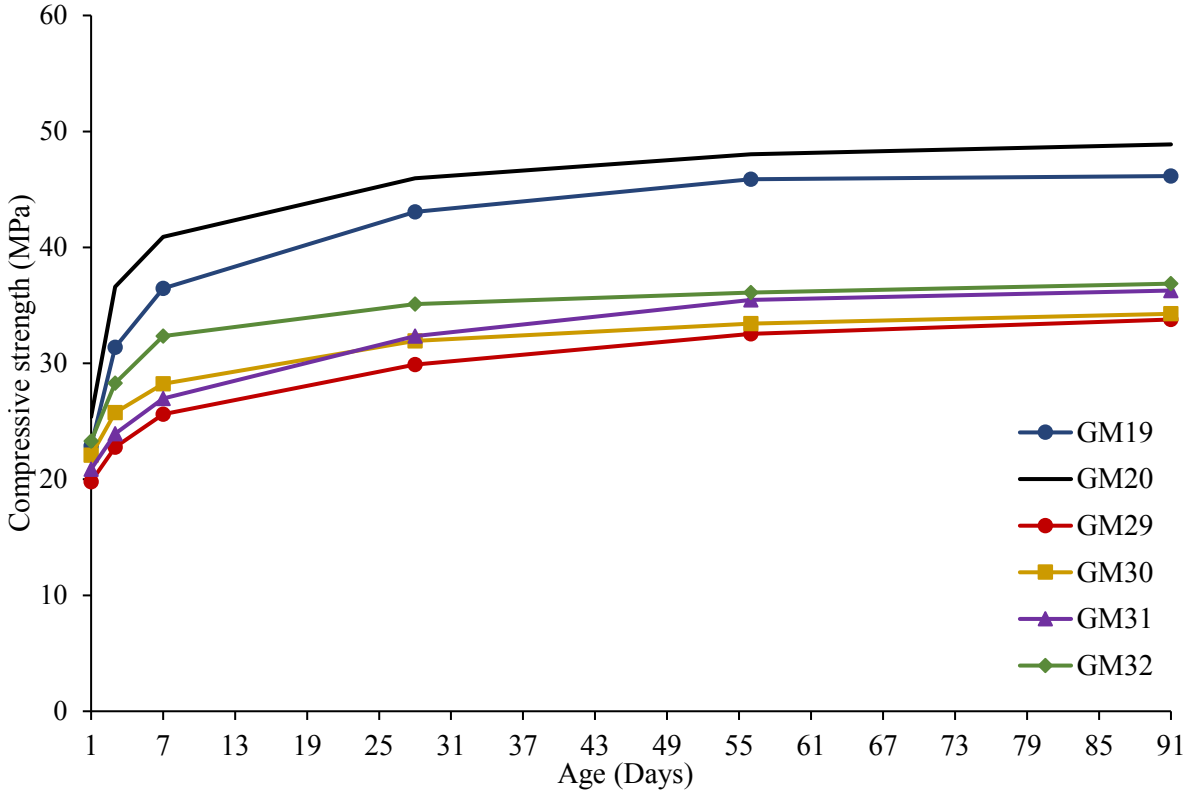

Figure 3.30: Effect of SP addition type on compressive strength gain of GPM mixes.

From the results, it was observed that GPM mixes possess early strength gain property. The strength gain were significantly higher at early ages compared to the strength of PCM. The compressive strength of PCM at various ages is furnished in Fig. 3.31. The 1 day strength of GPM was in the range of 50 - 70 % of the strength at 28 days and 3 days strength was in the range of 70 - 85 % of the strength at 28 days. The corresponding values in case of PCM were found to be 18 % and 55 %. High amount of FA in the mix played similar role in retarding setting time and increasing workability of the mix as done by lower amount of SP. However, such high amount of FA causes slow strength gain and even lower compressive strength compared to others. Addition of SP of PE origin on the other hand, can be an alternative to the mentioned issue as it retards setting time, increases workability and at the same time does not slow down the strength gain when added in lower dosage.

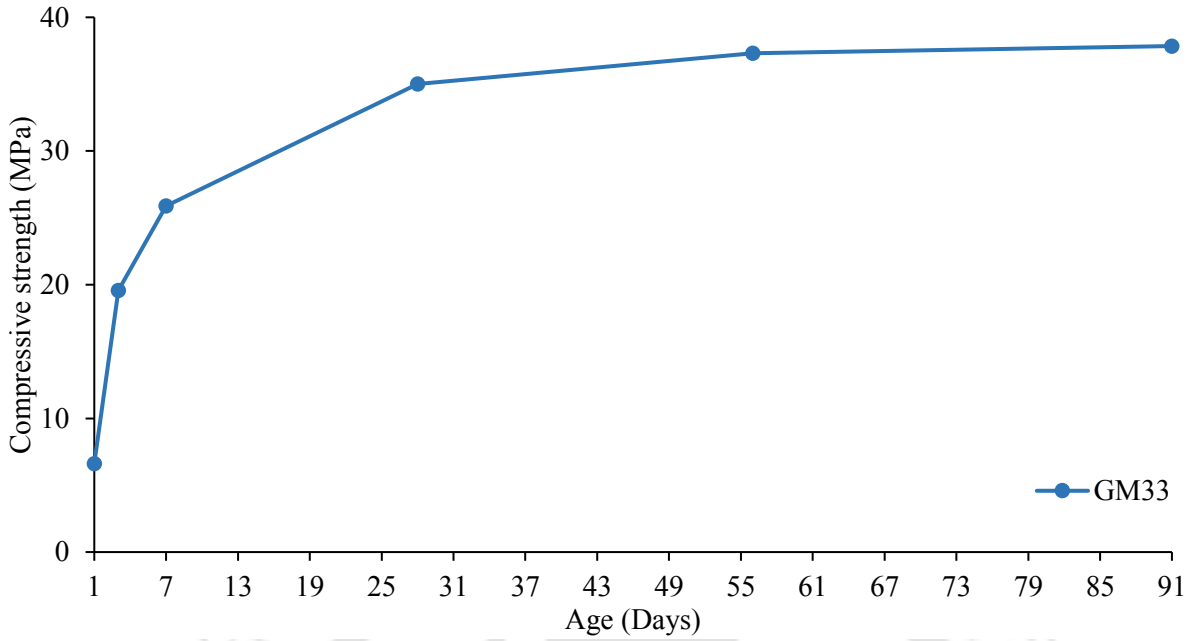

Figure 3.31: Compressive strength of PCM mixes.

3.3.4 Microstructure study of geopolymer mixes

Fig. 3.32 represents the microstructure of mixes GM8 (NaOH activated geopolymer containing only UGGBS) and GM14 (NaOH activated geopolymer containing 70 % UGGBS and 30 % FA) captured at 3 and 28 days. At 3 days, GM8 consisted of denser matrix compared to GM14. Large number of unreacted and/or partially reacted FA particles were seen which were due to curing of the mortar mixes at ambient temperature. FA particles react slowly at ambient temperature and hence unable to contribute to the early strength gain [107]. At 28 days, no significant change in the matrix of GM8 was observed as most of the reaction products were formed at early age. However, slight dense matrix was observed when compared with matrix at 3 days. In the matrix of GM14, the amount of unreacted and/or partially reacted FA particles decreased, the matrix was more dense thereby confirming the participation of FA particles in formation of geopolymer and hence strength enhancement.

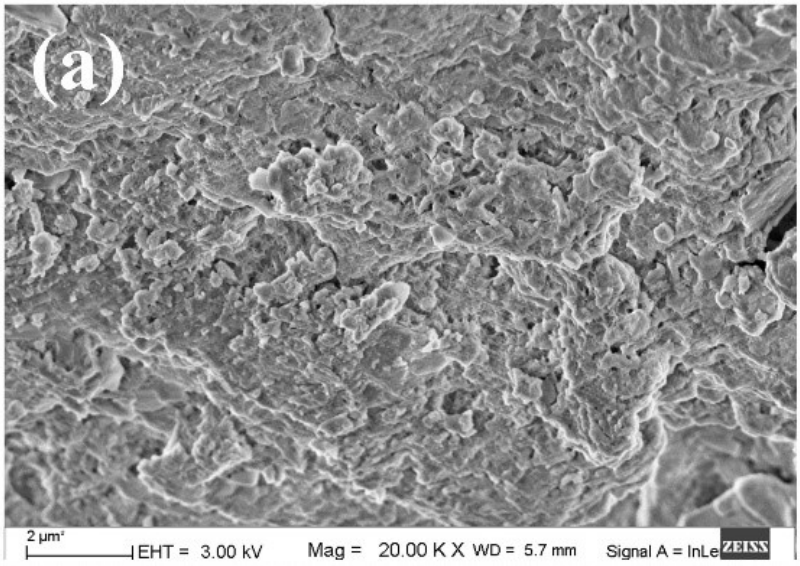

Figure 3.32 (a): FESEM images of geopolymer mix, GM8 at 3 days.

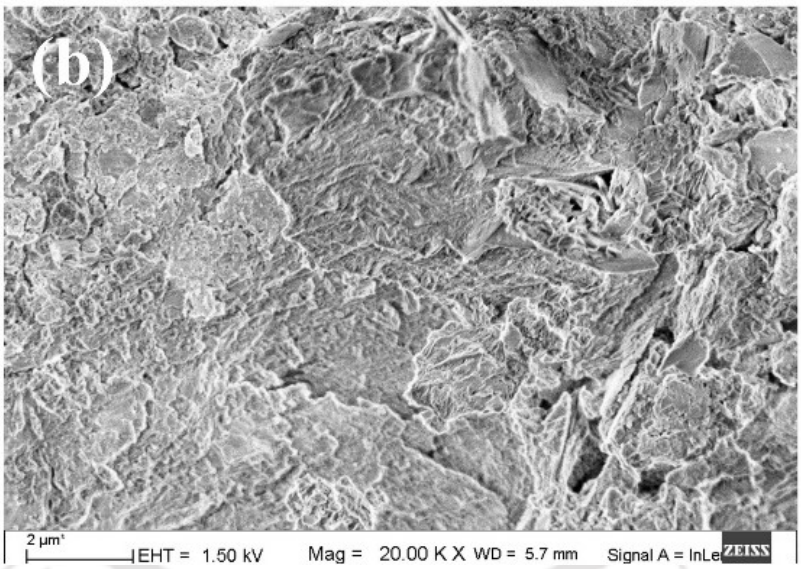

Figure 3.32 (b): FESEM images of geopolymer mix, GM8 at 28 days.

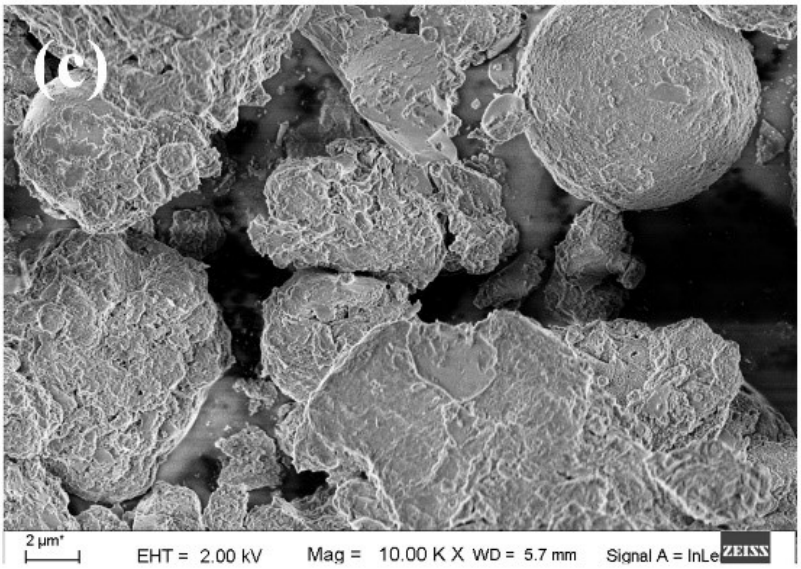

Figure 3.32 (c): FESEM images of geopolymer mix, GM14 at 3 days.

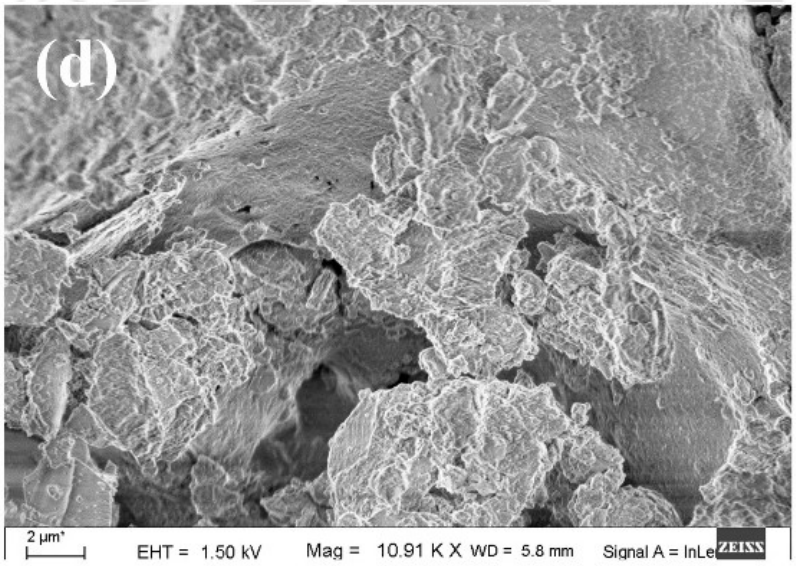

Figure 3.32 (d): FESEM images of geopolymer mix, GM14 at 28 days.

3.3.5 Statistical analysis of test data

For statistical analysis, mean (μ), standard deviation (σ) and coefficient of variation (ρ) of the data obtained from compressive strength test were calculated. For clarity of presentation μ, σ and ρ of strength test results of 3 and 28 days are only presented in Table 3.3. From the table, it can be seen that σ of the data are in the range of 0.125 MPa to 0.899 MPa while ρ are in the range of 0.01 to 0.035. The values of ρ in the table are insignificant. This infact indicates that deviation from mean result is low and hence precision and reproducibility of the experimental results is ensured [118,119].

Table 3.4: Statistical result of compressive strength test data.

Mix	3 Days			28 Days		
	μ (N/mm^2)	σ (N/mm^2)	ρ	μ (N/mm^2)	σ (N/mm^2)	ρ
GM1	13.03	0.125	0.010	22.63	0.793	0.035
GM2	26.40	0.163	0.006	34.80	0.455	0.013
GM3	14.60	0.432	0.030	24.20	0.455	0.019
GM4	40.20	0.245	0.006	47.00	0.408	0.009
GM5	26.60	0.294	0.011	33.67	0.899	0.027
GM6	43.40	0.294	0.007	50.71	0.285	0.006
GM7	25.20	0.141	0.006	32.30	0.668	0.021
GM8	46.30	0.616	0.013	52.90	0.535	0.010
GM9	37.16	0.408	0.011	48.68	0.605	0.012
GM10	36.58	0.479	0.013	47.68	0.591	0.012
GM11	26.82	0.435	0.016	37.06	0.584	0.016
GM12	18.02	0.376	0.021	27.62	0.506	0.018
GM13	41.56	0.589	0.014	49.66	0.589	0.012
GM14	39.17	0.524	0.013	48.94	0.719	0.015
GM15	31.72	0.599	0.019	42.42	0.615	0.014
GM16	22.07	0.476	0.022	30.98	0.467	0.015
GM17	29.86	0.562	0.019	40.98	0.678	0.017
GM18	38.39	0.671	0.017	49.06	0.754	0.015
GM19	31.38	0.564	0.018	43.06	0.531	0.012
GM20	36.59	0.649	0.018	45.96	0.760	0.017
GM21	19.19	0.562	0.029	27.58	0.525	0.019
GM22	24.58	0.506	0.021	35.62	0.466	0.013
GM23	25.71	0.586	0.023	38.61	0.693	0.018
GM24	30.60	0.432	0.014	40.58	0.460	0.011
GM25	24.60	0.474	0.019	33.00	0.589	0.018
GM26	25.35	0.541	0.021	35.20	0.600	0.017
GM27	13.05	0.278	0.021	18.46	0.335	0.018
GM28	20.40	0.503	0.025	25.63	0.425	0.017
GM29	22.78	0.472	0.021	29.90	0.572	0.019
GM30	25.74	0.419	0.016	31.94	0.678	0.021

Table 3.4: Statistical result of compressive strength test data. (Continued)

Mix	3 Days			28 Days		
	μ (N/mm^2)	σ (N/mm^2)	ρ	μ (N/mm^2)	σ (N/mm^2)	ρ
GM31	23.91	0.443	0.019	32.35	0.528	0.016
GM32	28.27	0.495	0.017	35.11	0.431	0.012
CM1	20.98	0.672	0.032	35.02	0.524	0.015

3.4. Closure

This chapter consists of the results of laboratory experiments performed on 32 numbers of ultra-fine ground granulated blast furnace slag (UGGBS) based geopolymer mortar (GPM) mixes possessing various quantities of components to evaluate the fresh and hardened state properties. Admixtures such as flyash (FA) and superplasticizer (SP) were added to the mixes and their influence on setting time, workability and strength gain was observed. Various mortar mixes were prepared by two different types of alkali activator which included combination of sodium silicate (Na_2SiO_3) and sodium hydroxide (NaOH) solution; and only NaOH solution to observe the influence on the mentioned properties. In few mixes, alkali activator concentration was also altered keeping parameters such as FA and SP content fixed. Influence of time of addition of SP in the mixes was also observed. Tests were also performed on a Portland cement mortar (PCM) mix which was considered as controlled mix. The important observations from the study are as follows:-

i. Very low amount of alkali activator in a GPM is not sufficient to start geopolymerisation. Increment in the alkali activator amount in the mix causes improvement in its fresh and hardened state.

ii. Na_2SiO_3 free UGGBS based geopolymer mortar mixes possess higher setting time, better workability and superior strength gain property compared to that containing Na_2SiO_3.

iii. Addition of FA in the mixes retards the early setting property and improves the workability of the mixes. However, FA addition higher than 30 % of total binder content results in reduction in the early strength gain property of the mixes. It also causes reduction in the strength at later ages.

iv. Both SN and PE based SP retards the early setting property and improves the workability of the mixes. Change in the trend of the influence of these admixtures has been observed at higher dosage i.e. beyond 1.5 % SP dosage. SN based ones shows

significant impact on setting time and workability at dosage above 1.5 % of total binder content while, PE based ones shows better performance upto dosage 1.5 % compared to SN based SP. Strength gain property exhibited by mixes with PE based SP has been found better than SN based ones. SP dosage higher than 1.5 % of total binder content lead to low strength of the mixes.

v. Alkali concentration has significant role in regulating the setting time, workability and strength gain of the mixes. Increase in alkali concentration reduces the setting time and workability of the mixes. However, in mixes with PE based SP, such reduction is significant at NaOH concentration higher than 10 M. Low (8 M) and high (14 M) concentration of NaOH solution results in similar pattern of reduced rate of strength gain in the mixes. Maximum rate of strength gain and strength at all ages has been observed in mixes with NaOH concentration of 10 M.

vi. Variations in time of addition of SP in the mixes are found responsible for the variations in the setting time, workability and rate of strength gain. Superior results have been shown by the mixes, when Type I SP addition was adopted in the mixes i.e. SP was added after the addition of alkali activator.

vii. The GPM possesses better fresh and hardened state properties compared to PCM. The early age strength of UGGBS based GPM is significantly higher than PCM.

Chapter 4

Development and Testing of Geopolymer Concrete

4.1 Introduction

Blast furnace slag (BFS) based geopolymer concrete (GPC) has the potential of replacing the conventional Portland cement concrete (PCC) in the construction industry and hence can reduce the CO_2 emission that otherwise results due to manufacturing of Portland cement (PC), the prime component in any construction project. Due to the expansion of construction industry, the demand for concrete has increased significantly. Hence, for meeting the demand, huge quantity of PC is required to be manufactured. This eventually can lead to enhanced accumulation of CO_2 in the atmosphere. Therefore, the use of GPC as an alternate to PCC can contribute towards fulfillment of the demand for concrete without increase of CO_2 in the atmosphere. The speciality of BFS based GPC is that unlike flyash (FA) based GPC, it can gain strength even when cured at ambient temperature [90, 107]. Of late, numerous researchers have dedicated their attention towards the study of fresh and hardened state properties of BFS based GPC [20, 22, 46, 101].

Numerous researchers in the past have tried to use geopolymer mortar (GPM) and GPC as concrete repairing agent. Hu et al. [50] established that metakaolin (MK) based geopolymeric system possess high early strength and thus can be advantageously used as

concrete repairing agent. The mechanical properties such as compressive, bond strength and abrasion resistance of MK based geopolymeric systems were found to be better than PC based systems. Investigation on the mechanical properties of ambient temperature cured blended and unblended FA and slag based GPC was carried out by Manjunatha et al. [120]. Slag based GPC exhibited superior performance among others including conventional PCC. Increase in slag content in the mixes progressively increased the strength and improved bonding.

Duan et al. [71] prepared a novel concrete repairing agent using MK based geopolymer. It possessed properties such as water resistance, fast setting, hydrophobic surface, high compressive and bond strength. Sarker [43] found that compared to PCC, GPC shows better bonding capacity with rebars. The cracking patterns of GPC specimens under the bond test were similar to that of PCC specimens.

Increase in fineness of binding material leads to early strength gain in GPM and GPC. Early age strength is a desirable property of concrete repairing and strengthening agent [121]. Collins and Sanjayan [20] prepared slag based geopolymer concrete specimens by replacing 10% of slag by ultra-fine FA (UFA), ultra-fine slag (UFS) and condensed silica fume (CSF). From test results, it was observed that remarkable improvement in workability occurred due to addition of UFA. Notable improvement in strength occurred even at early ages due to addition of UFS and CSF. Enhanced ultimate strength of slag based GPM was reported by Oner et al. [25] due to increase in fineness of binder. Finer binder contribute to accelerated strength gain and improved durability of the geopolymeric systems [22, 38, 39]. However, increase in fineness of the binder lead to accelerated setting and low workability of mortar or concrete compared to that with same binder of lower fineness [20]. In case of ultra-fine ground granulated blast furnace slag (UGGBS) based geopolymer mixes, high fineness contribute towards accelerated strength gain, however such high fineness and angular shape of slag particles contribute towards loss in setting time and workability of the mixes.

This chapter presents the works undertaken in the thesis to develop UGGBS based GPC possessing such fresh and hardened state properties that make the GPC advantageous to be used as concrete jacketing agent. Such concrete can be used to repair damaged RC members or strengthen them to withstand higher loads. FA and superplasticizer (SP) were added to the GPC to alter the properties and arrive at satisfactory workability, compressive and bond strength. Effect of variation of alkali activator concentration and time of addition of SP in GPC was also noted and compared with that of PCC. In this study, slump test, compressive strength, rebar pull-out and slant shear tests were performed.

4.2 Experimental Investigation

Geopolymer concrete (GPC) specimens were cast using ultra-fine ground granulated blast furnace slag (UGGBS) to conduct laboratory experiments to evaluate the fresh and hardened state properties. The tests included slump test, compressive strength test and bond test. Total 22 numbers of mixes including a controlled mix were tested at various days from the date of casting to observe the properties of GPC.

4.2.1 Materials

4.2.1.1 Geopolymer concrete

UGGBS was primarily used for preparing the geopolymer concrete (GPC). Flyash (FA) and superplasticizer (SP) were added to the GPC at various dosage levels. Both sulfonated naphthalene (SN) based SP and polycarboxylate ether (PE) based SP were used. The details of UGGBS, FA and SP have been presented in sub-section *2.2.2 Ultra-fine ground granulated blast furnace slag, 2.2.3 Flyash* and *2.2.6 Admixture* of Chapter 2. Locally available fine and coarse aggregates were used in the preparation of GPC. Their properties have been described in sub-section, *2.2.5 Aggregates* of Chapter 2. For activation of the geopolymerisation process, sodium hydroxide (NaOH) solution was used as alkali activator. NaOH solution was prepared using NaOH pellets which was available commercially. NaOH solution of required concentration was prepared by mixing NaOH pellets with distilled water 24 hours before the casting of specimens.

4.2.1.2 Portland cement concrete

Portland cement concrete (PCC) was prepared using ordinary Portland cement (OPC) 43 grade. Sub-section, *2.2.1 Portland cement* of Chapter 2 presents the details of the properties of the OPC. The fine and coarse aggregates used in the preparation of PCC were same as used in preparation of GPC. Portable water available in the laboratory was used for PCC preparation.

4.2.1.3 Reinforcement

Bond test specimens were cast using 16 mm diameter tor steel bars partially embedded centrally and vertically within them. Sub-section, *2.2.7 Steel reinforcement bars* of Chapter 2 presents the details of the rebar used.

4.2.2 Mix proportions

Mix proportion of the UGGBS based GPC is presented in Table 4.1. Hereafter, UGGBS and FA are together referred as total binding agent. NaOH solution is also referred as alkali activator solution. The alkali activator solution/total binding agent (a/b) ratio of 0.66 was maintained in GPC throughout the study.

The concrete mixes were prepared to study the effect of following on workability, compressive strength and bond strength of GPC:-

i. Addition of FA of varying amounts of 20, 30, 40 and 50 % by weight of total binding agent.
ii. Addition of SP of varying amounts of 0.5, 1.5 and 3 % by weight of total binding agent.
iii. Variation of NaOH concentrations of 8, 10, 12 and 14 molar (M).
iv. Variation in the time of addition of SP.

NaOH as the alkali activator; the lower and upper limits of FA and SP content; and the lower and upper limits of NaOH concentrations were set based on the study of past works by various authors in the same field of research mentioned in sub-section, *3.2.2 Mix proportions* of Chapter 3. SP of both SN and PE types were added to the GPC in either of the following three types:-

a. Type I: SP added after the addition of NaOH solution to the mix.
b. Type II: SP was mixed with NaOH solution and then added to the mix.
c. Type III: SP added before the addition of NaOH solution to the mix.

Table 4.1: Mix proportion for GPC (kg/m^3).

Mix	UGGBS	FA quantity and % in total binding agent	NaOH concentration (Molarity, M)	SP (% of total binding agent)	SP type	w/s	SP addition type	Mix group
GC1	358	0 (0)	10	-	-	0.40	Type I	G1
GC2	286.4	71.6 (20)		-	-			
GC3	250.6	107.4 (30)		-	-			
GC4	214.8	143.2 (40)		-	-			
GC5	179	179 (50)		-	-			
GC6	250.6	107.4 (30)	10	0.5	SN	0.40	Type I	G2 (including G3)
GC7	250.6	107.4 (30)		0.5	PE			
GC8	250.6	107.4 (30)		1.5	SN			
GC9	250.6	107.4 (30)		1.5	PE			
GC10	250.6	107.4 (30)		3	SN			
GC11	250.6	107.4 (30)		3	PE			
GC12	250.6	107.4 (30)	8	1.5	SN	0.43	Type I	G3 (including GC8 and GC9)
GC13	250.6	107.4 (30)	8	1.5	PE	0.43		
GC14	250.6	107.4 (30)	12	1.5	SN	0.37		
GC15	250.6	107.4 (30)	12	1.5	PE	0.37		
GC16	250.6	107.4 (30)	14	1.5	SN	0.34		
GC17	250.6	107.4 (30)	14	1.5	PE	0.34		
GC18	250.6	107.4 (30)	10	1.5	SN	0.40	Type II	G4 (including GC8 and GC9)
GC19	250.6	107.4 (30)		1.5	PE		Type II	
GC20	250.6	107.4 (30)		1.5	SN		Type III	
GC21	250.6	107.4 (30)		1.5	PE		Type III	

Note: *Fine aggregate = 611 kg/m^3, coarse aggregate = 1208 kg/m^3, NaOH = 236.28 kg/m^3, w/s = water to total solid ratio. The figures inside parenthesis indicate the % values.*

The difference in all the three types depends upon the time of SP addition. In Type I, the SP was added to the wet mix which consisted of UGGBS, FA, fine and coarse aggregates; and NaOH solution. After the addition of SP to the wet mix, it was blended thoroughly so that the SP got homogenously distributed. In Type II, SP was added to the NaOH solution

and stirred properly. Later, the SP containing NaOH solution was added to the dry mix. In Type III, SP was added to the dry mix prior to the addition of NaOH solution. On addition of the SP, it was thoroughly mixed for homogenous distribution. NaOH solution was added to the mix at the end of this step of SP addition.

Controlled mix was prepared using PCC. Table 4.2 presents the mix proportion of PCC. The substrates for preparing slant shear test specimens were also cast using PCC. CC1 is the mix for substrate concrete. CC2 denotes controlled mix. The water/cement (w/c) and water/solid (w/s) ratios of PCC and GPC were same (except that of GC12 to GC17 and CC1).

Table 4.2: Mix proportion for PCC (kg/m^3).

Mix	Cement	Fine Aggregate	Coarse aggregate	Water/cement (w/c)
CC1	360	680	1128	0.55
CC2	425	630	1190	0.40

4.2.3 Specimen preparation and curing

Following are the steps that were involved while preparing UGGBS based GPC specimens:-

i. Dry mix was manually composed by thoroughly mixing UGGBS, FA, fine and coarse aggregates for 2 minutes.
ii. To this dry mix, NaOH solution was added and the mixing processes was further continued for 3 minutes.
iii. SP was added to the mix by either of Type I, Type II or Type III method.
iv. On being ready, the fresh GPC was placed into the respective moulds for compressive strength, pull-out and slant shear tests. Fig. 4.1 shows freshly prepared GPC for slump test. The colour of the fresh GPC is dark brownish grey colour.

Figure 4.1: Freshly prepared GPC.

For preparation of PCC, procedures mentioned in IS 516 1959 [122] were followed. The curing of the specimens were conducted in similar way as that of the GPC specimens.

Compressive strength test was conducted on 150 mm cubes as per IS 516 1959 [122]. The freshly prepared concrete was placed into the cube moulds in three layers, each being compacted using an electric operated vibration table. The moulds were kept at ambient temperature of 20 ± 2 ºC. After 24 hours from the time of casting, the specimens were demolded and submerged inside water tank, maintaining temperature of 20 ± 2 ºC and stored till the arrival of test day. Fig. 4.2 shows the cubes being cured inside the water tank.

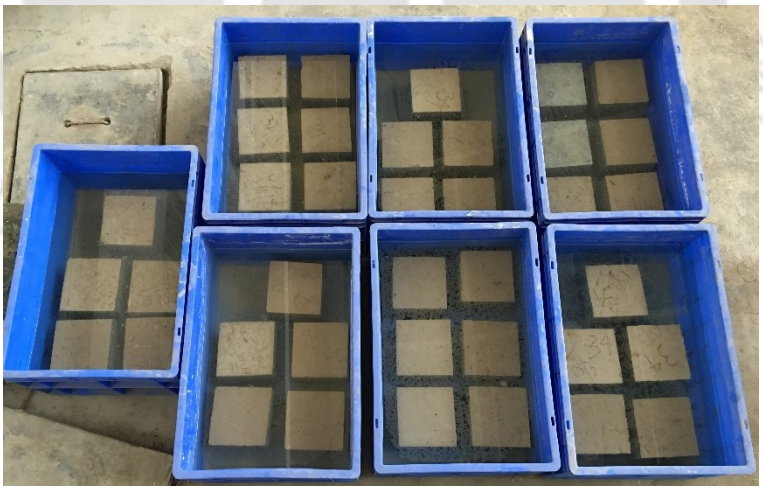

Figure 4.2: Concrete cubes under curing.

The size of cube specimens for pull-out test was also 150 mm. Provisions mentioned in IS 2770 1967 [123] were followed for the preparation of the specimens. Fig. 4.3 presents the special arrangements that were made for casting of the specimens for pull-out test. The

special arrangement was provided to facilitate the vertical erection of the rebar that was supposed to be embedded partially inside the fresh concrete. A hole was also provided at the base plate of the cube to allow 5 mm length of the bar to remain outside the cube and also to facilitate the vertical erection of the rebar. Fig. 4.4 shows the details of the pull-out test specimen. The embedded length of rebar inside the cube was 50 mm. The remaining part of the rebar inside the cube was covered using poly vinyl chloride (PVC) tube to break the contact between the GPC and the surface of the rebar. PVC tube was used since it does not possess any reactive phenomenon with concrete. It is also water resistant, can withstand moderate temperature without deformation and is flexible. Before placing the concrete inside the pull-out test specimen, the rebar was placed inside the mould and allowed to stand vertical with the help of the special arrangement. The freshly prepared concrete was poured inside the mould in three layers taking care that the rebar did not dislocate from its position. For compaction of the concrete the moulds were vibrated after pouring of concrete in each layer. The moulds were kept at ambient temperature of 20 ± 2 ºC. On completing of 24 hours from the time of casting, the specimens were demolded and submerged inside water tank, maintaining the temperature of 20 ± 2 ºC and stored till the arrival of test day. Fig. 4.5 shows the cubes being cured inside the water tank.

Figure 4.3: Mould for pull-out test specimens.

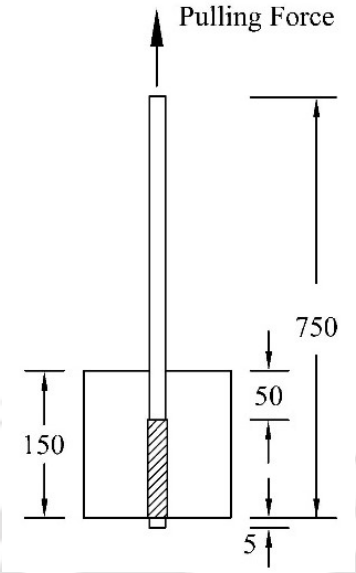

Figure 4.4: Details of specimens for pull-out test (All dimensions are in mm).

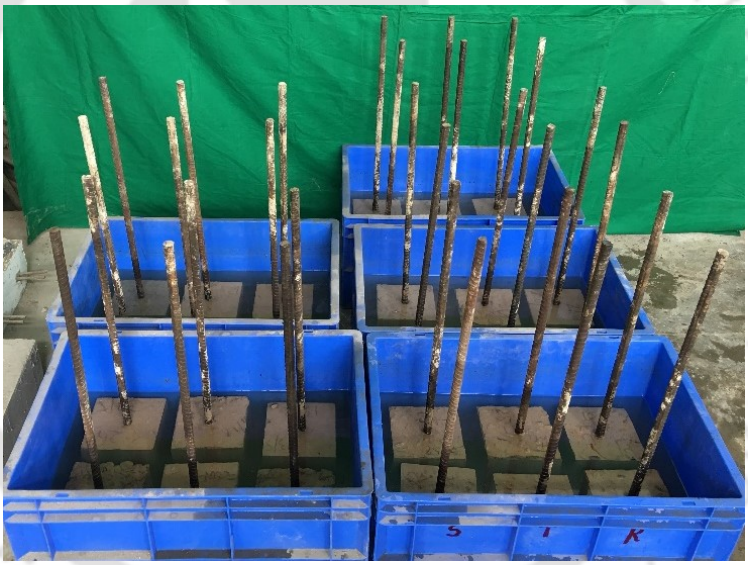

Figure 4.5: Pull-out test specimens under curing.

In the slant shear test specimens, the GPC constituted half of the volume. The other half, i.e. the substrate was prepared using PCC, mix CC1 (see Fig. 4.6). The PCC substrates were prepared with the help of dummy specimens which were cast, cured for 28 days and hand finished to give the perfect shape and slant angle of 30° along the surface 'ab' as shown in Fig. 4.6. The volume of each dummy specimen was half of that of cylindrical mould of size 75 mm diameter and 150 mm height [124]. Prior to the casting of the PCC substrate for slant shear test, the dummy specimens were placed into the cylindrical moulds with the surface 'ab' covered with polyvinyl sheet which acted as debonding media between the PCC substrates and dummy specimens. The fresh concrete for PCC substrate was prepared and

placed into the moulds such that it occupied the other half of volume of the mould and kept for 24 hours at temperature of 20 ± 2 ºC. The size of the moulds were taken as 75 mm diameter and 150 mm height to economize the cost of the experimental study. Moreover, this study deals with the comparative behaviour of various mixes. Hence, the size effect on strength due to use of small moulds for slant shear test was not taken into account. The specimens were later demoulded and cured till 28 days from date of casting by submerging inside water tank, maintaining water temperature at 20 ± 2 ºC. After 28 days, the PCC substrates were cured in the open air till 2, 6 and 12 months from the date of casting, Fig. 4.7. At the end of open air curing period, the substrates' surfaces 'ab' were carefully cleaned to peel off the dust layer, placed into the moulds and then the new GPC or PCC (CC2) was poured for each mix. The specimens were again kept into the mould for 24 hours at 20 ± 2 ºC. After 24 hours, these were demoulded and cured by submerging inside water tank maintaining temperature of 20 ± 2 ºC till the arrival of test day (Fig. 4.8).

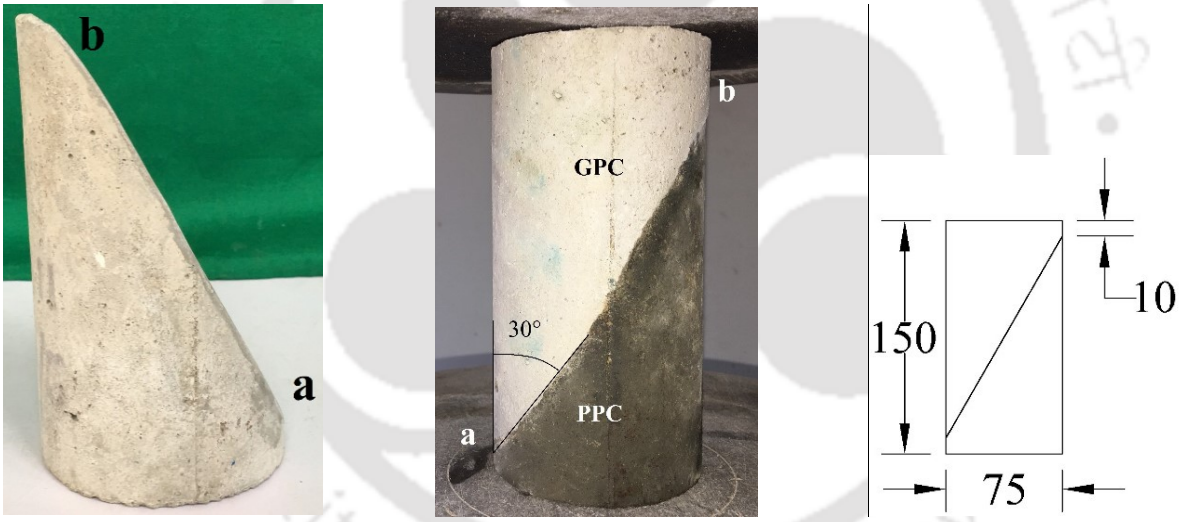

(a) (b) (c)

Figure 4.6: (a) PCC substrate for slant shear specimen, (b) slant shear specimen, (c) details of specimens for slant shear test (All dimensions are in mm).

Figure 4.7: Curing of PCC substrates in water and open air.

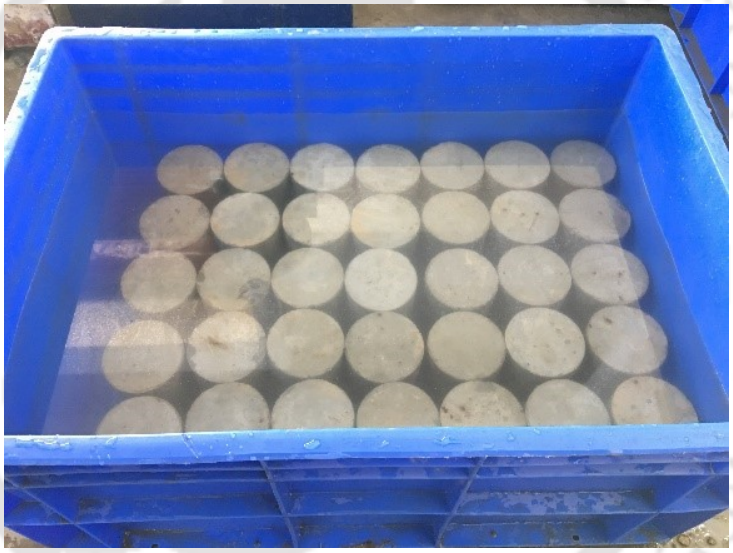

Figure 4.8: Curing of slant shear specimens in water.

4.2.4 Experiments

The workability of GPC and PCC was determined in the laboratory by conducting the slump test as per IS 1199 1959 [125]. The test was performed at 5, 15 and 30 mins from the time of mixing of dry GPC mix and NaOH solution. The slump test was conducted at the aforementioned time intervals to evaluate the slump retention capacity of GPC and PCC.

Compressive strength test was conducted on the GPC and PCC specimens at 1, 3, 7, 28 and 56 days as per IS 516 1959 [122] to evaluate the compressive strength of GPC mixes at early and later ages. The test was conducted in electronic compressive strength testing machine (CTM) of capacity 3000 kN consisting of digital display.

Bond strength of GPC and PCC mixes was evaluated on the basis of bond strength with rebar (BS_r) and with 2, 6 and 12 months old PCC substrate (BS_c). Pull-out test was carried out at 3 and 28 days to determine the bond strength with rebar as per IS 2770 1967 [123]. Fig. 4.9 shows the test set up in the UTM. The test was conducted in electronic Universal Testing Machine (UTM) of 1000 kN capacity. The rate of loading was 2 kN/min. The test setup for slant shear test is presented in Fig 4.10. The slant shear test as per ASTM C882/882M-13a [124] was conducted on the GPC and PCC mixes at 3 and 28 days to determine the bond strength with PCC substrate. The test was conducted in 2000 kN capacity electronic CTM.

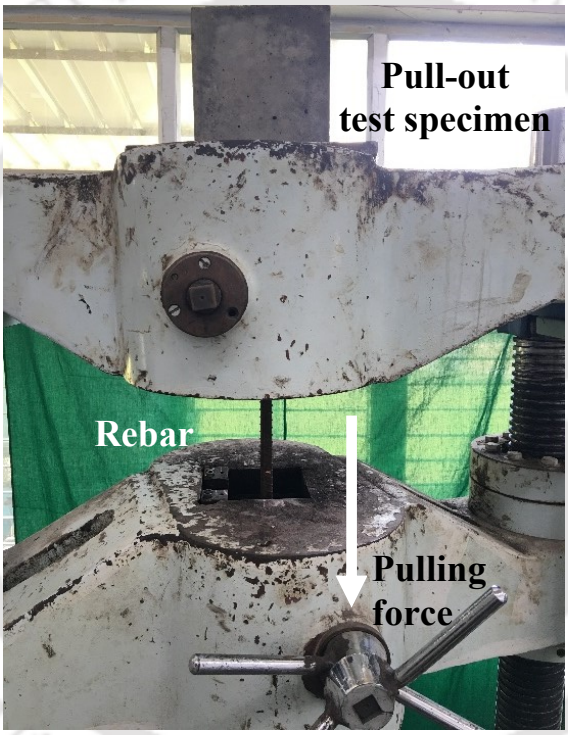

Figure 4.9: Test setup for pull-out test.

The BS_r and BS_c were evaluated using the following equations:-

$$BS_r = \frac{F_r}{A_r} \tag{4.1}$$

$$BS_c = \frac{F_c}{A_c} \tag{4.2}$$

Figure 4.10: Test setup for slant shear test.

Here, Fr and Fc are the loads carried by the specimen at failure in pull-out and slant shear tests respectively. Ar and Ac are the areas of surface of the embedded length of the bar and surface of PCC substrate shown by 'ab' in Fig. 4.6 (b).

In each type of test, 3 numbers of specimen per mix for each selected day were prepared and tested. The results presented are the average of the test result values of each specimen per mix for each selected day.

For statistical analysis, mean (μ), standard deviation (σ) and coefficient of variation (ρ) of the data obtained from compressive strength were calculated. The μ, σ and ρ of strength test results at 3 and 28 days only are presented. Both σ and ρ help in knowing the quality control in test procedures and indicate the precision and repeatability of the test method.

4.3 Experimental Observations

4.3.1. Workability

Fig. 4.11 presents the results from the slump test performed at various time interval. Ultra-fine ground granulated blast furnace slag (UGGBS) as the only binding agent showed very poor workability in the geopolymer concrete (GPC) mix. The slump value at 5 mins was found to be only 25 mm which eventually reached to 0 at 15 mins. The mix acquired the shape of the slump cone with no sign of movement (Fig. 4.12). High liquid demand due to high fineness and instant formation of the geopolymerisation products led to loss in workability of the mix [20, 104, 105]. Addition of flyash (FA) in the mix caused monotonous increase in

slump value (Fig. 4.11). The slump retaining property of the mixes improved because of two prime factors: (i) FA particles improved the mobility of the mix components because of its smooth spherical shape which eventually contributed to delay of setting, (ii) FA at ambient temperature is unable to form geopolymerisation products instantly, thus allowing more time for setting of the mix [90, 106, 107].

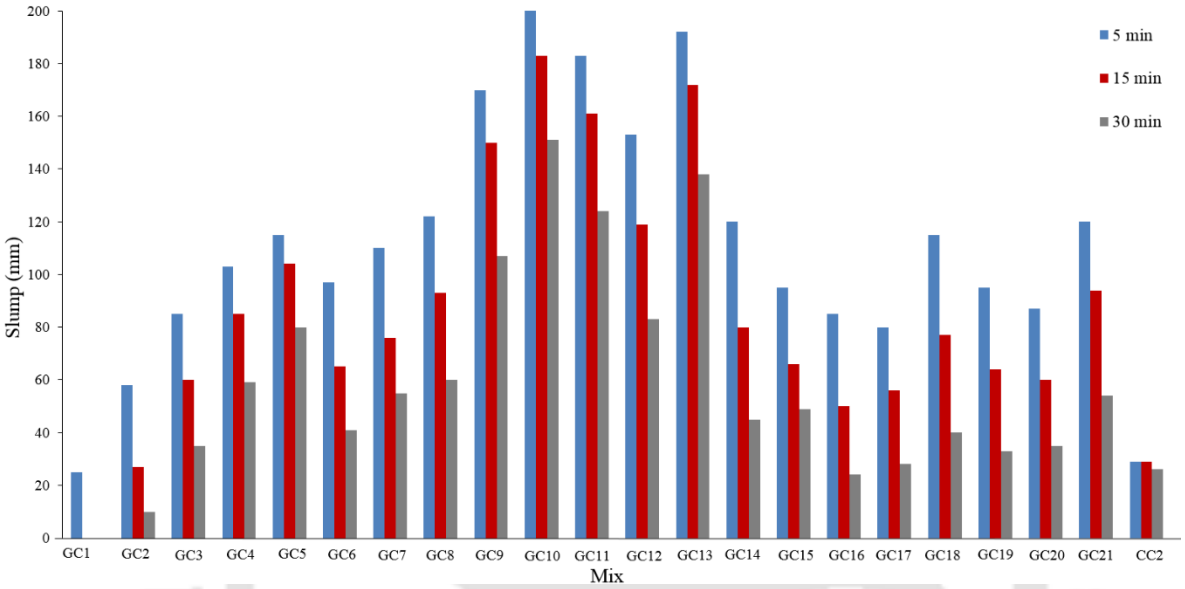

Figure 4.11: Results from slump test.

Figure 4.12: Dry slump.

Addition of SP in the mixes contributed towards the release of the liquid component in the mixes which were trapped in the flocs formed by the solid particles. This eventually increased the amount of available liquid component in the mix for better mobility of particles and hence improved the workability. PE based SP improved the workability of the mixes more efficiently compared to SN based SP. Increase in workability and slump retention capacity was monotonous due to increase in SP content. However, at very high SP content (3%), segregation was observed in the fresh mixes. This resulted in erroneous slump value of mixes with high SP dosage.

Depletion in slump value was observed due to increase in NaOH concentration in mixes with 30% FA and 1.5% SP dosage. Increase in NaOH concentration resulted in the increase in the total amount of solids in the solution (seen as w/s in Table 4.1). This caused the viscosity of the solution to increase and hence obstruction to mobility of the particles. Increase in NaOH concentration also led to deterioration in the slump retention capacity of the fresh mix. Similar observations were made by Lee and Lee [108] and Karakoca et al. [111] in their investigations on geopolymer mixes. Results showed that reduction in slump value and retention property was monotonous due to increase in NaOH concentration regardless of SP types in the mixes.

SP addition type also played significant role in controlling the workability of the mixes. Type I PE based SP addition outperformed all other types. Type II and III SP addition resulted in mixes with almost similar workability. The performance of PE based SP when mixed with NaOH activator (Type II) was lower than SN based SP. This is in contradiction with the performance trend of SP when mixed by other two methods. The performance of PE based SP when mixed with NaOH activator (Type II) was lower than SN based SP. This is in contradiction with the performance trend of SP when mixed by other two methods. A change in appearance of the NaOH solution from transparent to whitish colour occurred on addition of the PE based SP. This indicated a possible chemical change in the solution. Detailed study in this regard is presented by Palacios and Puertas [115].

Results show the slump value of PCC mix, CC2 to be lowest compared to GPC mixes. However, the slump value was approximately equal to that of GPC mix, GC1 which consisted of only UGGBS. The slump retention property of CC2 was pronouncedly high compared to the GPC mixes. The result of slump test of CC2 is supported by the setting time test result of CM2 (subsection, *3.3.1 Setting time* of Chapter 3).

4.3.2 Compressive strength

The compressive strengths of UGGBS based GPC mixes with various amounts of FA content are presented in Fig. 4.13. With the addition of FA, considerable loss in compressive strength was observed though the workability improved. The rate of strength gain also reduced. Since, FA has low calcium oxide (CaO) content, the total CaO content of the mix got reduced as the FA content increased. Therefore, the contribution of CaO towards strength attainment of mixes was reduced. Moreover, the specimens were cured at ambient temperature. But in case of FA based geopolymer, elevated temperature curing is required for SiO_2 and Al_2O to form the geopolymerisation products and hence, the contribution towards attaining of strength was reduced due to increase in the FA content in the mixes [69, 82, 90, 103, 107, 126]. The mixes containing high amount of FA exhibited very low early strength. At later ages, the mixes attained significantly higher strength compared to that attained at early ages. The mixes without any FA content or low FA content (less than 40 %), could attain high strength at early ages. About 50, 80 and 90 % of 28 days strength were attained by these mixes at 1, 3 and 7 days respectively. At high FA content, the strength development mechanism in the mix was more affected by FA. Hence, early strength development was not observed in the mixes with high FA content.

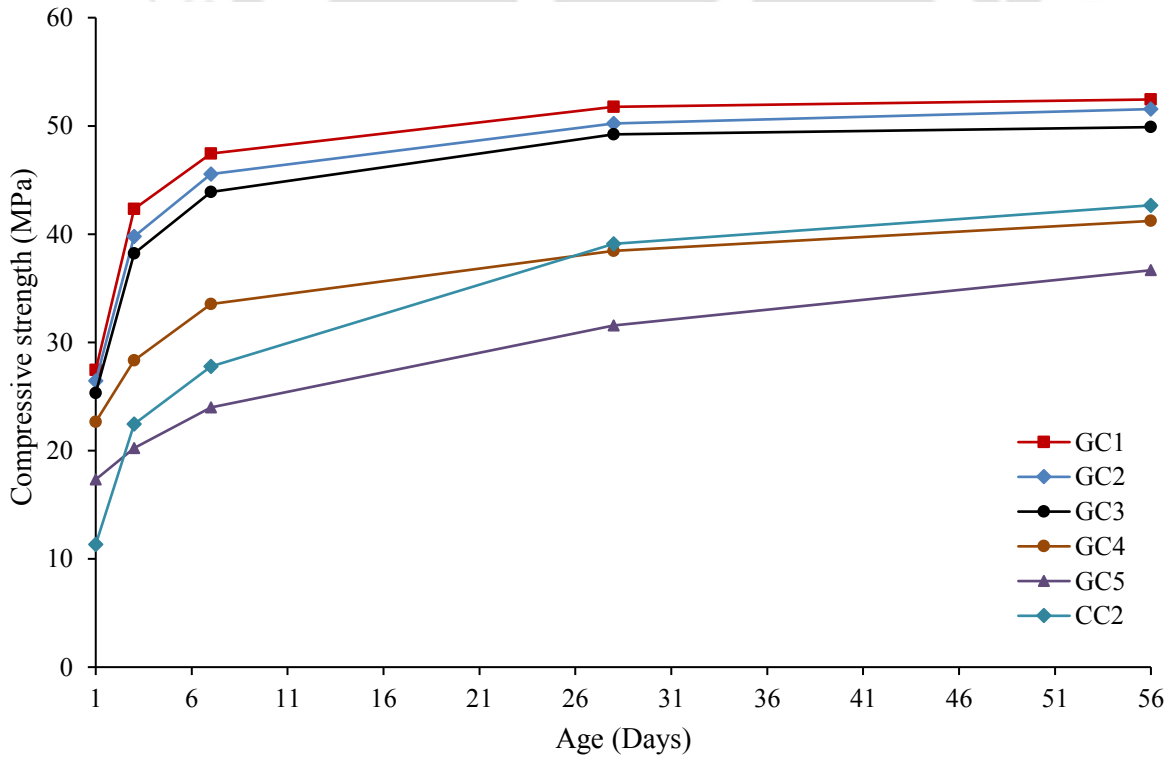

Figure 4.13: Effect of FA content on compressive strength of GPC.

Variation of compressive strength was observed in the UGGBS based GPC mixes with constant FA content of 30 % and varying dosage of both types of SP (see Fig. 4.14). GPC mix with 0.5 % PE based SP dosage attained maximum strength at all selected days. The strength of this mix at 1 and 3 days was around 60 and 80 % of that at 28 days. The improvement of strength of the mixes due to the addition of PE based SP was because of the fact that it improved mobility of the particles in the mixes leading to their even distribution and thus forming of homogenous concrete mixes. Mixes with PE based SP attained higher strength than SN based ones for each SP dosage. Moreover, the rate of strength gain was also higher in mixes with PE based SP. Drop in strength at early and later ages was observed in case of mix with dosage higher than 0.5 % PE based SP. In case of GPC mixes with SN based SP, addition of SP and the increment in the quantity led to monotonous loss in compressive strength (Fig. 4.14). At 3 % SP dosage, due to segregation the mix particles were not distributed homogenously resulting into GPC with very low strength. This phenomenon was pronouncedly observed in mix with 3 % SN based SP.

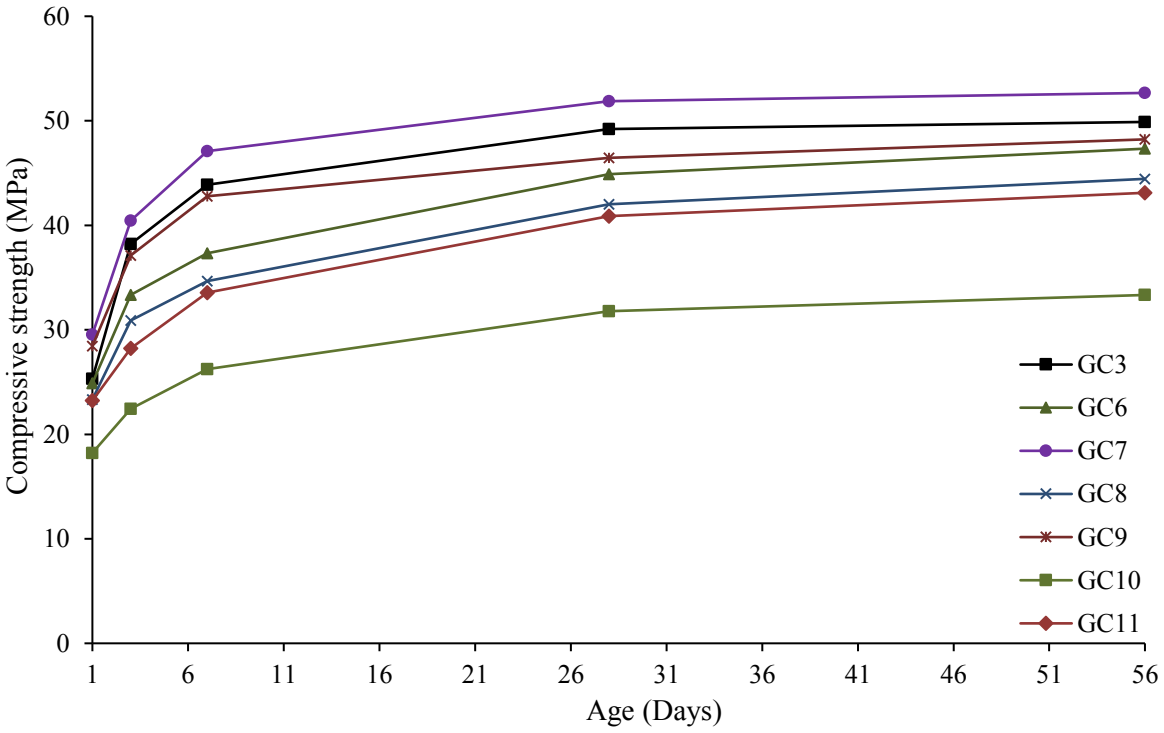

Figure 4.14: Effect of SP type and content on compressive strength of mixes.

The effect of concentration of NaOH on compressive strength of UGGBS based GPC at constant FA content of 30 % and SP of 1.5 % can be seen in Fig. 4.15. GPC mixes with 10 M NaOH exhibited maximum strength at early and later ages. Moreover, the rate of strength

gain was also observed to be higher irrespective of SP type. At 8 M NaOH concentration, the rate of strength gain of mixes were lower than that of mixes with 10 M NaOH concentration. This was in line with results obtained in earlier studies [21, 32] where the rate of strength gain was explained to be dependent on alkali concentration. Lower NaOH concentration led to slow rate of formation of polymerisation product with lower structural strength. However, the results for mixes with 12 and 14 M NaOH concentration were contradicting with the previous studies on geopolymeric systems. While other studies revealed that rate of strength gain and strength at specified days increase with alkali concentration [29], but in the present study, the compressive strength and rate of strength gain were lowered due to increase in NaOH concentration. At high NaOH concentration, the pH of the liquid component in the mixes was high. The dissolution of Si, Al, Ca ions were enhanced. This increased the concentration of the ions in the mixes, limiting the ions' mobility and hence delayed the formation of coagulated structures, i.e. delayed the polymerisation process [21]. Moreover, loss of workability at high NaOH concentration resulted in a non-homogenous GPC matrix. Hence, low rate of strength gain and low strength were exhibited by the mixes with higher NaOH concentration. The behaviour was in conformity with the results of sub-section, *3.3.3 Compressive strength* of Chapter 3. The rate of strength gain was lower for mixes with SN based SP compared to the PE based ones, irrespective of NaOH concentration.

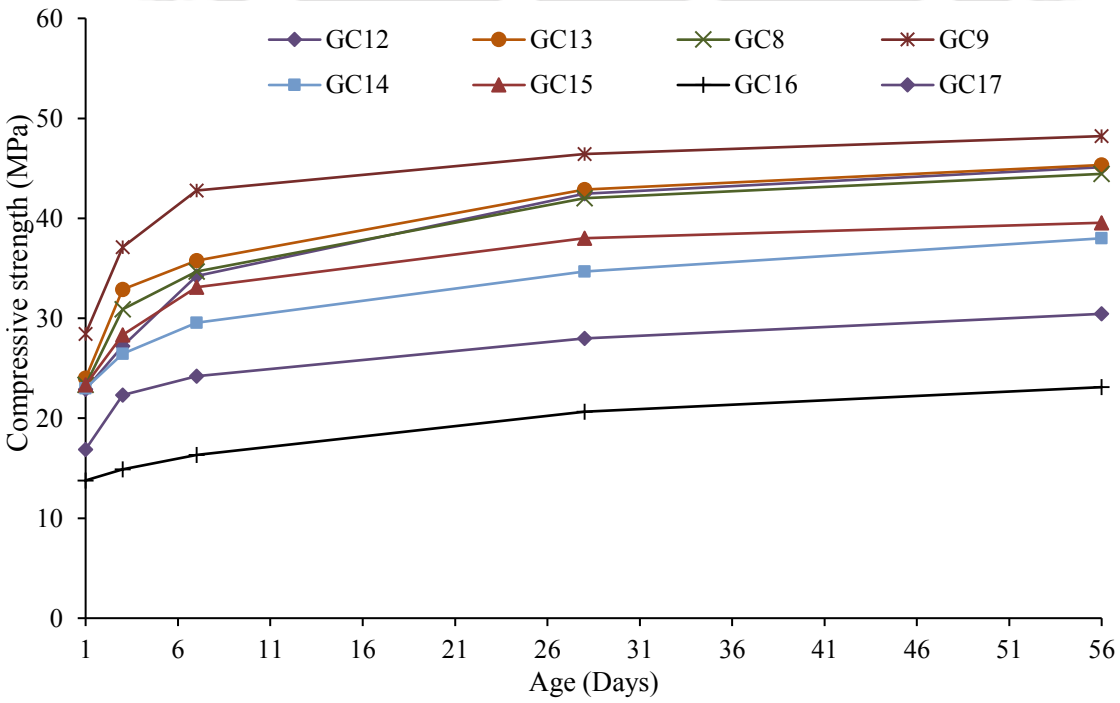

Figure 4.15: Effect of alkali concentration on compressive strength of mixes.

UGGBS based GPC with Type I SP addition exhibited better rate of strength gain than other methods (Fig. 4.16). This was observed in case of mixes with both SN and PE based SP. Mixes with Type II and III SP addition exhibited low strengths. In all, mixes with PE based SP showed superior performance in all types of SP addition methods.

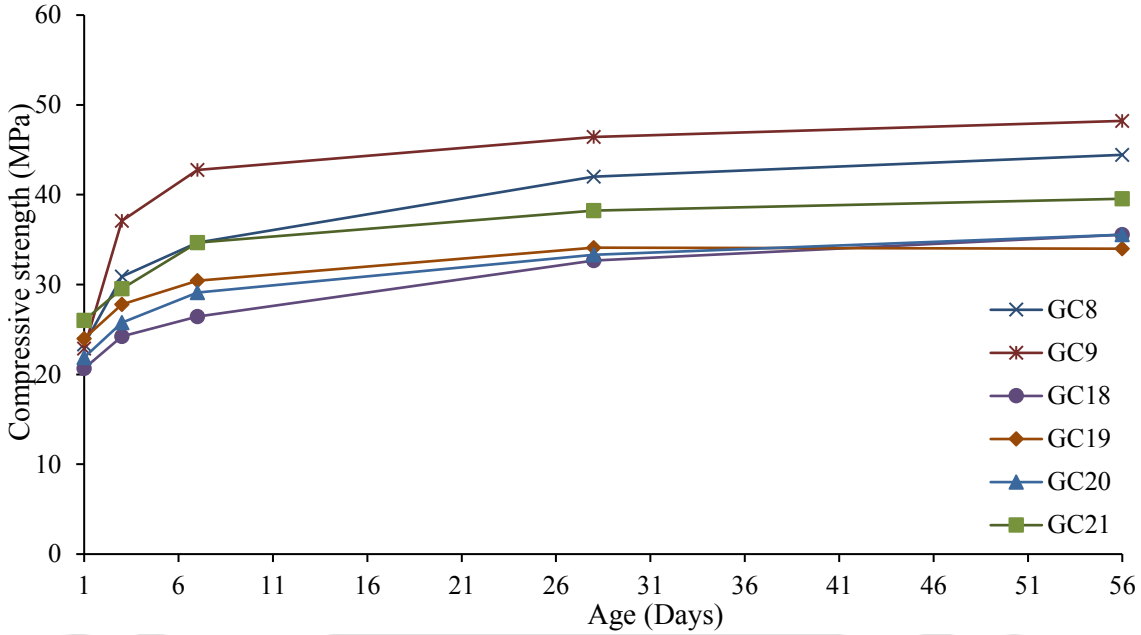

Figure 4.16: Effect of SP addition type on compressive strength of mixes.

GPC mixes exhibited higher early strength compared to PCC mix, CC2. However, at later ages, CC2 developed higher strength (Fig 4.13). Due to poor workability, the cement matrix was non-homogenous and hence retained large number of pores which acted as source for cracking of concrete due to action of compressive load. Moreover, due to non-homogenous matrix, the interfacial transition zone (ITZ) was very weak and hence concrete cracking occurred from that region too.

Statistical analysis of test data

The statistical analysis of compressive strength data was carried out for 22 numbers of mixes to find out mean (μ), standard deviation (σ) and coefficient of variation (ρ). Both 3 and 28 days strength results were analyzed and shown separately in Table 4.3.

From Table 4.3, it can be seen that standard deviation (σ) of the data are in the range of 0.089 MPa to 0.533 MPa while coefficient of variation (ρ) are in the range of 0.002 to 0.018. The small magnitude of the ρ is an indication of precision and reproducibility of the test results [118, 119].

Table 4.3. Statistical result of compressive strength test data.

Mix	3 Days			28 Days		
	μ (N/mm^2)	σ (N/mm^2)	ρ	μ (N/mm^2)	σ (N/mm^2)	ρ
GC1	42.33	0.111	0.003	51.78	0.222	0.004
GC2	39.78	0.133	0.003	50.22	0.133	0.003
GC3	38.22	0.133	0.003	49.22	0.156	0.003
GC4	28.33	0.156	0.005	38.44	0.222	0.006
GC5	20.22	0.222	0.011	31.56	0.178	0.006
GC6	33.33	0.000	0.000	44.89	0.089	0.002
GC7	40.44	0.178	0.004	51.89	0.333	0.006
GC8	30.89	0.178	0.006	42.00	0.222	0.005
GC9	37.11	0.089	0.002	46.44	0.200	0.004
GC10	22.44	0.178	0.008	31.78	0.133	0.004
GC11	28.22	0.222	0.008	40.89	0.356	0.009
GC12	27.22	0.156	0.006	42.44	0.200	0.005
GC13	32.89	0.178	0.005	42.89	0.222	0.005
GC14	26.44	0.133	0.005	34.67	0.311	0.009
GC15	28.33	0.111	0.004	38.00	0.133	0.004
GC16	14.89	0.311	0.021	20.67	0.133	0.006
GC17	22.33	0.200	0.009	28.00	0.222	0.008
GC18	24.22	0.311	0.013	32.67	0.311	0.010
GC19	27.78	0.267	0.010	34.11	0.333	0.010
GC20	25.78	0.444	0.017	33.33	0.356	0.011
GC21	29.56	0.533	0.018	38.22	0.444	0.012
CC2	22.44	0.222	0.010	39.11	0.133	0.003

4.3.3. Bond strength (pull-out)

Results from pull-out test on UGGBS based GPC mixes are presented in Fig. 4.17. Five geopolymer mixes (GC1 to GC5) and one Portland cement concrete mix (CC2) were studied. Information of flyash (FA) content in geopolymer mixes is given in the 3rd column of Table 4.1. It is evident that the strength of mix with 30 % FA content (GC3) is the highest compared to others. Addition of FA provided better mobility to mix particles and resulted in homogenous matrix. This led to better bonding of the matrix with the rebar surface. However, addition of high amount of FA (> 30%) led to reduced bond strength. The slow rate of strength

gain and reduced strength of FA based geopolymer compared to UGGBS based ones, may be attributed to occurrence of such phenomenon.

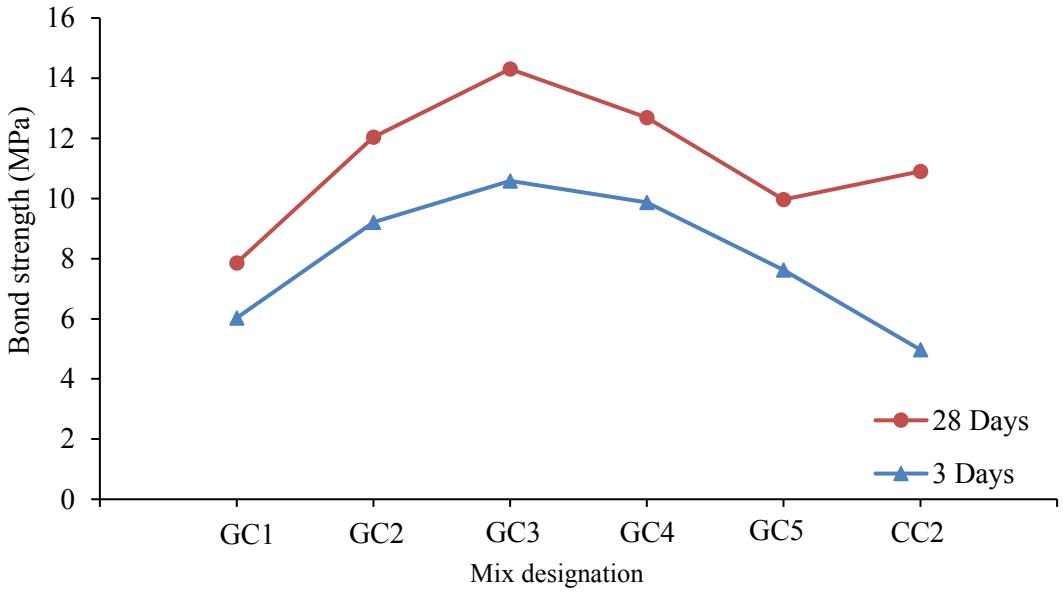

Figure 4.17: Effect of FA content on bond strength of GPC with rebar.

Enhanced bond strength was observed due to addition of PE based SP in the GPC mixes with constant FA content of 30 % in Fig. 4.18. PE based SP when added to the mixes produced homogenous mix due to better workability and mobility to the mix particles leading to better bond between the matrix and the rebar. However, dosage of PE based SP higher than 1.5 % caused segregation in the mix and hence it attained significantly low bond strength. The behaviour observed was rather different for mixes with SN based SP. Addition of SN based SP caused monotonous reduction in bond strength of the mixes with the rebar surface asserting the fact that such type of SP is not suitable for UGGBS based geopolymer mixes. The test results of mixes with SN based SP were in agreement with that of compressive strength test results.

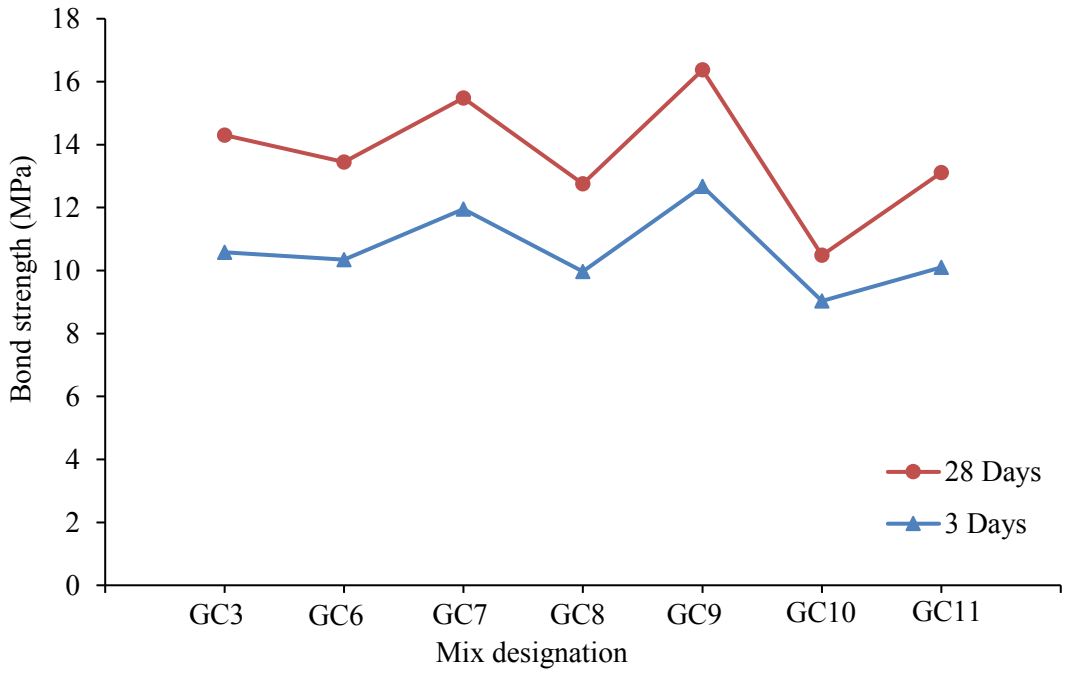

Figure 4.18: Effect of SP type and content on bond strength of GPC with rebar.

Fig. 4.19 presents the variation of bond strength with change of NaOH concentration in UGGBS based GPC mixes with constant FA and SP content. Lower NaOH concentration of 8 M had similar effect on the mixes as that of 12 M concentration. The mixes with 8 M concentration attained low strength because of the fact that lower concentration cause slow polymerisation process [27] and formation of end products with low structural strengths. On the other hand, slow strength gain and attainment of low bond strength with mixes activated by 12 M NaOH was primarily related to the fact that high NaOH concentration produced high pH in the liquid component and delayed the polymerisation process. This eventually led to low strength gain in the mixes [21]. Moreover, higher NaOH concentration led to lower workability and hence formation of non-homogenous matrix resulting in poor bond between the GPC matrix and rebar. The fall of strength was drastic for mixes with 12 M NaOH onwards. Mixes with 14 M NaOH were poor in terms of workability and setting time and hence, resulted in specimens with large pores (see Fig. 4.20) and exhibited poor results. PE based SP contained mixes showed better bond strength with rebar at both early and later ages compared to SN based SP ones, irrespective of the NaOH concentration.

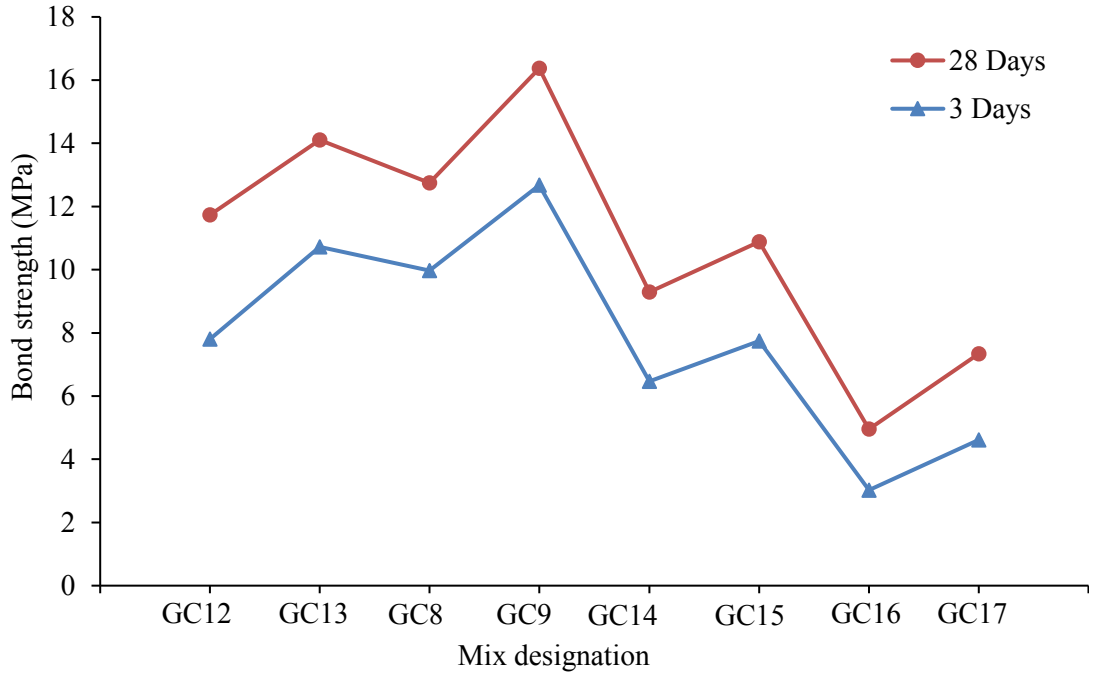

Figure 4.19: Effect of alkali concentration on bond strength of GPC with rebar.

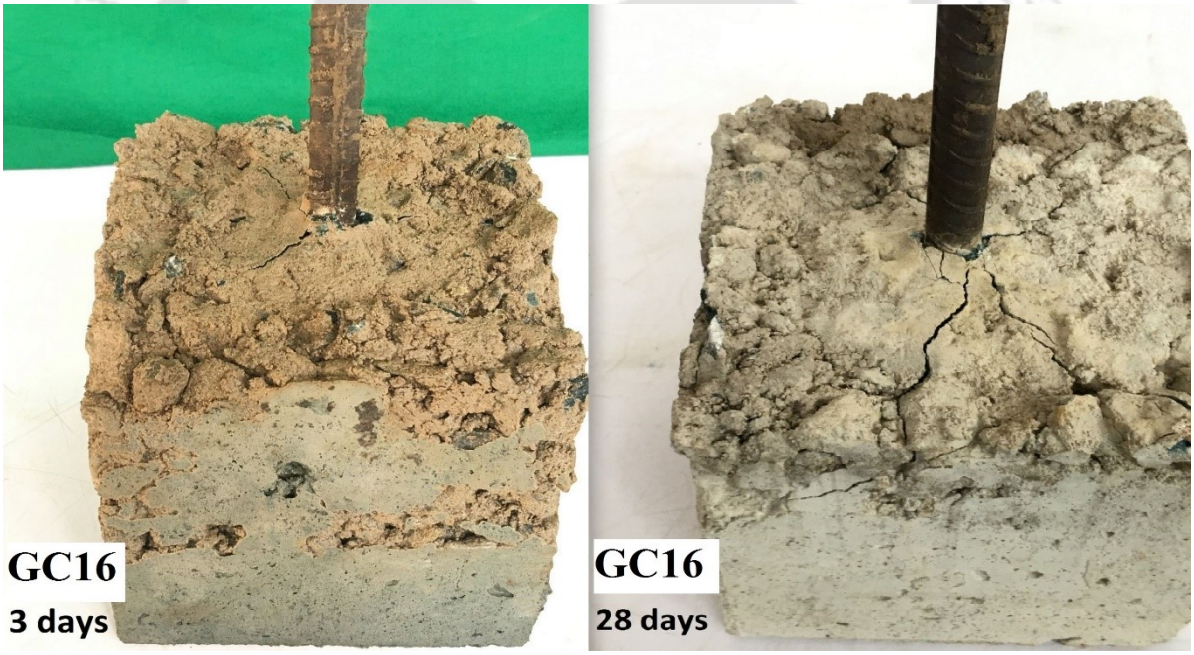

Figure 4.20: Pull-out test specimens of GC16.

Type I SP addition exhibited better bond strength with rebar than type II and III. This was in conformity with the compressive strength test results. Maximum bond strength at 3 and 28 days was observed in mixes with PE based SP added by Type I, Fig. 4.21.

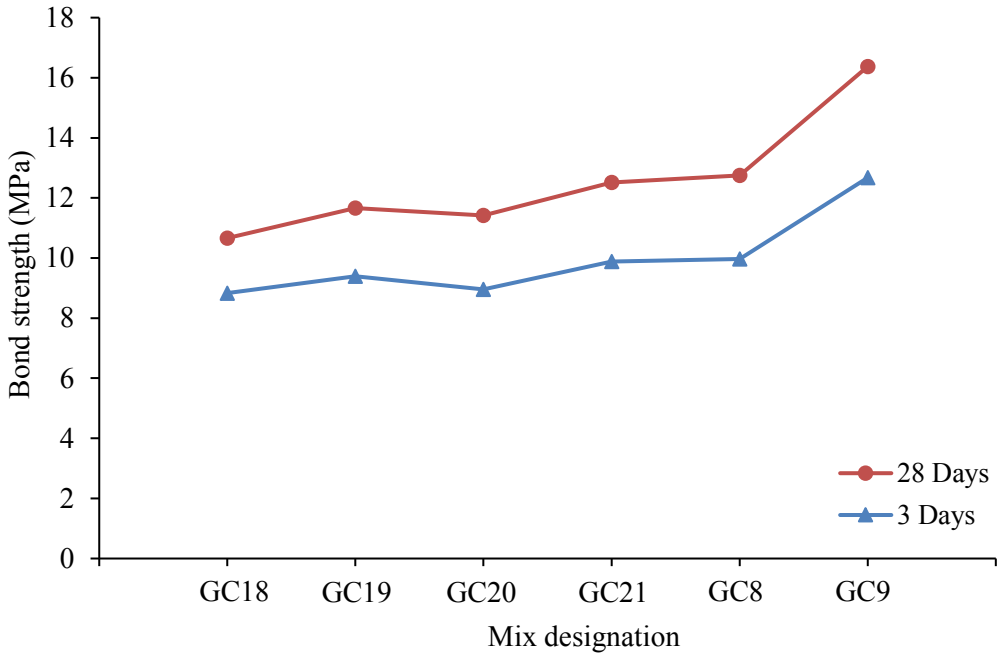

Figure 4.21: Effect of SP addition type on bond strength of GPC with rebar.

On examining the specimens after failure in the pull-out strength test, it was observed that in the specimens with higher slump value and bond strength wide cracks were visible (see Fig. 4.22) that originated from the interface of GPC matrix and rebar and travelled to the surface of the specimen indicating strong bond between both. On the other hand, specimens in Fig. 4.23 with lower slump value and bond strength failed without any visible cracks development. This gave an indication that failure of such specimens occurred due to weak bond between GPC matrix and rebar surface. In this case, since the bond failure happened between GPC matrix and rebar surface, hence no cracks travelled to the concrete surface and therefore no cracks are visible.

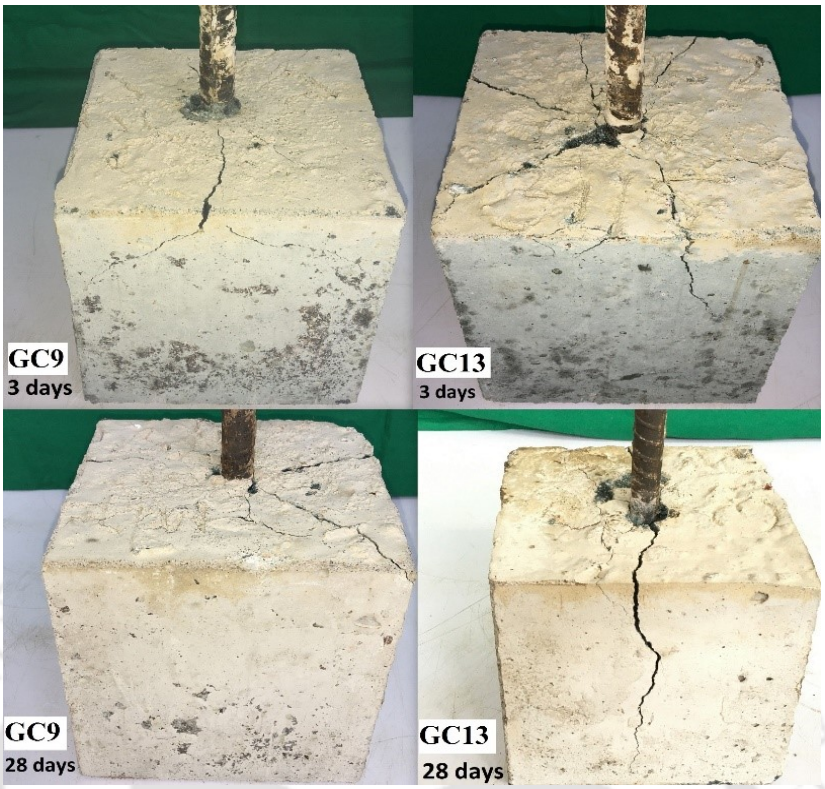

Figure 4.22: Pull-out test specimens with visible cracks after failure.

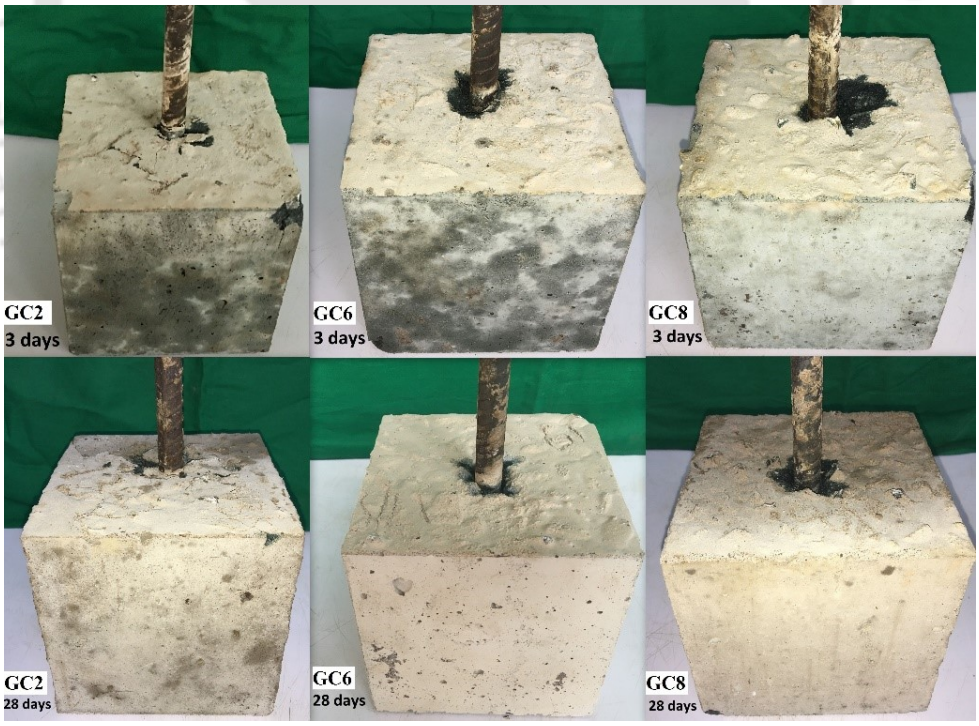

Figure 4.23: Pull-out test specimens without any visible crack after failure.

To observe the influence of workability and compressive strength on the bond strength of UGGBS based GPC with rebar, results from pull-out test have been plotted as function of

slump value and compressive strength in Fig. 4.24 (a) - (d) and 4.25 (a) - (d) respectively. Linear trend-lines have been plotted along with their coefficients of determination (R^2). The trend lines show difference in bonding behaviour due to workability and compressive strength. No definite relation could be concluded between workability and the bond strength. Increase in slump value in some mixes led to improved bond strength. While in others especially when high quantity SPs were added, bond strength of GPC with rebar reduced due to increase in slump value. The relation between workability and bond strength of GPC with rebar does not hold good and consistent (R^2 values range from 0.1168 to 0.6972).

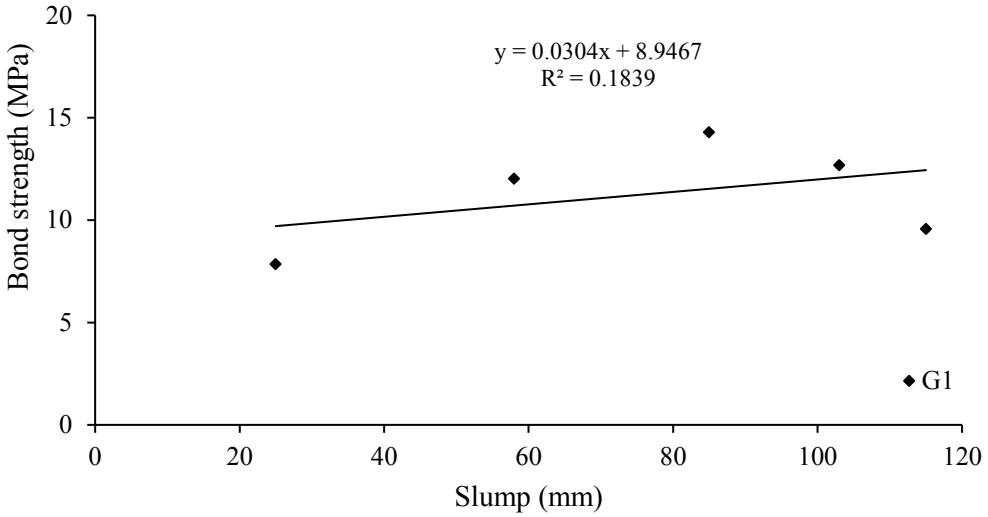

Figure 4.24 (a): Influence of workability on bond strength of GPC with rebar for mix group G1.

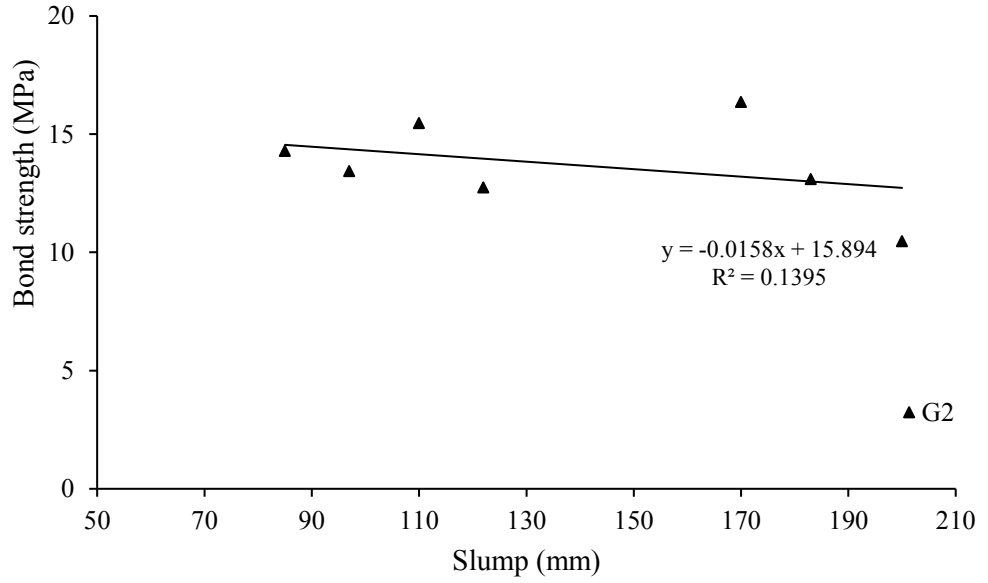

Figure 4.24 (b): Influence of workability on bond strength of GPC with rebar for mix group G2.

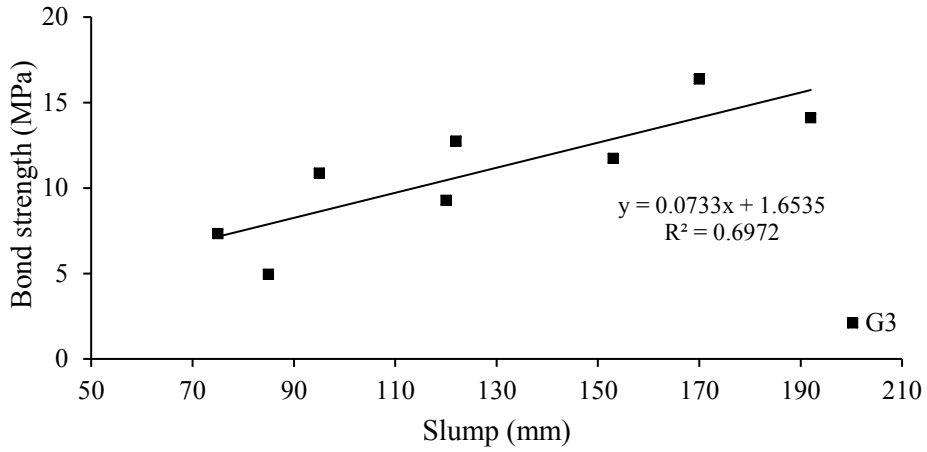

Figure 4.24 (c): Influence of workability on bond strength of GPC with rebar for mix group G3.

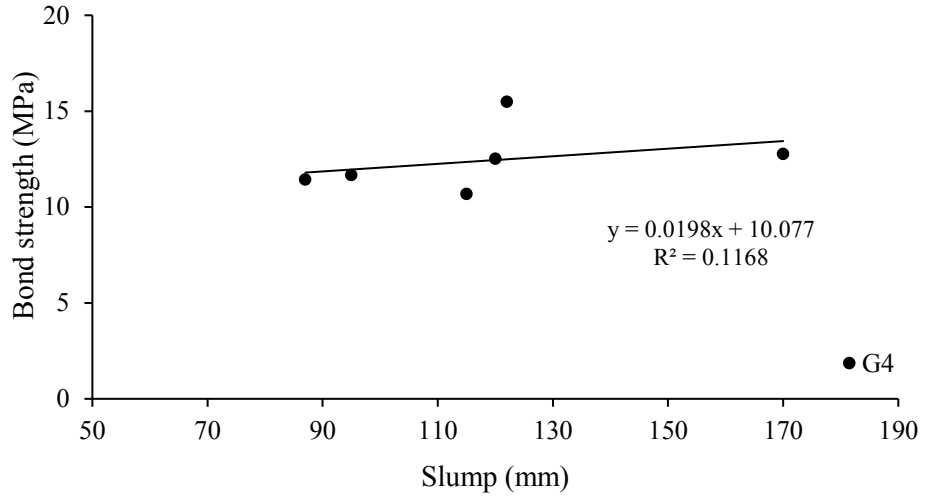

Figure 4.24 (d): Influence of workability on bond strength of GPC with rebar for mix group G4.

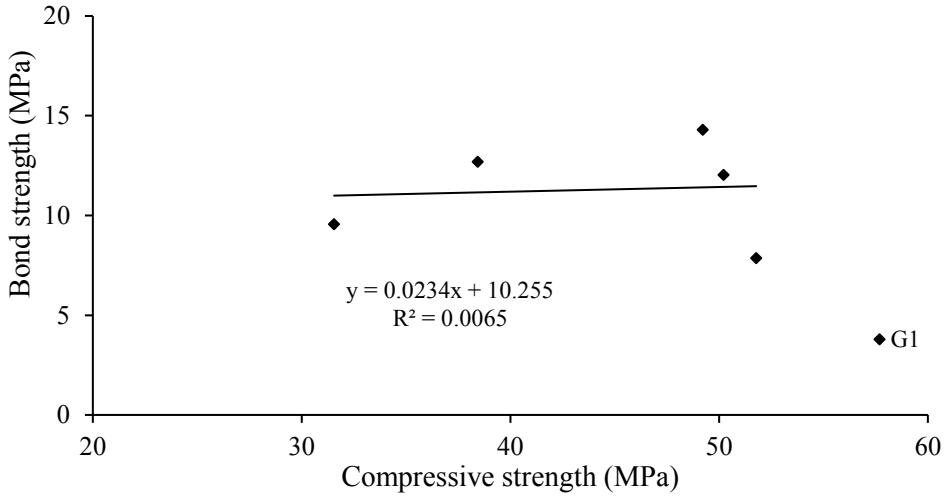

Figure 4.25 (a): Influence of compressive strength on bond strength of GPC with rebar for mix group G1.

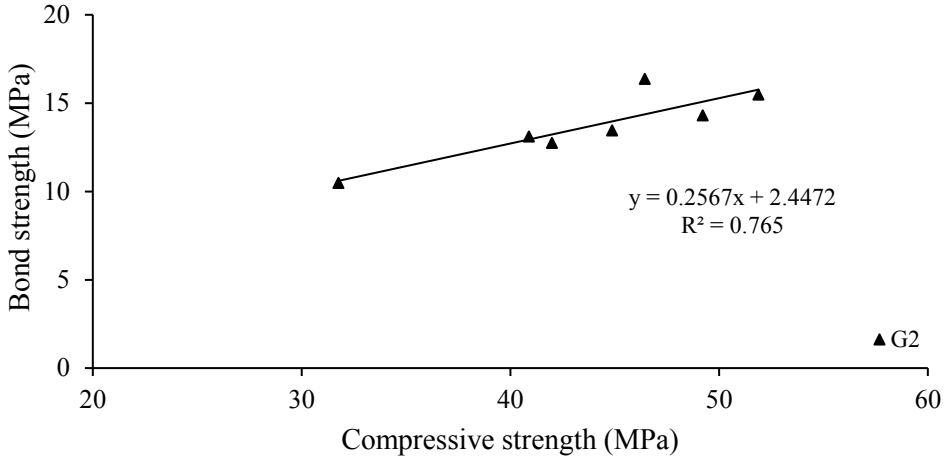

Figure 4.25 (b): Influence of compressive strength on bond strength of GPC with rebar for mix group G2.

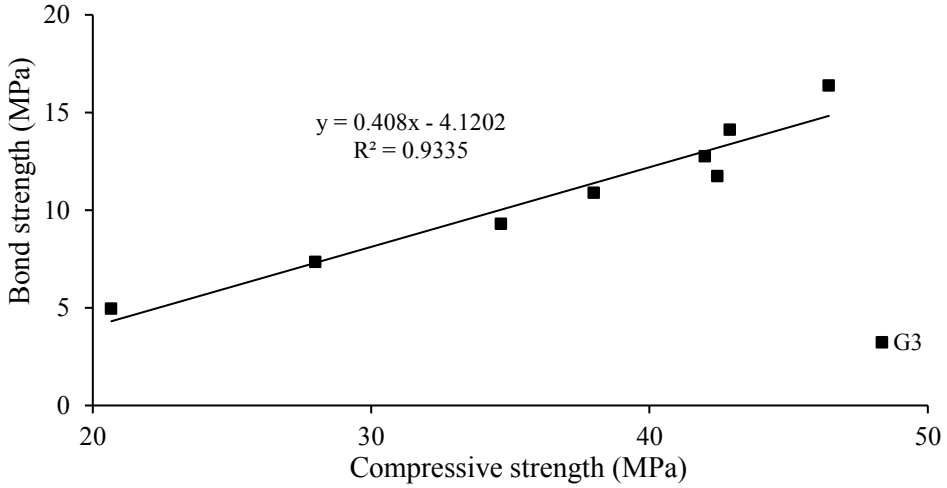

Figure 4.25 (c): Influence of compressive strength on bond strength of GPC with rebar for mix group G3.

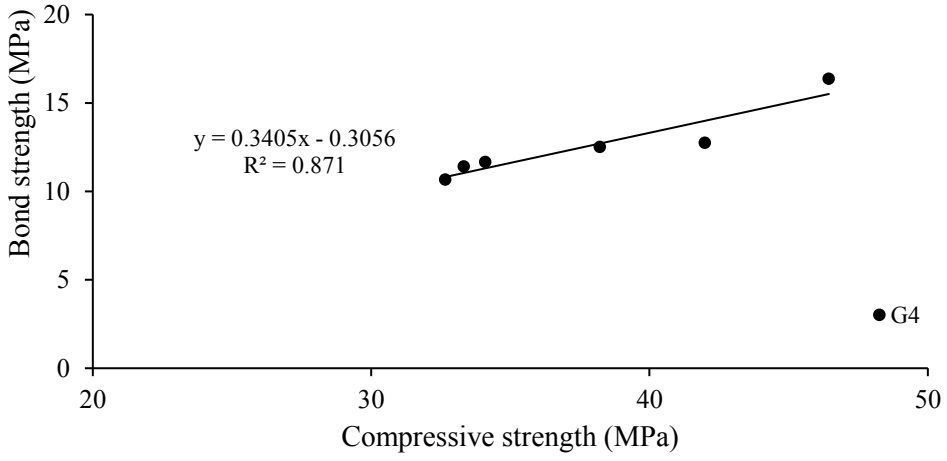

Figure 4.25 (d): Influence of compressive strength on bond strength of GPC with rebar for mix group G4.

The trend-lines for various GPC mix groups show increasing effect in bond strength of UGGBS based GPC with rebar due to increase in compressive strength. Pronounced effect in increase of bond strength with increase in compressive strength was observed in case of G3 GPC mixes ($R^2 = 0.916$). In case of G1 GPC mixes, a slight increase in bond strength of GPC with rebar was observed due to higher value of compressive strength. Nevertheless, the relation in G1 GPC mixes was not found to be consistent ($R^2 = 0.0152$).

4.3.4. Bond strength (slant shear)

Figs. 4.26 (a) - (c) present the results from slant shear test on UGGBS based GPC. As before five geopolymer concrete mixes (GC1 to GC5) and one Portland cement concrete mix (CC2) were selected for study. Flyash (FA) content in the geopolymer mixes varies from 0 to 30 % in an increment of 10 % (See Table 4.1 for details). Insignificant variation in strengths of the mixes have been observed due to addition of FA upto 30 % content, i.e. mix GC1 to GC3. Amount higher than 30 % FA in the mixes caused pronounced and monotonous decrease in the bond strength. Higher amount of FA in the mix caused pronounced reduction in strength due to the reason specified in the section 3.3. The slight improvement of strength at 20 % FA content was because FA addition improved workability that eventually produced homogenous mix and better bonding of the mix matrix to the PCC substrate surface.

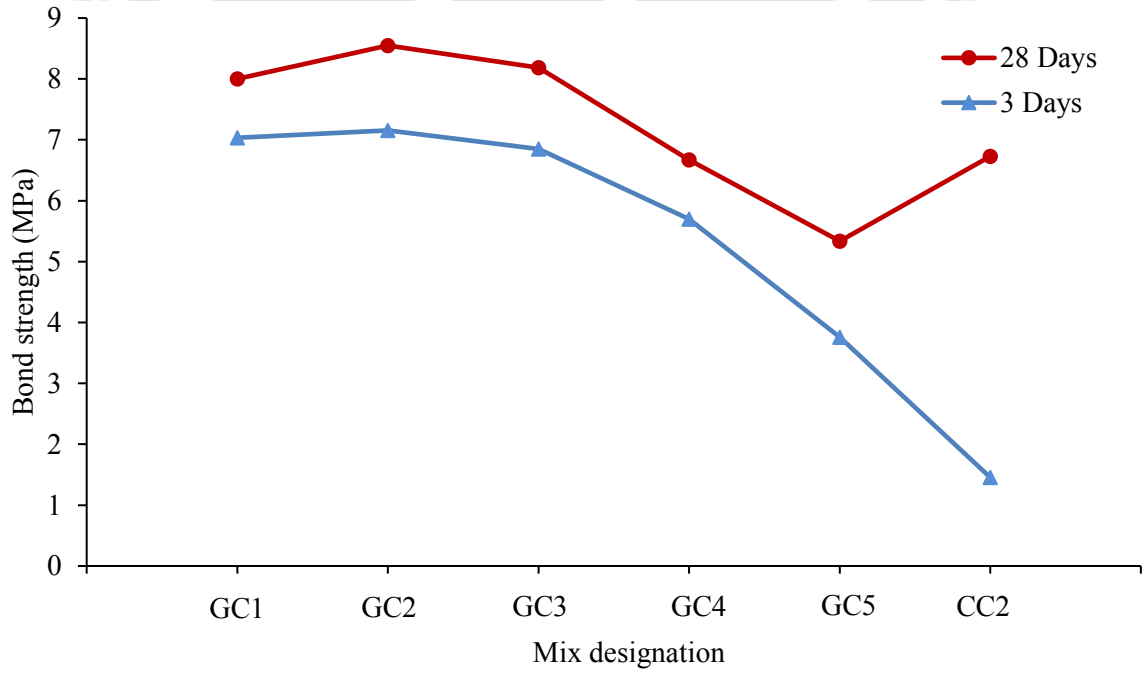

Figure 4.26 (a): Effect of FA content on bond strength of GPC and PCC with 2 months old substrate.

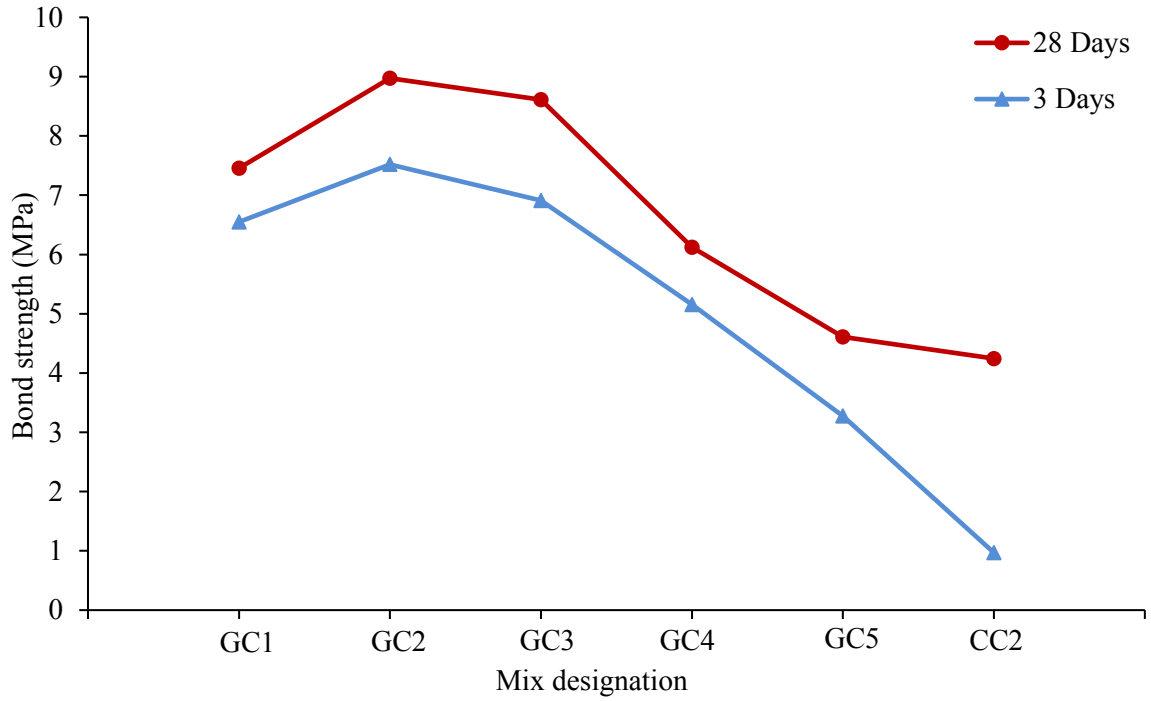

Figure 4.26 (b): Effect of FA content on bond strength of GPC and PCC with 6 months old substrate.

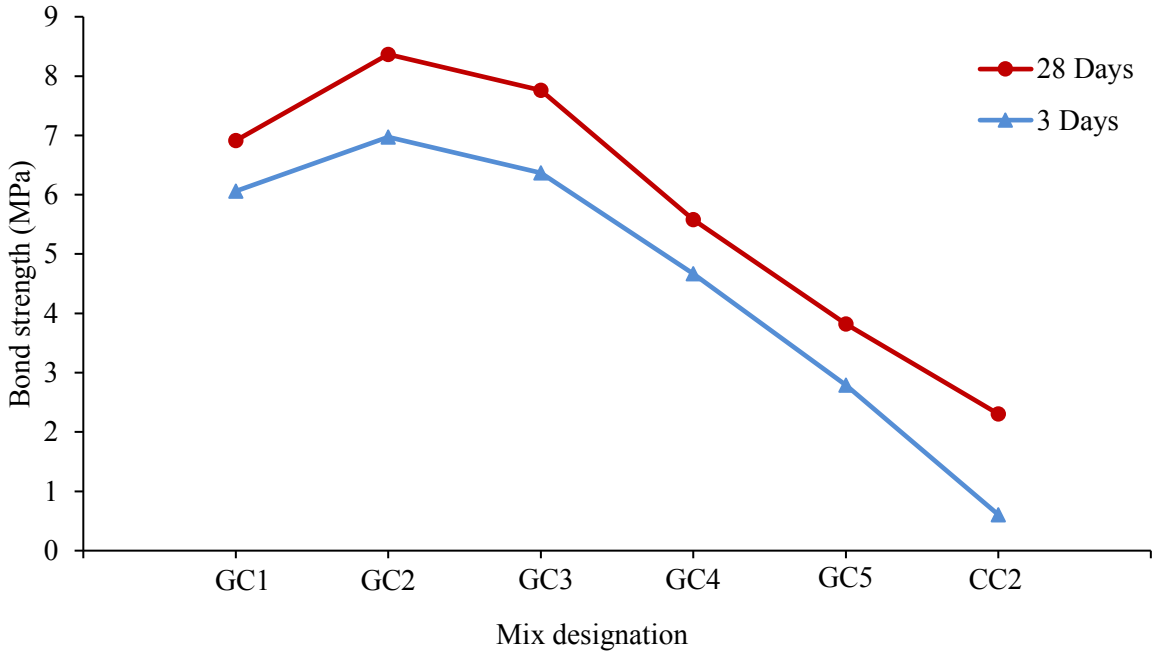

Figure 4.26 (c): Effect of FA content on bond strength of GPC and PCC with 12 months old substrate.

It has been observed that the bond strength of GPC with PCC gradually decreases with the ageing of the PCC {Figs. 4.26 (a) – (c)}. This decreasing trend was followed by mixes

with 0 or high (>30 %) FA content. The mixes with 20 and 30 % FA content achieved higher bond strength with 6 months old PCC substrate compared to that with 2 months old PCC substrate. This is because, the compressive strength and bond strength of GPC mixes with 20 and 30 % FA content was higher than other mixes. Moreover, at 6 months age, PCC substrate also achieved more strength than 2 months age. Hence, all the components (GPC, interface and PCC) in the specimens as a whole exhibited high strength. Therefore, better bond strength was observed. Nevertheless, in case of the specimens with 12 months old substrate, the bond strength deteriorated in all the specimens irrespective of FA content as the bond of GPC with PCC was not sufficiently developed. The observation was same for both early (3 days) and later (28 days) ages bond strength of the specimens.

Figs. 4.27 (a) – (c) show bond strength in the mixes at certain amount of PE based SP. The content of polycarboxylate ether (PE) based SP in the mixes can be seen in Table 4.1. The bond strength of mixes reduced monotonously as the amount of SN based SP in the mixes increased. Maximum bond strength was attained by mix containing 0.5 % PE based SP. Amount higher than this though increased workability but reduced the bond strength. The results from the slant shear test are in line with the compressive strength test results. Very high amount of SP caused segregation in the mix that eventually restricted formation of proper bonds within the geopolymer matrix and bond between the GPC and PCC surface. However, on inspection of the specimens after failure in the test, it was noticed that in mixes with low bond strength, the bond between the GPC and PCC interface was weaker than the bond within the GPC or PCC matrix. The failure surface was along the interface of the GPC and PCC (see Fig. 4.28). On the other hand, as seen in see Fig. 4.29, the failure surface for GPC with higher bond strength was not only along the interface of the GPC and PCC but also within the GPC and PCC matrix.

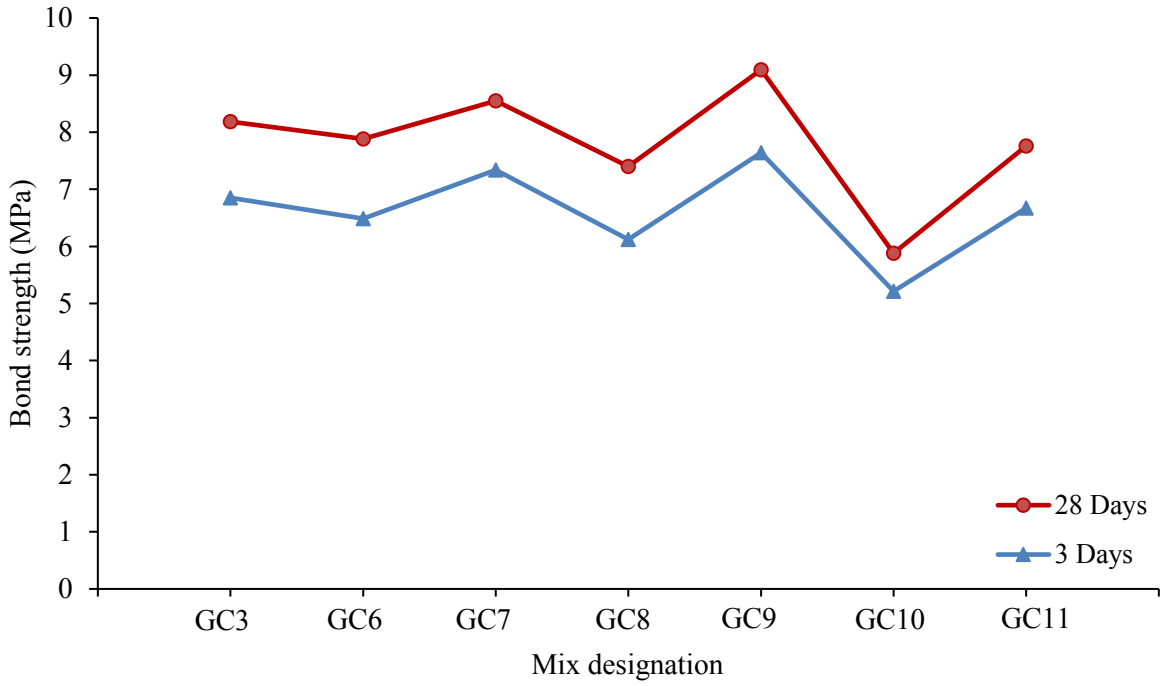

Figure 4.27 (a): Effect of SP content on bond strength of GPC and PCC with 2 months old substrate.

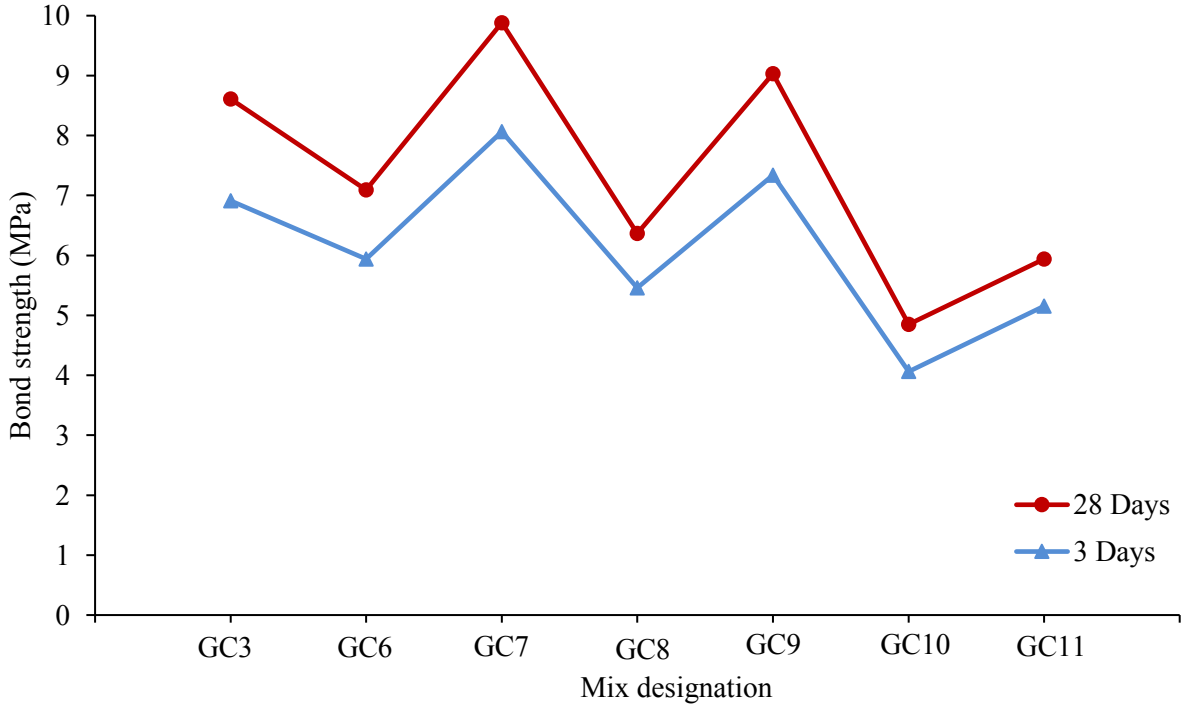

Figure 4.27 (b): Effect of SP content on bond strength of GPC and PCC with 6 months old substrate.

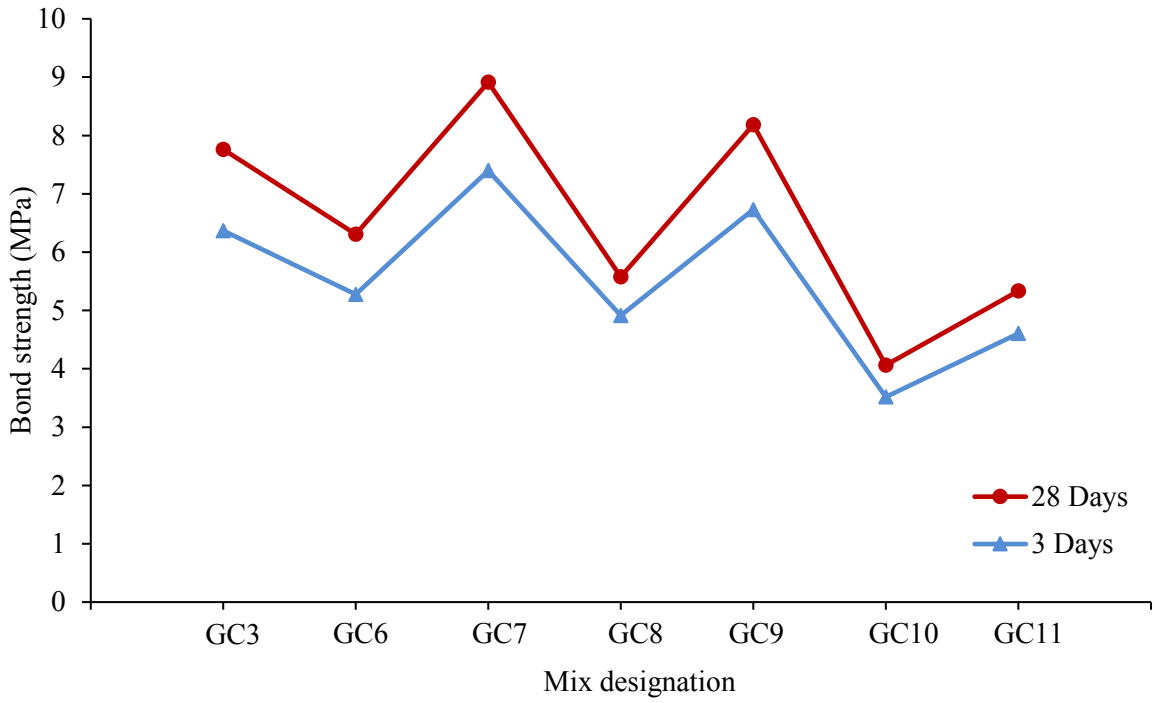

Figure 4.27 (c): Effect of SP content on bond strength of GPC and PCC with 12 months old substrate.

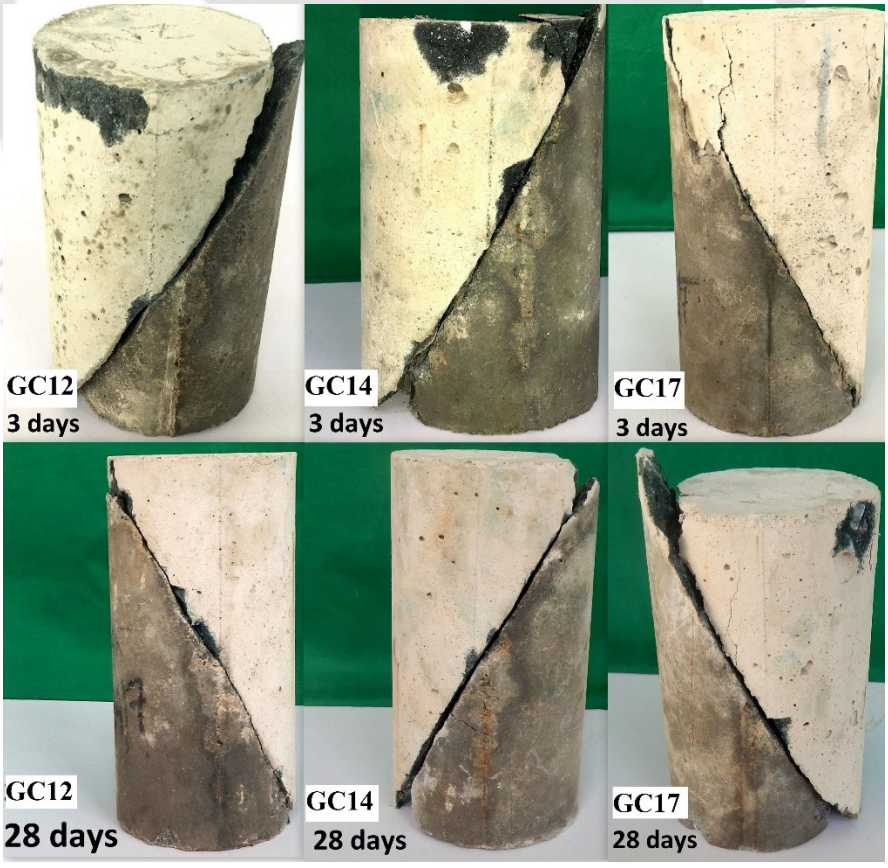

Figure 4.28: Slant shear test specimens with failure plane along GPC-PCC interface.

Figure 4.29: Slant shear test specimens with cracks in GPC and PCC region.

It has been observed that due to ageing of PCC substrate, the bond strength deteriorated at both early (3 days) and later (28 days) ages. This was evident for all the mixes containing varying SP contents except for GC7 mix which contained PE based SP of 0.5 % dosage. Due to the individual strength attainment of the PCC substrate, GPC and the interface, the mix specimens with 6 months old substrate exhibited higher bond strength than those with 2 months old substrate. Mix specimens with 12 months old substrate exhibited significant bond strength reducing trend.

It can be observed from Figs. 4.30 (a) - (c) that, increase in bond strength occurred in the UGGBS based GPC with constant FA and SP content, on increasing the NaOH concentration. However, this was true only upto 10 M concentration. Higher concentration led to reduction in the bond strength. At higher NaOH concentration, the strength tend to decrease monotonously. The phenomenon occurred in mixes containing both the types of SP. Due to high alkalinity and delay in polymerisation, the bond formation of GPC matrix with the PCC was not proper. Mixes containing SN based SP showed lower strength compared to those containing PE based SP regardless of NaOH concentration.

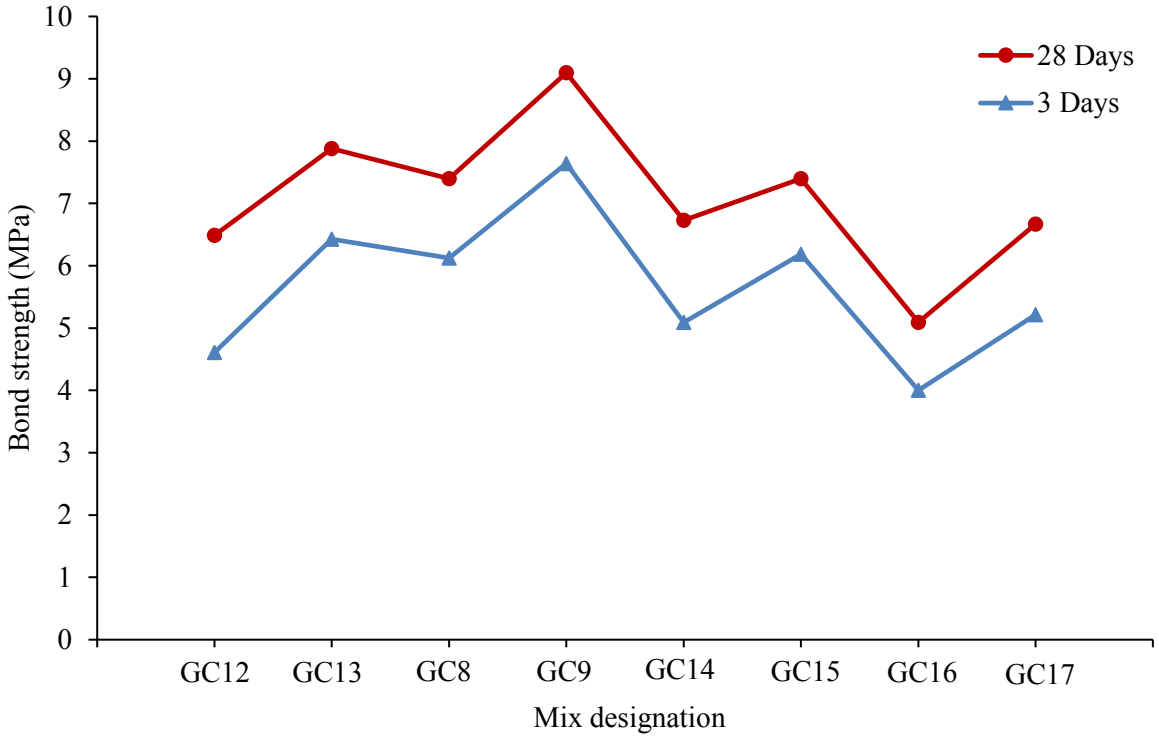

Figure 4.30 (a): Effect of alkali concentration on bond strength of GPC and PCC with 2 months old substrate.

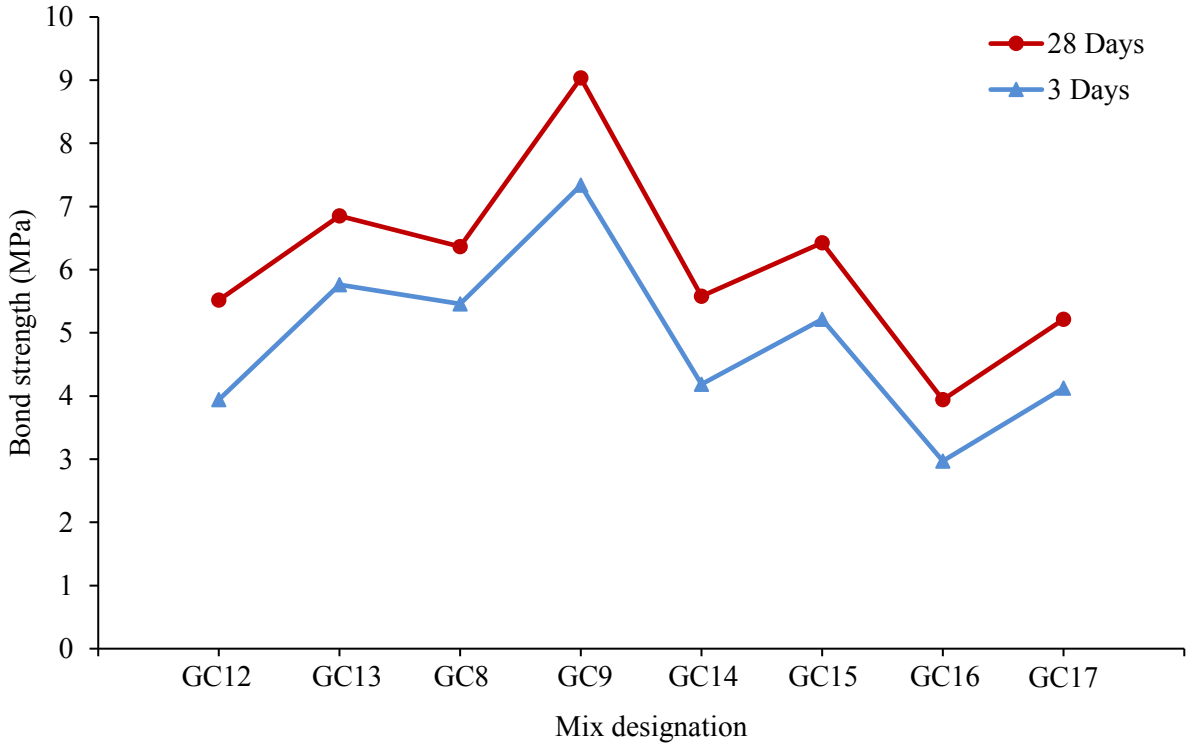

Figure 4.30 (b): Effect of alkali concentration on bond strength of GPC and PCC with 6 months old substrate.

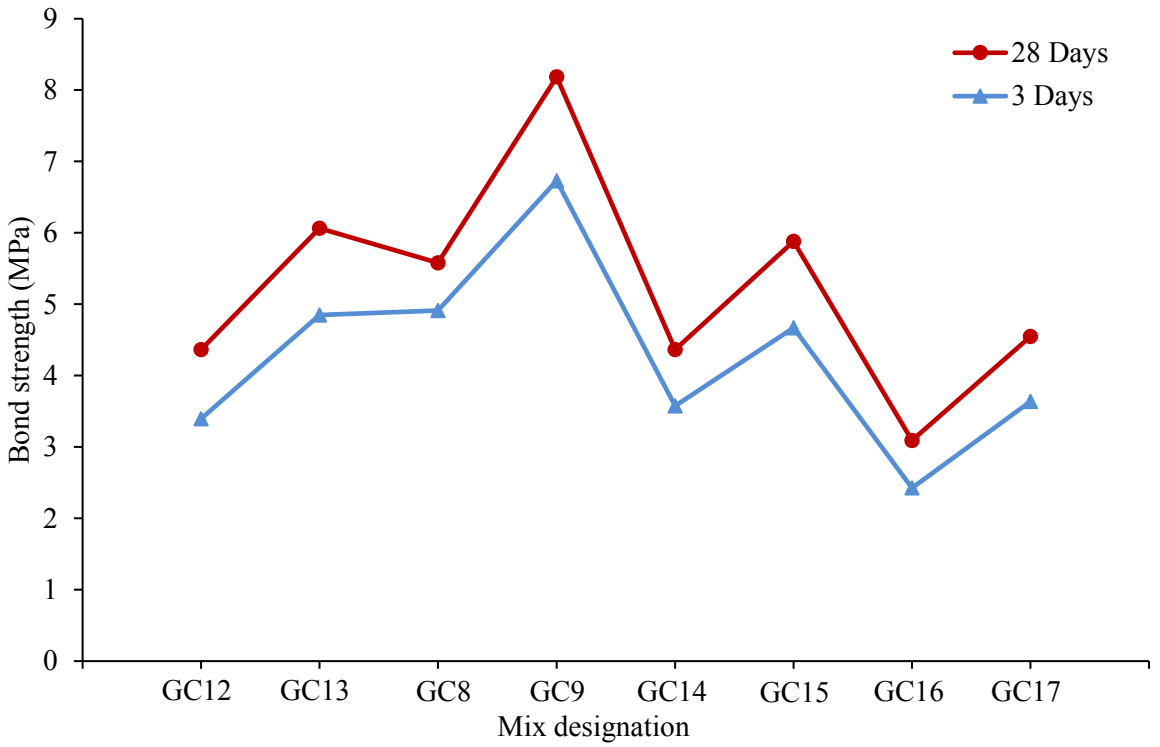

Figure 4.30 (c): Effect of alkali concentration on bond strength of GPC and PCC with 12 months old substrate.

The substrate ageing showed similar strength decreasing effect in all the mixes with various alkali concentration. However, the specimens with 10 M alkali concentration exhibited lower strength deterioration at early and later ages than other mixes. Such effect has been observed as the bond strength of the mix with the substrate is higher than others. The compressive strength of the mix as shown in Fig. 4.15 is also higher than other mixes. Higher compressive and better bonding capacity with substrate resulted in high bond strength even with 12 months old substrate. The bond strength deterioration was more for mixes with SN based SP irrespective of alkali concentration. The later age bond strength deterioration was more prominent in these mixes.

Bond strength results for mixes with various methods of SP addition are found to be in line with the compressive and pull-out strength test results. Type I SP addition outperformed other types, Figs. 4.31 (a) – (c). Type II and III addition showed insignificant difference in the results for a given type of SP. PE based SP performed better in each type of addition. The SP addition type had similar effect on bond strength with PCC substrate of all ages for a particular mix. Type I PE based SP addition exhibited minimum bond strength deterioration at early and later ages.

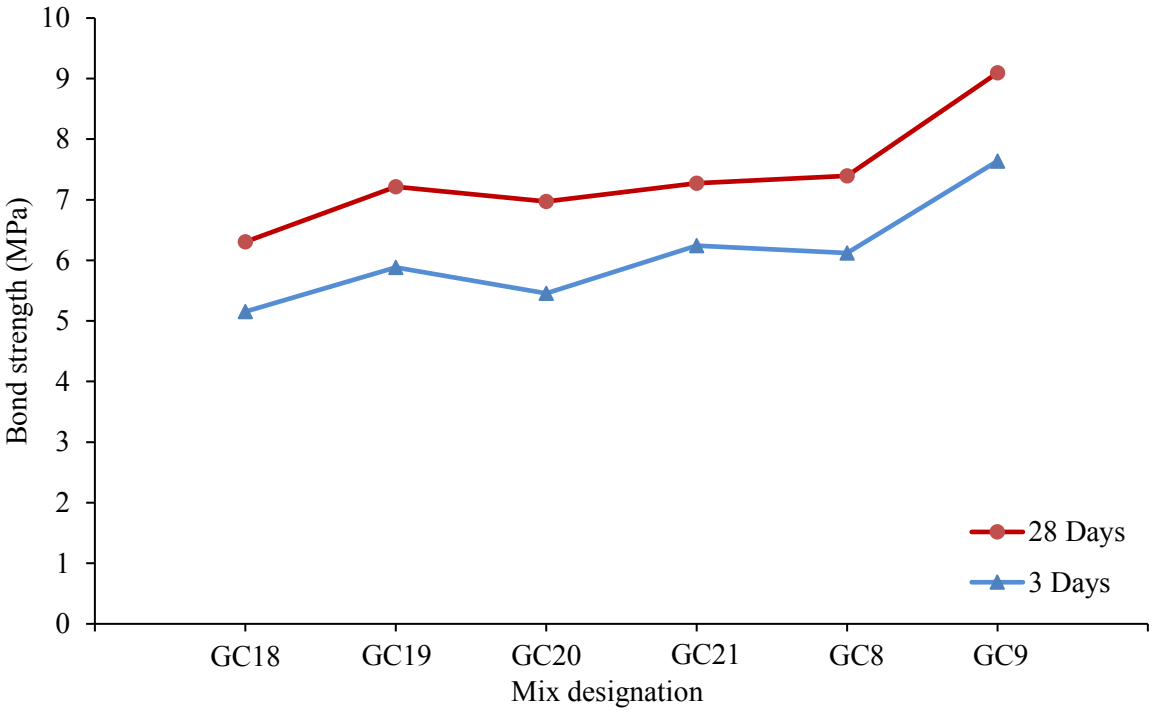

Figure 4.31 (a): Effect of SP addition type on bond strength of GPC and PCC with 2 months old substrate.

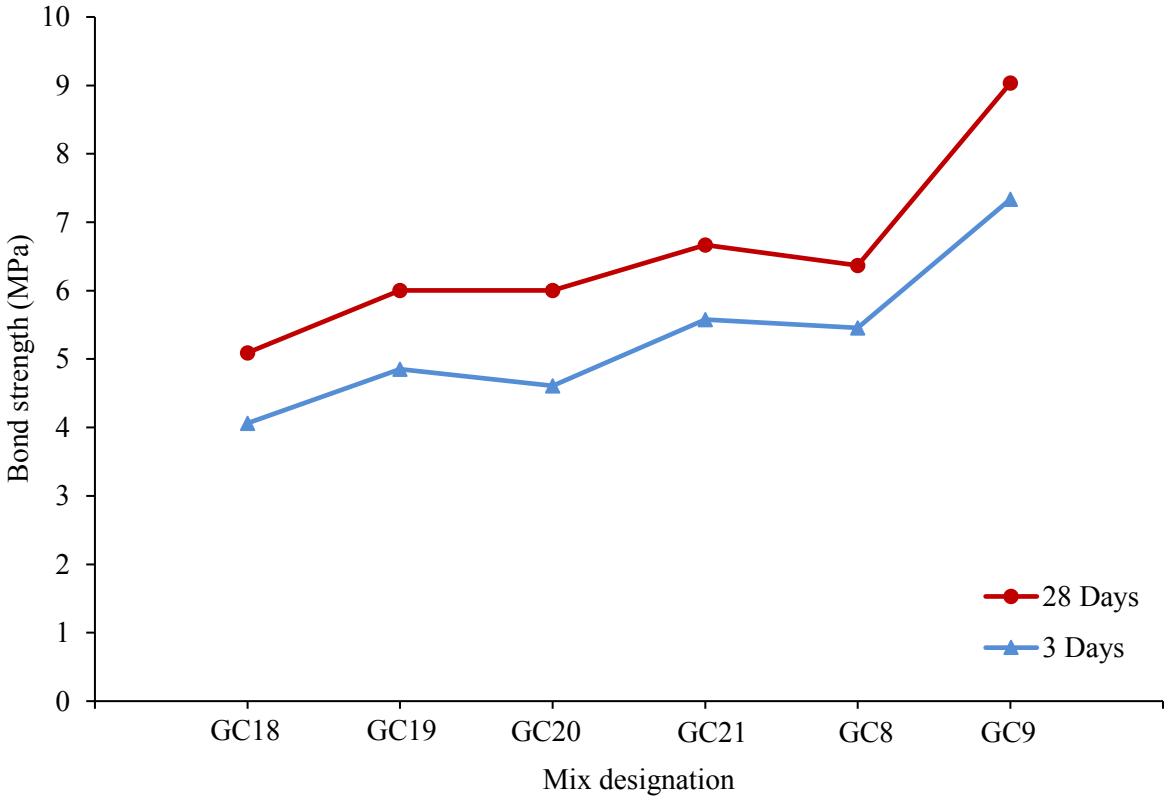

Figure 4.31 (b): Effect of SP addition type on bond strength of GPC and PCC with 6 months old substrate.

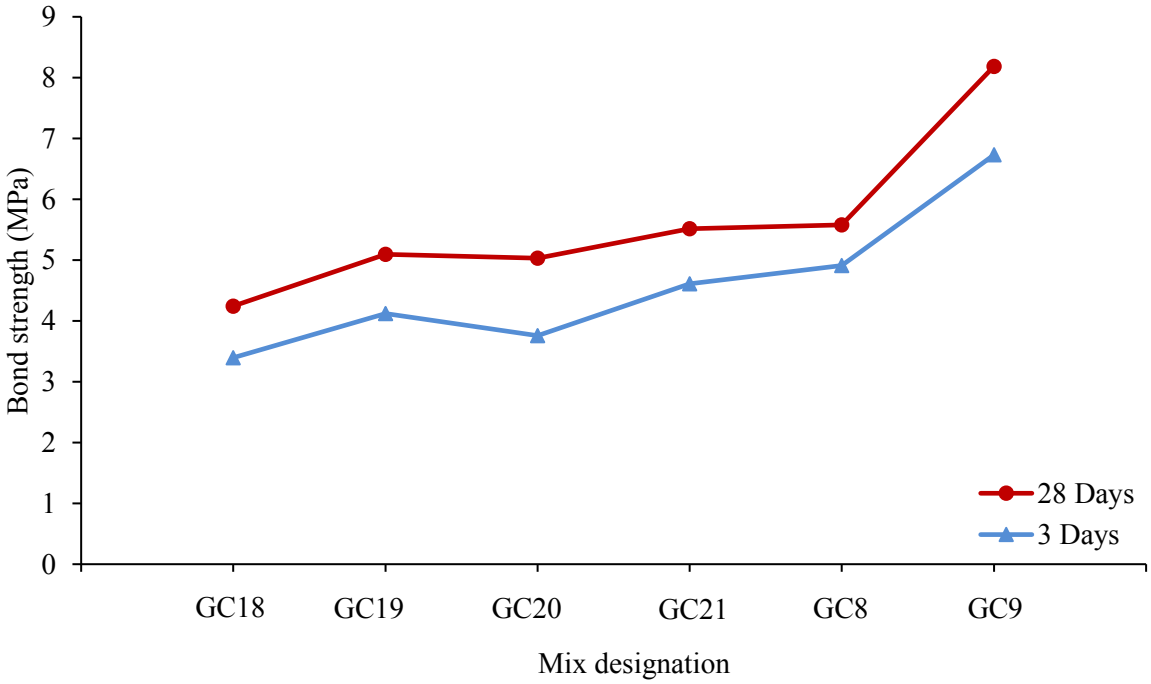

Figure 4.31 (c): Effect of SP addition type on bond strength of GPC and PCC with 12 months old substrate.

Figure 4.32 (a) – (d) show the variation of bond strength with slump value. The bond strength was based on slant shear test. From the plots, no definite relation could be established between workability and bond strength. Increase in slump value in some mixes led to improved bond strength while in other mixes especially when high quantity of FA and SPs were added, bond strength deteriorated with the increase in slump value. The relation between workability and bond strength of UGGBS based GPC with PCC does not hold good and is inconsistent (R^2 values range from 0.289 – 0.593).

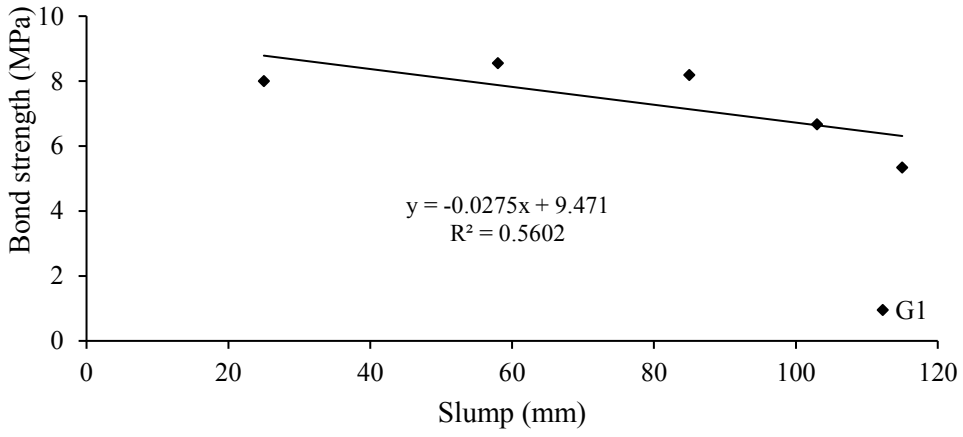

Figure 4.32 (a): Influence of workability on bond strength of GPC with PCC for mix group G1.

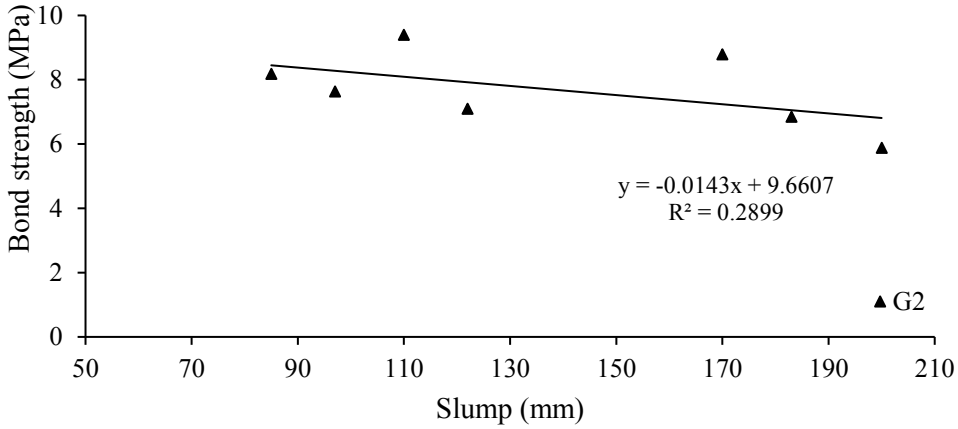

Figure 4.32 (b): Influence of workability on bond strength of GPC with PCC for mix group G2.

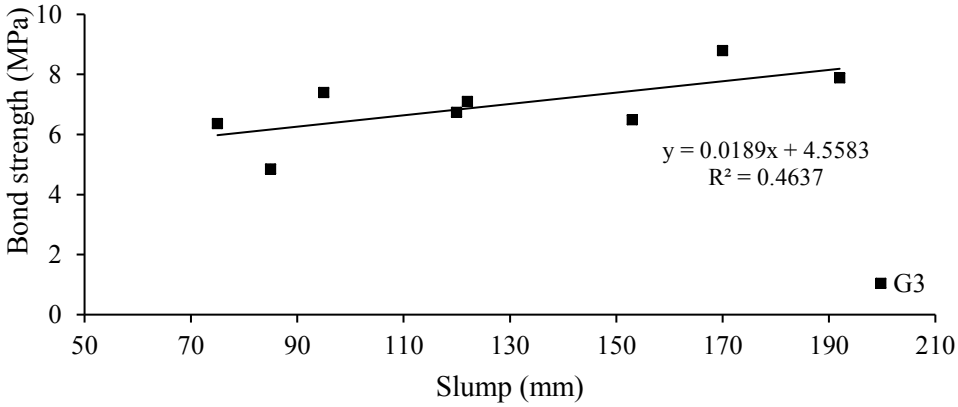

Figure 4.32 (c): Influence of workability on bond strength of GPC with PCC for mix group G3.

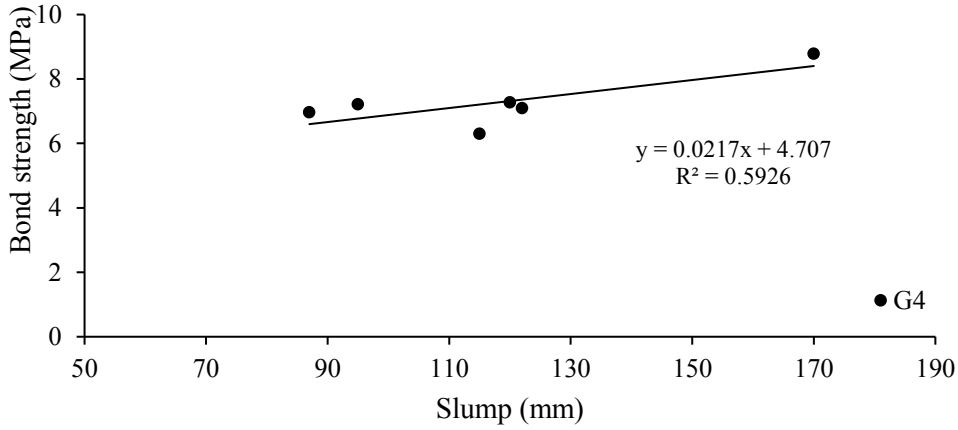

Figure 4.32 (d): Influence of workability on bond strength of GPC with PCC for mix group G4.

The relation between bond strength and compressive strength of UGGBS based GPC mix (G1 to G4) is shown in Figure 4.33 (a) – (d). The trend-lines for various UGGBS based GPC mix groups show that increase in compressive strength increases the bond strength of GPC with PCC. Effect was prominent in case of G1 GPC mixes ($R^2 = 0.972$). In case of GPC mixes, G2 and G4 relation between the bond strength of GPC with PCC and compressive strength was found to be moderately consistent (R^2 range from 0.711 to 0.785). It may be mentioned that bond strength indicates the new and old concrete bond that were determined by slant shear test.

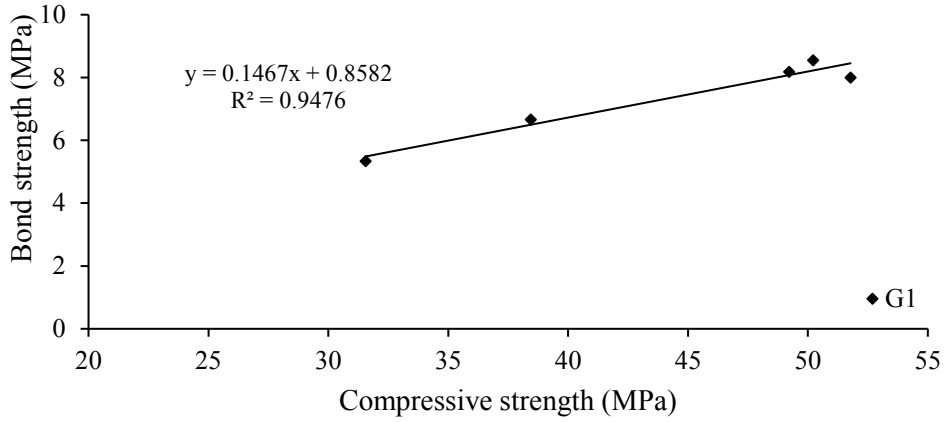

Figure 4.33 (a): Influence of compressive strength on bond strength of GPC with PCC for mix group G1.

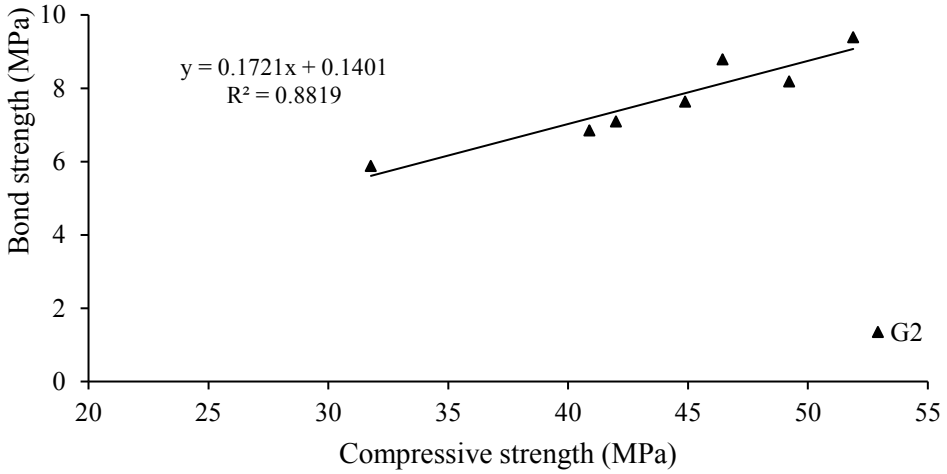

Figure 4.33 (b): Influence of compressive strength on bond strength of GPC with PCC for mix group G2.

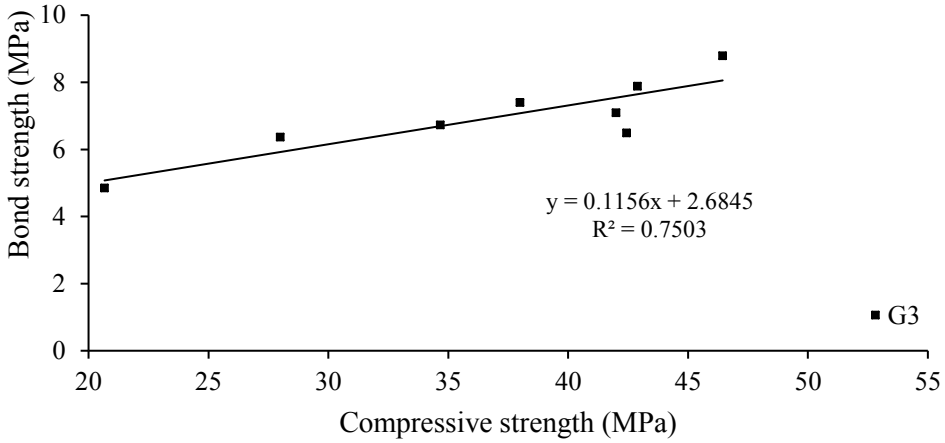

Figure 4.33 (c): Influence of compressive strength on bond strength of GPC with PCC for mix group G3.

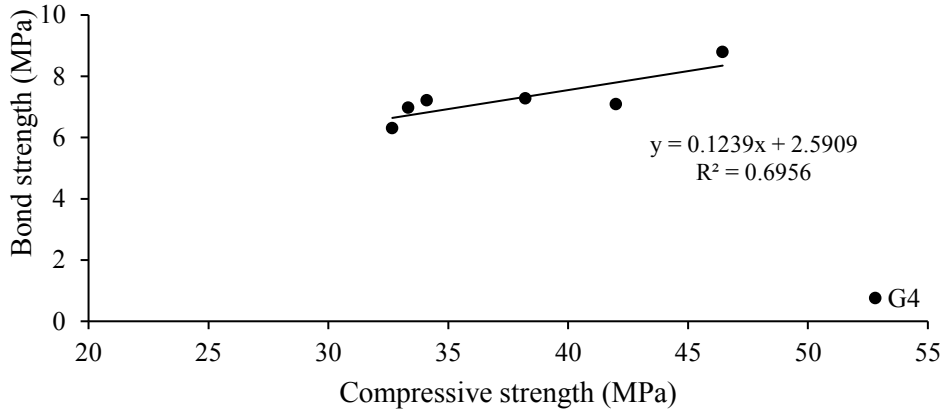

Figure 4.33 (d): Influence of compressive strength on bond strength of GPC with PCC for mix group G4.

4.4. Closure

Results of laboratory experiments performed on 21 different ultra-fine ground granulated blast furnace slag (UGGBS) based geopolymer concrete (GPC) mixes to evaluate the workability, compressive and bond strength are presented in this chapter. Tests were also performed on a Portland cement concrete (PCC) mix which was considered as controlled mix. The important observations from the study are as follows:-

i. UGGBS based GPC has strong potential to be used as an agent for concrete repairing and strengthening of reinforced concrete structures. GPC possess superior fresh and hardened state properties as compared to PCC.

ii. The speciality of UGGBS based GPC is that at 1 day it can develop strength of about 60 % of that at 28 days. The bond strength of the GPC with rebar and PCC surface is found

to be satisfactory at both early and later ages. However, UGGBS alone as binder creates workability issues.

iii. Addition of flyash (FA) to the UGGBS based GPC contribute towards monotonous improvement in workability. The strength on the other hand reduces. However, such reduction in strength is significant for mixes with high FA content. In such mixes, both early and later strengths are negatively affected. In case of bond strength results, the addition of FA improves the performance of the mixes but upto low FA content level.

iv. Workability of the UGGBS based GPC improves due to addition of superplasticizer (SP). Polycarboxylate ether (PE) based SP perform better than sulfonated naphthalene (SN) based SP at all dosage level. At high dosage, segregation occurs in the mixes and leads to erroneous workability results. The compressive and bond strength of the mixes improve till lower level of PE based SP dosage. In case of mixes with SN based SP, the addition of SP cause monotonous reduction in compressive and bond strength.

v. High workability of GPC mixes is observed when low concentration sodium hydroxide (NaOH) is used. Increase in concentration of NaOH leads to deterioration of workability property which is pronounced when NaOH concentration is higher than 10 M. Mixes with 10 M NaOH concentration are found to exhibit highest compressive and bond strengths at early and later ages compared to mixes with NaOH concentration of 8, 12 and 14 M. Higher NaOH concentration cause monotonous decrease in the compressive and bond strength.

vi. Time of addition of SP shows significant influence on fresh and hardened state properties of UGGBS based GPC. Type I SP addition prove to be reasonable for the mix process as it contribute towards better performance in terms of workability and strength. The other types of SP addition are not beneficial in improving the properties of the mixes.

Chapter 5

Repairing of RC Beams using Geopolymer Mortar

5.1 Introduction

The concrete in reinforced concrete (RC) structures undergo cracking due to numerous factors such as overloading on the structures, earthquake and other naturally occurring phenomenon, accidental impacts including man-made impacts, etc. Cracks in concrete are also induced due to its shrinkage, thermal stresses, chemical reaction, weathering, ageing, corrosion in steel, etc. Such cracks in concrete of RC structures if remain unattended are likely to enlarge and propagate away from the surface towards the inner region of the members. The cracks provide lead-way for intrusions of water and harmful ions in the concrete leading to physio-chemical reactions within. This result in further enlargement of the cracks, disintegration and strength loss in the concrete. Thus, the RC structures suffer structural weakness and loss in durability. Cracks may also appear due to overloading and corrosion in reinforcement in RC structures and walls. Fig. 5.1 shows some of the reasons of RC structural failure. The presence of crack in concrete also affects the overall appearance of an RC structure. Moreover, due to the presence of crack in concrete, the load carrying capacity of a member reduces compared to its designed capacity. Such member shows very poor performance when being subjected by repeated loading. The fatigue or cyclic load capacity reduces drastically in such member.

(a) Failure due to overloading in beam.

(b) Failure due to corrosion in beam.

(c) Shrinkage cracks in concrete.

(d) Cracks in beam-column joint due to earthquake.

(e) Cracks in beam-column joint.

(f) Cracks in the wall.

Figure 5.1: Cracks in concrete in RC structural members and walls.

Repairing of RC structures possessing concrete cracks is essential since dismantling an RC structure and replacing it with a new one is a very costly affair, especially in developing nation like India. In recent years, the repairing of RC structures is one of the most crucial and emerging field of research in the construction industry. The challenges in repairing of the RC

structures are attempted to be well addressed by various researchers and engineers engaged in this field.

Repairing of RC structures is carried out at local level in the structure, i.e. the repairing is performed in the RC members. The repairing of the RC members is performed primarily to address the following issues:-

i. Restoration of the load carrying capacity of the member being damaged due to the loads that was underestimated while designing.
ii. Avoiding the prematured failure that occur due to propagation and widening of the cracks induced due to various reasons.
iii. Restoration of load carrying capacity of corrosion affected members.

Due to advancement in technology in the construction industry, wide range of products and methods for repairing of RC structural members are available. However in present day, it is necessary for such techniques to be cost effective and fast in processing time. Many structures that were built in the past are carrying cracks in their members. Immediate attention is necessary to avoid further degradation and loss of the utility of the structures. However, the techniques of repairing is necessary to be cost efficient and rapid.

The process of repairing of RC structural members includes the following:-

i. The cracks in the members are identified.
ii. The identified cracks are then cleaned by brushing, jet watering or air blowing to make them free from loose concrete particles and dust.
iii. The repairing agent is then filled into the cracks to fill it completely.
iv. The repaired members are allowed to be cured if necessary.

RC elements are repaired and strengthened by several ways since long time. Various materials and methodologies were employed to repair RC elements and tested to evaluate the short-term and long-term performances. Chajes et al. [55] employed externally bonded composite fabrics consisting of amramid, E-glass and graphite fibres for strengthening of RC beams. Effectiveness of Portland cement (PC) based reinforced concrete jacketing of damaged RC beams was studied by Altun [59]. Issa and Deb [60] investigated the performance of gravity filled epoxy in concrete. Metakaolin based geopolymer mortar (GPM) was used by Vasconcelos et al. [51] for repairing of concrete. Polymer modified mortar (PMM) was used for controlling cracks in RC beams by Ahmad et al. [61].

The present work deals with the study of repairing of RC beams using ultra-fine ground granulated blast-furnace slag (UGGBS) based GPM. Generally, the early strength

gain of repairing agent is advantageous property in repairing technology. Moreover, the bond between the repairing agent and old concrete is of concerning issue in repairing works. In the present study it is established that GPM possesses early strength gain property (Chapter 3). The superior bond strength of geopolymer systems as established in Chapter 4 is also contributing factor which makes it suitable to be used as RC structural members repairing agent. Compared to other materials such as glass, graphite fibres, epoxy, polymer modified mortar, the cost of preparation of ultra-fine ground granulated blast-furnace slag (UGGBS) based GPM is significantly lower which makes it suitable to be used as RC structural members repairing agent. Hence, repairing of RC beams were performed using GPM. The performance of GPM repaired beam is compared with that of Portland cement mortar (PCM) repaired beam to conclude regarding the effectiveness of geopolymer as a repairing agent. Following aspects have been thoroughly studied:-

i. Load and displacement at yielding of beam.
ii. Ultimate load and corresponding displacement.
iii. Ductility ratio (DR), defined as the ratio between the deflection at ultimate load and deflection at yield load.
iv. Strength enhancement ratio (SER), defined as the ratio between ultimate load of the repaired beam and that of the controlled beam.
v. Load at development of first crack
vi. Cracking pattern.

Here, the controlled beam is the beam prior to any repairing. In case of partially damaged repaired beams, the beam, B3 with the following specification was considered as controlled beam:-

i. Cross-sectional size: 150 mm × 200 mm
ii. Length: 2 m
iii. Main reinforcement: 2 numbers of 12 mm diameter tor steel bars at top and bottom.
iv. Stirrups: 2 legged 8 mm diameter tor steel bars at 100 mm centre to centre till 500 mm length from the end on both sides and remaining middle portion of 930 mm length was provided with 2 legged 8 mm diameter tor steel bars as stirrups at 185 mm centre to centre.

5.2 Experimental Investigation

Reinforced concrete (RC) beams were cast using Portland cement concrete (PCC). The beams were subjected to four point loading till development of cracks. The repairing of the cracks was done using Portland cement paste (PCP) and Portland cement mortar (PCM); and geopolymer paste (GPP) and geopolymer mortar (GPM). Total 7 numbers of beams were cast for this purpose.

5.2.1 Materials

The materials that were used in the process of casting of the RC beams and thereafter their repairing are described elaborately in this section under the following heads:-

5.2.1.1 Geopolymer paste

The fine cracks in the repaired beams were filled using GPP. The paste was prepared using ultra-fine ground granulated blast furnace slag (UGGBS). The properties of UGGBS have been discussed in sub-section, *2.2.2 Ultra-fine ground granulated blast furnace slag* of Chapter 2. Table 5.1 presents the mix proportion of the GPP used as repairing agent. Total three numbers of mixes were prepared and tested to evaluate the efficiency in terms of fresh and hardened state properties. The mix consisted of 70 % UGGBS and 30 % flyash (FA). This percentage was selected as this gives optimum result in terms of workability and strength as found in Chapter 3. Moreover, from the results presented in Chapter 3, 10 M sodium hydroxide (NaOH) was decided to be used as alkali activator. Here, total binder refers to UGGBS and FA together. Alkali in alkali/ total binder (a/b) ratio refers to NaOH solution. The solid in the water/solid (w/s) ratio refers to binder and the NaOH solids in the solution. The tests were performed as per guidelines of IS 1727 1967 [81]. Workability test was performed using flow table. The procedure is described in sub-section, *3.2.4 Experiments* of Chapter 3. The result is reported in terms of flow index (FI) as defined by equation 5.1.

$$FI = \frac{FD - ID}{ID} \times 100 \tag{5.1}$$

Here, FI is the flow index in percent. FD is the average final base diameter of mortar mass measured on four diameters after jolting as per the codal provisions [81], ID is the original base diameter, which is 100 mm. While performing the experiment for workability, it was observed that the addition of high quantity of alkali activator led to highly flowable

GPP. However, when the such GPP was placed in the cube mould, the solid particles settled at the bottom. Compressive strength test was performed at 3 and 28 days on 50 mm cube of GPP to observe early and later age strength development behaviour.

Table 5.1: Mix proportion for GPP.

Mix	Binder		Alkali/binder	Water/solid
	UGGBS	FA	(a/b)	(w/s)
GP1	70	30	0.55	0.34
GP2			0.60	0.37
GP3			0.65	0.39

From the results in Table 5.2, it was found that the GPP having a/b ratio of 0.60 possessed satisfactory workability and compressive strength. The paste having a/b ratio of 0.55 resulted in lowest workability. Lowest compressive strength was found in the GPP having a/b ratio of 0.65. The low strength attainment is presumed due to the segregation of GPP constituents. Therefore, GPP GP2 was decided to be used as repairing paste.

Table 5.2: Workability and compressive strength tests result of GPP.

Mix	Alkali/binder	Compressive strength (N/mm^2)		Workability
	(a/b)	3 days	28 days	(FI)
GP1	0.55	42.40	51.07	96.67
GP2	0.60	37.33	48.00	158
GP3	0.65	24.27	29.87	200

5.2.1.2 Portland cement paste

The fine cracks in the beams which were not possible to be filled up by the repairing PCM were filled using Portland cement paste (PCP). Ordinary Portland cement (OPC) 43 grade was used for preparing the paste. The properties of OPC are discussed in sub-section, *2.2.1 Portland cement* of Chapter 2. Table 5.3 shows the water/cement (w/c) of the PCP tested for using as repairing agent. The mix proportion was selected such that the w/c ratio of PCP almost matches with total water/solid (w/s) ratio of GPP. Laboratory tests were performed to evaluate the fresh and hardened state properties of the PCP. The tests were performed as per guidelines of IS 1727 1967 [81]. Similar to the tests conducted for evaluation of fresh and hardened state properties of GPP, flow table and compressive strength tests were performed

on the PCP. Compressive strength test was conducted at 3 and 28 days on 50 mm cube of PCP to observe early and later age strength development behaviour.

The test results are presented in in Table 5.3. It was found that the PCP exhibited lower compressive strength at early age than GPP. The strength at 28 days was high and was almost equivalent to that of GPP. However, the PCP possessed very low workability. The FI was 36.67.

Table 5.3: Workability and compressive strength tests result of PCP.

Mix	Water/cement (w/c)	Compressive strength (N/mm^2)		Workability (FI)
		3 days	28 days	
CP1	0.40	27.07	46.00	36.67

5.2.1.3 Geopolymer mortar

Geopolymer mortar (GPM) was prepared primarily using UGGBS. FA and superplasticizer (SP) were added as admixtures. The details of UGGBS, FA and SP are presented in sub-section *2.2.2 Ultra-fine ground granulated blast furnace slag, 2.2.3 Flyash* and *2.2.6 Admixture* of Chapter 2. The fine aggregate used in the preparation are described in sub-section, *2.2.5 Aggregates* of Chapter 2. NaOH solution was used as alkali activator. Mix GM20 was selected for repairing from among all the GPM mixes presented in Table 3.1 in Chapter 3. Table 5.4 presents the mix proportion of GM20. Here, UGGBS and FA are together termed as binder. Total solid in the mix considers all the solid particles contributed by UGGBS, FA and NaOH. This was determined to find the value of water/solid ratio (w/s) in GPM which was considered equivalent to w/c of PCM mix used. The SP was added to the fresh GPM after the addition of the NaOH solution.

Table 5.4: Mix proportion for GM20 (kg).

UGGBS	FA	NaOH concentration (Molarity, M)	SP (% of binding agent)	SP type	w/s
70	30	10	1.5	PE	0.4

Note: *Fine aggregate = 300 kg*, *NaOH = 60 kg*.

The selection of GM20 as repairing agent was on the basis of fresh and hardened state properties of the GPM mixes. Compressive strength test was conducted on 50 mm cubes of

GPM in Compression Testing Machine and results of 3 and 28 days are presented in the table. Workability test was performed using flow table when the mortar was in fresh state. The result is reported in terms of flow index (FI) as defined by equation 5.1 in sub-section *5.2.1.1 Geopolymer paste*. Vicat apparatus was used for conducting the setting time test. The tests were conducted as per relevant IS Code of Practice [81].

GM20 offered appreciable workability. The setting time was also found to be sufficient for placing the mortar into the cracks. The strengths attained at both early and later ages were also comparatively high. The fresh and hardened state properties of the GPM mix GM20 are presented in Table 5.5.

Table 5.5: Fresh and hardened state properties of GM20.

Test	Result
Initial setting time	58 minutes
Final setting time	88 minutes
Workability	83.67 (FI)
Compressive strength (3 days)	36.60 N/mm^2
Compressive strength (28 days)	45.96 N/mm^2

5.2.1.4 Portland cement mortar (PCM)

Portland cement mortar (PCM) was used for repairing the cracks in the RC beams. The mortar was prepared using OPC as described in sub-section, *2.2.1 Portland cement* of Chapter 2. Fine aggregate that was used for preparation of GPM was also used for preparation of PCM. Table 5.6 presents the mix proportion of CM1 which was used for preparing the PCM. The fresh and hardened state properties of CM1 are shown in Table 5.7. The tests performed were similar to the tests performed in case of GPM.

Table 5.6: Mix proportion for PCM (kg).

Mix	Cement	Fine Aggregate	Water/cement (w/c)
CM1	100	300	0.40

Table 5.7: Fresh and hardened state properties of CM1.

Test	Result
Initial setting time	95 minutes
Final setting time	265 minutes
Workability	19.67 (FI)
Compressive strength (3 days)	19.58 N/mm^2
Compressive strength (28 days)	35.02 N/mm^2

5.2.1.5 Portland cement concrete

Portland cement concrete (PCC) was prepared using ordinary Portland cement. The details of OPC as described in sub-section, *2.2.1 Portland cement* of Chapter 2. The fine and coarse aggregates used in the preparation have been described in sub-section, *2.2.5 Aggregates* of Chapter 2. The mix proportion for PCC has been presented in Table 5.8.

Table 5.8: Mix proportion for PCC (kg/m^3).

Mix	Cement	Fine Aggregate	Coarse aggregate	Water/cement (w/c)
CC1	360	680	1128	0.55

Mix CC1 was used for preparation of PCC for casting of RC beams. Table 5.9 presents the fresh and hardened state properties of the mix. Compressive strength test was performed on 150 mm cubes of PCC in Compression Testing Machine and results of 3 and 28 days have been presented in the table. Prism specimens of size 150 mm × 150 mm × 700 mm were cast and tested applying four point loading at 3 and 28 days to determine the flexural strength of PCC. For determining the tensile strength, PCC cylinders of 150 mm diameter and 300 mm height were cast and tested in the Universal Testing Machine (UTM). Workability was evaluated from slump test performed using slump cone when the concrete was in fresh state. The tests were performed as per relevant IS Code of Practice [122, 125, 127].

Table 5.9: Fresh and hardened state properties of CC1.

Test	Result
Workability (Slump)	90 mm
Compressive strength (3 days)	15.14 N/mm^2
Compressive strength (28 days)	28.04 N/mm^2
Tensile strength (3 days)	0.90 N/mm^2
Tensile strength (28 days)	2.17 N/mm^2
Flexural strength (3 days)	1.12 N/mm^2
Flexural strength (28 days)	2.56 N/mm^2

5.2.1.6 Reinforcement

RC beams were cast with 2 numbers of 12 mm diameter tor steel bars IS 432 (Part 1) 1982 [95] at top and bottom as main reinforcement. Stirrups were provided using 2 legged 8 mm diameter tor steel bars. Sub-section, *2.2.7 Steel reinforcement bars* of Chapter 2 presents the details of the rebars used.

5.2.2 Method of beam preparation and repairing with mortar

Seven numbers of RC beams were cast for the purpose of testing of repaired beams. The beams in undamaged state were considered as controlled beams. The beams were of 1.8 m span and designed as doubly reinforced concrete beams having theoretical ultimate load carrying capacity of 53.78 kN. The design which was carried out to decide the beam size and reinforcement in case of preparing the RC beams is presented in Appendix B. The design was done to limit the load carrying capacity of the beam and also to create the condition of failure due to bending i.e., flexural failure. The RC beams were of size 150 mm × 200 mm and length 2 m. The reinforcement details are presented in Fig 5.2. Main reinforcement of 2 numbers of 12 mm diameter tor steel bars at top and bottom was provided. Stirrups were provided using 2 legged 8 mm diameter tor steel bars at 100 mm centre to centre till 500 mm length from the end on both sides and remaining middle portion of 930 mm length was provided with 2 legged 8 mm diameter tor steel bars as stirrups at 185 mm centre to centre. Fig. 5.3 shows the reinforcement provided in the RC beams. The size of repaired RC beams was restricted to its original size of 150 mm × 200 mm and length 2 m, Fig. 2.

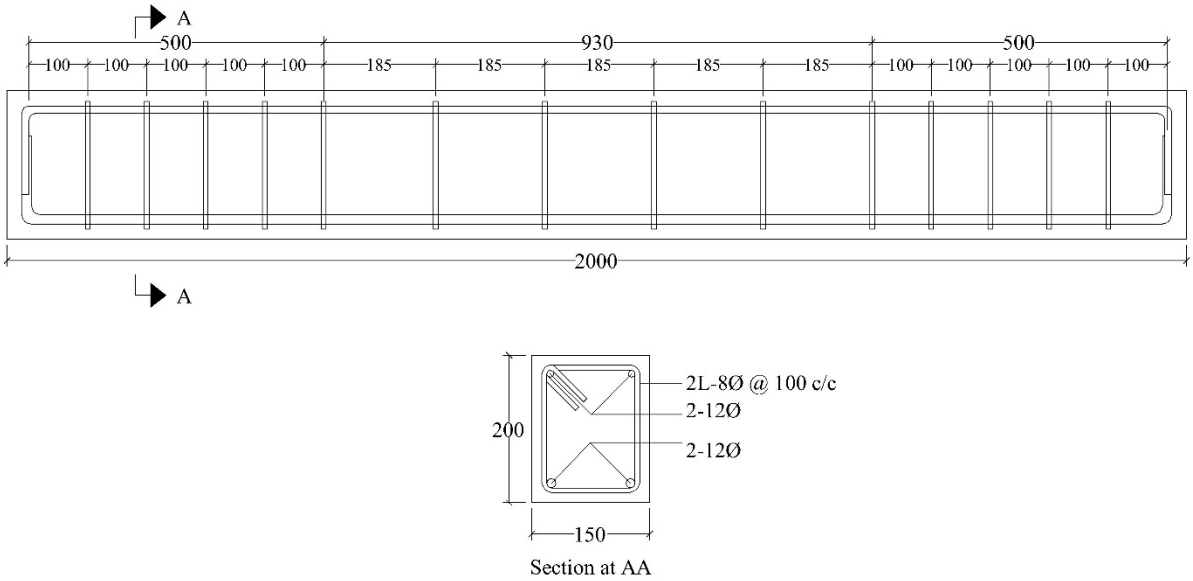

Figure 5.2: Details of controlled and repaired RC beams (*All dimensions are in mm*).

Figure 5.3: Reinforcement provided in the RC beams.

The parameters required for the design were collected from the mechanical tests which were carried out on the PCC (CM1). For evaluation of the mechanical properties, laboratory tests such as compressive, tensile and flexural strengths tests were conducted on cube specimens of size 150 mm, cylinder specimens of diameter 150 mm and height 300 mm; and prisms of size 150 mm × 150 mm × 700 mm respectively. Using the design results, the RC beams were cast to size 150 mm × 200 mm × 2000 mm.

The casting of the RC beams was carried out as per guidelines laid in IS 516 1959 [122]. The formworks for RC beams were prepared and reinforcements as mentioned in the preceding paragraph were placed inside it (Fig. 5.4). The PCC (CM1) was prepared and placed inside the formworks in total three layers. After placing the concrete in each layer, it

was vibrated using a needle vibrator as shown in Fig. 5.5 to release the air bubbles and fill up the voids in the concrete. This helped the concrete to get placed homogenously inside the formworks. On completion of placing of concrete, the formworks were left undisturbed for 24 hours in the laboratory. After 24 hours from the time of casting, the formworks were removed from the RC beams. The curing of the beams were carried out in the laboratory at ambient temperature of 20 ± 2 ºC for 3 and 28 days by wrapping them with wet rags.

Figure 5.4: Formwork used for casting RC beams.

Figure 5.5: Needle vibrator used for compaction of concrete in RC beams.

On completion of the curing period, the RC beams were uncovered from the wet rags and allowed to surface dry. A fine layer of white wash was applied over the surface of the beams so that the cracks that were supposed to develop due to the loading in the test are clearly visible. The RC beams were later subjected to static flexural load using MTS actuator

(Maximum load: 250 kN; Maximum displacement: 250 mm) till targeted load is applied. Displacement based loading at the rate of 0.01 mm/s was monotonically applied. The RC beams were divided into 2 groups based on the damage level due to the loads subjected from the actuator. The groups are as follows:-

i. *Fully damaged beams* - Four numbers of RC beams were loaded till failure. In these RC beams, the monotonic static load was applied to achieve the ultimate load. The cracks in the beams were induced in the region of pure tension. Most of the cracks were wide with minimum width of 5 mm which propagated towards the core of the beam. This can be observed from Fig. 5.6.

Figure 5.6: Cracks in fully damaged RC beam.

ii. *Partially damaged beams* - Three numbers of RC beams were loaded upto 60 % of their ultimate load carrying capacity as found by the procedure followed in beams in group (i). The ultimate load in this case was considered as the ultimate load of controlled beam, B3. At such load range, the beams remained in their elastic stage. This was observed from the load- deflection curve of the controlled beam. The cracks in the beams were induced in the region of pure tension however the enlargement was restricted. Most of the cracks were of maximum width of 1 mm. Further, the cracks did not propagate towards the core of the beam as evident from Fig 5.7.

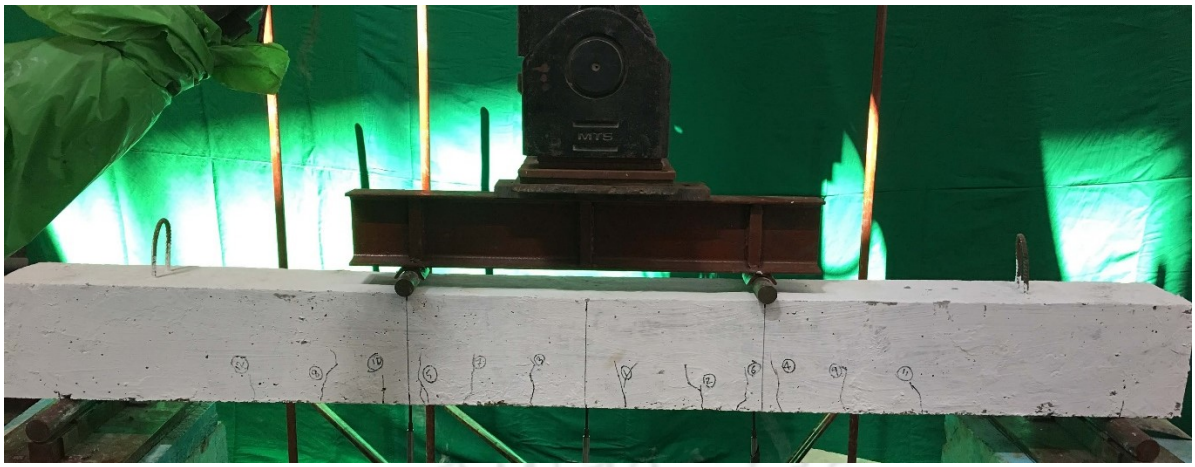

Figure 5.7: Cracks in partially damaged RC beam.

The cracks that were developed due to the application of load on the RC beams were identified and marked. These cracks were then enlarged upto a depth of maximum 50 mm and width of maximum 40 mm using hammer and concrete-breaking bit to facilitate easy and effective application and penetration of repairing material (paste and mortar) as shown in Fig. 5.8. Beyond 50 mm depth, the cracks are presumed to be very fine in nature. The broken concrete bits in the cracks were removed carefully with the help of brush such that no free particles remained attached to the surface of the cracks. The beams were subjected to air blow with the help of air blower as shown in Fig. 5.9 to remove the dust and minute free particles from the surface and ready it for further treatment. Minute inspection was done to ensure that no free particles remain inside the cracks. This method of crack cleaning and surface preparation is similar to that used by the field engineers and technical persons while repairing concrete structures with epoxy resin, cement grout, etc.

Figure 5.8: Crack width in the damaged RC beam after enlargement for repairing.

Figure 5.9: Use of air blower for removal of dust particles from inside the cracks.

The repairing paste (GPP or PCP) was first applied to fill the cracks followed by the application of repairing mortar. Due to high flowabilty of the paste, it could penetrate inside the fine cracks which were not wide enough to allow the accommodation of mortar. But those fine cracks were significant to act as the source of crack development in the repaired RC beam. Hence, the fine cracks were arrested by repairing paste. The paste was applied using a syringe used in treatment related to female hygiene in hospitals, Fig. 5.10. The use of such syringe facilitated better penetration of the paste into the fine cracks.

Figure 5.10: Application of repairing paste inside the cracks using syringe.

The large cracks were filled up by the repairing mortar (GPM or PCM). The repairing mortar was placed inside the cracks with the help of trowel, Fig. 5.11. It was compacted with the tamping bar for better placement and removal of voids within. The mortar was continued to be placed inside the cracks till the original cross-sectional size of the beam was restored as shown in Fig. 5.12. On completion of the cracks filling process, the beams were wrapped with wet rags and cured at ambient temperature of 20 ± 2 ºC till arrival of test day. On the test day, the wet rags were removed and the beams were exposed to air blower for drying the surface.

Figure 5.11: Application of repairing mortar inside the cracks using trowel.

Figure 5.12: Mortar repaired damaged RC beam.

5.2.3 Experimental setup

The experimental setup for testing the controlled and repaired RC beams is presented in Fig. 5.13. The experimental setup and testing method was same for controlled and repaired RC beams. The beams were subjected to static flexural load using MTS actuator (Maximum load: 250 kN; Maximum displacement: 250 mm). The tests were performed by applying four point loading. Displacement based loading was monotonically applied at the rate of 0.01 mm/s. The load in controlled beams was continued to be applied till the targeted load was reached. However, in case of repaired beams the load was applied till failure of the beams. The load application was halted when the load started to fall and reached 75 % of the ultimate load achieved. The midspan displacement was recorded using spring mounted linear variable differential transformer (LVDT), L2 of capacity 100 mm. Two additional LVDTs, L1 and L3 were used to monitor the loading uniformity. The additional LVDTs were placed below the point of contact of rollers of spreader beam with RC beam as shown in Fig. 5.13 by L1 and L3. However, results from these LVDTs were not considered to prepare the load-deflection curves. Load-deflection curves are drawn according to the record of the central LVDT, L2.

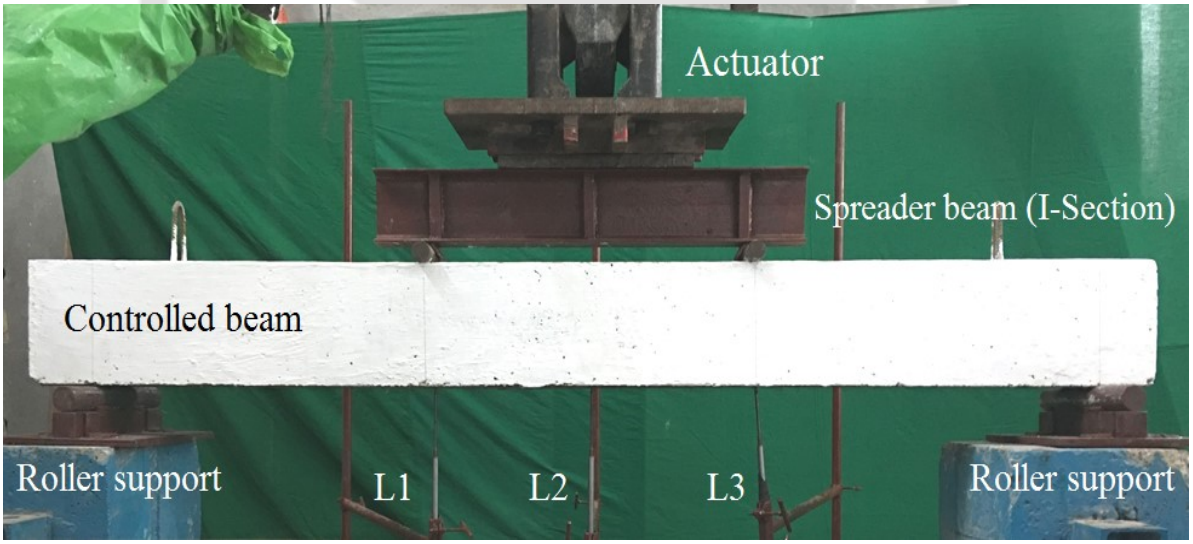

Figure 5.13: Setup for 4 point loading bending test of RC beam.

The PCM repaired fully damaged beams were tested at 3rd and 28th day of casting. PCM repaired partially damaged beams were tested only at 28th day of casting. The 3 days test for PCM repaired beam was not included since at 3 days, the strength gain by PCM is very low as being observed from the results of compressive strength test presented in sub-section, *3.3.3 Compressive strength* of Chapter 4. The GPM repaired fully and partially

damaged beams were tested at 3rd and 28th day of casting to observe the behaviour of GPM repaired RC beam at both early and later ages.

5.3 Experimental observations

The results form static flexural load test on the repaired Reinforced concrete (RC) beams are presented in Table 5.10. The repaired beams were denoted by adding the letter 'R' along with the beam number for each corresponding beam. The applied load and corresponding midspan displacement data obtained experimentally were utilized to prepare the load-deflection curve of each RC beam to make conclusive remarks. The crack pattern was also observed for arriving at suitable conclusions.

Table 5.10: Results from static flexural test on RC beams.

Beam No.	Test Day	Repairing Agent	Yield Load (kN)	Deflection at Yield Load (mm)	Ultimate Load (kN)	Deflection at Ultimate Load (mm)	Load at 1st Crack (kN)	DR	SER	Moment Capacity (kNm)
B1	28	-	52.95	5.23	62.62	21.46	19.44	4.10	-	18.78
B2	28	-	52.49	6.73	61.01	20.39	21.57	3.03	-	18.30
B3	28	-	54.10	6.43	62.84	21.06	21.25	3.27	-	18.85
B4	28	-	53.59	6.56	62.18	21.30	20.30	3.25	-	18.65
B1R	3	PCM	17.68	5.94	22.16	17.17	4.10	2.89	0.35	6.65
B2R	3	GPM	44.24	7.83	54.66	28.34	12.67	3.62	0.89	16.40
B3R	28	PCM	33.57	7.38	41.91	24.22	8.89	3.28	0.67	12.57
B4R	28	GPM	49.31	7.69	61.02	30.80	16.82	4.00	0.98	18.31
B5	28	-	*Considered data from results of B3*				19.85	-	-	18.85
B6	28	-	*Considered data from results of B3*				20.79	-	-	18.85
B7	28	-	*Considered data from results of B3*				20.37	-	-	18.85
B5R	3	GPM	55.64	8.79	63.75	31.74	21.03	3.61	1.01	19.13
B6R	28	PCM	43.29	9.73	49.42	26.81	22.49	2.75	0.79	14.83
B7R	28	GPM	56.97	8.96	69.56	41.06	23.22	4.58	1.11	20.87

5.3.1 Fully damaged RC beams

The load deflection curves from static flexural load test on Portland cement mortar (PCM) and geopolymer mortar (GPM) repaired fully damaged RC beams at 3 days are presented in Fig. 5.14. The beam, B1R repaired using PCM could sustain maximum load of 22.16 kN. This load was about 35 % of the load achieved by the controlled beam. On observing the load

deflection curve in Fig. 5.14, it was noted that the stiffness of the PCM repaired beam, B1R degraded by 75 % compared to that of controlled beam. The ductility ratio (DR) was found to be 2.89 which was lower than that of controlled beam, B1. The first crack in the repaired RC beam occurred very early at 4.01 kN followed by subsequent cracks whereas the first crack in the controlled beam occurred at 19.44 kN. The appearance of first crack at very early stage is attributed to the fact that PCM gains very low compressive and bond strength at early ages. Therefore, it was unable to arrest the cracks in the repaired beam effectively. Hence, the PCM filled up cracks propagated and further widened. This remark is supported by the observation that the cracks in the PCM repaired beam, B1R appeared in the same location as that of the cracks in the controlled beam. At 19.49 kN, the crack no. 4 and 9 in B1R started widening and continued to widen. It was observed from Fig. 5.15 (a) and (b) that the PCM which was placed inside the crack while repairing, spalled out from crack no. 4 and 9. On close observation of the cracks (Fig. 5.16), it was noted that spalling occurred since the PCM separated out from the old concrete surface of the cracks mainly due to bond failure between PCM and older concrete of the beam. This phenomenon was supported by the results of slant shear test presented in sub-section, *4.3.4. Bond strength (slant shear)* of Chapter 4 where PC system at early ages showed poor bond strength with concrete substrate of various ages.

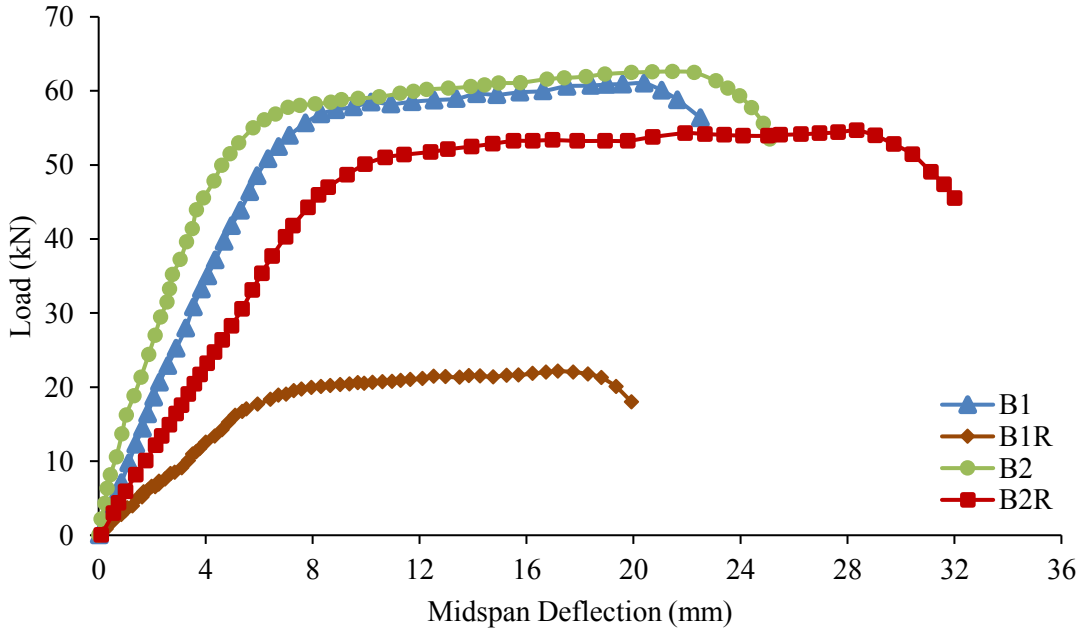

Figure 5.14: Load-deflection curves for PCM and GPM repaired fully damaged beams at 3 days.
Key: *B1, B2 - Controlled beams, B1R - PCM repaired beam, B2R - GPM repaired beam.*

Figure 5.15 (a): Cracks in controlled beam, B1.

Figure 5.15 (b): Cracks in PCM repaired beam, B1R.

Figure 5.16: Enlarged view of cracks in PCM repaired beam, B1R.

The GPM repaired beam, B2R attained an ultimate load of 54.66 kN at 3 days of repair which was around 89 % of the load attained by controlled beam. The stiffness degradation in the repaired beam as observed from Fig. 5.14 was found to be lower than that of the PCM repaired beam. The 1st crack occurred at 12.67 kN. The first crack in controlled beam occurred at 21.57 kN. The appearance of first crack was delayed due to the use of GPM as repairing agent compared to the use of PCM as repairing agent. The early compressive and bond strength development of GPM played significant role in arresting the cracks and hence the crack development and propagation in the GPM repaired beam, B2R was delayed in comparison with the PCM repaired beam, B1R. Moreover, some cracks were generated at

new locations which were not developed in the case of loading on the controlled beam. However, the significantly wider cracks in the controlled beams opened up again in the repaired beams indicating that the GPM was adequate enough to arrest only the cracks with small width. Crack number 1 and 2 started to widen at 50.5 kN. GPM spalling from the cracks was not observed (Fig. 5.17 (b)) even when the cracks 1 and 2 opened wide at 53 kN along with widening of crack no. 3, 5 and 8. The GPM remained attached to the older concrete surface in the cracks. The better compressive and bond strength of GPM led to achievement of higher ultimate strength without mortar spalling from the cracks. The ductility ratio (DR) was found to be 3.62 which was significantly higher than the DR of the controlled beam, B2.

Figure 5.17 (a): Cracks in controlled beam, B2.

Figure 5.17 (b): Cracks in GPM repaired beam, B2R

Fig. 5.18 presents the load deflection curve from the static flexural load test on the PCM and GPM repaired fully damaged RC beams at 28 days. The behaviour of the RC beams repaired by PCM at 28 days was in conjunction with the behaviour RC beams repaired by PCM at 3 days. The PCM repaired RC beam, B3R attained around 67 % of the load attained by controlled beam, B3. The stiffness degradation of the repaired beams was about 65 % when compared to controlled beams. No improvement in ductility was observed in the PCM

repaired beam, B3R as the DR was 2.64 for repaired and 3.27 for controlled beam. The 1st crack occurred at 8.89 kN which was around 42 % of the load for appearance of 1st crack in controlled beam. The widening of cracks occurred at 32.26 kN load, the mortar & concrete spalled out from some cracks and the region between them due to debonding at load 41.82 kN load. The debonding issue as observed is again attributed to the poor performance in case of bond strength between Portland cement systems and older concrete substrate. However, the strength achievement was higher at 28 days comparted to strength achievement at 3 days. But the performance of PCM repaired fully damaged RC beam at 28 days was inferior to that of GPM repaired fully damaged RC beam at 3 days.

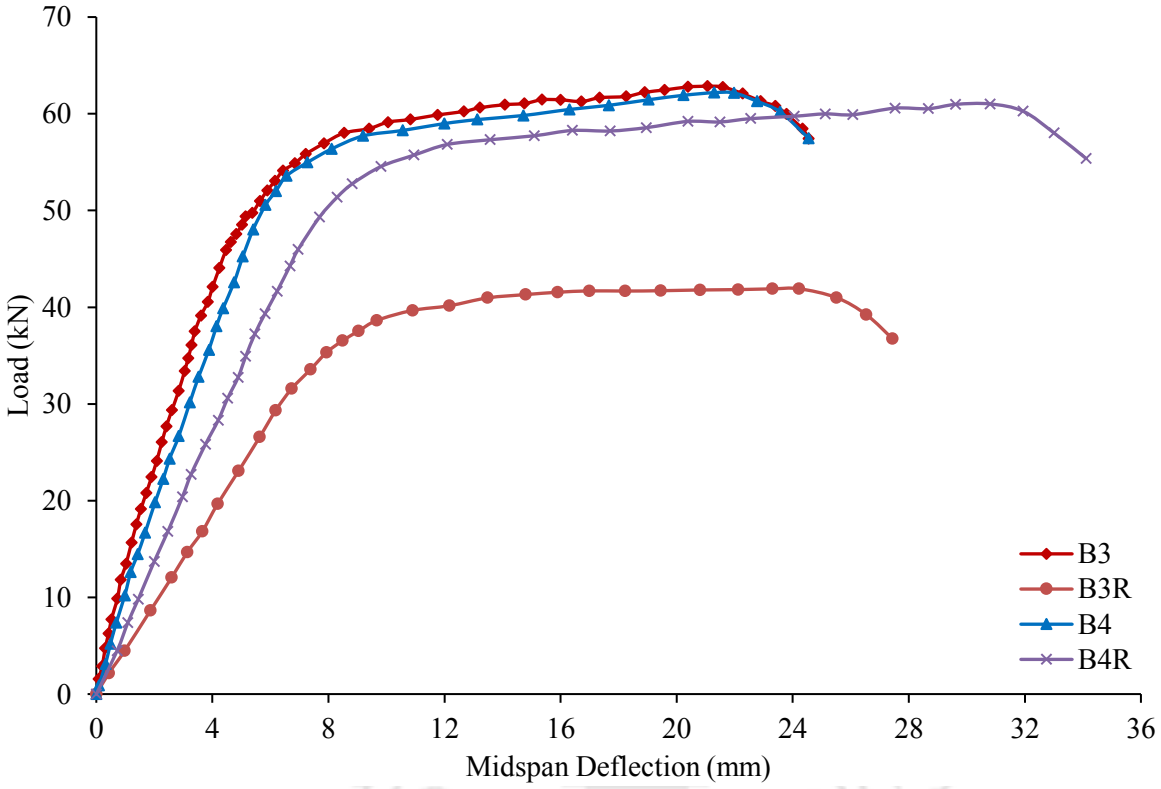

Figure 5.18: Load-deflection curves for PCM and GPM repaired fully damaged beams at 28 days.
Key: *B3, B4 - Controlled beams, B3R - PCM repaired beam, B4R - GPM repaired beam.*

The GPM repaired fully damaged RC beam, B4R at 28 days showed similar results as showed by GPM repaired fully damaged RC beam at 3 days. At 28 days, it attained 61.02 kN ultimate load which is around 98 % of that of controlled beam. Significant improvement in ductility was observed in the GPM repaired beam. The ductility ratio was 4.00 which was around 23 % higher than controlled beam. The appearance and widening of cracks occurred at higher loads compared to the PCM repaired ones. The 1st crack of controlled beam occurred

at around at 21.30 kN. In case of repaired beam, 1st crack occurred at 16.82 kN. The crack 1, 3, 5 and 12 widened at around 50 kN. At 56 kN, further widening of cracks occurred without any spalling of concrete from the filled up cracks. Observation of the cracks showed no bonding failure of GPM from older concrete surface in the cracks. The high bond strength of GPM played significant role in this regard.

5.3.2 Partially damaged RC beams

The load-deflection curve for the PCM repaired partially damaged RC beam test at 28 days is presented in Fig. 5.19. PCM repaired partially damaged RC beam, B6R showed comparatively low stiffness degradation compared to the PCM repaired fully damaged beam. The stiffness degradation was 55 % compared to the controlled beam. The strength achieved by the PCM repaired beam, B6R at 28 days was 49.42 kN. The 1st crack (fine in appearance) in B6R appeared at 22.49 kN, delayed in appearing compared to the controlled beam. At 29.50 kN, the cracks 3, 8 and 10 started widening and continued to widen till the mortar spalled out from them, Fig. 5.20. The mortar debonding was observed in this case. The DR was 2.75 which was found to be lower compared to the controlled beam.

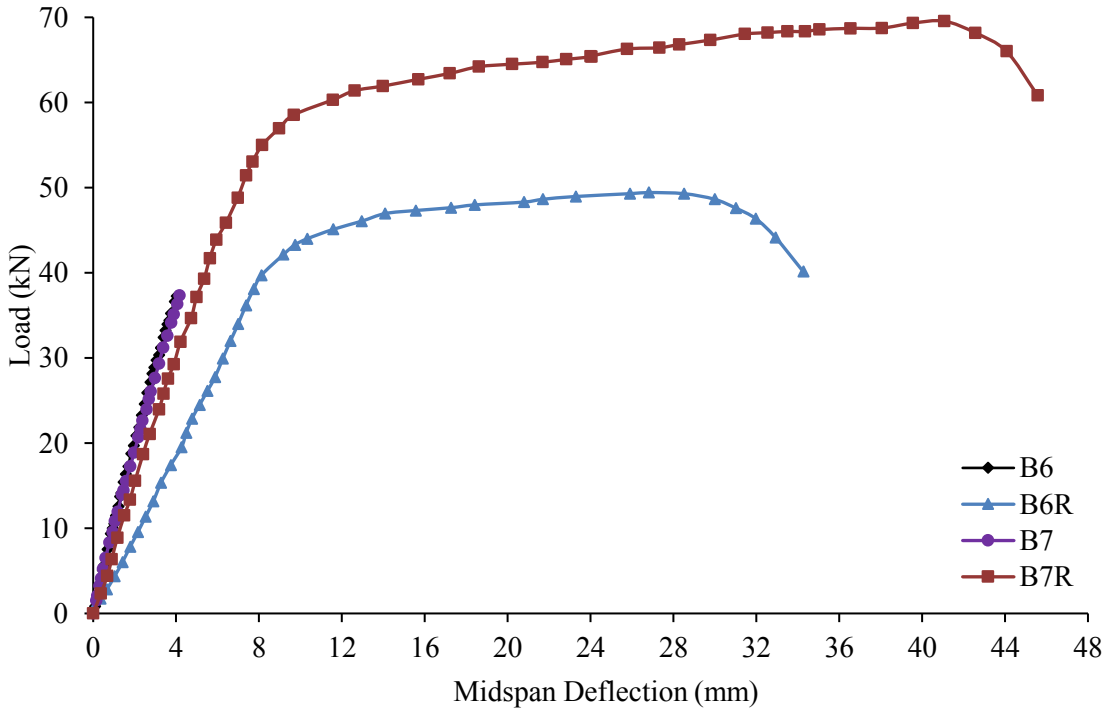

Figure 5.19: Load-deflection curves for PCM and GPM repaired partially damaged beams at 28 days. Key: *B6, B7 - Controlled beams, B6R - PCM repaired beam, B7R - GPM repaired beam.*

Figure 5.20: Cracks in PCM repaired beam, B6R

The load-deflection curve for GPM repaired partially damaged RC beam, B5R and B7R at 3 and 28 days respectively are presented in Fig. 5.21 and Fig 5.19 respectively. The results showed appreciable performance of the repaired beams, B5R and B7R in both early and later ages. The stiffness degradation was observed to be very less compared to PCM repaired ones at both early and later ages. The strength achieved by B5R was 63.75 kN at 3 days. This was marginally higher than the controlled beam. The strength achieved by B7R was 68.50 kN at 28 days of repairing. The strength enhancement ratio (SER) was 1.01 and 1.11 for B5R and B7R respectively. The strength was significantly enhanced compared to the controlled beam.

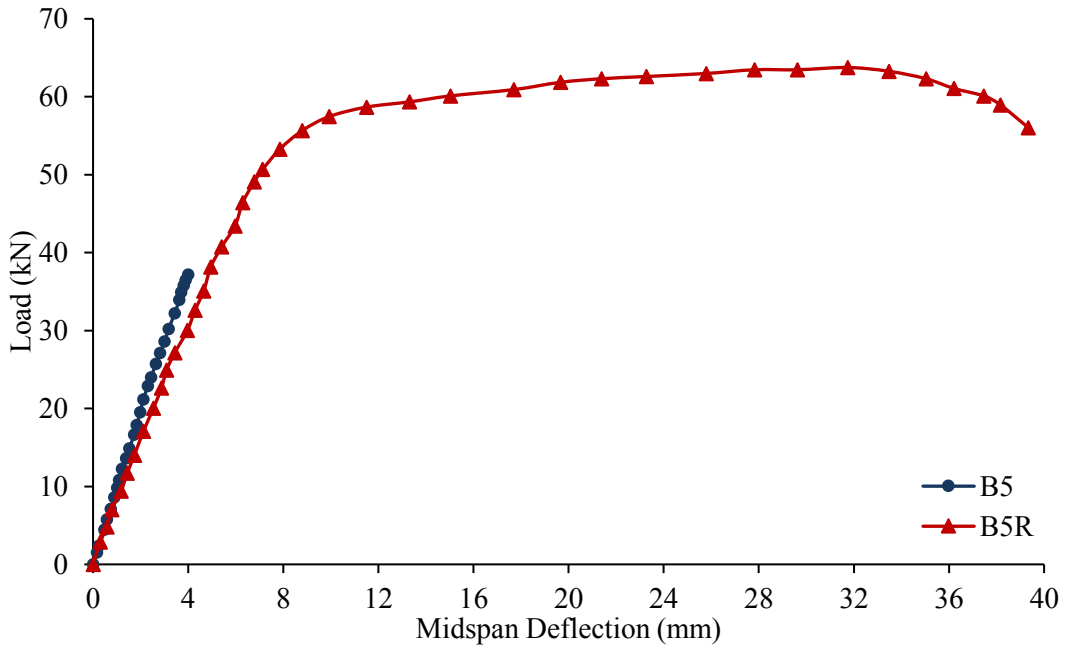

Figure 5.21: Load-deflection curves for GPM repaired partially damaged beams at 3 days.

Key: *B5 - Controlled beam, B5R - GPM repaired beam.*

In B5R, 1st crack appeared at 21.03 kN. The cracks 2, 16 and 8 started widening at around 59 kN load. At 63 kN, the cracks further widened, however no mortar spalling was observed due to the good bond between GPM and older concrete surface in the cracks. Similar observations were also noted for GPM repaired partially damaged RC beam, B7R which was tested at 28 days. The 1st crack occurred at 23.22 kN. The subsequent cracks occurred at higher loads and mostly at new locations indicating the fact that GPM was effective in arresting the cracks generated in the controlled beams, B7 (Fig. 5.22 (a) and (b)). Very slight widening of cracks were observed in this beam from 64 KN load onwards. Cracks 2, 3, and 4 widened at 64 kN and continued widening till failure. No spalling of mortar from the cracks was observed. The DR of GPM repaired beams tested at 3 and 28 days was 3.61 and 4.58. These were significantly higher compared to controlled RC beams and also higher than the values exhibited by GPM and PCM repaired fully damaged RC beams.

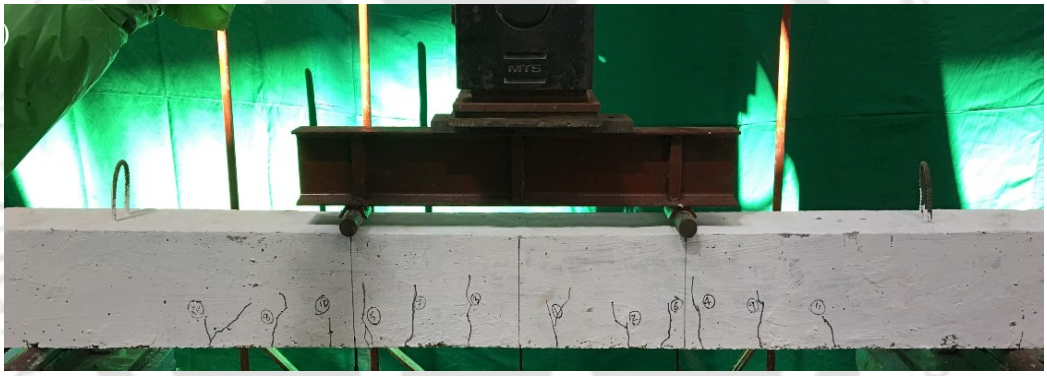

Figure 5.22 (a): Cracks in controlled beam, B7.

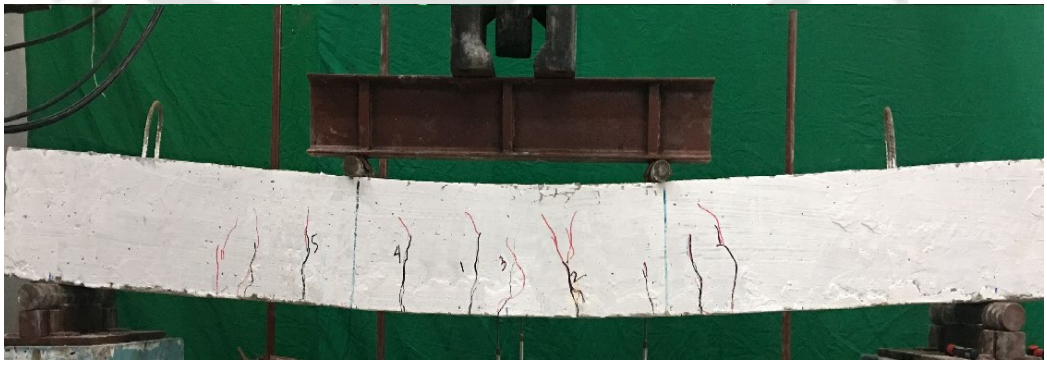

Figure 5.22 (b): Cracks in GPM repaired beam, B7R.

5.4 Closure

The behaviour of geopolymer mortar (GPM) repaired reinforced concrete (RC) beams is presented in this chapter by performing static flexural test in the laboratory. Total seven numbers of RC beams of size 150 mm × 200 mm and length 2 m including controlled beam were cast for these purpose. After 28 days of curing, static flexural load was applied using MTS actuator on three numbers of specimen upto the ultimate load and on other three number of specimen up to 60 % of the ultimate load (partially damaged state where the beams sustained 60 % of the ultimate load). The beams were repaired to restore the original size of the RC beams using GPM and Portland cement mortar (PCM) and were retested on completion of curing.

The results of the study reveal that GPM have strong potential to be used effectively as RC structural member repairing agent. Ultra-fine ground granulated blast-furnace slag (UGGBS) based GPM possess early strength achievement property which makes is most advantageous to be used as repairing agent and hence can be used to repair damaged RC structural members and put to re-use earlier. At 3 days, the GPM exhibited strength as high as around 85 % of 28 days strength. It was observed that, mortar repaired partially damaged RC beams behaved superior to mortar repaired fully damaged RC beams when subjected to static flexural load. Hence, it is recommended that repairing of the RC structural member at early period with GPM is the effective way of restoring the structure to its functional use at the earliest period possible. The findings of the present study are expected to be useful for repairing RC structural members damaged due to various reasons.

Chapter 6

Jacketing of RC Beams using Geopolymer Concrete

6.1 Introduction

Reinforced concrete (RC) structures often require strengthening to increase the capacity to sustain loads. This requirement arises due to additional loads to be carried, deterioration of load carrying members due to environmental effects, errors while designing, ageing of structures or upgradation to conform to new codal requirements. The strengthening can be done globally or locally in a structure. Global strengthening involves addition of shear walls, bracing, mass reduction, base isolation, supplemental damping, etc. Local strengthening involves jacketing of members, strengthening of footings, providing micro-piles below column, etc. Various methods have been employed by researchers for repairing or strengthening of RC structural members [59, 128 - 131]. Among the various methods of local strengthening scheme, jacketing of structural members is popularly used.

Jacketing is the process of restoring a damaged structural member to its original configuration. This process also enhances the capacity of an un-damaged structural member. It is carried out by encasement of the member using suitable agents. It increases the load carrying capacity, stiffness and ductility of the member. Jacketing is successfully used by

many researchers including and Altun et al. [59]; and Cheong and Mac Alevey [128] for strengthening of RC structures.

The success of jacketing depends upon the monolithic behaviour of the composite member, i.e. the jacketed region and the original member together. This can be achieved by maintaining proper bonding between the original member and the jacketing agent. Steel, concrete, and fibre-reinforced polymer (FRP) are some of the agents that are employed for jacketing RC structural members. In some cases, FRP and steel undergo prematured debonding from the old concrete surface and cause the jacketing agent to peel off. This makes such jacketing method to be ineffective.

Concrete is more consistent as jacketing agent than FRP and steel. It shows better bonding than FRP and steel with old concrete surface. Fig. 6.1 (a) and (b) present the cross-sectional and longitudinal sectional view of concrete jacketed RC member. Concrete jacketing involves providing additional concrete and reinforcement over the RC structural members. It is easy to implement and comparatively cost effective. This method though increases the member size, but it leads to increase in member stiffness and thus make the member capable of accommodating large deformations [128].

The process of concrete jacketing includes the following:-

i. The surface of the member to be jacketed is roughened.
ii. Incase of damaged RC member consisting of cracks, epoxy resin or cement grout is usually applied to penetrate into the cracks prior to jacketing.
iii. Steel connectors such as dowel bars are provided perpendicular into the hole made in the concrete surface of the member and cement or epoxy grouted into the hole.
iv. New longitudinal and transverse reinforcement bars are placed around the member.
v. New concrete is provided to encase the member and embed the new reinforcements.

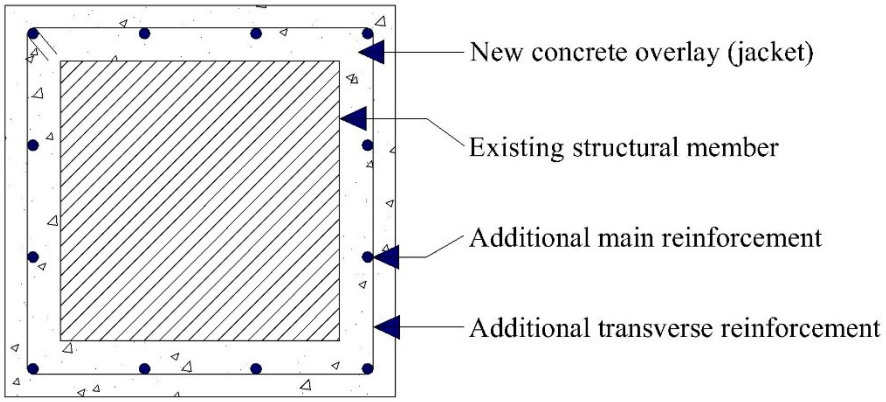

(a) Cross-section

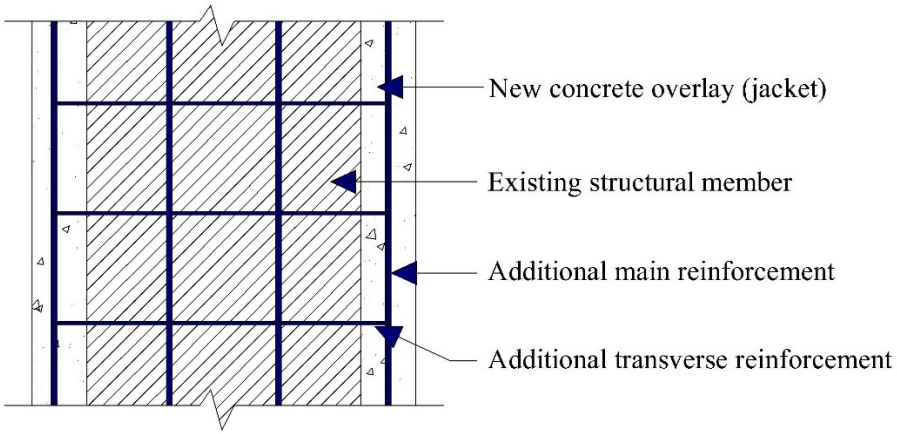

(b) Longitudinal section

Figure 6.1: Concrete jacketed RC member

In the present work, jacketing of RC beams were done using ultra-fine slag based geopolymer concrete (GPC). Generally, the weak bond between the old and new concrete is the concerning issue in concrete jacketing. However, in the present study it is established that GPC possesses superior bond strength (Chapter 4). Therefore, jacketing of RC beams were performed using GPC. The performance of GPC jacketed beam is compared with that of Portland cement concrete (PCC) jacketed beam to conclude regarding the effectiveness of geopolymer as a jacketing agent. Following aspects are thoroughly studied:-

i. Load and displacement at yielding of beam.
ii. Ultimate load and corresponding displacement.

iii. Ductility ratio (DR), defined as the ratio between the deflection at ultimate load and deflection at yield load.

iv. Strength enhancement ratio (SER), defined as the ratio between ultimate load of the jacketed beam and that of the controlled beam.

v. Load at development of first crack

vi. Cracking pattern.

Here, the controlled beam is the beam prior to jacketing in case of fully damaged beam and in case of partially and undamaged beams, controlled beam is considered as B3.

6.2 Experimental investigation

The process of the laboratory testing started with the casting of Reinforced concrete (RC) beams using PCC. The jacketing was done using PCC and GPC. Total nine numbers of beams were cast for this purpose.

6.2.1 Materials

The materials used for preparation of RC beams and jacketing thereafter are elaborately discussed as given in the following sub-sections:-

6.2.1.1 Portland cement concrete

Portland cement concrete (PCC) was prepared using Portland cement (PC) as described in sub-section, *2.2.1 Portland cement* of Chapter 2. The fine and coarse aggregates used in the preparation are described in sub-section, *2.2.5 Aggregates* of Chapter 2. The mix proportion for PCC is presented in Table 6.1.

Table 6.1: Mix proportion for PCC (kg/m^3).

Mix	Cement	Fine Aggregate	Coarse aggregate	Water/cement (w/c)
CC1	360	680	1128	0.55
CC2	425	630	1190	0.40

Two numbers of PCC mixes were used in this study. Mix CC1 was used for preparation of PCC for casting of RC beams and mix CC2 was used for preparing the PCC for jacketing the RC beams. For the purpose of ease in placement of the concrete inside the formwork of jacketed beam, the maximum size of coarse aggregate was restricted to 16 mm. The water/cement (w/c) ratio of CC2 was selected as 0.40 to match with the water/solid (w/s)

ratio of GPC used for jacketing. Table 6.2 presents the fresh and hardened state properties of the CC1 and CC2. The tests were performed as per relevant IS Code of Practice [122, 125, 127].

Table 6.2: Fresh and hardened state test results of PCC mixes.

Test	Result	
	CC1	CC2
Workability (Slump)	90 mm	29 mm
Compressive strength (3 days)	15.14 N/mm^2	22.44 N/mm^2
Compressive strength (28 days)	28.04 N/mm^2	39.11 N/mm^2
Tensile strength (3 days)	0.90 N/mm^2	1.28 N/mm^2
Tensile strength (28 days)	2.17 N/mm^2	2.67 N/mm^2
Flexural strength (3 days)	1.12 N/mm^2	1.81 N/mm^2
Flexural strength (28 days)	2.56 N/mm^2	4.22 N/mm^2

6.2.1.2 Geopolymer concrete

Ultra-fine ground granulated blast furnace slag (UGGBS) was used for preparation of the Geopolymer concrete (GPC). Flyash (FA) and superplasticizer (SP) were added as admixtures. The details of UGGBS, FA and SP are presented in the sub-*section 2.2.2 Ultra-fine ground granulated blast furnace slag*, *2.2.3 Flyash* and *2.2.6 Admixture* of Chapter 2. Fine and coarse aggregates were same as that used in preparation of PCC. Mix GC9 was selected for jacketing from among the GPC mixes presented in Table 4.1 in Chapter 4. Table 6.3 presents the mix proportion of GC9.

Table 6.3: Mix proportion for GC9 (kg/m^3).

UGGBS	FA	NaOH concentration (Molarity, M)	SP (% of total binding agent)	SP type	w/s	SP addition type
250.6	107.4	10	1.5	PE	0.4	Type I

Note: *Fine aggregate = 611 kg/m^3, coarse aggregate = 1208 kg/m^3, NaOH = 236.28 kg/m^3, w/s = water to total solid ratio*

The selection was on the basis of fresh and hardened state properties including the bond behaviour. This mix offered appreciable workability and strength at both early and later ages. The bond strength was also found to be satisfactory. Table 6.4 presents the fresh and hardened state properties of the GPC mix GC9.

Table 6.4: Fresh and hardened state test results on GC9.

Test	Result
Workability (Slump)	170 mm
Compressive strength (3 days)	37.11 N/mm^2
Compressive strength (28 days)	46.44 N/mm^2
Tensile strength (3 days)	2.43 N/mm^2
Tensile strength (28 days)	3.25 N/mm^2
Flexural strength (3 days)	5.17 N/mm^2
Flexural strength (28 days)	6.63 N/mm^2

6.2.1.3 Reinforcement

RC beams were cast with 2 numbers of 12 mm diameter tor steel bars conforming to IS 432 (Part 1) 1982 [95] at top and bottom as main reinforcement. Stirrups were provided using 2 legged 8 mm diameter tor steel bars. Sub-section, *2.2.7 Steel reinforcement bars* of Chapter 2 presents the details of the rebars used.

6.2.2 Method of beam preparation and jacketing

Doubly reinforced concrete beams were designed for span of 1.8 m and theoretical ultimate load carrying capacity of 53.78 kN. Total 9 numbers of RC beams were cast for the purpose of jacketing. Appendix B presents the preliminary design which was performed to decide the beam size and reinforcement in case of preparing RC beams and jacketed RC beams. The aim of the design was to limit the load carrying capacity of the beam. The RC beams were of size 150 mm × 200 mm and length 2 m. The detail of the reinforcement is presented in Fig 6.2. Main reinforcement of 2 numbers of 12 mm diameter tor steel bars at top and bottom was provided. Stirrups were provided using 2 legged 8 mm diameter tor steel bars at 100 mm centre to centre till 500 mm length from the end on both sides and remaining middle portion of 930 mm length was provided with 2 legged 8 mm diameter tor steel bars as stirrups at 185 mm centre to centre.

The jacketed RC beams were of size of 250 mm × 300 mm and length 2 m. Fig. 6.3 presents the details of the jacketed beam and the reinforcement provided in it. The jacketing was done increasing the width and depth by 100 mm. The jacketed region was provided with extra main reinforcement of 2 numbers of 12 mm diameter tor steel bars at top and bottom and stirrups using 2 legged 8 mm diameter tor steel bars at 80 mm centre to centre till 560

mm length from the end on both sides and remaining middle portion of 930 mm length was provided with 2 legged 8 mm diameter tor steel bars as stirrups at 160 mm centre to centre.

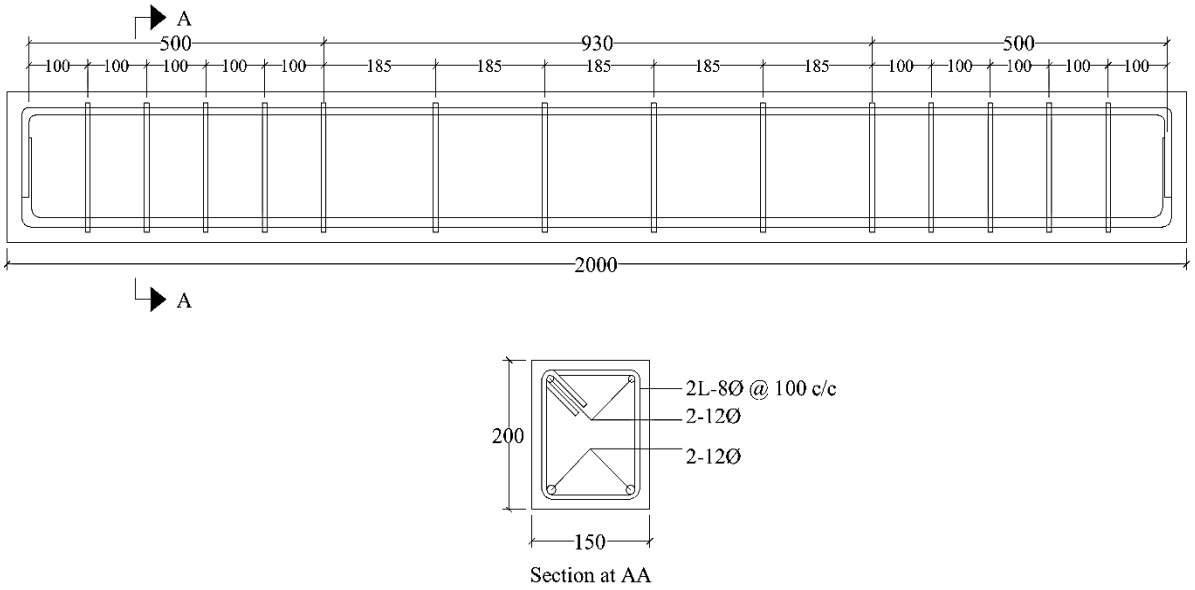

Figure 6.2: Details of RC beams (*All dimensions are in mm*).

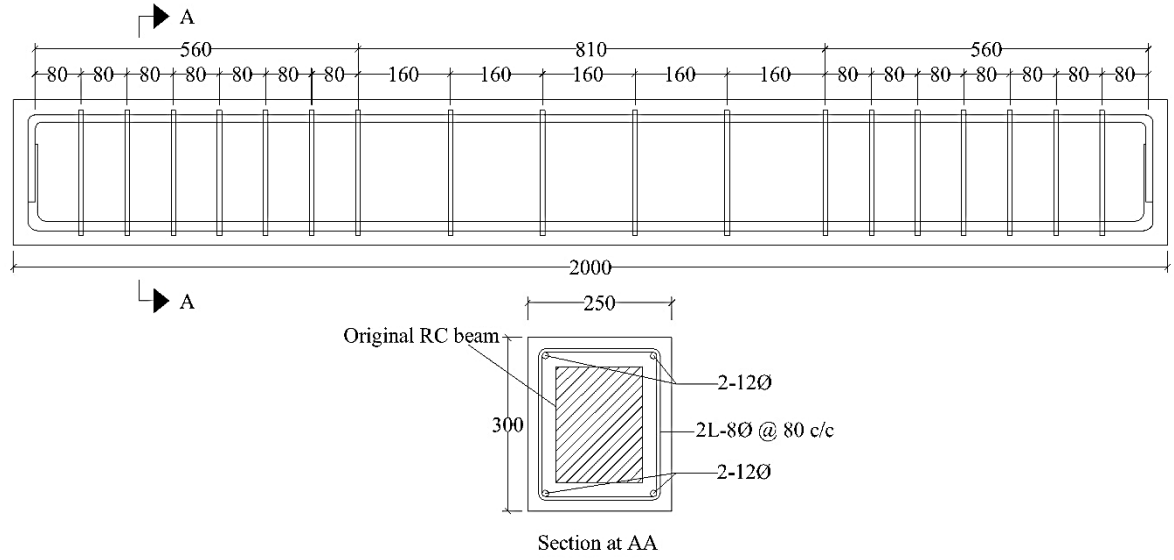

Figure 6.3: Details of jacketed RC beams (*All dimensions are in mm*).

Prior to the process of jacketing, cube specimens of size 150 mm, cylinder specimens of diameter 150 mm and height 300 mm; and prisms of size 150 mm × 150 mm × 700 mm were cast using plain GPC (GC9) and PCC (CM1) and tested for evaluation of compressive, tensile and flexural strengths respectively. The RC beams were cast to size of 150 mm × 200

mm × 2000 mm as decided from the design presented in Appendix B prepared using the compressive strength test results. The RC beams were cast as per the guidelines laid in IS 516 1959 [122] and cured in the laboratory for 28 days by wrapping with wet rags at ambient temperature of 20 ± 2 ºC. On completion of the curing period, the RC beams were subjected to monotonic static load using MTS actuator (Maximum load: 250kN; Maximum displacement: 250 mm). The setup and procedure for application of lad on the controlled beam is similar to that of the case of load application in the controlled beams for investigation of mortar repaired RC beams presented in sub-section, *5.2.3 Experimental setup* in Chapter 5. The RC beams were grouped under 3 categories based on the damage level due to the loads subjected from the actuator. The groups are as follows:-

i. *Fully damaged beams* - Three numbers of RC beams were loaded till failure. In these RC beams, the monotonic static load was applied to achieve the ultimate load. The cracks in the beam were induced in the region of pure tension. Most of the cracks were wide with minimum width of 5 mm and propagated towards the core of the beam.

ii. *Partially damaged beams* - Three numbers of RC beams were loaded by upto 60 % of their ultimate load capacity as found by the procedure followed in (i). The ultimate load of the controlled beam, B3 was considered as the ultimate load of the partially damaged beams. Till this load, the beams remained in their elastic stage. This was observed from the load- deflection curve of the controlled beam. The cracks were developed but enlargement was restricted. Further, the cracks did not propagate towards the core of the beam.

iii. *Undamaged beams* - Three numbers of RC beams were left unloaded and undamaged prior to jacketing.

The formwork for RC beam and its casting is shown in Fig 5.4 and 5.5 in sub-section, *5.2.2 Method of beam preparation and repairing with mortar* of Chapter 5. Fig 6.4 presents the process of preparation of the beam for jacketing. Post targeted loading, the cracks that were generated in fully and partially damaged beams were identified, cleaned and enlarged manually as seen in Fig 6.4 (a) and (b). The enlargement of crack was such that its maximum depth was 50 mm and width was 40 mm [Fig 6.4 (c)]. Beyond this depth, the cracks were presumed to be very fine in nature. The enlargement was done with the aim to provide an easy and effective application and penetration of the jacketing agent. The broken concrete bits inside the cracks were removed carefully with the help of air blower. Minute inspection was carried out to ensure that no free particles remain inside the cracks. The surface of the RC

beam was roughened by chipping uniformly all over to ensure that the jacketing agent gets properly bonded with the old concrete surface of the RC beam. The surface of the beam was cleaned and air blown to make it free from any loose and unwanted particles attached to it. This method of crack cleaning and surface preparation is similar to the method practiced by engineers and technical persons engaged in repair and strengthening of RC structures in site. The undamaged beams were simply subjected to surface chipping and air blow to make its surface dust and loose particles free.

Figure 6.4 (a): Removal of the loose particles from the surface by iron brushing.

Figure 6.4 (b): Removal of dust and fine particles by air blower.

Figure 6.4 (c): Crack ready for being repaired.

The extra reinforcement for jacketing was provided to drape over the prepared RC beams and then the whole system was placed inside the formwork as shown in Fig. 6.5. The concrete, either GPC or PCC for jacketing was provided in layers and vibrated to release the voids inside the concrete. Fig. 6.6 and 6.7 show the concrete being poured inside the formwork and the jacketed RC beam ready for curing. After completion of placing of concrete in the formwork, the beams were kept for 24 hours at ambient temperature of 20 ± 2 ºC. Later, the formworks were removed and the beams were further cured in the laboratory by wrapping with wet rags till arrival of the test day. On the test day, the wet rags were removed and the beams were exposed to air blower for drying of the surface.

Figure 6.5: Extra reinforcement for jacketing.

Figure 6.6: Jacketing concrete being placed inside the formwork.

Figure 6.7: Jacketed beam ready for curing.

6.2.3 Experimental setup

Fig. 6.8 presents the experimental setup for testing of the jacketed RC beams. The beams were subjected to static flexural loading using MTS actuator (Maximum load: 250 kN; Maximum displacement: 250 mm). The test was done under four point loading. Displacement based loading was monotonically applied at the rate of 0.01 mm/s. The load was continued to be applied till the targeted load was reached. The midspan displacement was recorded using spring mounted linear variable differential transformer (LVDT), L2 of capacity 100 mm which was placed in such a way that the piston tip touched the sofit of the beam. Two additional LVDTs, L1 and L3 of capacity 100 mm were used to monitor the loading uniformity. The additional LVDTs were placed below the point of contact of rollers of spreader beam with RC beam as shown in Fig. 6.5 by L1 and L3. However, results from these LVDTs have not been considered to prepare the load-deflection behaviour graphs. Load-deflection curves were drawn according to the record of the central LVDT, L2.

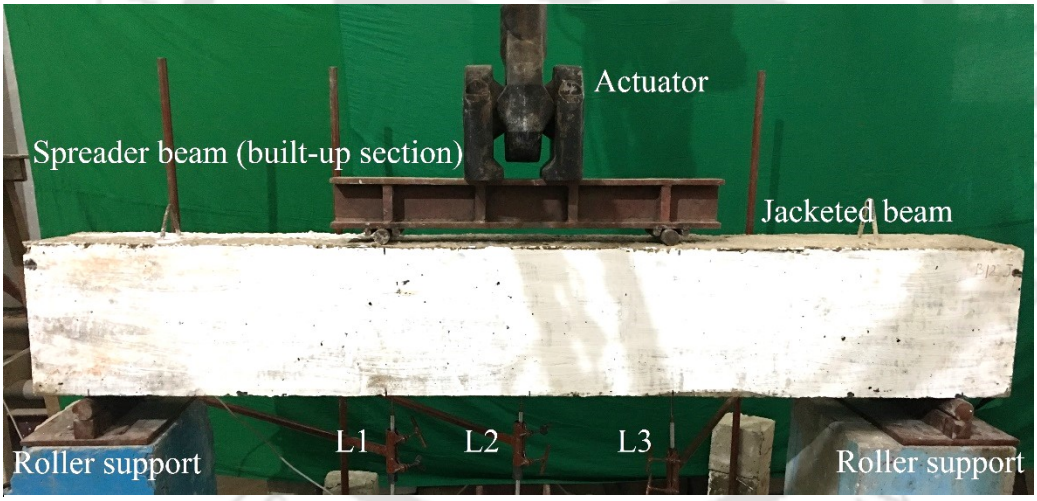

Figure 6.8: Setup for static flexural four point loading test of jacketed RC beam.

The PCC jacketed beams for all the three categories were tested at 28th day of casting. The GPC jacketed beam was tested at 3rd and 28th day of casting to see the behaviour of GPC jacketed RC beam at both early and later ages. The 3 days test for PCC jacketed beam was not included since at 3 days, the strength gain by PCC is very low as being observed from the results of compressive strength test presented in sub-section, *4.3.2 Compressive strength* of Chapter 4.

6.3 Experimental observations

Table 6.5 presents the results from the static flexural load test on the jacketed Reinforced concrete (RC) beams. To designate the jacketed beams, the letter 'J' is added along with the corresponding beam number. The load-deflection curve of each beam was prepared from the applied load and corresponding midspan deflection data of the RC beams experimentally obtained to arrive at various conclusions.

Table 6.5: Results from flexural load test on RC beams.

Beam No.	Test Day	Jacketing Agent	Yield Load (kN)	Deflection at Yield Load (mm)	Ultimate Load (kN)	Deflection at Ultimate Load (mm)	Load at 1st Crack (kN)	DR	SER	Moment Capacity (kNm)
B3	28	-	54.10	6.43	62.84	21.06	21.25	3.27	-	18.85
B8	28	-	54.45	6.63	62.55	20.27	22.00	3.06	-	18.77
B9	28	-	53.54	7.06	62.54	21.54	19.80	3.05	-	18.76
B10	28	-	47.46	6.21	61.07	20.81	19.82	3.35	-	18.32
B8J	3	GPC	142.94	6.10	185.67	32.53	57.31	5.33	2.97	55.7
B9J	28	PCC	121.85	6.76	150.94	26.87	51.40	3.97	2.41	45.28
B10J	28	GPC	159.54	5.46	214.00	32.04	66.72	5.87	3.50	64.2
B11	28	-	*Considered data from results of B3*				19.94	-	-	18.85
B12	28	-	*Considered data from results of B3*				19.51	-	-	18.85
B13	28	-	*Considered data from results of B3*				20.20	-	-	18.85
B11J	3	GPC	152.95	6.48	215.52	38.75	64.08	5.98	3.43	64.66
B12J	28	PCC	150.43	7.96	183.61	29.89	59.52	3.76	2.92	55.08
B13J	28	GPC	169.98	6.21	233.02	43.48	68.66	7.01	3.71	69.91
B14	28	-	*Considered data from results of B3*				-	-	-	18.85
B15	28	-	*Considered data from results of B3*				-	-	-	18.85
B16	28	-	*Considered data from results of B3*				-	-	-	18.85
B14J	3	GPC	153.22	7.06	217.52	43.48	66.56	6.16	3.46	65.26
B15J	28	PCC	148.99	8.17	197.22	32.81	61.24	4.02	3.14	59.17
B16J	28	GPC	181.70	6.58	236.37	47.95	73.91	7.29	3.76	70.91

6.3.1 Fully damaged RC beams

Fig. 6.9 presents the load-deflection data from the test of Portland cement concrete (PCC) and geopolymer concrete (GPC) jacketed fully damaged RC beam at 28 days. At 28 days, the PCC jacketed fully damaged beam attained an ultimate load of 150.94 kN. This was 2.41

times higher than that of the controlled beam, i.e. strength enhancement ratio (SER) was 2.41. The ductility ratio (DR) was 3.97. The first crack appeared early at 51.4 kN. It was observed from the Fig. 6.10 (a) and (b) that the cracks occurred mostly in the same pattern and over the same location where the cracks in the controlled beam occurred. The core beam being fully damaged contributed to loss of stiffness rapidly. Moreover, from the results of the flexural load test on Portland cement mortar (PCM) repaired fully damaged RC beams as presented in sub-section *5.3.1 Fully damaged RC beams* of Chapter 5, it can be inferred that the cracks initiated from the cracks present in the damaged beam due to poor bonding capacity of the PC system with concrete substrate. This phenomenon is related to the observation of the results from the slant shear strength test on PCC presented in sub-section, *4.3.4 Bond strength (slant shear)* of Chapter 4 for studying the bond strength behaviour of PCC with concrete substrate. Due to this bond issue, the cracks were not arrested properly and hence got opened up early and resulted in loss of stiffness, low ultimate strength and ductility.

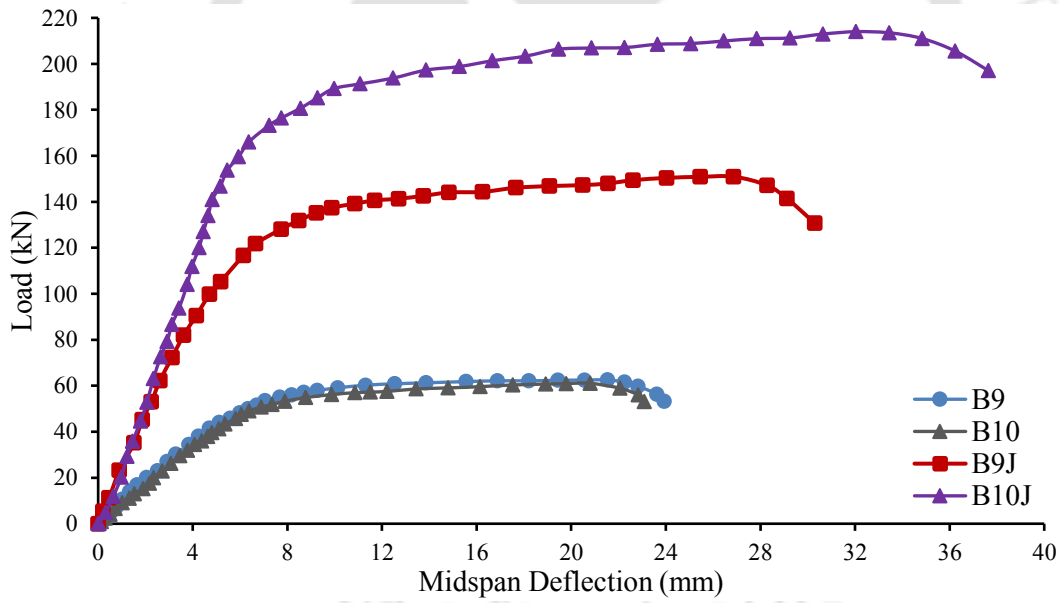

Figure 6.9: Load-deflection curves for PCC and GPC jacketed fully damaged beams at 28 days.
Key: *B9, B10 - Controlled beams, B9J - PCC jacketed beam, B10J - GPC jacketed beam.*

Figure 6.10 (a): Cracks in fully damaged RC beam, B9.

Figure 6.10 (b): Cracks in PCC jacketed RC beam, B9J.

Load-deflection curve for GPC jacketed fully damaged RC beam at 3 days is shown in Fig. 6.11. GPC as jacketing agent in the RC beams contributed towards achievement of ultimate load as high as 3.00 times than that of controlled beam even at 3 days. The SER in this case was quite higher than that of PCC jacketed RC beam at 28 days. The DR was 5.33, which was also higher at 3 days for GPC jacketed RC beam compared to that of PCC jacketed beams.

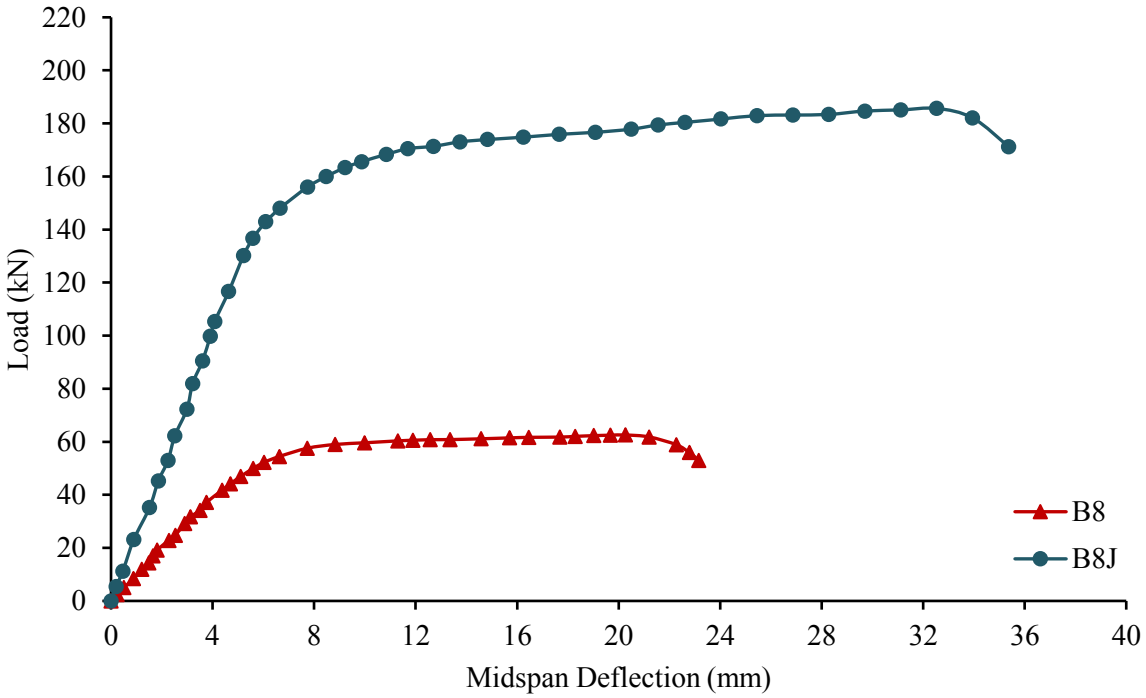

Figure 6.11: Load-deflection curves for GPC jacketed fully damaged beams at 3 days.

Key: *B8 - Controlled beam, B8J - GPC jacketed beam.*

At 28 days, the GPC jacketed RC beam exhibited marginal improvement in strength related behavior compared to 3 days. It was established from the results of compressive strength test furnished in sub-section, *3.3.3 Compressive strength and 4.3.2 Compressive strength* of chapter 3 and 4 respectively that at 3 days, geopolymeric systems using ultra-fine ground granulated blast furnace slag (UGGBS) develops around 80 % of the 28 days strength. The DR and SER increased marginally to reach values of 5.87 and 3.5 respectively. Higher ductility was observed due to the fact that GPC possesses higher tensile and flexural strength compared to PCC. Moreover, the cracks were filled up by the GP system which possesses good bonding property with concrete and hence restricted their early opening and propagation. These properties of GP system contributed towards slower stiffness degradation of GPC jacketed RC beam compared to the PCC jacketed RC beam at 28 days as seen in Fig. 9. The first crack occurred later than that in PCC jacketed ones. As observed in Fig. 6.12 (a) and (b), the cracks occurred in new locations in the jacketed RC beam. The first crack also appeared at different location compared to the original fully damaged beam. Jacketing of fully damaged beams contributed towards the improvement of the stiffness. However, better stiffness was exhibited in GPC jacketed beams.

Figure 6.12 (a): Cracks in fully damaged RC beam, B10.

Figure 6.12 (b): Cracks in GPC jacketed RC beam, B10J.

6.3.2 Partially damaged RC beams

The partially damaged RC beams on jacketing showed better strength achievement and ductility than fully damaged RC beams. The results of PCC and GPC jacketed partially damaged RC beam at 28 days are shown in Fig 6.13. The SER was higher than that of corresponding fully damaged RC beams. PCC jacketed partially damaged beam attained an ultimate load of 183.61 kN. The SER and DR were 2.92 and 3.76 respectively. Higher values were shown due to the fact that the RC beam was initially partially damaged. The beam was still in elastic state till the point when the load application was terminated. Hence, cracks were not fully formed and hence in the jacketed partially damaged RC beam, the first crack appearance was found later compared to that in jacketed fully damaged RC beams. The first crack appeared at 59.52 kN.

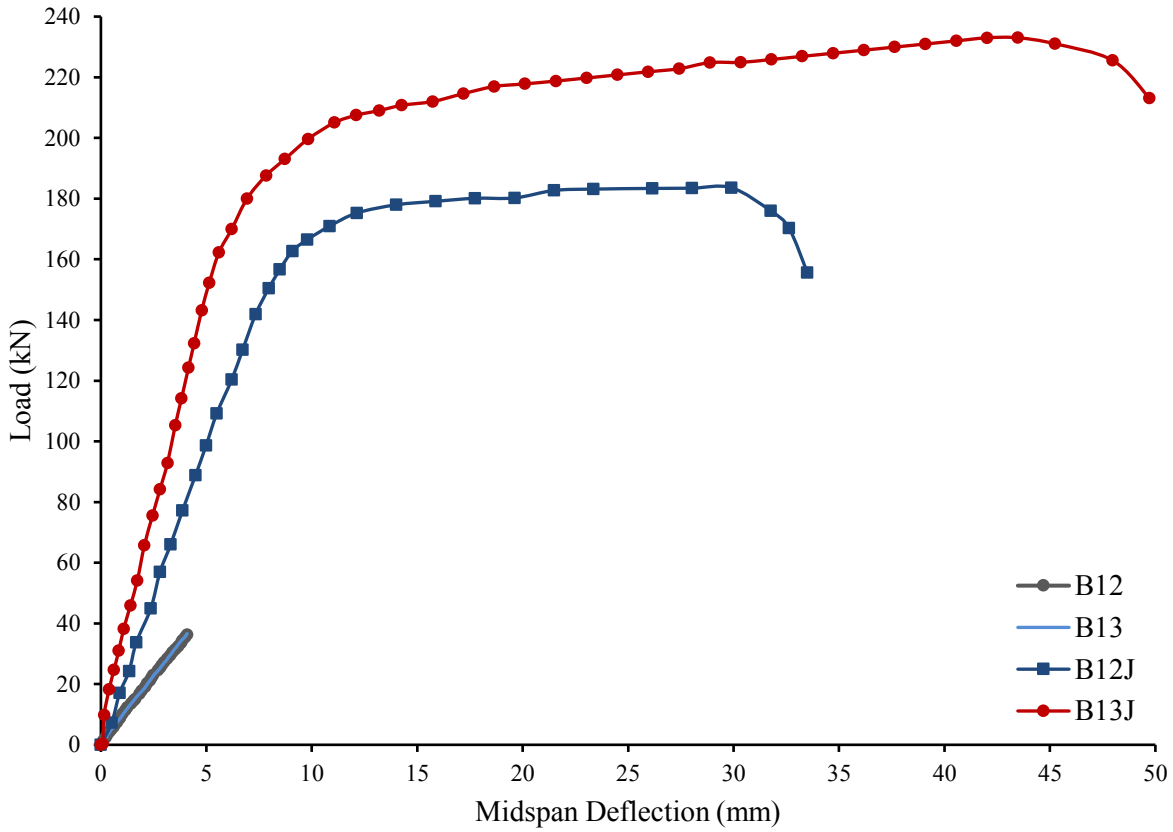

Figure 6.13: Load-deflection curves for PCC and GPC jacketed partially damaged beams at 28 days.
Key: *B12, B13 - Controlled beams, B12J - PCC jacketed beam, B13J - GPC jacketed beam.*

Fig. 6.14 presents the load-deflection data from the test of GPC jacketed partially damaged RC beam at 3 days. The beam exhibited higher load carrying capacity than PCC jacketed beams at 28 days. The ultimate loads of GPC jacketed RC beams at 3 and 28 days were 215.52 kN and 233.02 kN respectively. The corresponding SERs were 3.43 and 3.71 respectively. The DR of the GPC jacketed partially damaged beam at 3 and 28 days were 5.98 and 7.01 respectively. These were considerably higher than that of PCC jacketed partially damaged beam. GPC possesses higher tensile strength than PCC. This property contributed to the enhanced load carrying capacity of the GPC jacketed beams. Moreover, due to the higher tensile strength in GPC, which is due to the polymeric action in between the geopolymerisation products, higher ductility was observed in the jacketed beams compared to PCC jacketed beams. Partially damaged beams offered higher ductility when jacketed with GPC. Fig. 6.15 (a) and (b) show the cracks developed on the beams, B13 and B13J. The cracks being only surficial, did not contribute to the formation of early cracks in the jacketed RC beams. Moreover, due to good bond strength of GPC with PCC, the surficial cracks got

arrested properly on jacketing with GPC. Therefore, cracks at new locations were observed in the jacketed partially damaged RC beams. The initiation of cracks occurred at significantly higher loads compared to that in case of PCC jacketed partially damaged beams. The first crack appeared in GPC jacketed partially damaged beam at 64.08 kN and 68.66 kN at 3 and 28 days respectively. It was observed that the strength improvement, stiffness enhancement, ductility range, elastic limit load were higher for the partially damaged beams than their corresponding fully damaged RCC beams.

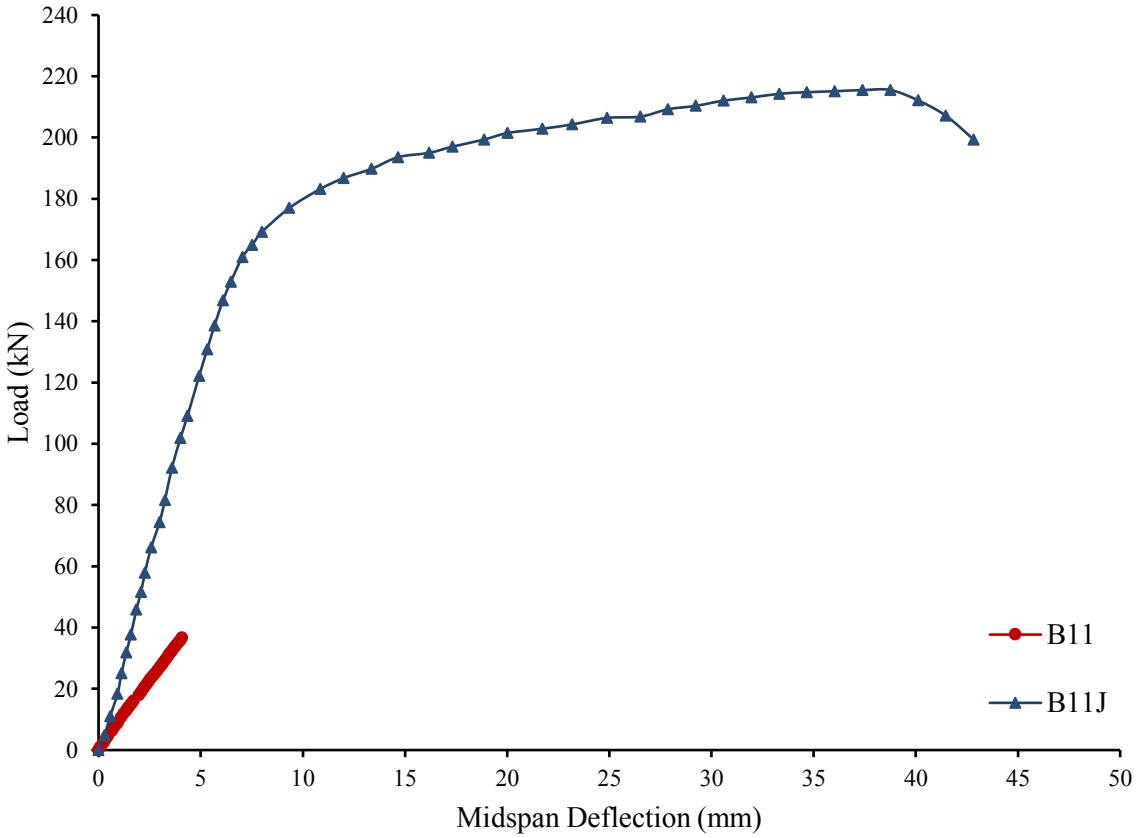

Figure 6.14: Load-deflection curves for GPC jacketed partially damaged beams at 3 days.
Key: *B11 - Controlled beam, B11J - GPC jacketed beam.*

Figure 6.15 (a): Cracks in partially damaged RC beam, B13.

Figure 6.15 (b): Cracks in GPC jacketed RC beam, B13J.

6.3.3 Undamaged RC beams

The beams without any damage prior to the jacketing showed strength achievement trends similar to that of partially damaged and jacketed RC beams. The load-deflection curves are presented in Fig. 6.16 and 6.17. For comparing the results, the load-deflection curve for beam B3 is also furnished. As seen from the Fig. 6.16, PCC jacketed beams attained ultimate load of 197.22 kN. The SER and DR were found to be 3.14 and 4.02 respectively. The undamaged RC beam in the core of jacketed RC beams behaved in the similar way as that by the partially damaged beam.

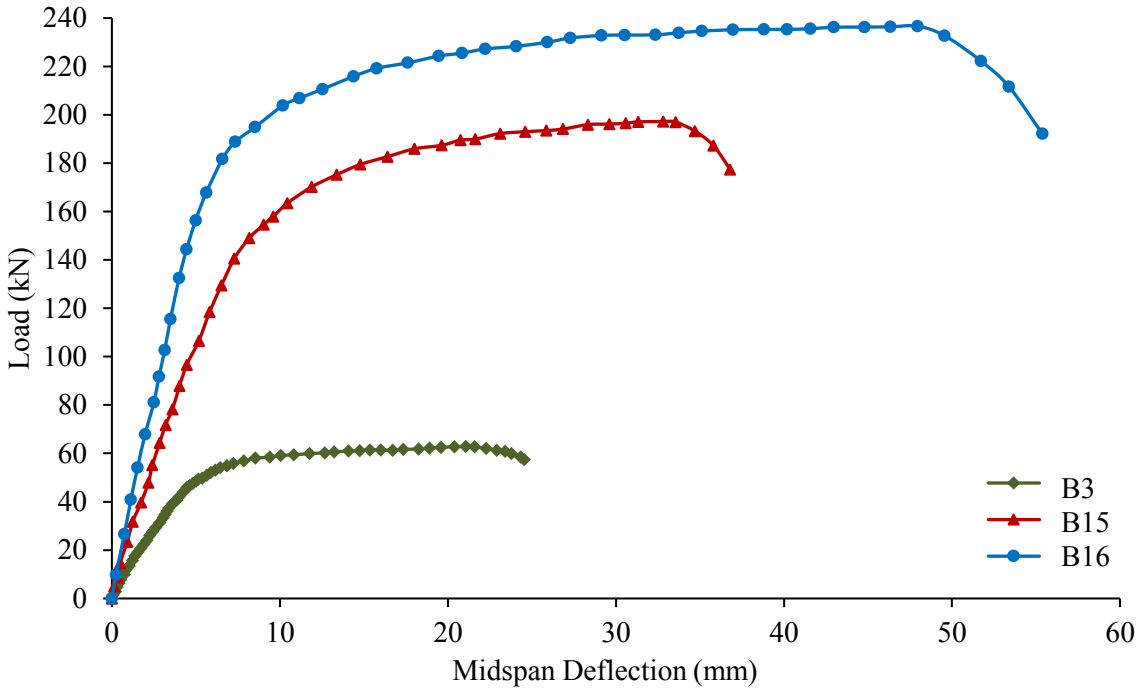

Figure 6.16: Load-deflection curves for PCC and GPC jacketed undamaged beams at 28 days.

Key: *B3 - Controlled beam, B15J - PCC jacketed beam, B16J - GPC jacketed beam.*

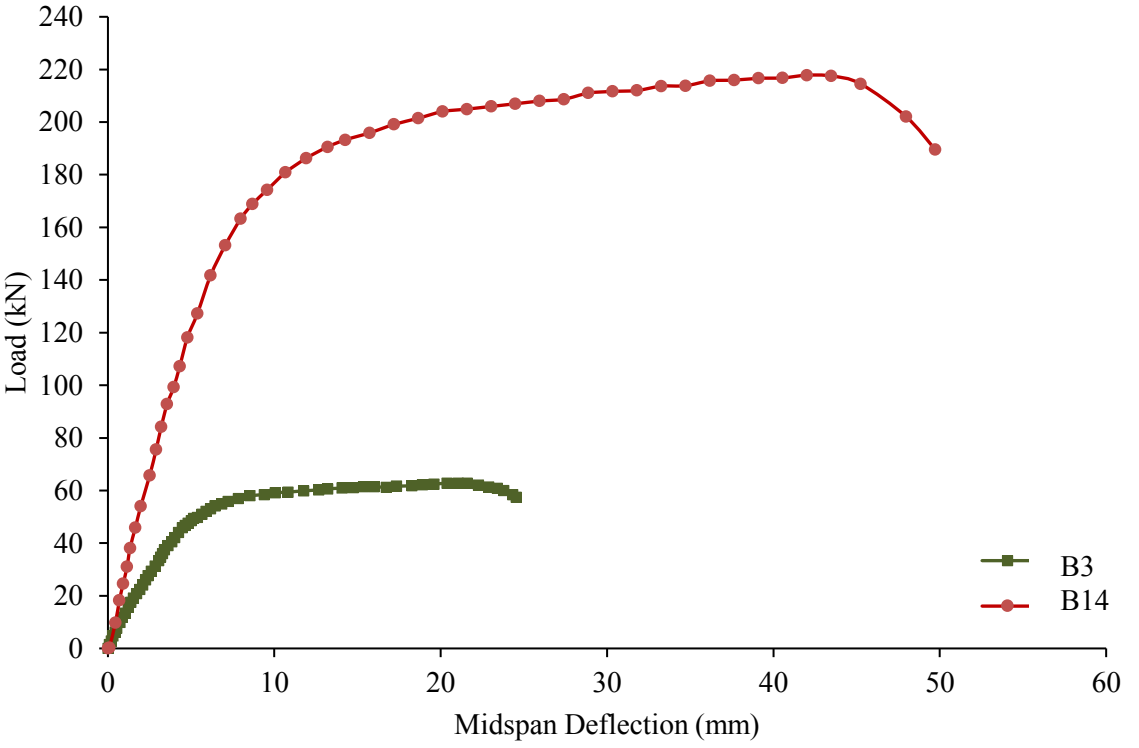

Figure 6.17: Load-deflection curves for GPC jacketed undamaged beams at 3 days.

Key: *B3 - Controlled beam, B14J - GPC jacketed beam.*

Figure 6.18: Cracks in GPC jacketed un-damaged RC beam, B16J.

At 3 and 28 days, GPC jacketed beam achieved SER of 3.46 and 3.76 respectively. However, these values were marginally improved as compared to the jacketed partially damaged beams. Fig. 6.18 shows the cracks developed in the GPC jacketed undamaged RC beam. It was observed that the cracks developed in similar pattern as that in partially damaged beams. The un-damaged RC beams in the core of jacketed beam behaved similar to that of partially damaged beam and hence the cracks developed in similar pattern in both the cases. Hence it can be inferred that jacketing of a partially damaged RC structural members is advantageous than the fully damaged beam. GPC can be used advantageously as jacketing agent to attain high load carrying capacity for partially and un-damaged beam. It was observed that, GPC jacketed beams showed better performance even at 3 days compared to PCC jacketed beams at 28 days. The maximum loads attained by the GPC jacketed beams at 3 and 28 days were 217.52 and 236.36 kN. Due to no prior cracks, the appearance of first crack occurred at significantly higher load in these beams compared to partially and fully damaged beams. The first crack in GPC jacketed beam at 3 and 28 days occurred at 66.56 kN and 73.91 kN respectively. Whereas first crack in PCC jacketed beam appeared at 61.24 kN. The SER and DR for GPC jacketed beams were as high as 3.46 and 6.16 respectively at 3 days; and 3.76 and 7.29 respectively at 28 days. These values for GPC jacketed undamaged beams differ insignificantly from those of GPC jacketed partially beams. In general, the SER, DR, stiffness improvement, ultimate strength and elastic limit load in these undamaged beams were higher than their corresponding partially and fully damaged beams.

6.4 Closure

A detailed study to understand the behaviour of geopolymer concrete (GPC) jacketed reinforced concrete (RC) beams was conducted in this chapter by performing static flexural test in the laboratory. Total ten numbers of RC beams of size 150 mm × 200 mm and length 2 m including controlled beam were cast for this purpose. After 28 days of curing, static flexural load was applied using MTS actuator on three numbers of RC beams upto the ultimate load and on other three number of RC beams up to 60% of the ultimate load (partially damaged state where the beams sustained 60% of the ultimate load). Three more RC beams were left undamaged (undamaged beams), i.e. no pre-loading before jacketing. The beams were jacketed to size of 250 mm × 300 mm and length 2 m using GPC and Portland cement concrete (PCC) and were retested on completion of curing.

The results of the study reveal that GPC can be used effectively as strengthening agent. Early strength achievement is the most important advantage of UGGBS based GPC and hence can be used where early removal of form work is needed so that damaged or strengthened structures can be put to re-use earlier. The strength at 3 days was as high as around 85 % of 28 days strength. The ductility of GPC was also high due to higher tensile strength than PCC. It was observed that, concrete jacketed partially damaged RC beams behaved very similar to concrete jacketed un-damaged RC beams when subjected to static flexural load. Hence, it is recommended that repairing and strengthening of the RC structural member at early period with GPC is the effective way of restoring the structure to its functional use at the earliest period possible. The findings of the present study may be useful for seismic retrofitting after an earthquake causes damage to RC members of different types.

Chapter 7

Summary and Conclusions

7.1 Overview

In the present study, ultra fine ground granulated blast furnace slag (UGGBS) based geopolymer mortar (GPM) and concrete (GPC) are developed with the aim of using these sustainable materials in repair and strengthening of reinforced concrete (RC) structures. Since repairing works are usually carried out by mortar whereas retrofitting/strengthening requires concrete, equal emphasis has been laid to develop GPM and GPC suitable for repairing and strengthening of RC structures.

The study was directed towards four major directions such as evaluation of the fresh and hardened state properties of geopolymer mortar (GPM), geopolymer concrete (GPM) and their effectiveness for the repairing and strengthening of RC beams.

In the present thesis, 32 numbers of UGGBS based GPM mixes were developed and detail tests were carried out to evaluate the fresh and hardened state properties. Admixtures such as flyash (FA) and superplasticizer (SP) were added to the mixes and their influence on setting time, workability and strength gain was observed. Two different types of alkali activator were used in the mixes which included combination of sodium silicate (Na_2SiO_3)

and sodium hydroxide (NaOH) solution; and only NaOH solution to observe their influence on the mentioned properties. In few mixes, alkali activator concentration was also altered keeping parameters such as FA and SP content fixed. Influence of time of addition of SP in the mixes was also observed. A controlled mortar mix was also prepared using Portland cement (PC) and similar tests as in case of GPM were conducted for comparison purpose.

Laboratory experiments were also conducted on UGGBS based GPC mixes to evaluate the workability, compressive and bond strength. Total 22 different mixes were prepared and tested including one controlled mix of Portland cement concrete (PCC). Special emphasis was given on the study of the bond strength of GPC with reinforcement bar and old PCC substrate. Special arrangements were made for casting of the specimens for rebar pull-out and slant shear tests for accessing bond strength.

Based on the results of GPM, suitable mix was selected for the repairing of RC beams. Total 7 numbers of RC beams of size 150 mm × 200 mm and length 2 m were subjected to different stages of damage by pre-loading the beams with different amounts of static flexural four point load. The damaged beams were repaired using GPM and Portland cement mortar (PCM) and retested by applying static flexural four point loading to observe the behaviour of the repaired beams due to static loading.

Strengthening of RC beams was also undertaken in this study. GPC was used as jacketing agent. The GPC mix was selected based on the results obtained from the tests on fresh and hardened state GPC. The RC beams were categorized into three different stages of damage which included undamaged, partially damaged and fully damaged beams. Total 10 number of RC beams of size 150 mm × 200 mm and length 2 m including a controlled beam were cast for this purpose. The beams were jacketed to size of 250 mm × 300 mm and length 2 m using GPC and PCC and were retested by application of static flexural four point load in the laboratory.

7.2 Major Conclusions and Recommendations

The significant observations and recommendations from the present study are outlined below as:-

1. Ultra fine ground granulated blast furnace slag (UGGBS) based geopolymeric mixes possess better fresh and hardened state properties; and develop higher early strength compared to Portland cement (PC) mix.

2. Sodium silicate (Na_2SiO_3) free UGGBS based geopolymer mixes possess higher setting time, better workability and superior strength gain property compared to that containing Na_2SiO_3.
3. Addition of flyash (FA) in the mixes retards the early setting property and improves the workability of the mixes. However, addition of very high amount of FA results in reduction in the early strength gain property of the mixes. It also leads to reduction in the strength at later ages.
4. Both sulfonated naphthalene (SN) and polycarboxylate ether (PE) based superplasticizer (SP) retards the early setting property and improves the workability of the geopolymer mixes. However, excess amount of this admixture in mixes lead to deterioration in performance related to setting time and early strength gain.
5. Increase in alkali concentration reduces the fresh state properties, however, the increased alkali concentration upto certain level contribute to the strength of the mixes.
6. Increase in alkali concentration reduces the setting time and workability of the geopolymer mixes. However, the increase in alkali concentration upto certain level contribute to the early and later age strength of the mixes.
7. Variations in time of addition of SP in the mixes are found responsible for the variations in the setting time, workability and rate of strength gain. Improved performance was shown by the mixes, when SP was added after the addition of alkali activator in the geopolymer mixes.
8. In case of bond strength results, the addition of FA and PE based SP improves the performance of the mixes but upto low content level of these admixtures
9. High sodium hydroxide (NaOH) concentration cause monotonous decrease in the bond strength of the geopolymer mixes.
10. UGGBS based geopolymer has strong potential to be used as concrete repairing and jacketing agent. The speciality of UGGBS based geopolymer is that at 1 day it can develop strength of about 60 % of that at 28 days.
11. GPM on using as concrete repairing agent show better performance than PCM. The GPM repaired fully damaged beams at 3 and 28 days could attain 89 and 98 % respectively of load attained by the controlled beam.

12. In case of GPM repaired partially damaged beams, the load attained were 1.01 and 1.11 times higher than the controlled beams at 3 and 28 days.
13. The ductile behaviour of the geopolymer mortar (GPM) repaired fully and partially damaged beams also enhanced compared to the controlled ones and Portland cement mortar (PCM) repaired beams.
14. Mortar repaired partially damaged reinforced concrete (RC) beams behaved superior to mortar repaired fully damaged RC beams when subjected to static flexural load.
15. Geopolymer concrete (GPC) jacketed beams performed more satisfactorily than Portland cement concrete (PCC) jacketed beams. The load carrying capacity of GPC jacketed beams enhanced by higher amounts than the increase in load capacity of PCC jacketed beams. Higher increase in ductility ratio was also observed in the GPC jacketed beams.
16. The level of damage also has significant influence on the performance of the strengthened structural members. The performance order decreased as: undamaged and jacketed: partially damaged and jacketed; and fully damaged and jacketed.
17. It was observed that, concrete jacketed partially damaged RC beams behaved very similar to concrete jacketed un-damaged RC beams when subjected to static flexural load.
18. It is recommended to prepare UGGBS based geopolymer as repairing agent with maximum 30 % of FA and 1.5 % of PE ether based SP for obtaining optimum results in terms of setting time, workability and strength including bond strength.
19. Repairing and strengthening of the RC structural member with geopolymer at initial stage of damage is recommended as it the effective way of restoring the structure to its functional use at the earliest period possible.

7.3 Scope for Future Work

From the present study, following future research works are recommended:-

1. The repairing and jacketing agent can be prepared using other by-products such as rice husk, metakaolin, etc. of high fineness.
2. Study on the bond behaviour and mechanism of interface of bond of slag based GPC with concrete and rebar.
3. The durability aspect, energy dissipation, stiffness behaviour in elastic and inelastic range, damage ratio, etc. of the repairing and jacketing agent can be explored.

4. The repairing of columns and beam-columns joints can be studied.
5. Dynamic loading can be included to examine the behavior of the repaired/strengthened beams.

APPENDIX

Appendix A

Mix Design For Portland Cement Concrete

IS 10262 2009 [97] was followed for the purpose of preparing the mix proportion for Portland cement concrete (PCC). Total two number of mixes were prepared for the purpose of conducting laboratory test in this study. Each mix was of different targent strength. Mix CC1 was designed with target strength of 20 N/mm^2 and mix CC2 with target strength of 35 N/mm^2. The minimum cement content and maximum water/cement (w/c) ratio were selected from Table 5 of IS 456 2000 [98]. Since, the concrete in both cases were cast and tested in the laboratory, standard deviation while finding the target strength was considered as 0.

A.1 Mix CC1

Given,

1.	Compressive strength of concrete	:	20 N/mm^2
2.	Maximum nominal size of aggregate	:	20 mm
3.	Minimum cement content	:	320 kg/m^3 (Table 5 [98])
4.	Maximum w/c ratio	:	0.55 (Table 5 [98])
5.	Workability	:	100 mm (slump)
6.	Grade of cement	:	OPC 43 grade
7.	Specific gravity of cement	:	3.08
8.	Specific gravity of:		
	a. CA	:	2.61
	b. FA	:	2.68
9.	Water absorption of:		
	a. CA	:	0.7 %
	b. FA	:	1.7 %
10.	Zone of FA	:	zone III

Target Strength for mix proportioning:

Target Strength of concrete at 28 days (f_{ck}') = Compressive strength of concrete at 28 days (f_{ck}) + standard deviation (σ)

Here,

σ = 0 (Since, casting of concrete specimens were done in controlled condition in laboratory.)

Therefore, $f_{ck}' = 20 + 0 = 20$ N/mm^2

Selection of w/c ratio:

Maximum w/c ratio = 0.55 (Table 5 [98])

Adopted w/c ratio = 0.55

Calculation of water content:

Maximum water content for 20 mm nominal maximum size aggregate and 25 - 50 mm slump range	= 186 kg (Table 2 [97])
Therefore, estimated water content for 20 mm nominal maximum size aggregate and 100 mm slump	= 186+(((2×3)/100)×186) = 197.16 kg

Calculation of cement content:

w/c = 0.55

Therefore, cement content = 197.16 ÷ 0.55 = 358.5 kg ≈ 360 kg (Approximated)

Proportion of volume of CA and FA:

Volume of CA corresponding to 20 mm size aggregate and FA (zone III) for w/c of 0.50	= 0.64 (Table 3 [97])
Here, w/c is 0.55	
Therefore, volume of CA	= 0.64 + (-1)×0.01 = 0.63
Volume of FA	= 1 - 0.63 = 0.37

Mix calculation:

1. Volume of concrete (a) = 1 m^3
2. Volume of cement (b) = (mass of cement/ specific gravity of cement)×(1/1000)

		= 0.117 m^3
3.	Volume of water (c)	= (mass of water/ specific gravity of water)×(1/1000)
		= 0.197 m^3
4.	Volume of aggragate (d)	= a-(b+c)
		= 0.686 m^3
5.	Mass of CA	= d×volume of CA×specific gravity of CA×1000
		= 1127.92 kg
6.	Mass of FA	= d×volume of FA×specific gravity of FA×1000
		= 680.19 kg

Mix proportion for CC1:

1.	Cement	= 360 kg
2.	FA	= 680 kg
3.	CA	= 1128 kg
4.	Water	= 197 kg
5.	w/c	= 0.548

A.2 Mix CC2

Given,

1.	Compressive strength of concrete	:	35 N/mm^2	
2.	Maximum nominal size of aggregate	:	35 mm	
3.	Minimum cement content	:	340 kg/m^3	(Table 5 [98])
4.	Maximum w/c ratio	:	0.45	(Table 5 [97])
5.	Workability	:	100 mm (slump)	
6.	Grade of cement	:	OPC 43 grade	
7.	Specific gravity of cement	:	3.08	
8.	Specific gravity of:			
	a. CA	:	2.61	
	b. FA	:	2.68	
9.	Water absorption of:			
	a. CA	:	0.7 %	

	b. FA	:	1.7 %
10.	Zone of FA	:	zone-III

Target Strength for mix proportioning:

Target Strength of concrete at 28 days (f_{ck}') = Compressive strength of concrete at 28 days (f_{ck}) + standard deviation (s)

Here,

s = 0 (Since, casting of concrete specimens were done in controlled condition in laboratory.)

Therefore, $f_{ck}' = 35 + 0 = 35$ N/mm^2

Selection of w/c ratio:

Maximum w/c ratio = 0.45 (Table 5 [98])

Adopted w/c ratio = 0.4

Calculation of water content:

Maximum water content for 20 mm nominal maximum size aggregate and 25 - 50 mm slump range	= 186 kg	(Table 2 [97])
Therefore, estimated water content for 20 mm nominal maximum size aggregate and 100 mm slump	= 160+(((2×3)/100)×186) = 171.16 kg	

Calculation of cement content:

w/c = 0.40

Therefore, cement content = 171.16 ÷ 0.4 = 427.9 kg ≈ 425 kg (Approximated)

Proportion of volume of CA and FA:

Volume of CA corresponding to 20 mm size aggregate and FA (zone III) for w/c of 0.50	= 0.64	(Table 3 [97])
Here, w/c is 0.40		
Therefore, volume of CA	= 0.64 + (2)×0.010 = 0.66	
Volume of FA	= 1- 0.66 = 0.34	

Mix calculation:

1. Volume of concrete (a) = 1 m^3
2. Volume of cement (b) = (mass of cement/ specific gravity of cement)×(1/1000)
   = 0.138 m^3
3. Volume of water (c) = (mass of water/ specific gravity of water)×(1/1000)
   = 0.171 m^3
4. Volume of aggragate (d) = a-(b+c)
   = 0.691 m^3
5. Mass of CA = d×volume of CA×specific gravity of CA×1000
   = 1190 kg
6. Mass of FA = d×volume of FA×specific gravity of FA×1000
   = 630 kg

Mix proportion for CC2:

1. Cement = 425 kg
2. FA = 630 kg
3. CA = 1190 kg
4. Water = 171 kg

Appendix B

Design of Reinforced Concrete Beam

B.1 Controlled Beam Weak in Flexure

The beams were designed without considering material factor of safety of concrete and steel. All the beams were designed as doubly reinforced beams. The beams were designed targeting a total load carrying capacity of 55 kN from the actuator. The design of beam is as follows:-

Let, it be assumed that 2-12 mm dia bars are provided at both top and bottom of the beam and 2-legged 8 mm dia bars are used as stirrups.

Here,

Area of tension steel, A_{st} = Area of compression steel, A_{sc} = 226.19 mm^2

Breadth, b = 150 mm

Overall depth, D = 200 mm

Clear cover = 25 mm

Effective cover, d_c = 31 mm

Efective depth, d = 200 – 31 = 169 mm

Span of the beam, L = 1800 mm

From cube test results, f_{ck} = 28.04 N/mm^2

From tensile test of 12 mm rebar, f_y = 550.87 N/mm^2

From tensile test of 8 mm rebar, f_y' = 542.74 N/mm^2

***Analysis of Beam*:**

Calculation of Neutral Axis (NA) Depth:-

The equilibrium equation for a doubly reinforced RC beam is given by

$$C_{uc} + C_{us} = T_u \quad \text{(B1)}$$

Where,

C_{uc} = Resultant compressive force in concrete

C_{us} = Resultant compressive force in the compressive steel

T_u =Resultant tensile force in tension steel

Let x be the NA depth.

Now,

$C_{uc} = 0.81 \times f_{ck} \times b \times x$ (Negelecting safety factors)

$= 0.81 \times 28.04 \times 150 \times x$

$= 3406.86 \times x$ N

$C_{us} = E_s \times \epsilon_{s1}$, where ϵ_{s1} is strain in compressive steel and E_s is modulus of elasticity of steel

$C_{us} = 2 \times 10^5 \times 0.0035 \times \frac{x-35}{x} \times A_{sc} = 158336.3 \times \frac{x-35}{x}$

$T_u = f_y \times A_{st}$

$= 550.87 \times 226.19$

$= 124603.87$ N

Substituting values in (B1),

$3406.86 \times x + 158336.3 \times \frac{x-35}{x} = 124603.87$

Solving for x,

$x = 33.3$ mm

Now, stress developed in compressive steel, $f_{sc} = 48.9$ N/mm^2

Moment carrying capacity of beam,

$M_u = C_{uc} \times (d - 0.42 \times x) + C_{us} \times (d - d_c)$

$= 16.14$ kNm

Load producing moment, $W_u = 4 \times \{M_u - (\text{moment due to selfweigth})\}/L$

$= 26.89$ kN

Ultimate Load carrying capacity of beam under simply supported condition, $2W_u$

$= 2 \times 26.89$ kN

$= 53.78$ kN

Shear force, $V_u = 27.57$ kN

***Design of shear reinforcement in beam*:**

Here, percentage of tensile reinforcement provided, $p_t = 0.892$ %

Corresponding shear stress for M20 and $p_t = 0.892$ %, (Table 19 [98])

$\tau_c = 0.61$ N/mm^2

Shear resisted by concrete,

$V_c = \tau_c \times b \times d$ (Cl. – 40.1 [98])

$= 0.61 \times 150 \times 169$

$= 15.46$ kN $< V_u$ (27.57 kN)

Hence, shear reinforcement is required.

Now, shear to be resisted by steel,

$V_{us} = V_u - V_c$

$= 27.57 - 15.46$

$= 12.10$ kN

Area of stirrup, $A_{sv} = 100.53$ mm^2

Let, S_v be the spacing of the stirrups and $f_y'' = f_y'/0.87 = 542.74/0.87$

$V_{us} = (0.87 \times f_y'' \times A_{sv} \times d) / S_v$ (Cl. - 40.4.a [98])

$S_v = 701.82$ mm

Minimum shear reinforcement (Cl. - 26.5.1.5 [98])

$S_{v(max)} = 0.75 \times d = 126.75$ mm (maximum)

Shear reinforcement is provided at minimum of $2 \times d = 338$ mm from either ends.

Development length required $= (\phi \times \sigma)/(4 \times \tau_{bd})$ (Cl. - 26.2.1 [98])

$= (12 \times 550.87)/(4 \times 1.2)$

$= 1377$ mm

Available length = 1800 mm

Therefore, 2-legged 8 mm diameter stirrups @ 100 mm c/c up to 500 mm from both ends and 2 -legged 8 mm diameter stirrups @ 185 mm c/c for remaining length of beam are provided.

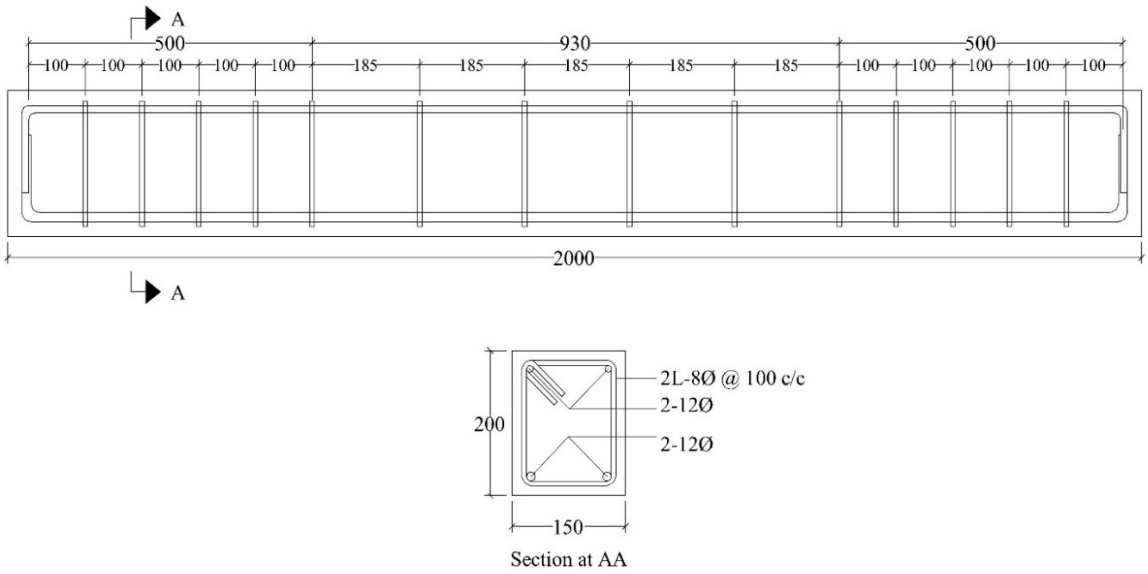

Figure B.1: Reinforcement details in the beam (*All dimensions are in mm*).

REFERENCES

[1] Aitcin, P. C. (2000). Cements of yesterday and today: concrete of tomorrow. *Cement and Concrete research*, 30(9), 1349-1359.

[2] Statista, https://www.statista.com/statistics/420530/production-of-cement-in india.

[3] Cement demand to see 4.5% growth in FY19, https://economictimes.indiatimes.com/industry/indl-goods/svs/cement/cement-demand-to-see-4-5-growth-in-fy19/article show/63094576.cms.

[4] Statista, the statistics portal, https://www.statista.com/statistics/267364/world-cement-production-by-country/.

[5] Statista, the statistics portal, https://www.statista.com/statistics/269322/cement-consumption-in-india-since-2004/.

[6] Statista, the statistics portal, https://www.statista.com/statistics/373845/global-cement-production-forecast/.

[7] Mehta, P. K. (2002). Greening of the concrete industry for sustainable development. *Concrete international*, 24(7), 23-28.

[8] Malhotra, V. M. (2002). Introduction: sustainable development and concrete technology. *Concrete International*, 24(7).

[9] Davidovits, J. (1982). *U.S. Patent No. 4349386*. Washington, DC: U.S. Patent and Trademark Office.

[10] Davidovits, J., and Morris, M. (2009). *Why the pharaohs built the Pyramids with fake stones*. Institut Géopolymère.

[11] Davidovits, J. (1988). Geopolymer chemistry and properties. *Geopolymer*, 88 (1), 25-48.

[12] Duxson, P., Fernández-Jiménez, A., Provis, J. L., Lukey, G. C., Palomo, A., and van Deventer, J. S. (2007). Geopolymer technology: the current state of the art. *Journal of materials science*, 42(9), 2917-2933.

[13] Indian Minerals Yearbook 2017, Indian Bureau of Mines, Ministry of Mines, Government of India, New Delhi.

[14] ASTM C618 - 17a, Standard Specification for Coal Fly Ash and Raw or Calcined Natural Pozzolan for Use in Concrete, *American Society for Testing and Materials*, 2013, West Conshohocken, US.

References

[15] Giddel, M. R., and Jivan, A. P. (2007, January). Waste to wealth, potential of rice husk in India a literature review. In *International conference on cleaner technologies and environmental Management PEC, Pondicherry, India* (Vol. 2, pp. 4-6).

[16] Davidovits, J. (1989). Geopolymers and geopolymeric materials. *Journal of Thermal Analysis and Calorimetry*, 35(2), 429-441.

[17] Douglas, E., and Brandstetr, J. (1990). A preliminary study on the alkali activation of ground granulated blast-furnace slag. *Cement and Concrete Research*, 20(5), 746-756.

[18] ASTM C109 / C109M - 16a, Standard Test Method for Compressive Strength of Hydraulic Cement Mortars (Using 2-in. or [50-mm] Cube Specimens), *American Society for Testing and Materials*, 2013, West Conshohocken, US.

[19] Douglas, E., Bilodeau, A., Brandstetr, J., and Malhotra, V. M. (1991). Alkali activated ground granulated blast-furnace slag concrete: preliminary investigation. *Cement and concrete research*, 21(1), 101-108.

[20] Collins, F., and Sanjayan, J. G. (1999). Effects of ultra-fine materials on workability and strength of concrete containing alkali-activated slag as the binder. *Cement and concrete research*, 29(3), 459-462.

[21] Alonso, S., and Palomo, A. (2001). Alkaline activation of metakaolin and calcium hydroxide mixtures: influence of temperature, activator concentration and solids ratio. *Materials Letters*, 47(1-2), 55-62.

[22] Brough, A. R., and Atkinson, A. (2002). Sodium silicate-based, alkali-activated slag mortars: Part I. Strength, hydration and microstructure. *Cement and concrete research*, 32(6), 865-879.

[23] Hardjito, D., Wallah, S. E., Sumajouw, D. M., and Rangan, B. V. (2004). On the development of fly ash-based geopolymer concrete. *Materials Journal*, 101(6), 467-472.

[24] Hardjito, D., and Rangan, B. V. (2005). Development and properties of low-calcium fly ash-based geopolymer concrete.

[25] Öner, M., Erdoğdu, K., and Günlü, A. (2003). Effect of components fineness on strength of blast furnace slag cement. *Cement and Concrete Research*, 33(4), 463-469.

[26] Barnett, S. J., Soutsos, M. N., Millard, S. G., and Bungey, J. H. (2006). Strength development of mortars containing ground granulated blast-furnace slag: Effect of curing temperature and determination of apparent activation energies. *Cement and Concrete Research*, 36(3), 434-440.

[27] Atiş, C. D., and Bilim, C. (2007). Wet and dry cured compressive strength of concrete containing ground granulated blast-furnace slag. *Building and Environment*, 42(8), 3060-3065.

[28] Chindaprasirt, P., De Silva, P., Sagoe-Crentsil, K., and Hanjitsuwan, S. (2012). Effect of SiO2 and Al2O3 on the setting and hardening of high calcium fly ash-based geopolymer systems. *Journal of Materials Science*, 47(12), 4876-4883.

[29] Altan, E., and Erdoğan, S. T. (2012). Alkali activation of a slag at ambient and elevated temperatures. *Cement and Concrete Composites*, 34(2), 131-139.

[30] Burciaga-Díaz, O., Díaz-Guillén, M. R., Fuentes, A. F., and Escalante-Garcia, J. I. (2013). Mortars of alkali-activated blast furnace slag with high aggregate: binder ratios. *Construction and Building Materials,* 44, 607-614.

[31] Tsai, C. J., Huang, R., Lin, W. T., and Chiang, H. W. (2014). Using GGBOS as the alkali activators in GGBS and GGBOS blended cements. *Construction and Building Materials*, 70, 501-507.

[32] Atiş, C. D., Görür, E. B., Karahan, O., Bilim, C., Ilkentapar, S., and Luga, E. (2015). Very high strength (120 MPa) class F fly ash geopolymer mortar activated at different NaOH amount, heat curing temperature and heat curing duration. *Construction and building materials*, 96, 673-678.

[33] Karthik, A., Sudalaimani, K., Vijayakumar, C. T., and Saravanakumar, S. S. (2018). Effect of bio-additives on physico-chemical properties of fly ash-ground granulated blast furnace slag based self-cured geopolymer mortars. *Journal of hazardous materials*.

[34] Patel, Y. J., and Shah, N. (2018). Enhancement of the properties of Ground Granulated Blast Furnace Slag based Self Compacting Geopolymer Concrete by incorporating Rice Husk Ash. *Construction and Building Materials*, 171, 654-662.

[35] Singhal, D., Junaid, M. T., Jindal, B. B., and Mehta, A. (2018). Mechanical and microstructural properties of fly ash based geopolymer concrete incorporating Alccofine at ambient curing. *Construction and Building Materials*, 180, 298-307.

[36] Askarian, M., Tao, Z., Adam, G., and Samali, B. (2018). Mechanical properties of ambient cured one-part hybrid OPC-geopolymer concrete. *Construction and Building Materials*, 186, 330-337.

[37] Li, G., and Zhao, X. (2003). Properties of concrete incorporating fly ash and ground granulated blast-furnace slag. *Cement and Concrete Composites*, 25(3), 293-299.

[38] Binici, H., Temiz, H., and Köse, M. M. (2007). The effect of fineness on the properties of the blended cements incorporating ground granulated blast furnace slag and ground basaltic pumice. *Construction and Building Materials*, 21(5), 1122-1128.

[39] Teng, S., Lim, T. Y. D., and Divsholi, B. S. (2013). Durability and mechanical properties of high strength concrete incorporating ultra fine ground granulated blast-furnace slag. *Construction and Building Materials*, 40, 875-881.

[40] Salas, D. A., Ramirez, A. D., Ulloa, N., Baykara, N., Boero, A. J. (2018). Life cycle assessment of geopolymer concrete. *Construction and Building Materials*, 190(30), 170-177.

[41] Luhar, S., Chaudhary, S., and Luhar, I. (2018). Thermal resistance of fly ash based rubberized geopolymer concrete. *Journal of Building Engineering*.

[42] Khan, M. I., Azizli, K., Sufian, S., and Man, Z. (2015). Sodium silicate-free geopolymers as coating materials: Effects of Na/Al and water/solid ratios on adhesion strength. *Ceramics International*, 41(2), 2794-2805.

[43] Sarker, P. K. (2011). Bond strength of reinforcing steel embedded in fly ash-based geopolymer concrete. *Materials and structures*, 44(5), 1021-1030.

[44] Ueng, T. H., Lyu, S. J., Chu, H. W., Lee, H. H., and Wang, T. T. (2012). Adhesion at interface of geopolymer and cement mortar under compression: an experimental study. *Construction and Building Materials*, 35, 204-210.

[45] Zheng, W., and Zhu, J. (2013). The effect of elevated temperature on bond performance of alkali-activated GGBFS paste. *Journal of Wuhan University of Technology-Mater. Sci. Ed.*, 28(4), 721-725.

[46] Phoo-ngernkham, T., Sata, V., Hanjitsuwan, S., Ridtirud, C., Hatanaka, S., and Chindaprasirt, P. (2015). High calcium fly ash geopolymer mortar containing Portland cement for use as repair material. *Construction and Building Materials*, 98, 482-488.

[47] Al-Azzawi, M., Yu, T., and Hadi, M. N. (2018). Factors Affecting the Bond Strength Between the Fly Ash-based Geopolymer Concrete and Steel Reinforcement. *Structures*, 14, 262-272.

[48] Perná, I., and Hanzlíček, T. (2016). The setting time of a clay-slag geopolymer matrix: the influence of blast-furnace-slag addition and the mixing method. *Journal of Cleaner Production*, 112, 1150-1155.

[49] Xiong, G., Liu, J., Li, G., and Xie, H. (2002). A way for improving interfacial transition zone between concrete substrate and repair materials. *Cement and concrete Research*, 32(12), 1877-1881.

[50] Hu, S., Wang, H., Zhang, G., and Ding, Q. (2008). Bonding and abrasion resistance of geopolymeric repair material made with steel slag. *Cement and concrete composites*, 30(3), 239-244.

[51] Vasconcelos, E., Fernandes, S., De Aguiar, J. B., and Pacheco-Torgal, F. (2011). Concrete retrofitting using metakaolin geopolymer mortars and CFRP. *Construction and Building Materials*, 25(8), 3213-3221.

[52] Popov, E. P., and Bertero, V. V. (1975). Repaired R/C members under cyclic loading. *Earthquake Engineering and Structural Dynamics*, 4(2), 129-144.

[53] Holman, J. W., and Cook, J. P. (1984). Steel plates for torsion repair of concrete beams. *Journal of Structural Engineering*, *110*(1), 10-18.

[54] Al-Mandil, M. Y., Khalil, H. S., Baluch, M. H., and Azad, A. K. (1990). Performance of epoxy-repaired concrete under thermal cycling. *Cement and concrete composites*, 12(1), 47-52.

[55] Chajes, M. J., Thomson Jr, T. A., and Farschman, C. A. (1995). Durability of concrete beams externally reinforced with composite fabrics. *Construction and building Materials*, 9(3), 141-148.

[56] Cairns, J., and Rafeeqi, S. F. A. (1997). Behaviour of reinforced concrete beams strengthened by external unbonded reinforcement. *Construction and Building Materials*, 11(5-6), 309-317.

[57] Nounu, G. and Chaudhary, Z (1999). Reinforced concrete repairs in beams. *Construction and building materials*, 13(4), 195-212.

[58] Li, A., Assih, J., and Delmas, Y. (2001). Shear strengthening of RC beams with externally bonded CFRP sheets. *Journal of Structural Engineering*, 127(4), 374-380.

[59] Altun, F. (2004). An experimental study of the jacketed reinforced-concrete beams under bending. *Construction and Building Materials*, 18(8), 611-618.

[60] Issa, C. A., and Debs, P. (2007). Experimental study of epoxy repairing of cracks in concrete. *Construction and Building Materials*, 21(1), 157-163.

[61] Ahmad, S., Elahi, A., Barbhuiya, S. A., and Farid, Y. (2012). Use of polymer modified mortar in controlling cracks in reinforced concrete beams. *Construction and Building Materials*, 27(1), 91-96.

[62] Pattnaik, R. R., and Rangaraju, P. R. (2014). Investigation on flexure test of composite beam of repair materials and substrate concrete for durable repair. *Journal of The Institution of Engineers (India): Series A*, 95(4), 203-209.

[63] Tomlinson, D., and Fam, A. (2014). Performance of concrete beams reinforced with basalt FRP for flexure and shear. *Journal of composites for construction*, 19(2), 04014036.

[64] Luna-Galiano, Y., Leiva, C., Villegas, R., Arroyo, F., Vilches, L., and Fernández-Pereira, C. (2018). Carbon fiber waste incorporation in blast furnace slag geopolymer-composites. *Materials Letters*.

[65] Raval, S. S., and Dave, U. V. (2013). Effectiveness of various methods of jacketing for RC beams. *Procedia Engineering*, 51, 230-239.

[66] Belal, M. F., Mohamed, H. M., and Morad, S. A. (2015). Behavior of reinforced concrete columns strengthened by steel jacket. *HBRC Journal*, 11(2), 201-212.

[67] Jamil, M. A., Zisan, M. B., Alam, M. A. M., and Alim, H. (2013). Restrengthening of RCC beam by beam jacketing. *Malaysian Journal of Civil Engineering*, 25(2).

[68] Júlio, E. N., Branco, F. A., and Silva, V. D. (2005). Reinforced concrete jacketing-interface influence on monotonic loading response. *ACI Structural Journal*, 102(2), 252.

[69] Swanepoel, J. C., and Strydom, C. A. (2002). Utilization of fly ash in a geopolymeric material. *Applied geochemistry*, 17(8), 1143-1148.

[70] Fernández-Jiménez, A., Palomo, A., and Criado, M. (2005). Microstructure development of alkali-activated fly ash cement: a descriptive model. *Cement and concrete research*, 35(6), 1204-1209.

[71] Duan, P., Yan, C., and Luo, W. (2016). A novel waterproof, fast setting and high early strength repair material derived from metakaolin geopolymer. *Construction and Building Materials*, 124, 69-73.

[72] Alanazi, H., Yang, M., Zhang, D., and Gao, Z. J. (2016). Bond strength of PCC pavement repairs using metakaolin-based geopolymer mortar. *Cement and Concrete Composites*, 65, 75-82.

[73] Zanotti, C., Borges, P. H., Bhutta, A., and Banthia, N. (2017). Bond strength between concrete substrate and metakaolin geopolymer repair mortar: Effect of curing regime and PVA fiber reinforcement. *Cement and Concrete Composites*, 80, 307-316.

[74] Aldahdooh, M. A. A., Bunnori, N. M., Johari, M. M., Jamrah, A., and Alnuaimi, A. (2016). Retrofitting of damaged reinforced concrete beams with a new green cementitious composites material. *Composite Structures*, 142, 27-34.

[75] IS 4031 (Part 6) - 1988. Methods of physical tests for hydraulic cement- Part 6: Determination of compressive strength of hydraulic cement (other than masonry cement). Bureau of Indian Standard, New Delhi, India

[76] IS 4031 (Part 1) - 1996. Methods of physical tests for hydraulic cement- Part 1: Determination of fineness by dry sieving. Bureau of Indian Standard, New Delhi, India

[77] IS 4031 (Part 4) - 1988. Methods of physical tests for hydraulic cement- Part 4: Determination of consistency of standard cement paste. Bureau of Indian Standard, New Delhi, India

[78] IS 4031 (Part 5) - 1988. Methods of physical tests for hydraulic cement- Part 5: Determination of initial and final setting time. Bureau of Indian Standard, New Delhi, India

[79] IS 4031 (Part 11) - 1988. Methods of physical tests for hydraulic cement- Part 11: Determination of Density. Bureau of Indian Standard, New Delhi, India

[80] IS 8112: 1989. 43 grade ordinary Portland cement- specification. Bureau of Indian Standard, New Delhi, India

[81] IS 1727-1967. Methods of test for pozzolanic materials. Bureau of Indian Standards, New Delhi, India

[82] Somna, K., Jaturapitakkul, C., Kajitvichyanukul, P., and Chindaprasirt, P. (2011). NaOH-activated ground fly ash geopolymer cured at ambient temperature. *Fuel*, 90(6), 2118-2124.

[83] De Vargas, A. S., Dal Molin, D. C., Masuero, Â. B., Vilela, A. C., Castro-Gomes, J., and de Gutierrez, R. M. (2014). Strength development of alkali-activated fly ash

produced with combined NaOH and Ca (OH) 2 activators. *Cement and Concrete Composites*, 53, 341-349.

[84] Morsy, M. S., Alsayed, S. H., Al-Salloum, Y., and Almusallam, T. (2014). Effect of sodium silicate to sodium hydroxide ratios on strength and microstructure of fly ash geopolymer binder. *Arabian journal for science and engineering*, 39(6), 4333-4339.

[85] Gu, K., Jin, F., Al-Tabbaa, A., Shi, B., and Liu, J. (2014). Mechanical and hydration properties of ground granulated blastfurnace slag pastes activated with MgO–CaO mixtures. *Construction and Building Materials*, 69, 101-108.

[86] Abdalqader, A. F., Jin, F., and Al-Tabbaa, A. (2016). Development of greener alkali-activated cement: utilisation of sodium carbonate for activating slag and fly ash mixtures. *Journal of Cleaner Production*, 113, 66-75.

[87] Sakulich, A. R., Anderson, E., Schauer, C. L., and Barsoum, M. W. (2010). Influence of Si: Al ratio on the microstructural and mechanical properties of a fine-limestone aggregate alkali-activated slag concrete. *Materials and Structures*, 43(7), 1025-1035.

[88] Yang, K. H., Song, J. K., Ashour, A. F., and Lee, E. T. (2008). Properties of cementless mortars activated by sodium silicate. *Construction and Building Materials*, 22(9), 1981-1989.

[89] Phoo-ngernkham, T., Maegawa, A., Mishima, N., Hatanaka, S., and Chindaprasirt, P. (2015). Effects of sodium hydroxide and sodium silicate solutions on compressive and shear bond strengths of FA–GBFS geopolymer. *Construction and Building Materials*, 91, 1-8.

[90] Görhan, G., and Kürklü, G. (2014). The influence of the NaOH solution on the properties of the fly ash-based geopolymer mortar cured at different temperatures. *Composites part b: engineering*, 58, 371-377.

[91] Xu, H., and Van Deventer, J. S. J. (2000). The geopolymerisation of alumino-silicate minerals. *International journal of mineral processing*, 59(3), 247-266.

[92] IS 2386 (Part III) 1963, Methods of test for aggregates for concrete – Part 3: Specific gravity, density, voids, absorption and bulking , Bureau of Indian Standard, New Delhi, India.

[93] IS 2386 (Part I) 1963, Methods of test for aggregates for concrete – Part 1: particle size and shape, Bureau of Indian Standard, New Delhi, India.

[94] IS 383 1970, Specification for coarse and fine aggregates from natural sources for concrete, Bureau of Indian Standard, New Delhi, India.

[95] IS 432 (Part I) 1982, Specification for mild steel and medium tensile steel bars and hard-drawn steel wire for concrete reinforcement – Part 1: mild steel and medium tensile steel bars, Bureau of Indian Standard, New Delhi, India.

[96] IS 1608 2005, Metallic materials - tensile testing at ambient temperature, Bureau of Indian Standard, New Delhi, India.

[97] IS 10262 2009. Concrete Mix Proportioning - Guidelines. Bureau of Indian Standard, New Delhi, India.

[98] IS 456 - 2000. Plain and Reinforced concrete - Code of Practice. Bureau of Indian Standard, New Delhi, India

[99] Khale, D., and Chaudhary, R. (2007). Mechanism of geopolymerization and factors influencing its development: a review. *Journal of materials science*, 42(3), 729-746.

[100] Law, D. W., Adam, A. A., Molyneaux, T. K., and Patnaikuni, I. (2012). Durability assessment of alkali activated slag (AAS) concrete. *Materials and Structures*, 45(9), 1425-1437.

[101] Kim, Y. J., Kim, S. C., and Kim, Y. T. (2003). Corrosion resistance and hydration heat of concrete containing ground granulated blast furnace slag. *KSCE Journal of Civil Engineering*, 7(4), 399-404.

[102] Pacheco-Torgal, F., Castro-Gomes, J., and Jalali, S. (2008). Alkali-activated binders: A review: Part 1. Historical background, terminology, reaction mechanisms and hydration products. *Construction and Building Materials*, 22(7), 1305-1314.

[103] Singh, B., Ishwarya, G., Gupta, M., and Bhattacharyya, S. K. (2015). Geopolymer concrete: A review of some recent developments. *Construction and building materials*, 85, 78-90.

[104] Zhu, J., Zhong, Q., Chen, G., and Li, D. (2012). Effect of particlesize of blast furnace slag on properties of portland cement. *Procedia Engineering*, 27, 231-236.

[105] Memon, F. A., Nuruddin, M. F., and Shafiq, N. (2013). Effect of silica fume on the fresh and hardened properties of fly ash-based self-compacting geopolymer concrete. *International Journal of Minerals, Metallurgy, and Materials*, 20(2), 205-213.

[106] Nath, P., and Sarker, P. K. (2014). Effect of GGBFS on setting, workability and early strength properties of fly ash geopolymer concrete cured in ambient condition. *Construction and Building Materials*, 66, 163-171.

[107] Yang, K. H., Song, J. K., Ashour, A. F., and Lee, E. T. (2008). Properties of cementless mortars activated by sodium silicate. *Construction and Building Materials*, 22(9), 1981-1989.

[108] Lee, N. K., and Lee, H. K. (2013). Setting and mechanical properties of alkali-activated fly ash/slag concrete manufactured at room temperature. *Construction and Building Materials*, 47, 1201-1209.

[109] Puertas, F., Martínez-Ramírez, S., Alonso, S., and Vazquez, T. (2000). Alkali-activated fly ash/slag cements: strength behaviour and hydration products. *Cement and Concrete Research*, 30(10), 1625-1632.

[110] Laskar, A. I., and Bhattacharjee, R. (2013). Effect of Plasticizer and Superplasticizer on Rheology of Fly-Ash-Based Geopolymer Concrete. *ACI materials journal*, 110(5).

[111] Karakoç, M. B., Türkmen, I., Maraş, M. M., Kantarci, F., Demirboğa, R., and Toprak, M. U. (2014). Mechanical properties and setting time of ferrochrome slag based geopolymer paste and mortar. *Construction and Building Materials*, 72, 283-292.

[112] Chang, J. J. (2003). A study on the setting characteristics of sodium silicate-activated slag pastes. *Cement and Concrete Research*, 33(7), 1005-1011.

[113] Criado, M., Palomo, A., Fernández-Jiménez, A., and Banfill, P. F. G. (2009). Alkali activated fly ash: effect of admixtures on paste rheology. *Rheologica Acta*, 48(4), 447-455.

[114] IS 8112 2013. Ordinary Portland cement, 43 Grade - Specification. Bureau of Indian Standard, New Delhi, India

[115] Palacios, M., and Puertas, F. (2005). Effect of superplasticizer and shrinkage-reducing admixtures on alkali-activated slag pastes and mortars. *Cement and concrete research*, 35(7), 1358-1367.

[116] Song, S., Sohn, D., Jennings, H. M., and Mason, T. O. (2000). Hydration of alkali-activated ground granulated blast furnace slag. *Journal of Materials Science*, 35(1), 249-257.

[117] Atiş, C. D., Görür, E. B., Karahan, O., Bilim, C., Ilkentapar, S., and Luga, E. (2015). Very high strength (120 MPa) class F fly ash geopolymer mortar activated at different NaOH amount, heat curing temperature and heat curing duration. *Construction and Building Materials*, 96, 673-678.

[118] Heinisch, O. (1965). Young, HD: Statistical Treatment of experimental Data. McGraw-Hill Book Comp., Inc., New York, London 1962. XV+ 172 Seiten, Preis 20 s. *Biometrische Zeitschrift*, 7(1), 72-72.

[119] Swamy, G. J., Sangamithra, A., and Chandrasekar, V. (2014). Response surface modeling and process optimization of aqueous extraction of natural pigments from Beta vulgaris using Box–Behnken design of experiments. *Dyes and Pigments*, 111, 64-74.

[120] Manjunatha, G. S., Radhakrishna, Venugopal, K., and Maruthi, S. V. (2014). Strength characteristics of open air cured geopolymer concrete. *Transactions of the Indian Ceramic Society*, 73(2), 149-156.

[121] Yun, K. K., and Choi, P. (2014). Causes and controls of cracking at bridge deck overlay with very-early strength latex-modified concrete. *Construction and Building Materials*, 56, 53-62.

[122] IS 516 1959, Methods of Tests for Strength of Concrete, Bureau of Indian Standard, New Delhi, India, 2004.

[123] IS 2770 1967, Methods of Testing Bond in Reinforced Concrete, Bureau of Indian Standard, New Delhi, India, 2002.

[124] ASTM C882/C882M – 13a, Standard Test Method for Bond Strength of Epoxy-Resin Systems used with Concrete by Slant Shear, vol. 04.02, Annual Book of ASTM Standard, United States, 2005.

[125] IS 1199 1959, Methods of Sampling and Analysis of Concrete, Bureau of Indian Standard, New Delhi, India, 2004.

[126] Kumar, S., Kumar, R., and Mehrotra, S. P. (2010). Influence of granulated blast furnace slag on the reaction, structure and properties of fly ash based geopolymer. *Journal of Materials Science*, 45(3), 607-615.

[127] IS 5816 1999, Splitting Tensile Strength of Concrete - Method of Test, Bureau of Indian Standard, New Delhi, India.

[128] Cheong, H. K., and MacAlevey, N. (2000). Experimental behavior of jacketed reinforced concrete beams. *Journal of Structural Engineering*, 126(6), 692-699.

[129] Hussain, M., Sharif, A., Baluch, I. B. M., and Al-Sulaimani, G. J. (1995). Flexural behavior of precracked reinforced concrete beams strengthened externally by steel plates. *Structural Journal*, 92(1), 14-23.

[130] Oh, B. H., Cho, J. Y., and Park, D. G. (2003). Static and fatigue behavior of reinforced concrete beams strengthened with steel plates for flexure. *Journal of structural engineering*, 129(4), 527-535.

[131] Sirju, K., and Sharma, A. K. (2001). Strengthening of reinforced concrete members under compression and bending. *Proceedings of the Institution of Civil Engineers-Structures and Buildings*, 146(2), 227-231.

PUBLICATIONS FROM THE THESIS

Journal:

1. Laskar, S. M., and Talukdar, S. "Development of ultrafine slag-based geopolymer mortar for use as repairing mortar." *ASCE Journal of Materials in Civil Engineering*, 29 (5), 2017.
2. Laskar, S. M., and Talukdar, S. "Preparation and tests for workability, compressive and bond strength of ultra-fine slag based geopolymer as concrete repairing agent." *Construction and Building Materials*, 154, pp 176–190, 2017.
3. Laskar, S. M., and Talukdar, S. "A study on the performance of damaged RC members repaired using ultra-fine slag based geopolymeric systems". (Under review in *Journal of Construction and Building Materials*)
4. Laskar, S. M., and Talukdar, S. "Slag based geopolymer concrete as reinforced concrete jacketing agent". (Under review in *ASCE Journal of Materials in Civil Engineering*)

Conference:

1. Laskar, S. M., and Talukdar, S. "Effect of alkaline solution of varying molarity and varying superplasticizer content on flyash based geopolymer." *International Conference on Construction, Real Estate, Infrastructure and Project Management (ICCRIP-2016)*, Oct 21-22, 2016, NICMAR, Pune, India.
2. Laskar, S. M., and Talukdar, S. "Effect of Addition of Flyash and Superplasticizer to Ultra-fine Slag Based Geopolymer Mortar." *Structural Engineering Convention (SEC 2016)*, Dec 21-23, 2016, CSIR-SERC, Chennai, India.
3. Laskar, S. M., and Talukdar, S. "Influence of Superplasticizer and Alkali Activator Concentration on Slag-Flyash Based Geopolymer." *ASCE India Conference 2017*, Dec 13-14, 2017, IIT Delhi, India.
4. Laskar, S. M., and Talukdar, S. "Potential Use of Geopolymer: A State of the Art." *International Conference on Infrastructure Development (ICID) 2018*, Dec 21-22, 2018, Jorhat Engineering College, Jorhat, Assam.